FULL-DAY WORKSHOP

RAWCON 98

1998 IEEE Radio and Wireless Conference

Sheraton Colorado Springs
Colorado Springs, Colorado, USA
August 9-12, 1998

http://rawcon.org

IEEE NIST ITS

Modeling and Simulation of Devices and Circuits for Wireless Communications

Organizer and Chair:
John F. Sevic
Spectrian Corp.

Sunday, August 9, 1998
8:00 a.m. - 5:00 pm
Ballroom 1
Sheraton Colorado Springs

RAWCON'98 Sunday Workshop

Modeling and Simulation of Devices and Circuits for Wireless Communication Systems

Organizer and Chairman:
John F. Sevic, *Spectrian Corp.*

Abstract

Commercial RF and microwave CAD packages have evolved to the point where predictive simulation is possible. When properly applied, CAD can reduce design cycle-time and provide insight that bench techniques alone cannot. Virtual prototyping and statistical optimization are possible, precluding the necessity of time-consuming pilot runs. Unfortunately, many CAD users are unfamiliar with rigorous modeling and characterization techniques. The result is often user frustration and alienation. Ultimately, many CAD users return to bench methods.

The purpose of this workshop is to introduce basic modeling and characterization techniques for RF and microwave CAD. Experts will discuss how to use simulation to complement the design process for wireless communication circuits. The emphasis will be on learning when to use simulation to an advantage, how to interpret results, and how to establish confidence in the models. Attendees of the workshop will learn to trust simulation in order to make engineering decisions.

A wide variety of topics will be covered, including simulation and modeling of passive lumped and distributed components, frequency-conversion circuits, and power amplifier circuits. Large-signal device modeling and characterization techniques will also be covered. Identification of the appropriate simulation method and model will be covered for each topic, and measured versus simulated examples will be given.

1998 IEEE RADIO AND WIRELESS CONFERENCE (RAWCON'98)
SUNDAY WORKSHOP

Modeling and Simulation of Devices and Circuits for Wireless Communications

August 9, 1998, 8:00 am - 5:00 pm

Time	Speaker	Affiliation	Topic
7:00 am	Registration		
8:00 am	Introduction		
8:15 am	Jeffrey Jargon	NIST	Microwave Network Theory and VNA Calibration
9:00 am	Wayne Struble	M/A-COM	Stability Analysis of Linear Circuits
10:00 am	Break		
10: 15 am	James Rautio	Sonnet Software, Inc.	Detailed Analysis of a High Temperature Superconducting Filter
11:15 am	Stephen Maas	Nonlinear Technologies, Inc.	Broadband Planar Monolithic Balanced Mixers and Frequency Multipliers
12:15	Lunch		
1:15 pm	Joe Staudinger	Motorola Semiconductor Products Sector	Behavioral Analysis Methods Applied to the Design and Simulation of Linear Power Amplifiers
2:15 pm	David Root	Hewlett-Packard Company	Elements of Measurement-Based Large-Signal Device Modeling
3:15 pm	Break		
3:30 pm	Thomas Brazil	University College Dublin	High-Frequency CAD - The Key to Success in Wireless Design
4:30 pm	Question and Answer Session		

Microwave Network Theory and VNA Calibration

Jeffrey A. Jargon
RF Technology Division
National Institute of Standards and Technology
Boulder, CO 80303 USA
TEL: 303-497-3596 | FAX: 303-497-3970 | E-Mail: jjargon@nist.gov

RAWCON '98 Sunday Workshop
August 9, 1998
Modeling and Simulation of Devices and Circuits for Wireless Communication Systems

Outline

- Introductory Remarks
- Microwave Circuit Theory
- Network Parameters
- Vector Network Analyzers
- Concluding Remarks
- References

Introductory Remarks

- Definition of a Linear Network.
- Role of Measurements in CAD.
- Importance of Vector Measurements.

Linear Networks

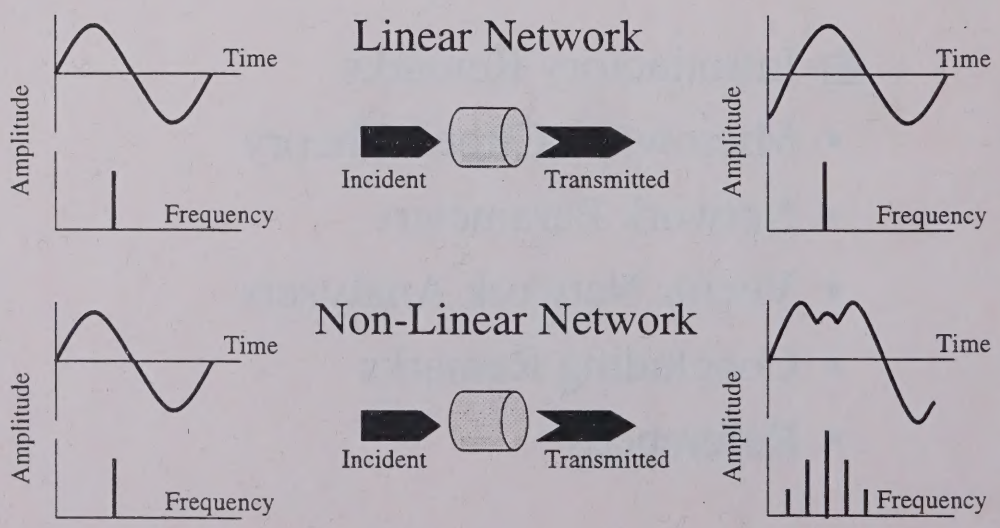

Role of Measurements in CAD

- Electrical CAD is critical to success.
- Measurements are important in two ways:
  - Validate elements that can be accurately modeled.
  - Provide database for elements that cannot be accurately modeled.

The Importance of Vector Measurements

- Complete Characterization of Linear Networks
- Complex Impedance
- Accurate Calibration Procedures
- Transformation to Time Domain

Outline

- Introductory Remarks
- Microwave Circuit Theory
- Network Parameters
- Vector Network Analyzers
- Concluding Remarks
- References

Microwave Circuit Theory

- Circuit Theory Assumptions
- Low-Frequency Circuit Theory
- Conventional Microwave Circuit Theory
- General Microwave Circuit Theory
- Fundamental Parameters
- Transmission Line Equivalent Circuit

Circuit Theory Assumptions

- The circuit is linear.
- The circuit is an interconnection of *n*-port components which interact only at the ports.
- The circuit behavior can be predicted solely from knowledge of these parameters.

Two Forms of Circuit Theory

Low-Frequency

- Applies to circuits much smaller than a wavelength.
- E-field line integral is virtually independent of path, thus voltage is well-defined.
- Fundamental quantities are voltage and current.
- Impedance parameters relate *v* and *i*.

Microwave

- Circuits may be much larger than a wavelength.
- E-field line integral depends on path, thus voltage is not well-defined.
- Uniform transmission lines are assumed.
- Fundamental quantities are modal wave amplitudes.
- Scattering parameters are primary, while impedance parameters are defined in terms of S-parameters.

Conventional Microwave Circuit Theory

Assumptions:

- Mode fields *et* and *ht* are real.
- Wave impedance η is constant.
- Characteristic impedance *Zo* is arbitrary but real.

Assumptions based on:

- Lossless conductors (loss included as perturbation).
- TE, TM, or TEM modes.

General Microwave Circuit Theory

Inhomogeneous Transmission Line Cross Section

- Hybrid modes (not TE, TM, or TEM).
- Common in planar structures.

Lossy Conductors

- Skin depth may be large compared to metals.
- Problem at low frequencies.
- Common in planar structures.

Complex Characteristic Impedance

Fundamental Parameters

Electrical Parameters:

- γ : **Propagation Constant** - signal distortion, loss, and delay.
- Z_o : **Characteristic Impedance** - signal reflection, circuit compatibility.

Physical Parameters:

- C, G : **capacitance** and **conductance** per unit length - material parameters of dielectric substrate.
- L, R : **inductance** and **resistance** per unit length - material parameters of conductors.

Transmission Line Equivalent Circuit

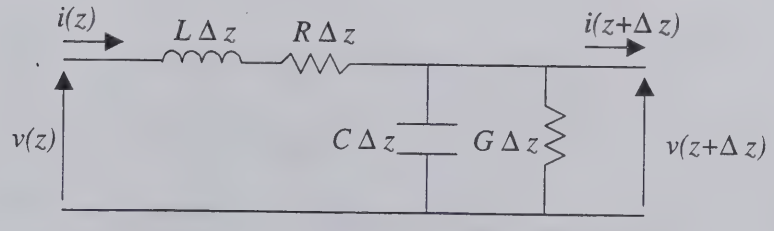

$$\frac{\gamma}{Z_o} = j\omega C + G \qquad \gamma Z_o = j\omega L + R$$

$$\gamma = \sqrt{(j\omega L + R)(j\omega C + G)} \qquad Z_o = \sqrt{(j\omega L + R)/(j\omega C + G)}$$

Characteristic Impedance of a CPW Line

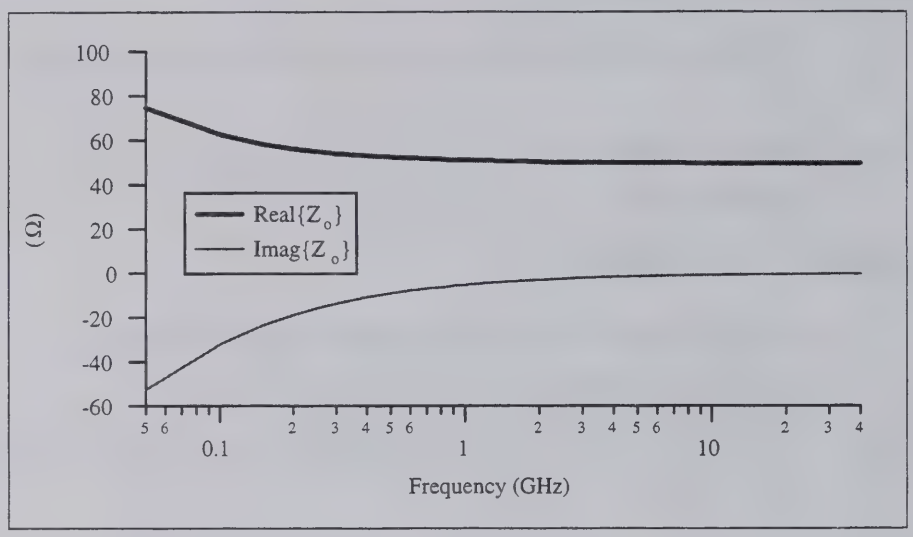

Resistance and Inductance of a CPW Line

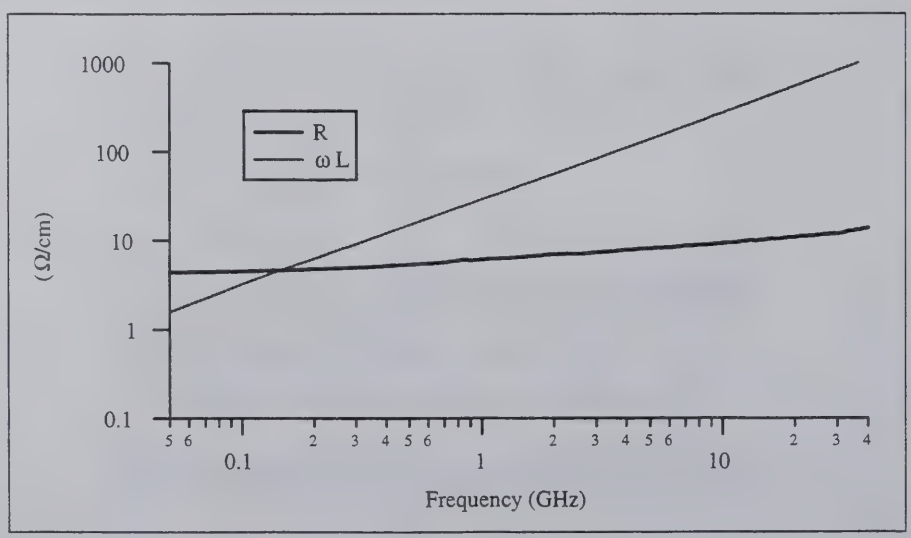

Outline

- Introductory Remarks
- Microwave Circuit Theory
- Network Parameters
- Vector Network Analyzers
- Concluding Remarks
- References

Network Parameters

- Scattering Parameters
- Traveling Waves
- Pseudo-Waves

Using S-Parameters

- At high frequencies, S-parameters are measured since it is difficult to measure total voltage or current.
- S-parameters are ratios of traveling waves.
- They are relatively easy to measure.
- They relate to common measurements such as reflection coefficient, insertion loss, and gain.
- S-parameters can be cascaded for multiple devices to predict system performance.
- They can be converted into Y and Z parameters.
- They are convenient for use with CAD programs.

Two-Port S-Parameters

Forward

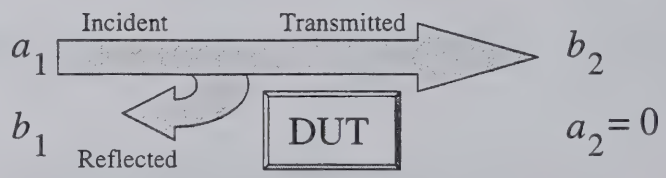

$$S_{11} = \frac{\text{Reflected}}{\text{Incident}} = \frac{b_1}{a_1} \Big| \; a_2 = 0 \qquad S_{21} = \frac{\text{Transmitted}}{\text{Incident}} = \frac{b_2}{a_1} \Big| \; a_2 = 0$$

Reverse

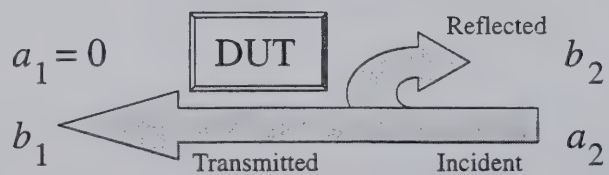

$$S_{12} = \frac{\text{Transmitted}}{\text{Incident}} = \frac{b_1}{a_2} \Big| \; a_1 = 0 \qquad S_{22} = \frac{\text{Reflected}}{\text{Incident}} = \frac{b_2}{a_2} \Big| \; a_1 = 0$$

S-Parameters in Matrix Form

$$\mathbf{b} = \mathbf{S}\,\mathbf{a} \qquad \begin{bmatrix} b_1 \\ b_2 \end{bmatrix} = \begin{bmatrix} S_{11} & S_{12} \\ S_{21} & S_{22} \end{bmatrix} \begin{bmatrix} a_1 \\ a_2 \end{bmatrix}$$

Traveling Waves

Traveling waves a_o and b_o:

$$a_o = \frac{\sqrt{\mathrm{Re}\{p_o\}}}{2v_o}(v + iZ_o) \qquad b_o = \frac{\sqrt{\mathrm{Re}\{p_o\}}}{2v_o}(v - iZ_o)$$

Power in terms of traveling waves:

$$P = |a_o|^2 - |b_o|^2 + 2\,\mathrm{Im}\{a_o b_o^*\}\frac{\mathrm{Im}\{Z_o\}}{\mathrm{Re}\{Z_o\}}$$

Pseudo-Waves

Pseudo-waves a and b are mathematical artifacts:

$$a(Z_{ref}) = \frac{|v_o|\sqrt{\mathrm{Re}\{Z_{ref}\}}}{v_o \quad 2|Z_{ref}|}(v + iZ_{ref})$$

$$b(Z_{ref}) = \frac{|v_o|\sqrt{\mathrm{Re}\{Z_{ref}\}}}{v_o \quad 2|Z_{ref}|}(v - iZ_{ref})$$

Power in terms of pseudo-waves:

$$P = |a|^2 - |b|^2 + 2\,\mathrm{Im}\{ab^*\}\frac{\mathrm{Im}\{Z_{ref}\}}{\mathrm{Re}\{Z_{ref}\}}$$

Scattering and Pseudo-Scattering Matrices

Scattering Matrix S^o

$$\mathbf{b}_o = \mathbf{S}^o\mathbf{a}_o \qquad \begin{bmatrix} b_{o1} \\ b_{o2} \end{bmatrix} = \begin{bmatrix} S^o_{11} & S^o_{12} \\ S^o_{21} & S^o_{22} \end{bmatrix}\begin{bmatrix} a_{o1} \\ a_{o2} \end{bmatrix}$$

Pseudo-Scattering Matrix S

$$\mathbf{b} = \mathbf{S}\,\mathbf{a} \qquad \begin{bmatrix} b_1 \\ b_2 \end{bmatrix} = \begin{bmatrix} S_{11} & S_{12} \\ S_{21} & S_{22} \end{bmatrix}\begin{bmatrix} a_1 \\ a_2 \end{bmatrix}$$

Outline

- Introductory Remarks
- Microwave Circuit Theory
- Network Parameters
- Vector Network Analyzers
- Concluding Remarks
- References

Vector Network Analyzers

- Architecture of Vector Network Analyzers.
- Calibration Function and Procedure.
- On-Wafer Calibration Issues.
- Verification Techniques.
- Time Domain Network Analysis.

VNA Block Diagram

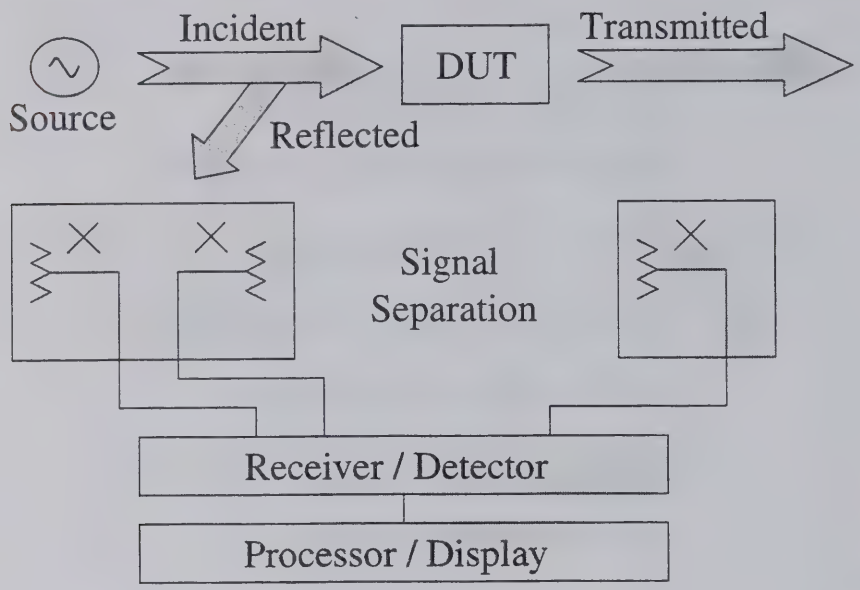

Three-Sampler VNA Diagram

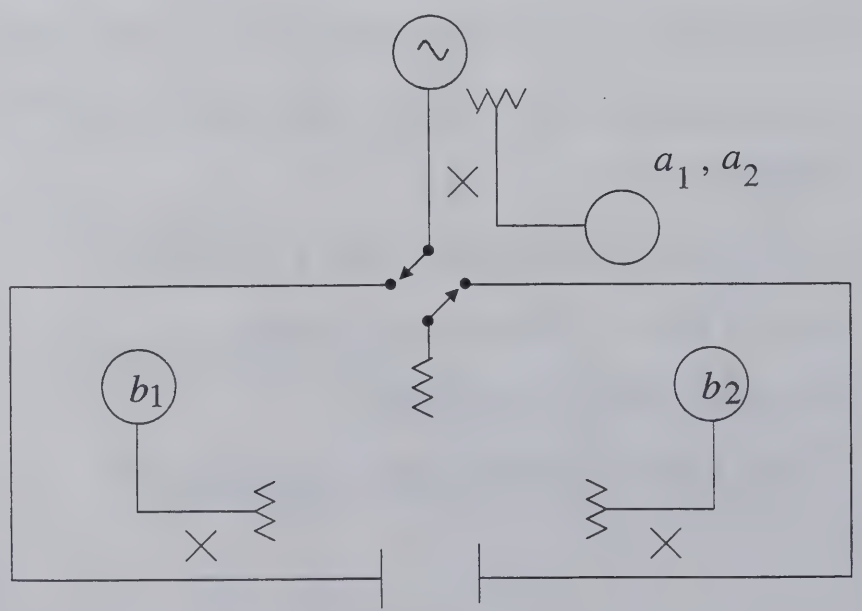

Four-Sampler VNA Diagram

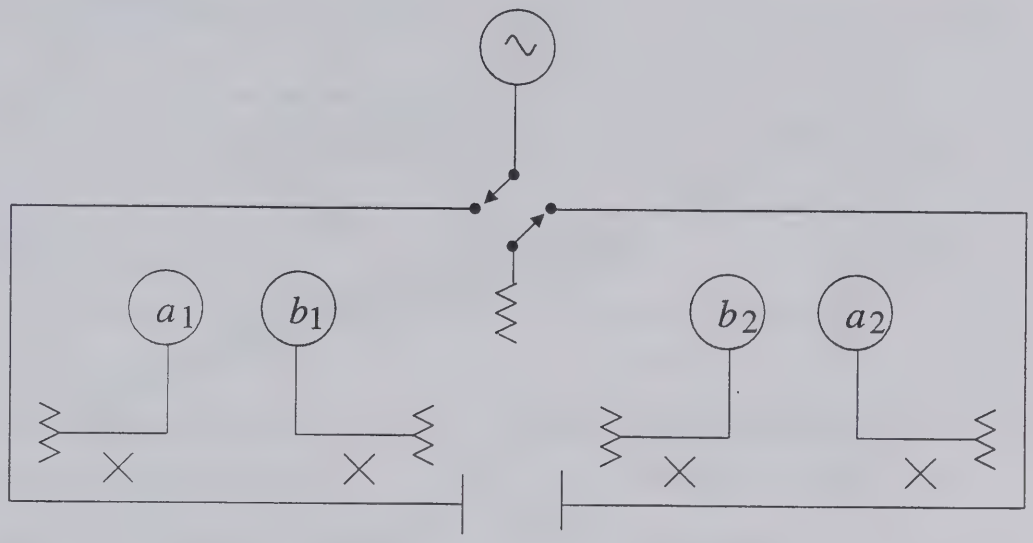

VNA Calibration: Function

- Accounts for serious imperfections in the network analyzer:
  - Directivity and crosstalk errors due to signal leakage.
  - Impedance mismatches in the source, receiver, and load.
  - Frequency response errors in the source and receiver.
  - Losses in the cables and connectors.

- Does not account for:
  - System drift.
  - Repeatability in the switches and connectors.
  - Instrument noise.
  - Errors in calibration standards.

Importance of Calibration

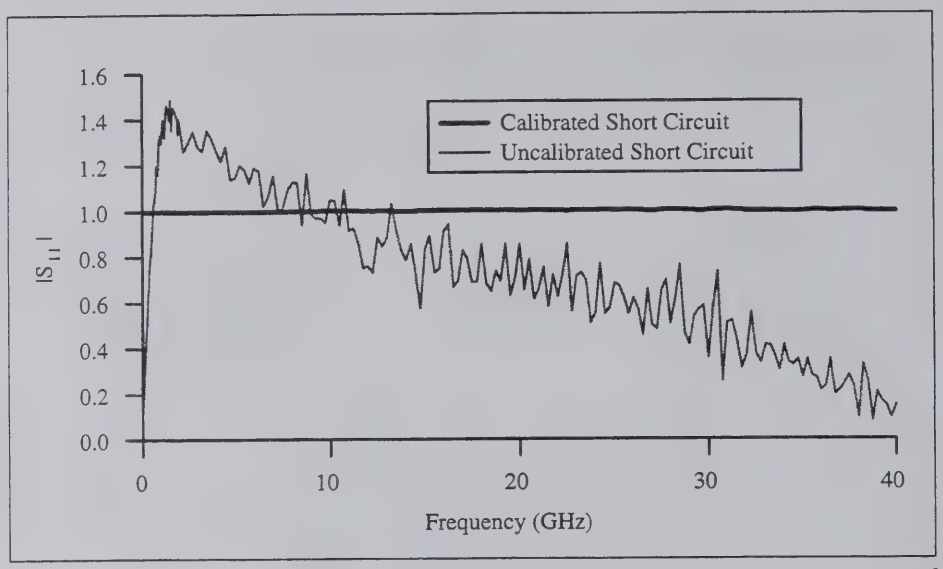

VNA Calibration: Procedure

Procedure:

- Measure known standards.
- Process data to determine error coefficients.
- Correct measured data for device under test.

Methods:

- Lumped-element standards (OSLT, LRM).
- Transmission line standards (TRL, Multiline TRL).
- Electronic transfer standards.

VNA 12-Term Error Model

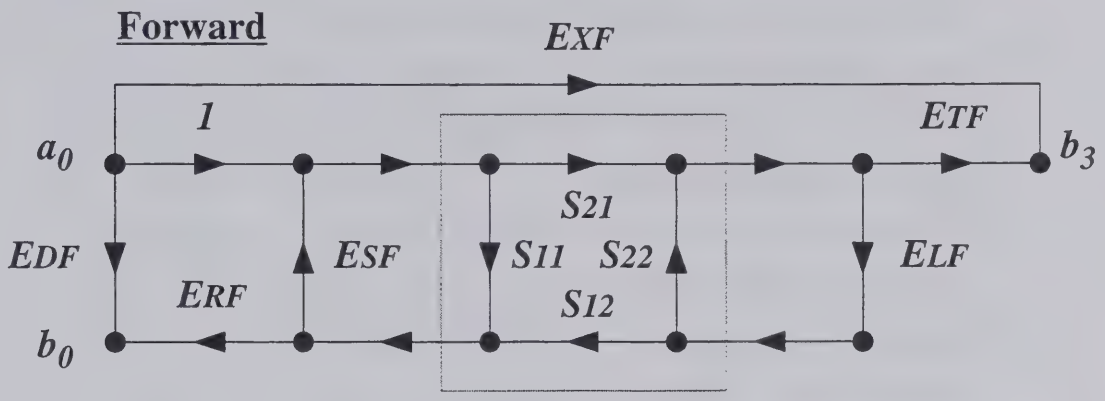

EDF = Directivity
ESF = Port 1 Match
ERF = Reflection Tracking
ETF = Transmission Tracking
ELF = Port 2 Match
EXF = Leakage

VNA 12-Term Error Model

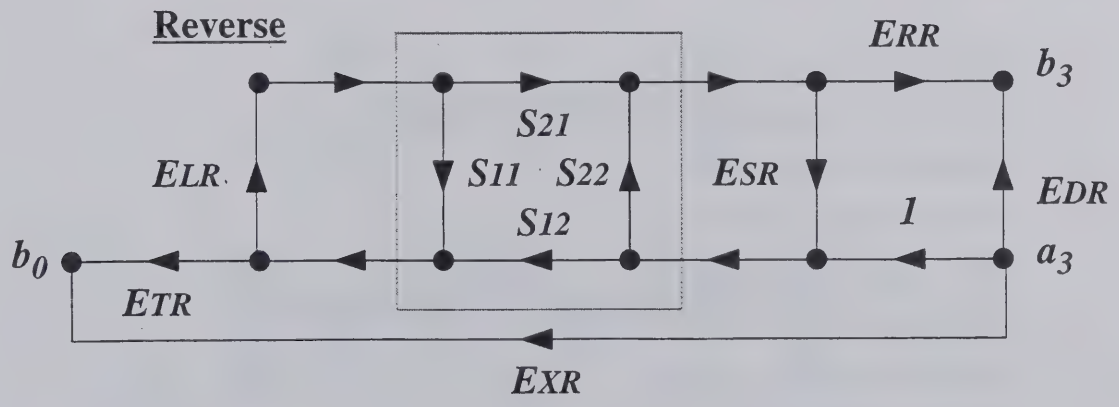

EDR = Directivity
ELR = Port 1 Match
ERR = Reflection Tracking
ETR = Transmission Tracking
ESR = Port 2 Match
EXR = Leakage

OSLT Calibration

- Most popular form of VNA calibration.
- Primarily used in coaxial environments.
- Uses lumped-elements.
- Originally intended for three-sampler VNAs.
- Variations are possible for four-samplers VNAs.

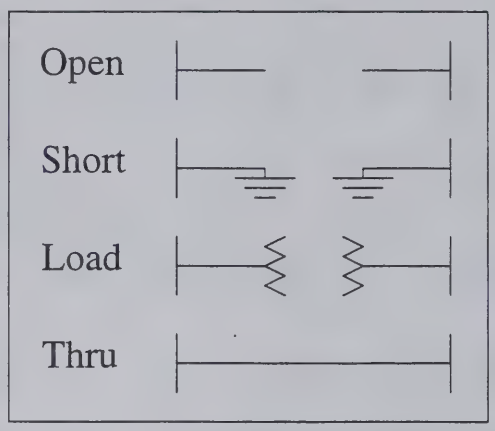

TRL Calibration

- Next most common form of VNA calibration.
- Primarily used in non-coaxial environments.
- Uses transmission lines as standards.
- Requires a four-sampler VNA architecture.
- Variations are possible for three-sampler VNAs.

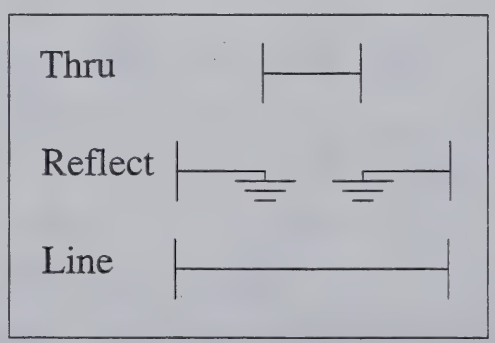

On-Wafer Calibration Issues

- Known load impedances are rare on planar structures.
- Known reflection coefficients are rare, except for transmission lines which have no reflection.
- On-wafer calibration:
  - Custom calibration standards correspond to DUT.
  - Calibrate out effect of transition and contact.
  - Accurately set reference plane and reference impedance.
- Off-wafer (probe-tip) calibration:
  - Generic, commercial calibration standards.
  - Ignore effect of transition and contact.
  - Reference plane confined to the probe tip.

Multiline TRL Calibration

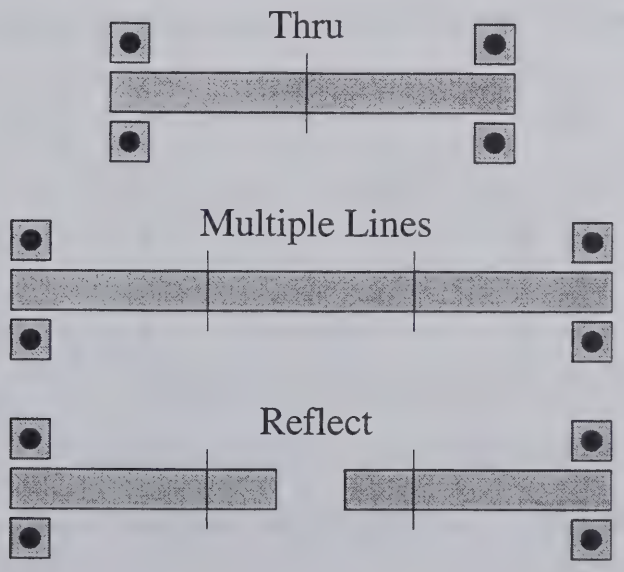

Multiline TRL Calibration

- Calibration standards are transmission lines.
- Standards are custom, and also large and numerous.
- Broadband.
- Accurately determines S-parameters.
- Accurately determines propagation constant, which allows the reference plane to be set and moved.
- Reference impedance is equal to the characteristic impedance of the line.
  - Can't measure pseudo-scattering parameters (i.e., 50 Ω).
  - Can't measure impedance parameters.

Measuring Characteristic Impedance

$$\frac{\gamma}{Z_o} \equiv j\omega C + G$$

$$Z_o = \frac{\gamma}{j\omega C + G}$$

Often, $j\omega C + G$ can be estimated.

When the dielectric loss is very low, then $j\omega C + G \approx j\omega C_{dc}$

Full Electrical Characterization

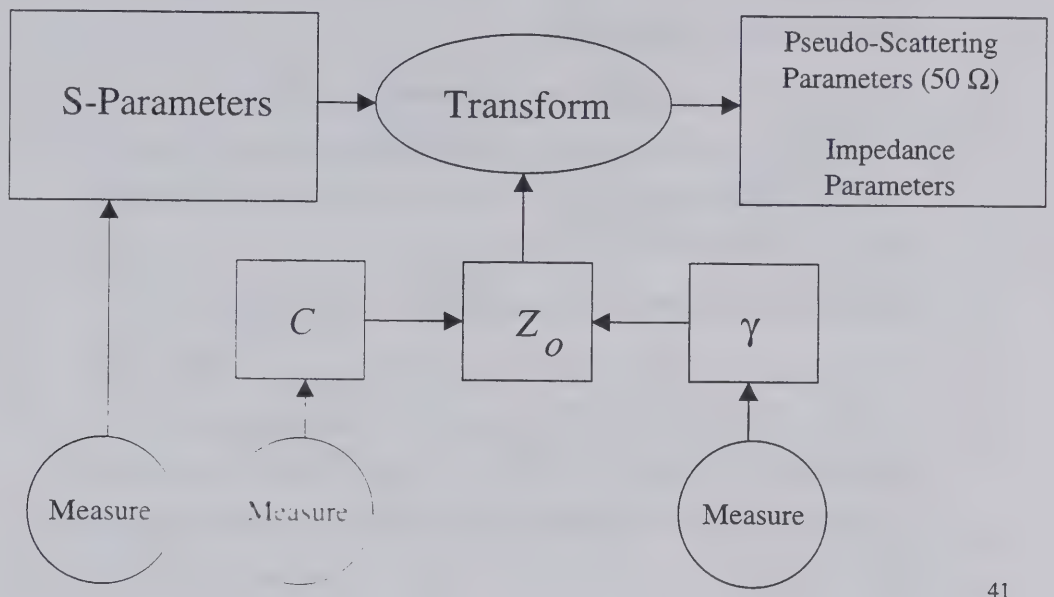

Comparing Calibrations

	OSLT	TRL	Multiline TRL
Small Cal. Set	yes	yes	no
Easy to Implement	yes	yes	no
Broadband	yes	no	yes
Commercially Available	yes	yes	no
Resetable Reference Impedance and Plane	no	no	yes
Complete Transmission Line Characterization	no	no	yes

Verification Techniques

Calibration Comparison

Two similar or different calibrations are performed on one VNA, and the error coefficients are compared to estimate the magnitude of the maximum differences in the S-parameters.

Network Analyzer Comparison

Verification devices are measured on two calibrated VNAs, and then the S-parameters are compared individually for each device, or the S-parameters are compared for an ensemble of devices to obtain a worst case bound.

Calibration Comparison Example

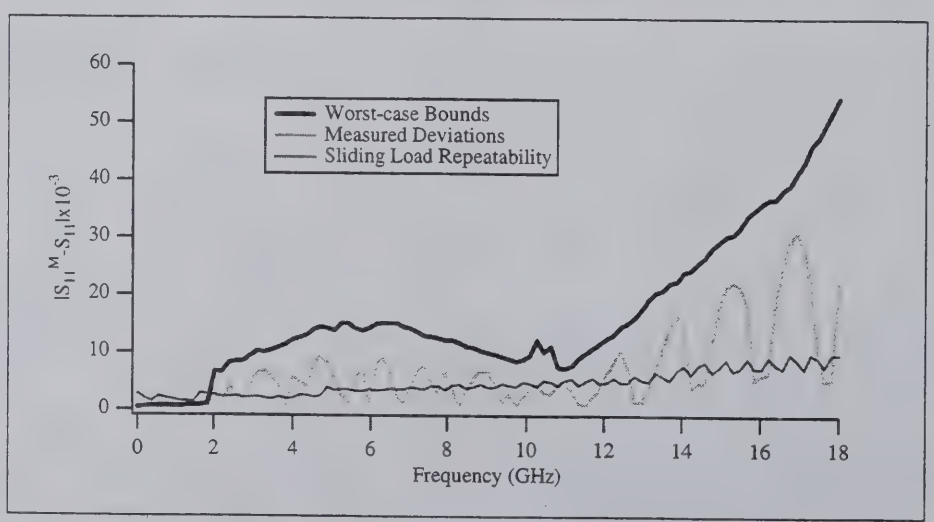

Worst-case error bounds and measured deviations for S11 between an OSLT calibration and a sliding load calibration.

VNA Comparison Example

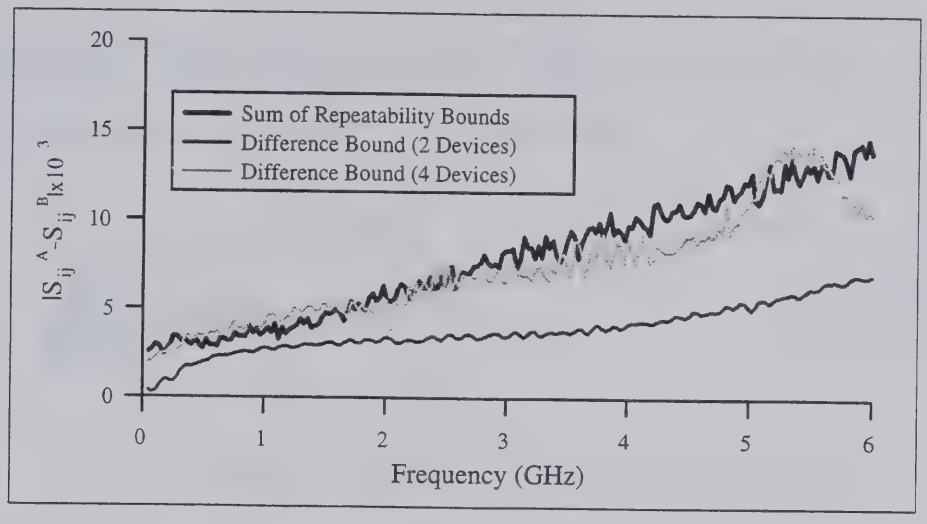

Comparison of a three-sampler VNA to a four-sampler VNA. Both VNAs calibrated using OSLT with identical standards.

Time Domain Network Analysis

- TDNA is the acquisition of frequency-domain network parameters using a digital sampling oscilloscope with time-domain reflection/transmission (TDR/T) capabilities.
- This is done by calibrating Fourier-transformed TDR/T waveforms using conventional VNA error models and calibration methods.
- The significance of TDNA is that it allows laboratories that already own lower priced oscilloscopes to make accurate frequency-domain measurements.
- The accuracy of TDNA measurements depend on the oscilloscope's settings, drift, jitter, time base distortion, voltage distortion, etc.

TDNA Measurement Example

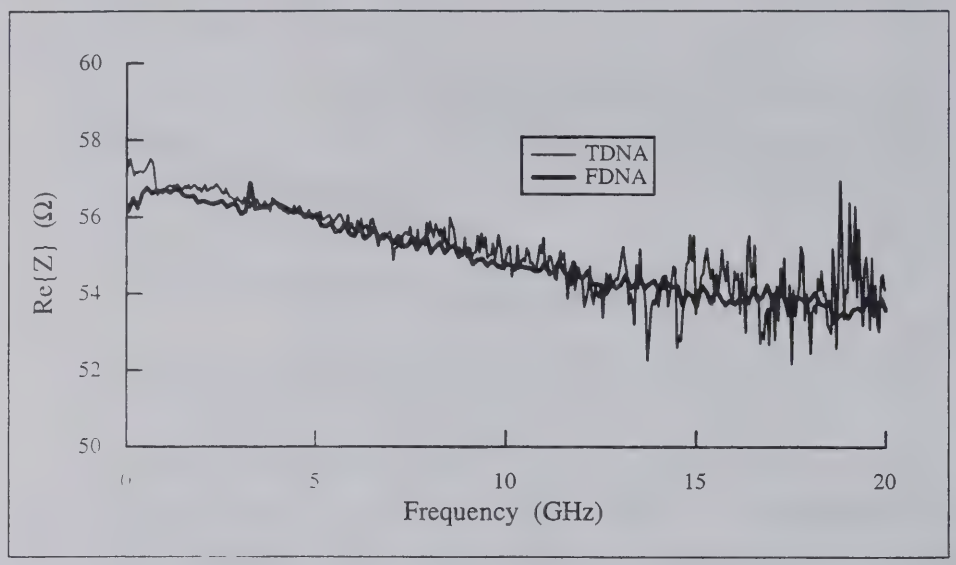

Outline

- Introductory Remarks
- Microwave Circuit Theory
- Network Parameters
- Vector Network Analyzers
- ▶ Concluding Remarks
- References

Concluding Remarks

Linear measurements are difficult especially when the following are present:

- Hybrid modes
- Lossy conductors
- Lossy substrates
- Complex characteristic impedance
- More than two ports

The Nonlinear Challenge

- To characterize a nonlinear device, one usually measures one or more of the following parameters: load pull, spectral regrowth, third order intercept point, adjacent channel power ratio, and 1 dB compression point.
- All of these parameters come from the same nonlinear behavior, although they are difficult to compare and correlate.
- Our goal: A general nonlinear network analyzer for measuring weakly nonlinear devices.

Outline

- Introductory Remarks
- Microwave Circuit Theory
- Network Parameters
- Vector Network Analyzers
- Concluding Remarks
- References

References, Part 1

General Waveguide Circuit Theory

R.B. Marks and D.F. Williams, "A General Waveguide Circuit Theory," *Journal of Research of the National Institute of Standards and Technology* 97, pp. 533-562, Sep.-Oct. 1992.

Fundamentals of Network Analysis

"Understanding the Fundamental Principles of Vector Network Analysis, Hewlett-Packard Application Note 1287-1, May 1997.

"Exploring the Architecture of Network Analyzers," Hewlett-Packard Application Note 1287-2, May 1997.

Network Analyzer Calibration

R.B. Marks, "Formulations of the Basic Vector Network Analyzer Error Model including Switch Terms," *50th ARFTG Conference Digest*, pp. 115-126, Dec. 1997.

"Applying Error Correction to Network Analyzer Measurements," Hewlett-Packard Application Note 1287-3, May 1997.

D. Rytting, "Network Analyzer Error Models and Calibration Methods," *RF & Microwave Measurements for Wireless Applications* (ARFTG/NIST Short Course Notes), Dec. 1996.

References, Part 2

R.B. Marks, J.A. Jargon, and D.K. Rytting, "Accuracy of Lumped-Element Calibrations for Four-Sampler Vector Network Analyzers," IEEE MTT-S International Microwave Symposium Digest, pp. , Jun. 1998.

G.F. Engen and C.A. Hoer, "Thru-Relect-Line: An Improved Technique for Calibrating the Dual Six-Port Automatic Network Analyzer," *IEEE Transactions on Microwave Theory and Techniques*, vol. 27, pp. 987-993, Dec. 1979.

H.J. Eul and B. Schiek, "A Generalized Theory and New Calibration Procedures for Network Analyzer Self-Calibration," *IEEE Transactions on Microwave Theory and Techniques*, vol. 39, pp. 724-731, Apr. 1991

R.B. Marks, "A Multiline Method of Network Analyzer Calibration," *IEEE Transactions on Microwave Theory and Techniques*, vol. 39, pp. 1205-1215, Jul. 1991.

K.J. Silvonen "A General Approach to Network Analyzer Calibration," *IEEE Transactions on Microwave Theory and Techniques*, vol. 40, pp. 754-759, Apr. 1992.

J.A. Jargon and R.B. Marks, "Two-Tier Multiline TRL for Calibration of Low-Cost Network Analyzers," 46th ARFTG Conference Digest, pp. 1-8, Dec, 1995.

References, Part 3

Measuring Characteristic Impedance and Capacitance

R.B. Marks and D.F. Williams, "Characteristic Impedance Determination using Propagation Constant Measurement," *IEEE Microwave and Guided Wave Letters* 1, pp. 141-143, Jun. 1991.

D.F. Williams and R.B. Marks, "Transmission Line Capacitance Measurement," *IEEE Microwave and Guided Wave Letters* 1, pp. 243-245, Sep. 1991.

VNA and Calibration Comparisons

D.F. Williams, R.B. Marks, and A. Davidson, "Comparison of On-Wafer Calibrations," *38th ARFTG Conference Digest*, pp. 68-81, Dec. 1991.

R.B. Marks, J.A. Jargon, and J.R. Juroshek, "Calibration Comparison Method for Vector Network Analyzers," *48th ARFTG Conference Digest*, pp. 38-45, Dec. 1996.

D.C. DeGroot, R.B. Marks, and J.A. Jargon, "A Method for Comparing Vector Network Analyzers," *50th ARFTG Conference Digest*, pp. 107-114, Dec. 1997.

J.R. Juroshek, C.M. Wang, and G.P. McCabe, "Statistical Analysis of Network Analyzer Measurements," *Cal Lab*, pp. 26-33, Jun. 1998.

References, Part 4

Time-Domain Network Analysis

T. Dhaene, L. Martens, and D. De Zutter, "Calibration and Normalization of Time Domain Network Analyzer Measurements, *IEEE Transactions on Microwave Theory and Techniques*, vol. 41, pp. 415-420, Mar. 1993.

R.B. Marks, L.A. Hayden, J.A. Jargon, and F. Williams, "Time Domain Network Analysis Using Multiline TRL Calibration," 44th ARFTG Conference Digest, pp. 47-55, Dec. 1994.

D.C DeGroot and R.B. Marks, "Optimizing Time-Domain Network Analysis," 46th ARFTG Conference Digest, pp. 19-28, Nov. 1995.

Nonlinear Network Analyzers

U. Lott, "Measurement of Magnitude and Phase of Harmonics Generated in Nonlinear Microwave Two-Ports," *IEEE Transactions on Microwave Theory and Techniques*, vol. 38, pp. 358-365, Apr. 1990.

J. Verspecht, "Calibration of a Measurement System for High Frequency Nonlinear Devices," Ph.D. Thesis, Vrije Universiteit Brussel, Spe. 1995.

AMP M/A-COM

Stability Analysis of Linear Circuits

Wayne Struble

M/A-COM

Integrated Semiconductor Business Unit

Abstract

- The purpose of this presentation is to show a method of determining the stability (or instability) of linear, passively terminated, multiport networks from the normalized network determinant function (NDF).
- This method is rigorous and can be calculated within commercially available steady-state circuit simulators.

Outline

AMP M/A-COM

- Background on stability concepts
- Normalized Determinant Function (NDF)
- Use and calculation of the NDF
- Calculating the NDF from return ratios
- A ring oscillator example
- Single active element example
- Libra implementation for MESFETs and PHEMTs
- NDF guidelines

BACKGROUND

Background

AMP M/A-COM

- Most GaAs MMIC designers use the well known Linvill or Rollett stability criteria (C or K) to determine the stability of linear two-port networks. This procedure is WRONG!
- Platzker et al. have shown that a separate test is required to determine the stability of the network; i.e. test for the existence of any zeroes of the network determinant in the right half plane (RHP), before the Linvill or Rollett stability criteria can be applied.

Background

AMP M/A-COM

- The network is stable if and only if no zeroes of the full network determinant exist in the RHP. If any zeroes do exist in the RHP, the network is unstable. This is RIGOROUS!
- Platzker's test applies the Principle of the Argument theorem to a normalized network determinant function (NDF) to determine the number of zeroes in the RHP of the full network determinant (and thus poles of the network).

WHAT IS THE NDF?

What is the NDF

- Platzker's normalized network determinant function NDF is simply the full network determinant, including all port terminations, divided by the resulting passive network determinant when all dependent sources (i.e. N voltage controlled or current controlled sources) contained within the network are set equal to zero.

$$\mathrm{NDF} = \frac{\Delta}{\Delta_{0N}}$$

What is the NDF

AMP M/A-COM

- Note that any linear network parameters such as Y, Z, H etc. can be used to calculate the above determinants.
- Δ_{0N} represents the determinant of a passive network and cannot contain any zeroes in the RHP. Therefore, zeroes in the RHP of the NDF correspond to zeroes in the RHP of the full network determinant.

AMP M/A-COM

HOW IS THE NDF USED TO DETERMINE STABILITY?

Using the NDF

AMP M/A-COM

- To determine stability, the complex quantity NDF is calculated for a given network along the frequency axis ζ from $+\clock$ to $-\clock$ and its locus is plotted in the complex plane.
- If the locus of the NDF encircles the origin (0,0) in a counterclockwise direction, the network determinant contains zeroes in the RHP. The number of encirclements is equal to the number of zeroes in the RHP.

Using the NDF

AMP M/A-COM

- A clockwise encirclement of the origin is not possible by construction of the NDF.
- This NDF test can be used on any physically realizable, passively terminated, linear multiport network.

AMP M/A-COM

HOW IS THE NDF CALCULATED?

Calculating the NDF

AMP M/A-COM

- Using the brute force approach, the NDF can be found by calculating the full network determinants Δ and Δ_{0N} at each frequency ζ.
- A faster approach to calculating the NDF is to first reduce the network to a parallel connection of two networks, one totally passive and one totally active.

Calculating the NDF

AMP M/A-COM

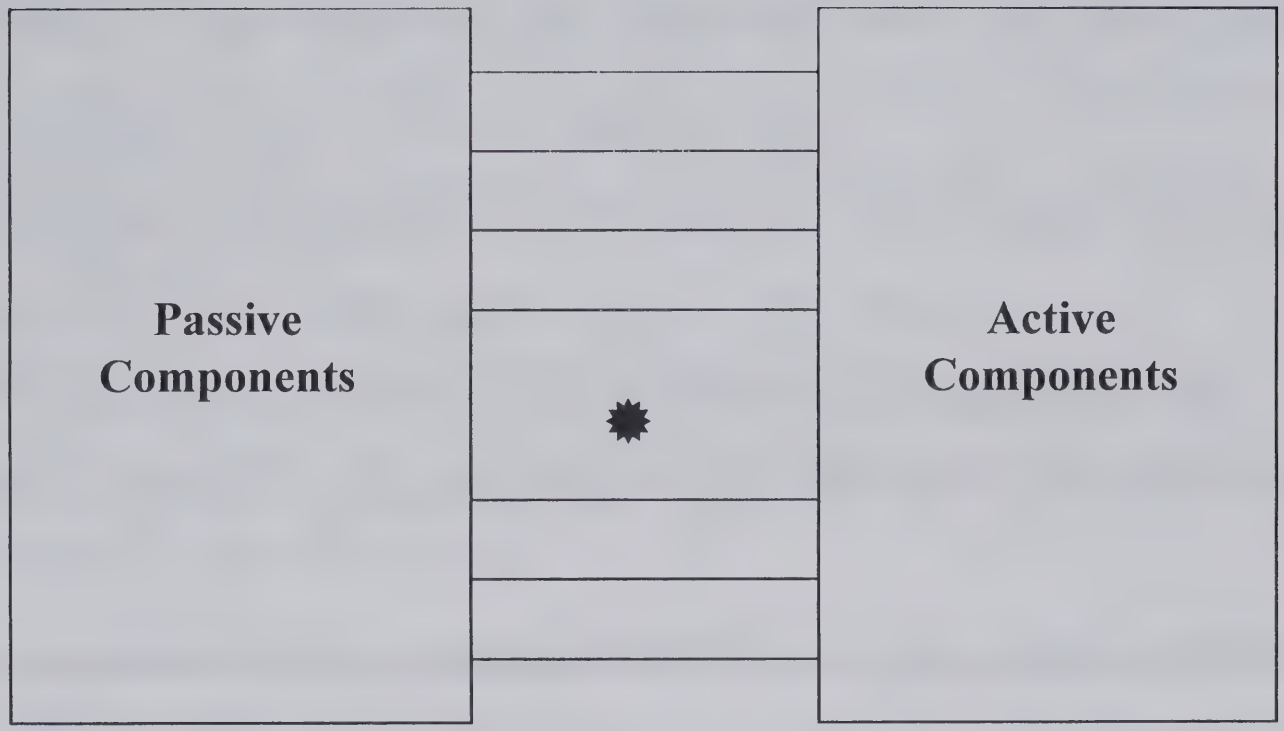

Calculating the NDF

AMP M/A-COM

- This reduces the number of nodes in the network, and thus the sizes of the relevant matrices, to between two and four times the number of dependent sources contained in the network (2N-4N) depending on connectivity.
- The network cannot be reduced any further than this due to the possibility of introducing poles in Δ. This will result in pole-zero cancellation in the NDF.

Calculating the NDF

AMP M/A-COM

- In networks containing more than five dependent sources, direct calculation of the NDF becomes difficult using commercially available circuit simulators.
- This is due to the limitation in the sizes of matrices that can be saved by the simulators for external calculations.
- Also, calculation of the NDF inside a circuit simulator is desirable since it allows for sensitivity analysis or optimization.

Calculating the NDF

AMP M/A-COM

- To this end, I have derived an alternative way of easily calculating the NDF within commercial circuit simulators using the concept of Return Ratios.

AMP M/A-COM

A METHOD OF CALCULATING THE NDF USING RETURN RATIOS

NDF from Return Ratios

AMP M/A-COM

- The Return Ratio (RR) of a dependent source was first presented by Bode and is defined as the Return Difference minus one or,

$$\mathbf{RR} \equiv \frac{\Delta}{\Delta_0} - \mathbf{1}$$

- Where Δ is the full network determinant and Δ_0 represents the full network determinant where the dependent source is set equal to zero.

NDF from Return Ratios

AMP M/A-COM

- For networks containing a single dependent source, the Return Ratio is equivalent to the NDF and can be used as a rigorous check for stability.

$$\mathbf{NDF} = \frac{\Delta}{\Delta_{01}} = \mathbf{RR_1} + \mathbf{1}$$

- If the network contains more than one dependent source, Δ_{01} may contain zeroes in the RHP due to other dependent sources, and a single Return Ratio calculation is not sufficient for a rigorous assessment of stability.

NDF from Return Ratios

AMP M/A-COM

- However, the concept can be extended to networks with N dependent sources by rearranging the previous equation into the form,

$$\Delta = (\mathbf{RR_1} + \mathbf{1}) \cdot \Delta_{\mathbf{01}}$$

- and realizing that,

$$\Delta_{\mathbf{01}} = (\mathbf{RR_2} + \mathbf{1}) \cdot \Delta_{\mathbf{02}}$$

- Where RR_2 is the Return Ratio of a second dependent source in the network with the first dependent source set to zero.

NDF from Return Ratios

AMP M/A-COM

- By substituting Δ_{01} into the previous equation,

$$\Delta_{01} = (RR_2 + 1) \cdot \Delta_{02} \qquad \Delta = (RR_1 + 1)(RR_2 + 1) \cdot \Delta_{02}$$

- By continuous substitution,

$$\Delta = (RR_1 + 1)(RR_2 + 1)(RR_3 + 1)\ldots(RR_N + 1) \cdot \Delta_{0N}$$

- or,

$$NDF = (RR_1 + 1)(RR_2 + 1)(RR_3 + 1)\ldots(RR_N + 1)$$

NDF from Return Ratios

AMP M/A-COM

- For each successive Return Ratio calculation RR_i (i = 2-N), the network is physically changed by setting all previous dependent sources to zero.

HOW IS THE RETURN RATIO OF A DEPENDENT SOURCE CALCULATED?

Return Ratio of a Source

AMP M/A-COM

- The Return Ratio of a dependent source embedded within a network is calculated by replacing the dependent source, which is controlled by an internal voltage or current, with an identical source that is controlled by an external voltage or current.
- The stimulus from this new source will result in some amount of feedback to the controlling voltage or current of the original dependent source.

Return Ratio of a Source

AMP M/A-COM

- The negative ratio of the voltage or current returned, to the external voltage or current stimulus, is the Return Ratio of the dependent source.

Return Ratio of a Source

$$RR = \frac{-V_{13}}{V_{ext}}$$

AMP M/A-COM

ORIGINAL NETWORK

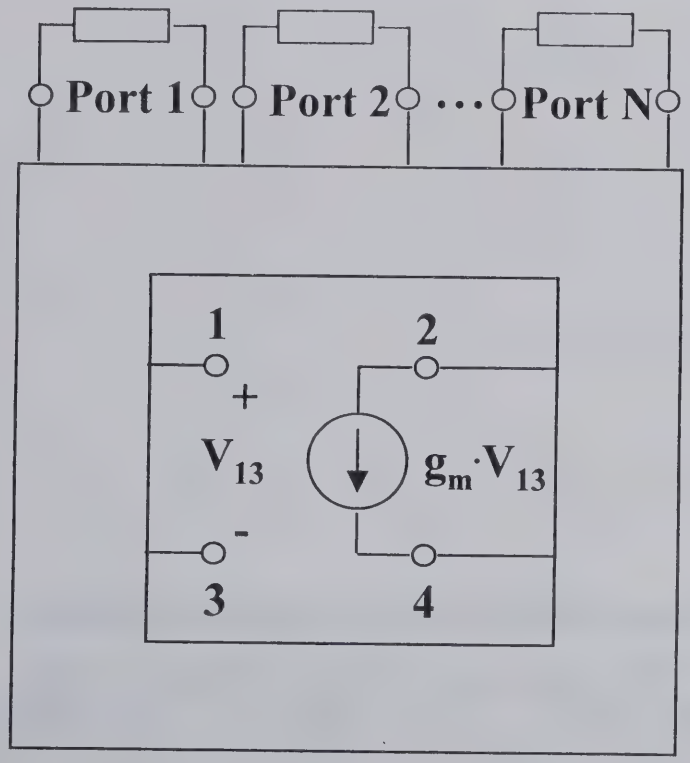

RETURN RATIO NETWORK

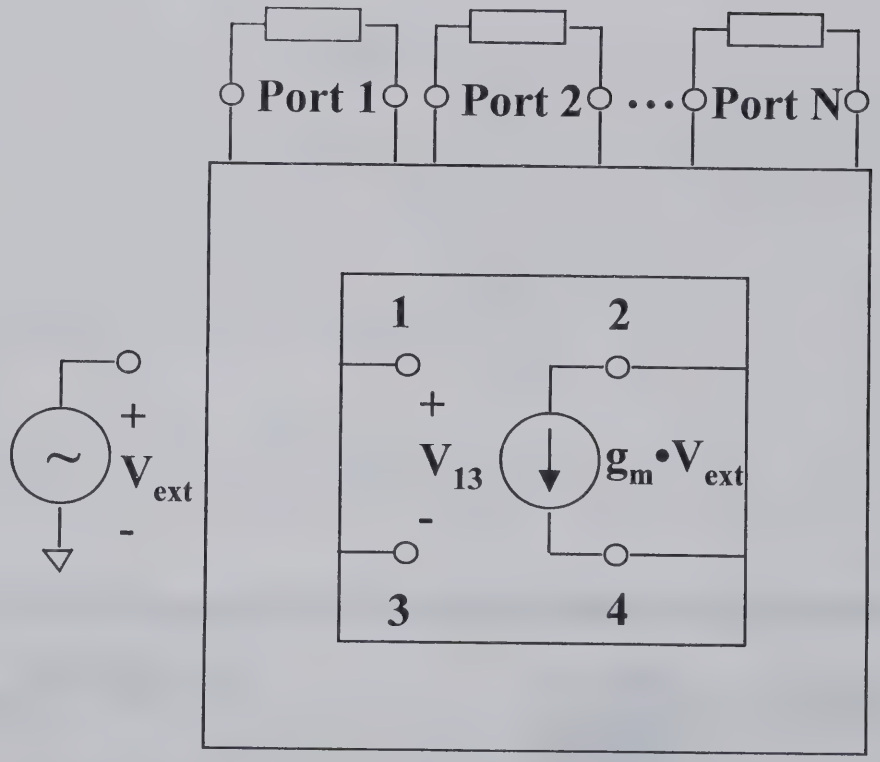

AMP M/A-COM

RING OSCILLATOR EXAMPLE

Ring Oscillator Example

AMP M/A-COM

- The following example is a ring oscillator containing two dependent sources.
- The NDF of the oscillator is calculated from two Return Ratios (one Return Ratio for each dependent source in the network).
- The order of the Return Ratio calculations is unimportant as long as after calculating the Return Ratio of any given dependent source, it is set to zero in the Return Ratio calculations of all following dependent sources.

Ring Oscillator Schematic

AMP M/A-COM

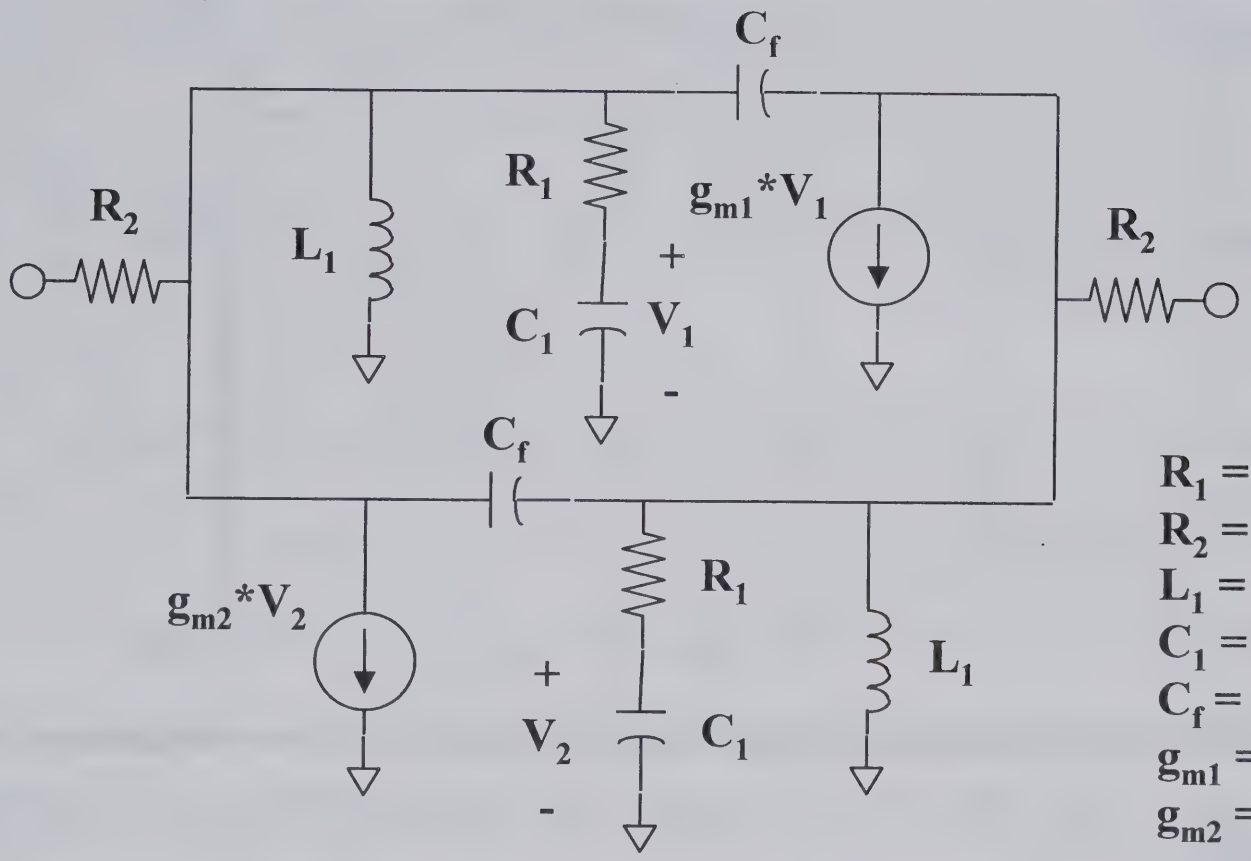

$R_1 = 10\Omega$
$R_2 = 50\Omega$
$L_1 = 560pH$
$C_1 = 16pF$
$C_f = 0.1pF$
$g_{m1} = 500mS$
$g_{m2} = 400mS$

Ring Oscillator k-factor and |S|

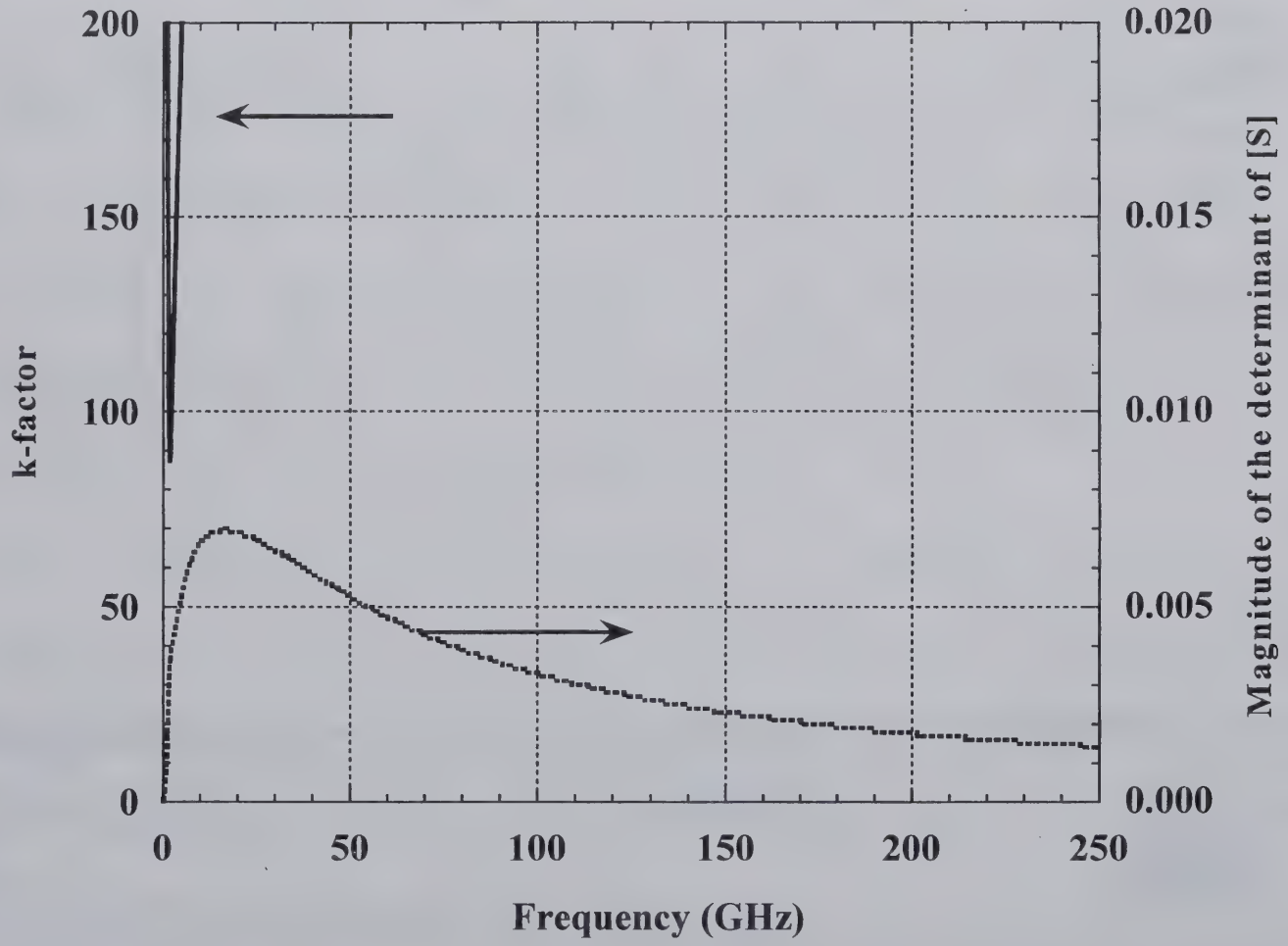

Ring Oscillator k-factor and |S|

AMP M/A-COM

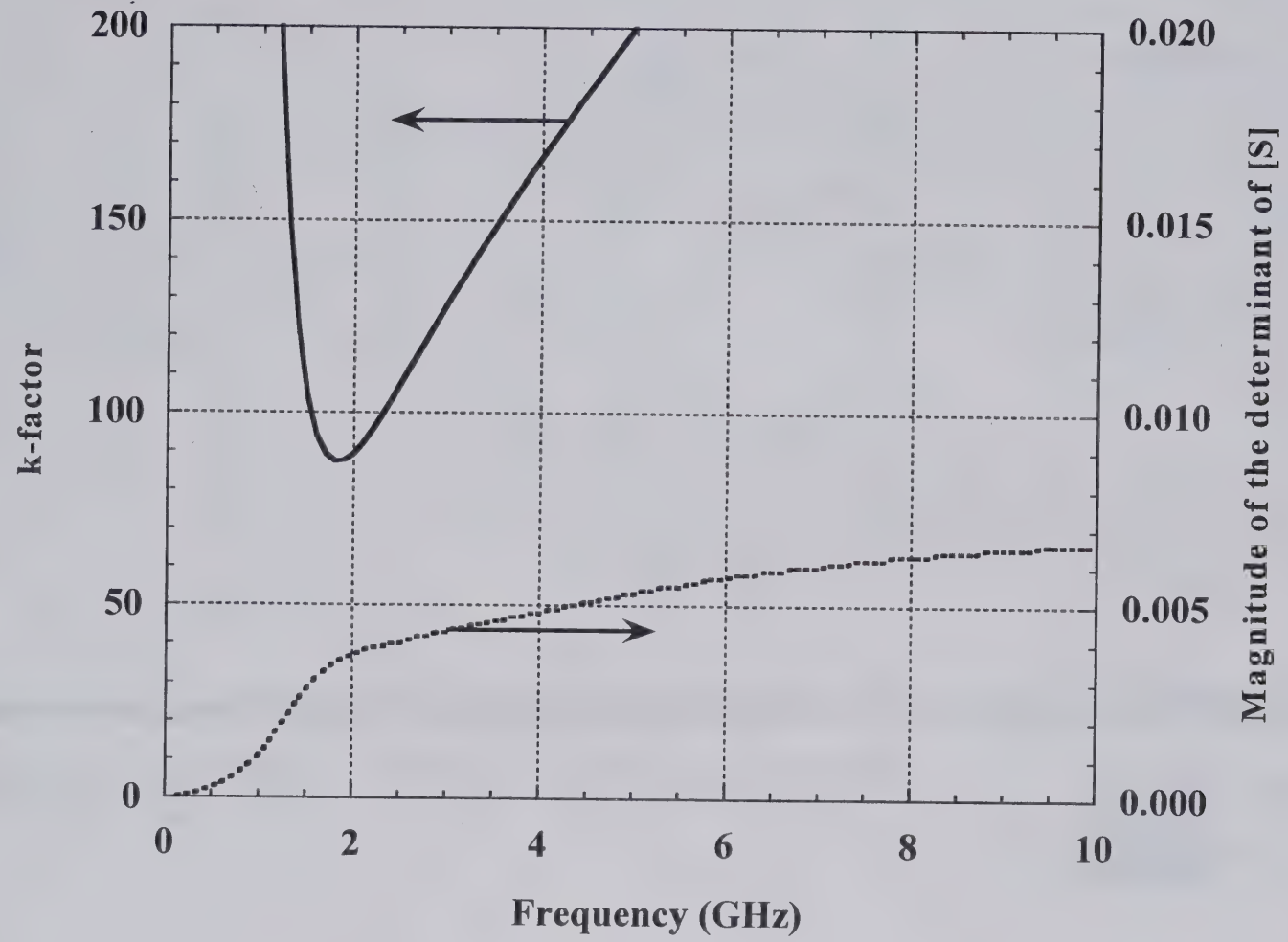

Return Ratio RR_1 Schematic

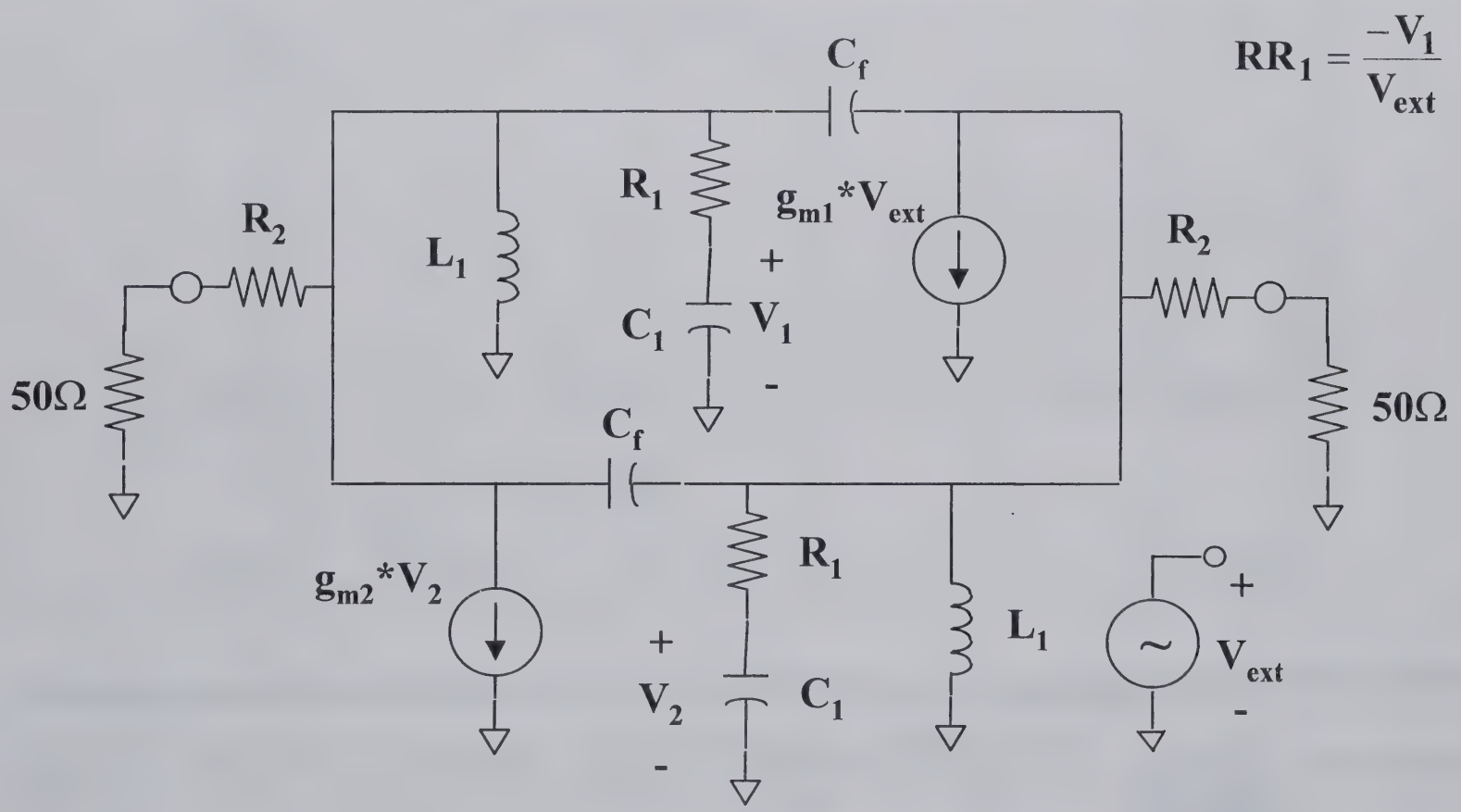

Return Ratio RR_2 Schematic

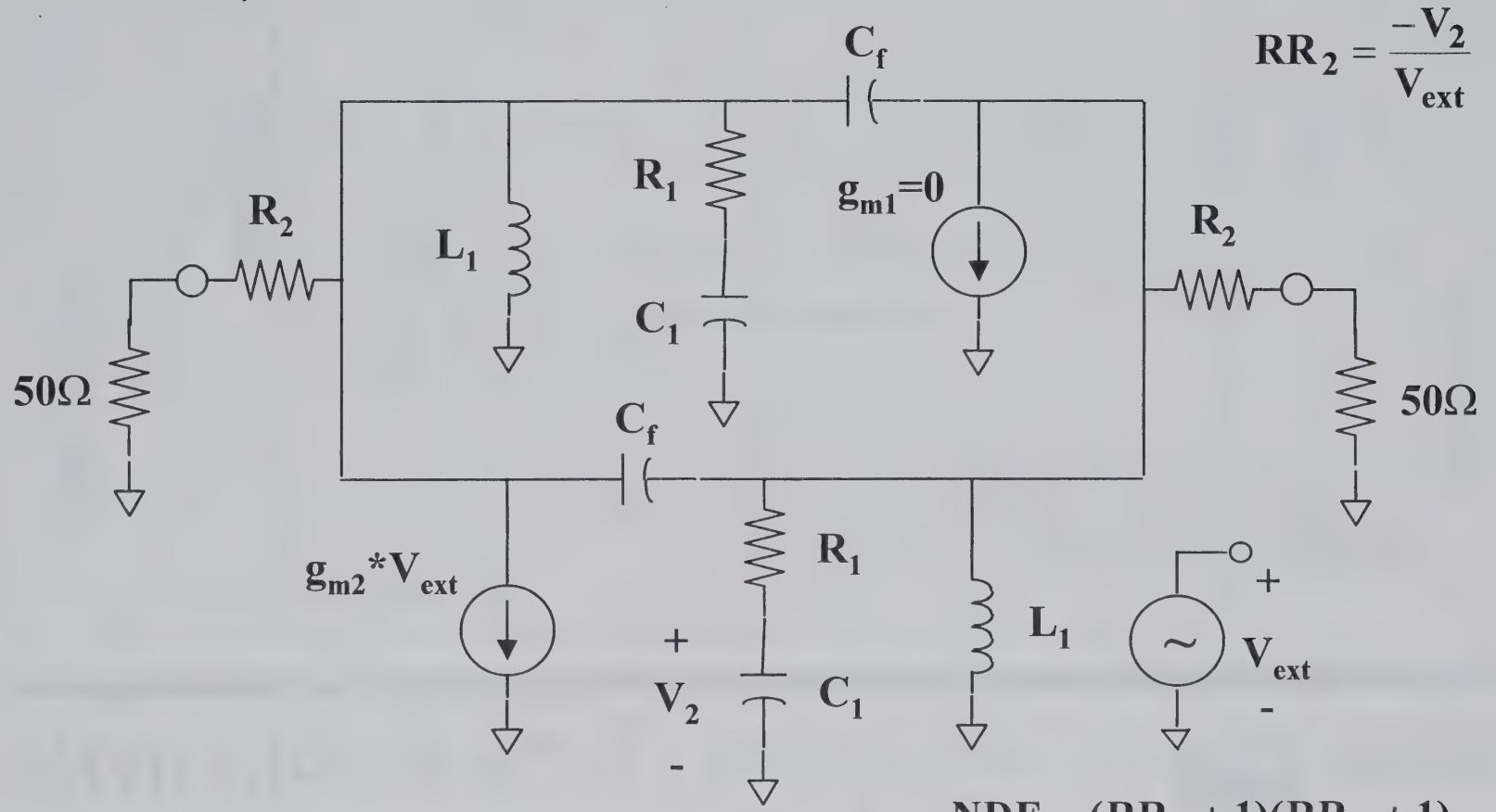

NDF Plot of Ring Oscillator

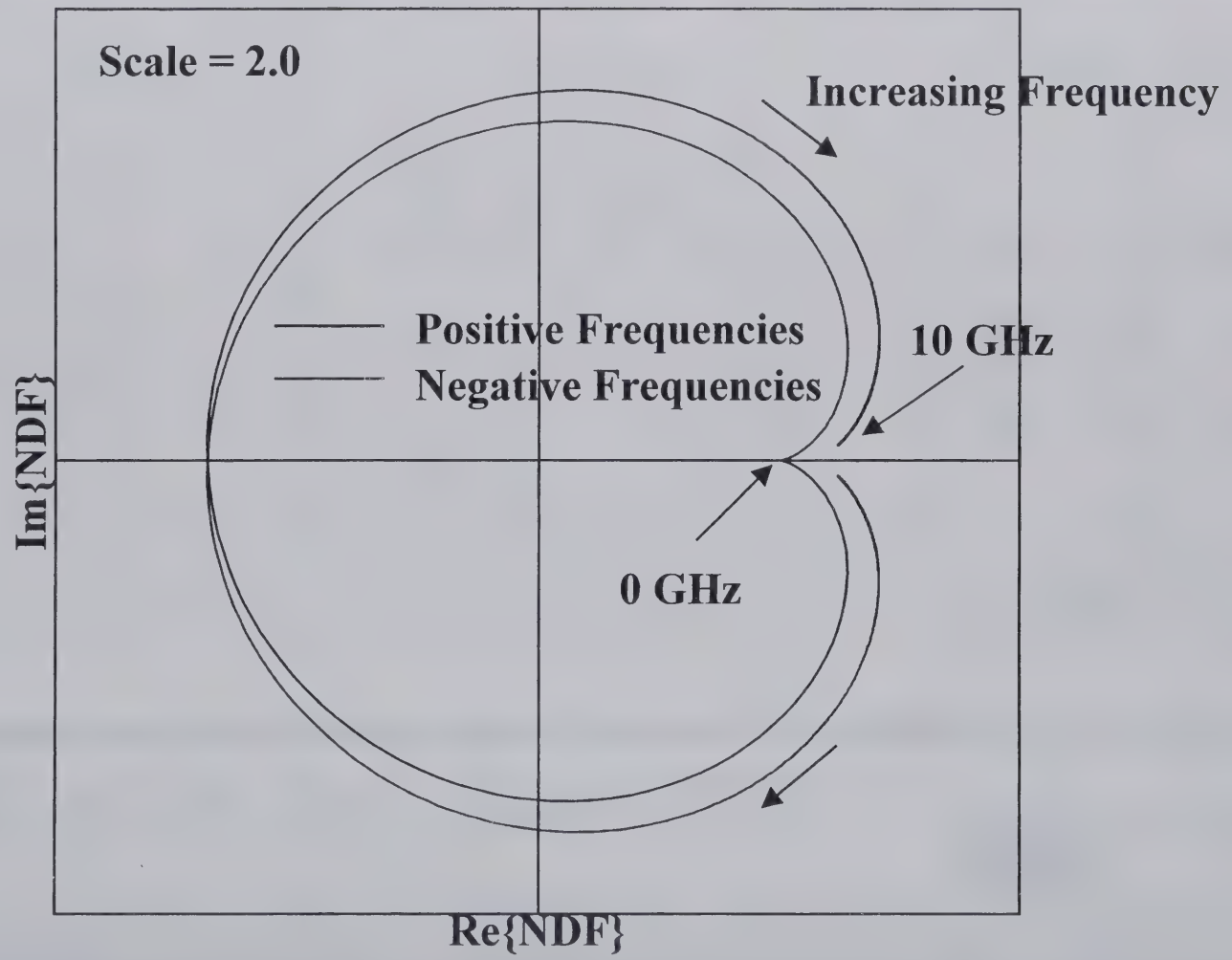

NDF Encirclement Plot

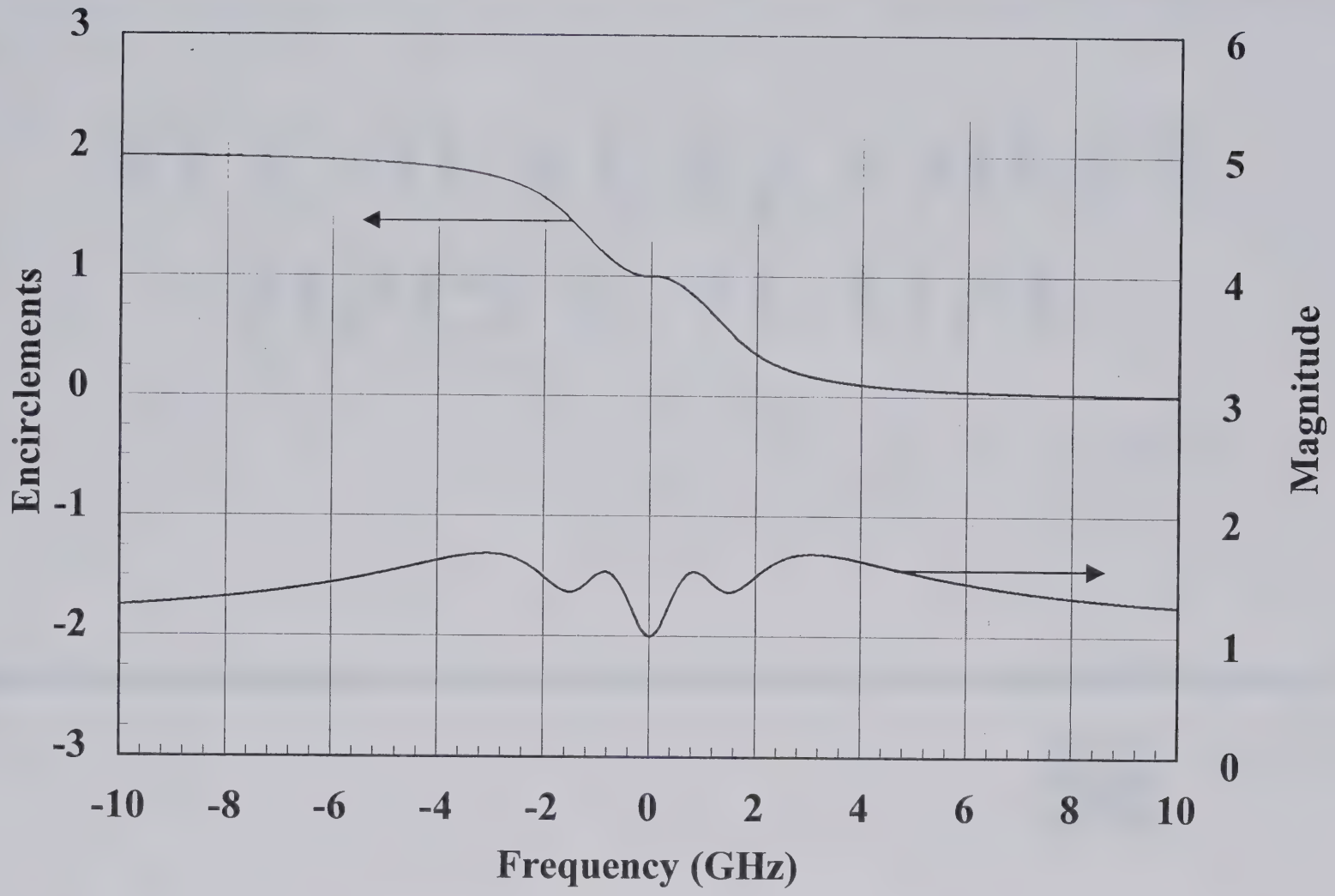

AMP M/A-COM

SINGLE ACTIVE ELEMENT EXAMPLE

Single Active Element Example

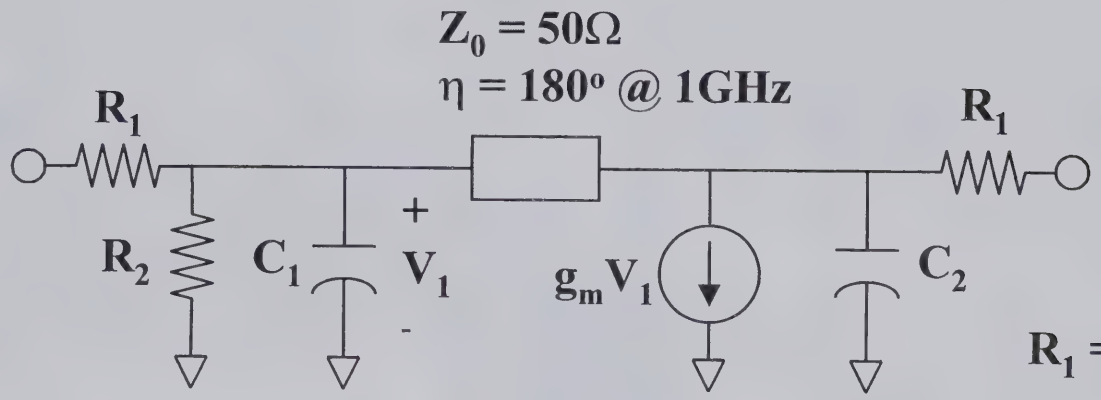

$R_1 = 100\Omega$

$R_2 = 10\Omega$

$C_1 = 0.1pF$

$C_2 = 10pF$

$g_m = 1.0S$

k-factor and |S|

AMP M/A-COM

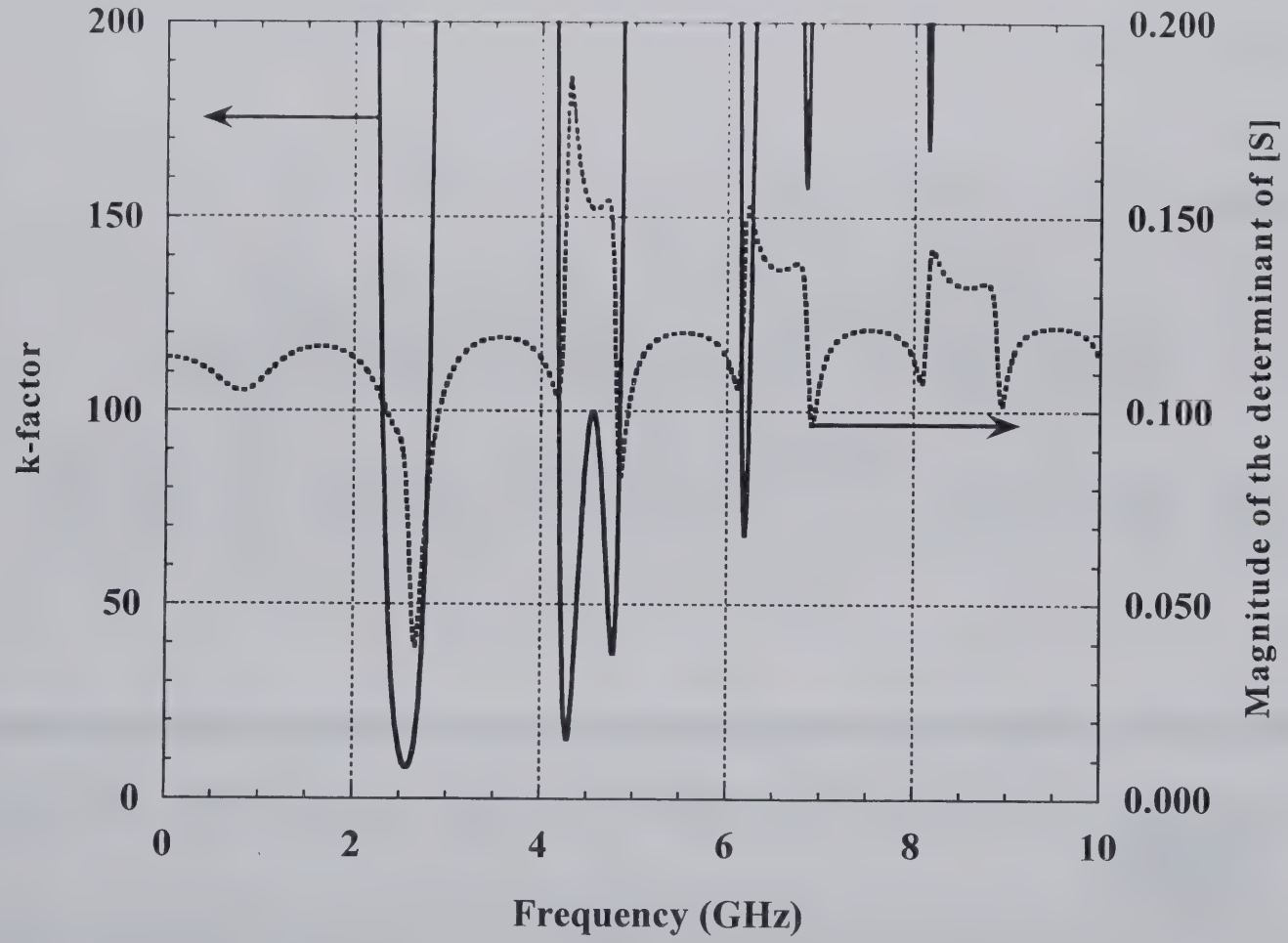

NDF Plot (scale = 10)

AMP M/A-COM

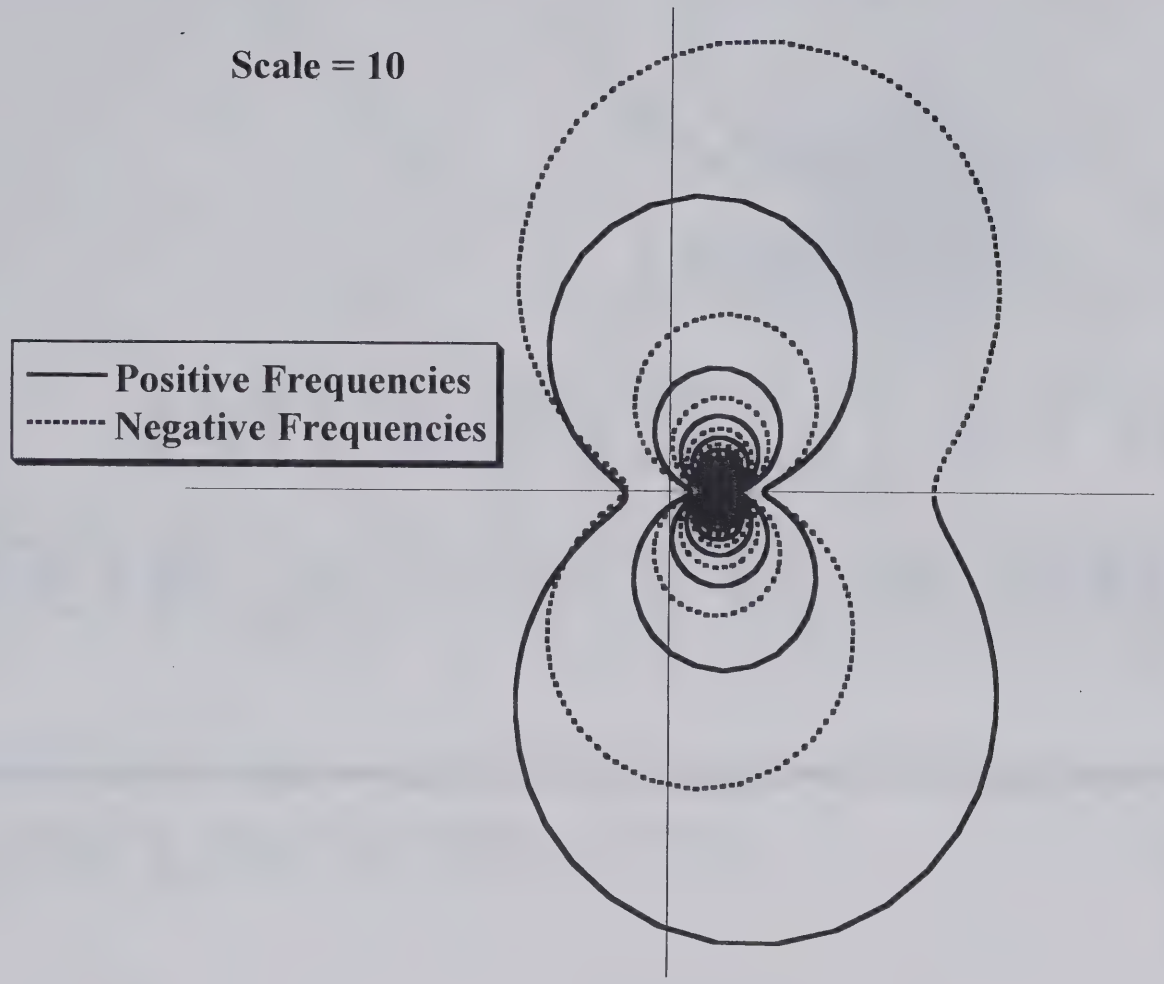

NDF Plot (scale = 2)

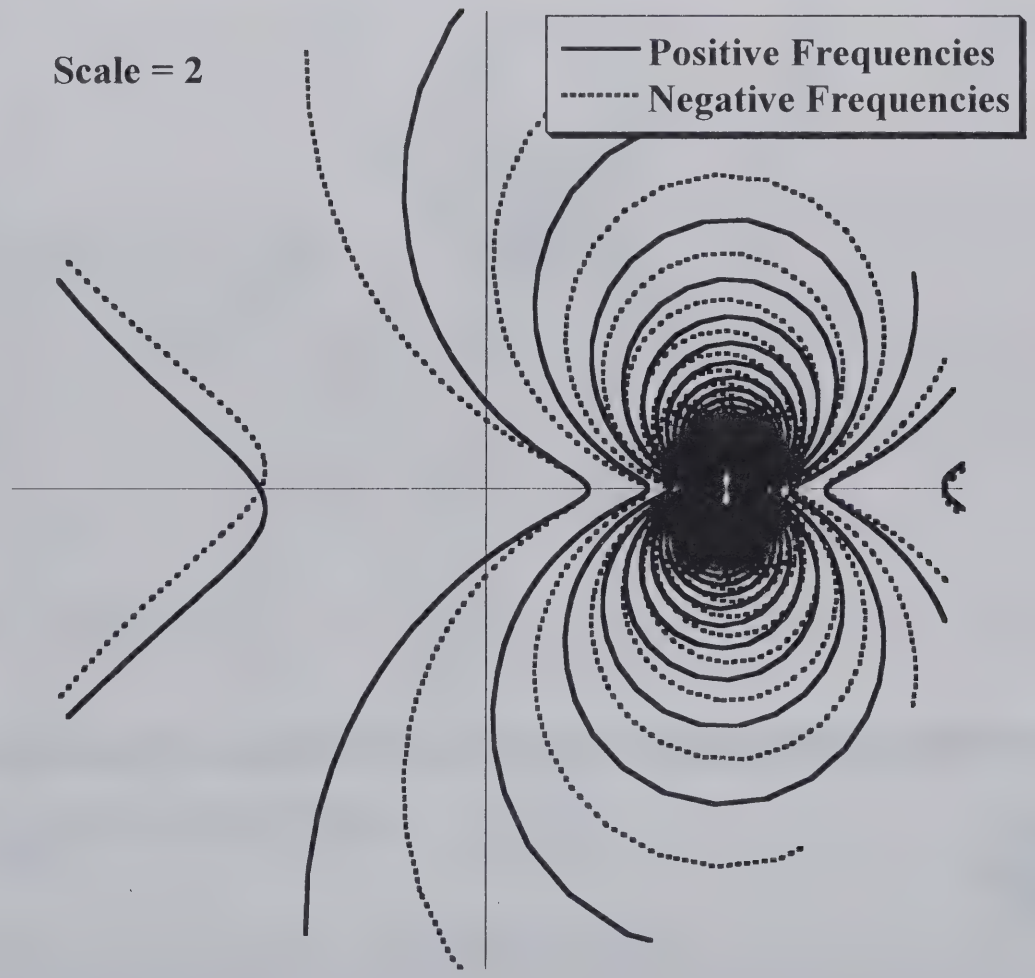

AMP M/A-COM

LIBRA IMPLEMENTATION FOR MESFETs & PHEMTs

Libra DSCR FET Model

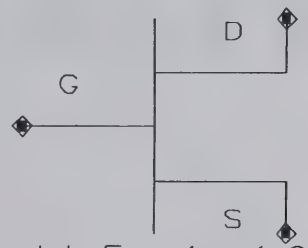

lh5_4x100_lh5_6110452704_dscr
X1
UGW=100
NGF=4
INDEX=1

DSCR FET Schematic

AMP M/A-COM

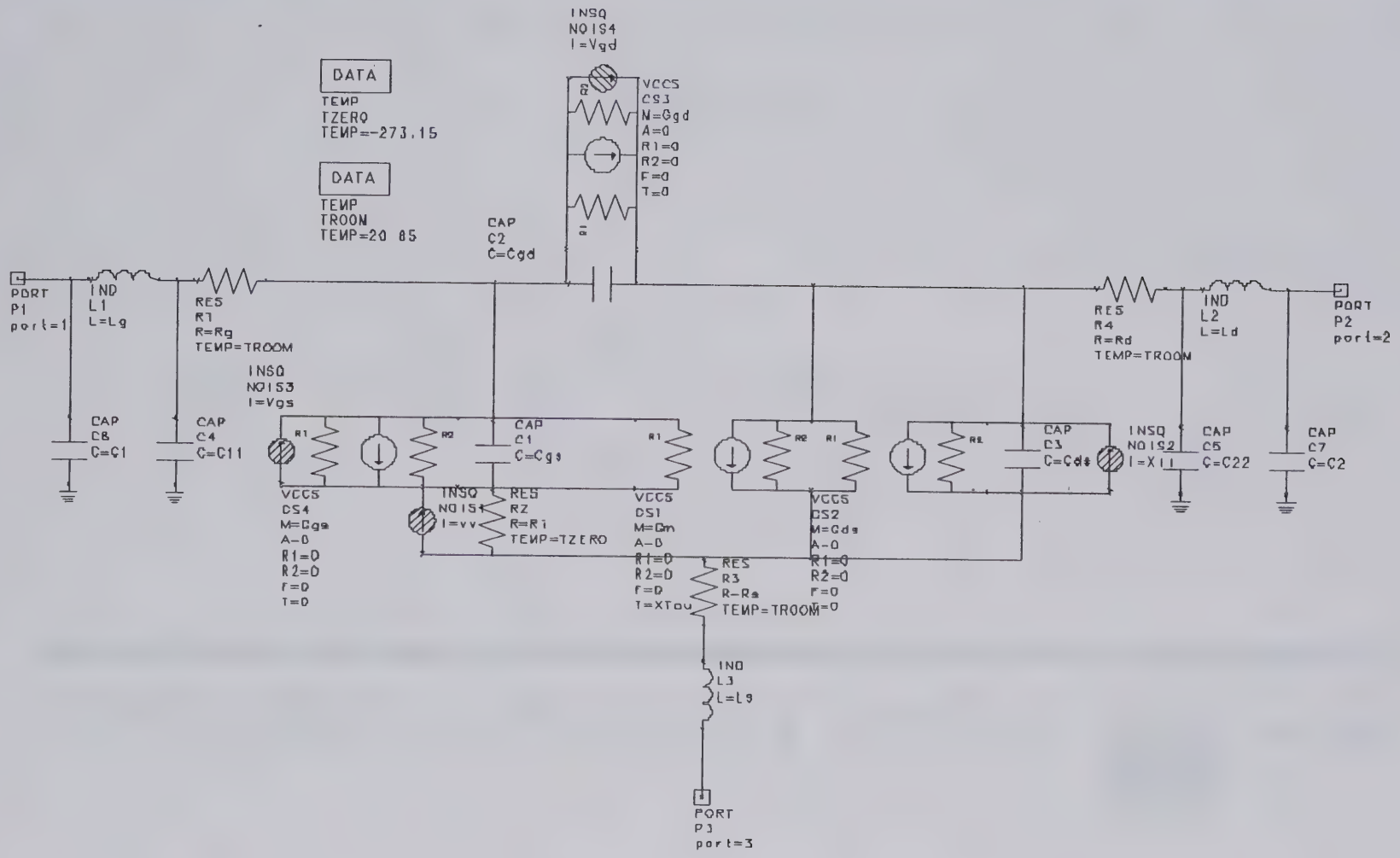

Libra Return Ratio FET Model

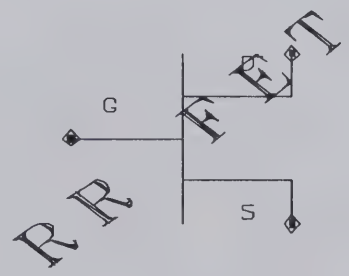

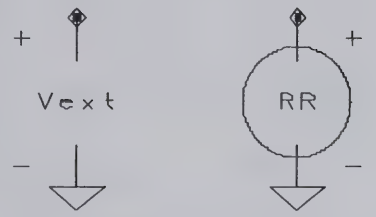

lh5_4x100_lh5_6110452704_rrfet
X1
UGW=100
NGF=4
INDEX=1

Return Ratio FET Schematic

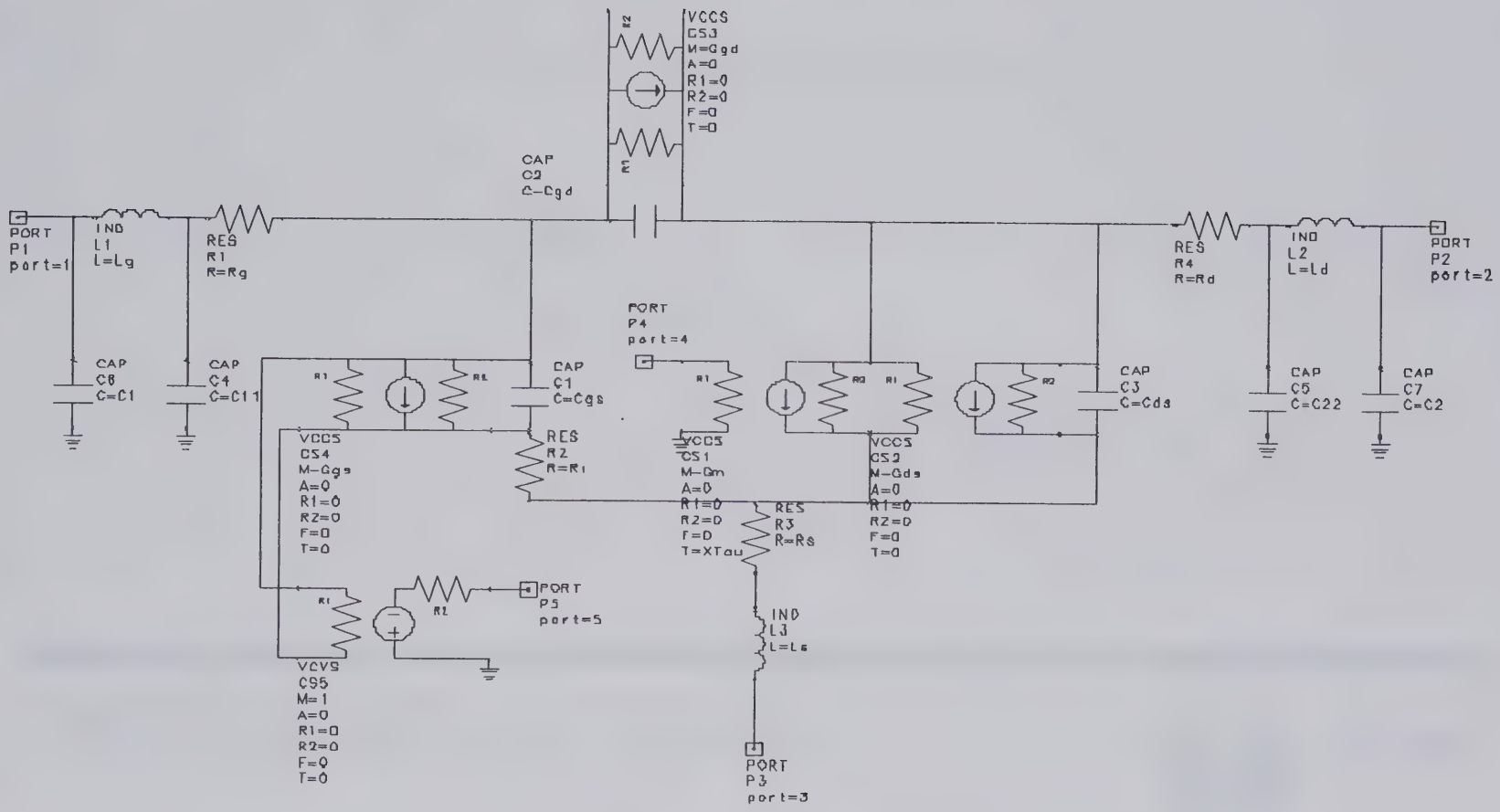

Libra Dead FET Model

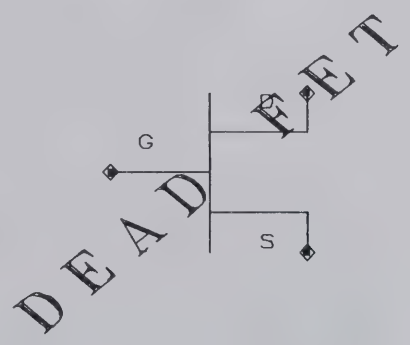


```
lh5_4x100_lh5_6110452704_deadfet
X1
UGW=100
NGF=4
INDEX=1
```

Dead FET Schematic

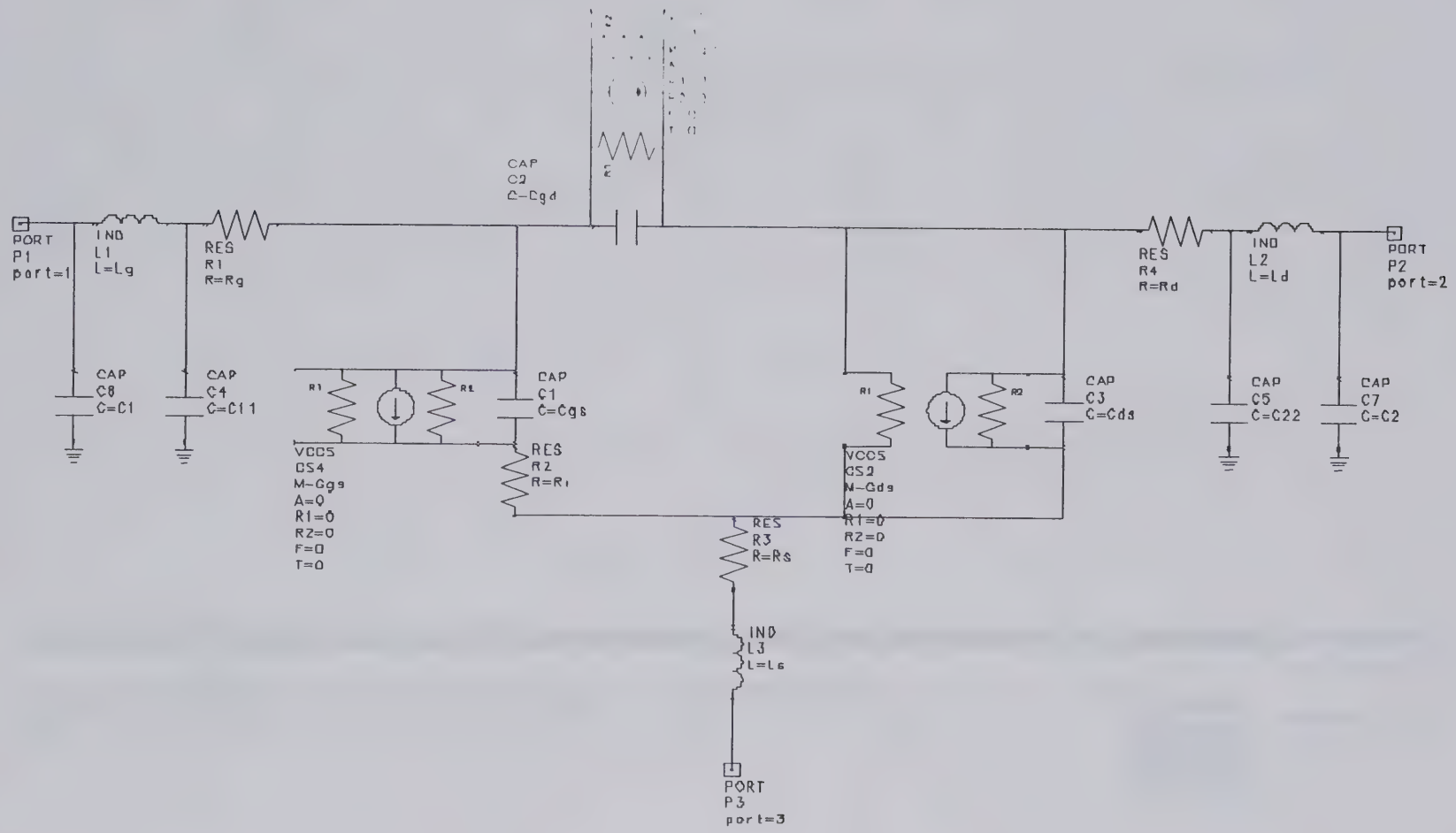

3-Stage Amplifier Example

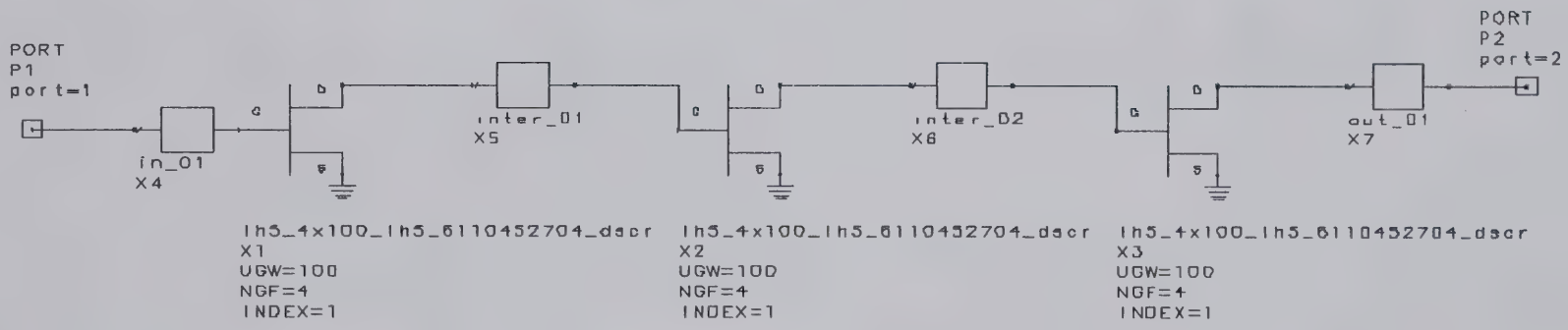

3-Stage NDF Schematic

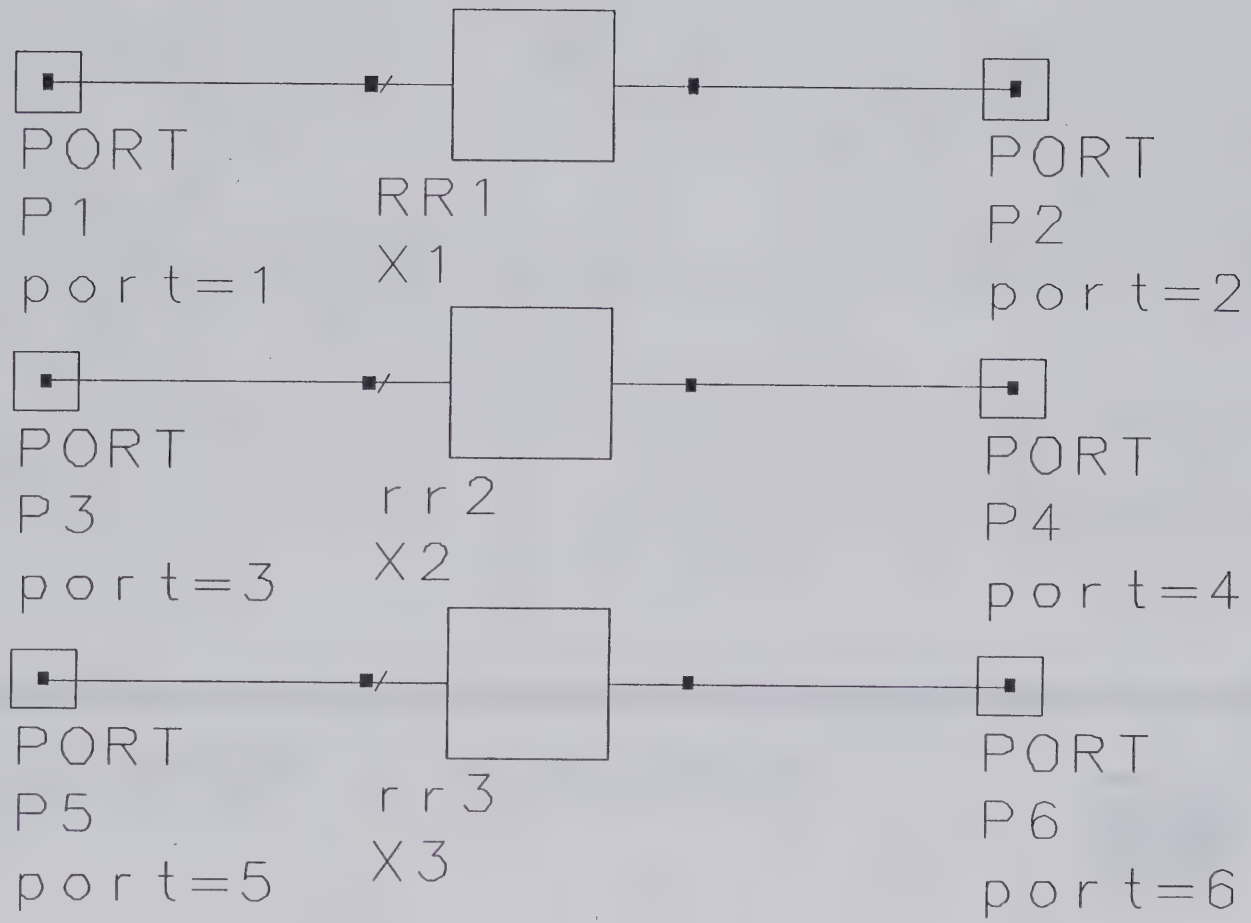

Return Ratio 1 Schematic

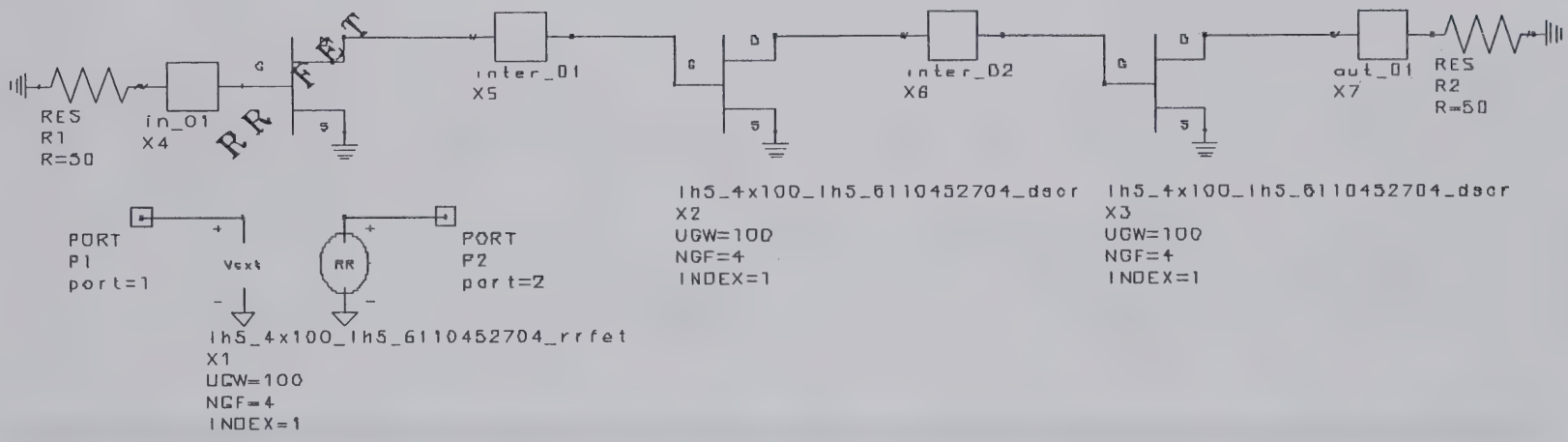

Return Ratio 2 Schematic

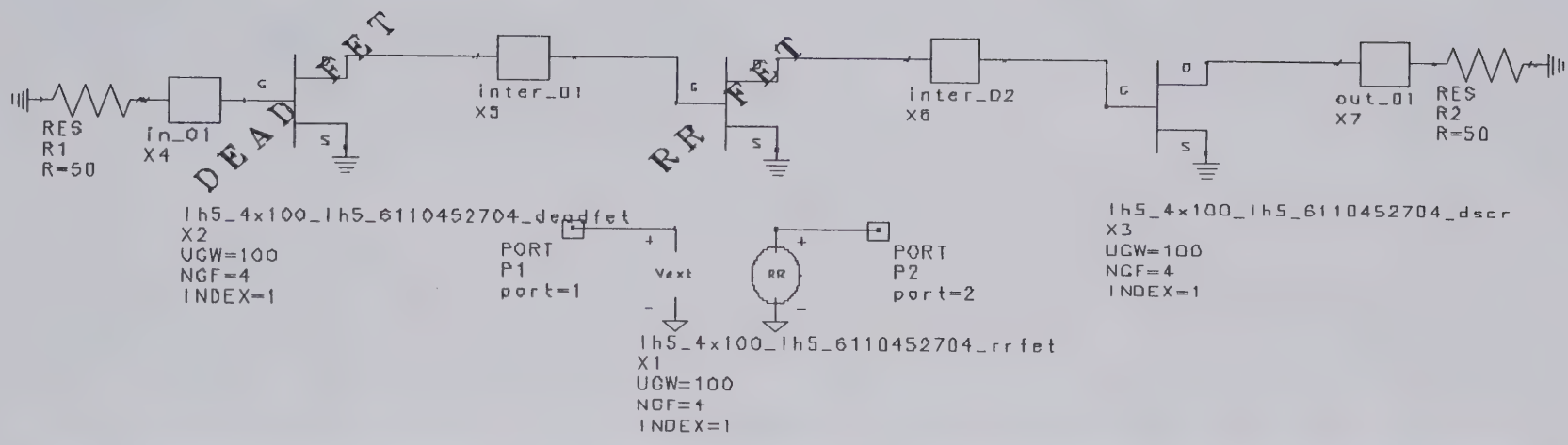

Return Ratio 3 Schematic

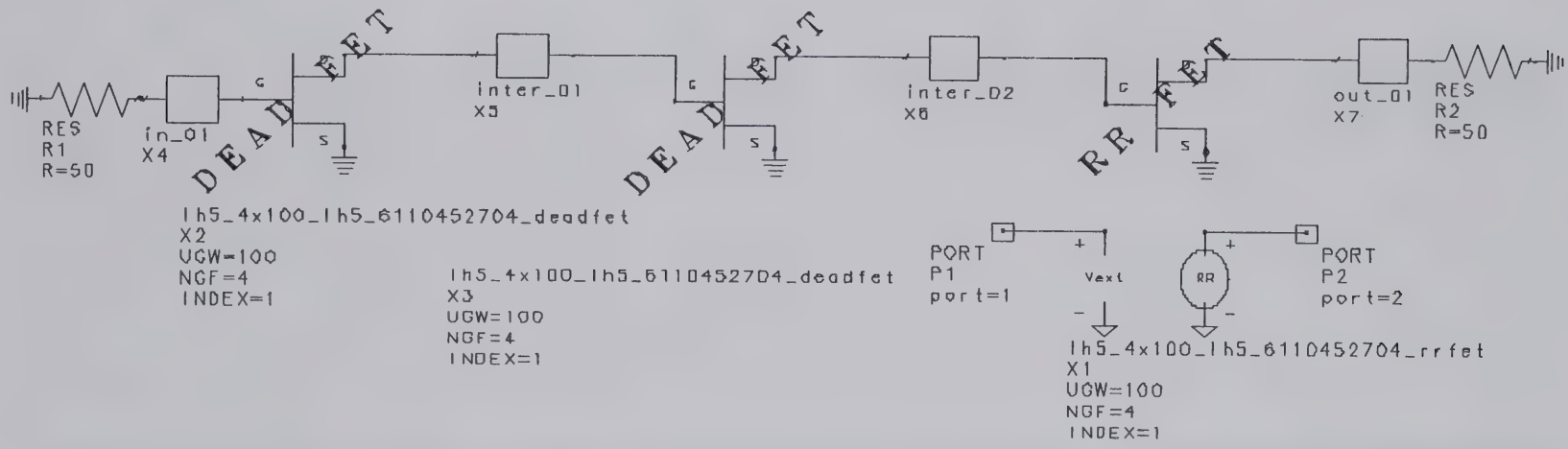

NDF Test Bench

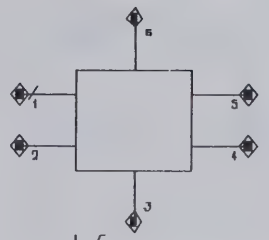

OUTPUT
EQUATION
OUT_EQN
_OUTEQN
NDF=(RR1*.5+1)*(RR2*.5+1)*(RR3*.5+1)
NDFC=CNJ(NDF)

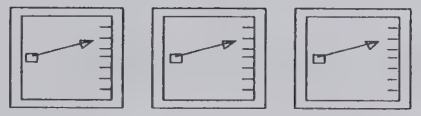

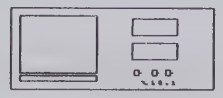

FREQUENCY
FPLAN
value=SWEEP 0.01 100 0.01

AMP M/A-COM

NDF GUIDELINES

NDF Polar Plots

AMP M/A-COM

- Regardless of stability, the polar plot for physically realizable networks will always begin and end at ζ = +/-🕓 on the real axis at (1,0) by construction.
- The NDF does not specifically determine the frequency of oscillation (if an encirclement occurs). However, the frequency where the NDF plot crosses 180 degrees is generally close to the frequency of oscillation.

NDF Polar Plots

AMP M/A-COM

- One exception to this rule is if the NDF plot touches the origin (0,0) at some frequency. If this happens, then this frequency is at least one frequency of oscillation.
- Encirclements of the origin (from $\zeta = +\infty$ to $-\infty$) in a clockwise direction are not possible by construction of the NDF.

NDF Encirclement Plots

AMP M/A-COM

- A stable network will always have a cumulative NDF phase/360 of zero. That is, sweeping from $\zeta = +\infty$ to $\zeta = -\infty$ the plot will begin (by definition) and end at zero encirclements.
- It is unimportant if the encirclement plot rises above +1 or below -1 so long as it returns to zero at $\zeta = -\infty$.

NDF Encirclement Plots

AMP M/A-COM

- A unstable network will always have a cumulative NDF phase/360 of some multiple of 2. That is, sweeping from $\zeta = +\infty$ to $\zeta = -\infty$ the plot will begin at zero and end at +2,4,6... encirclements.
- Negative numbers of encirclements or odd numbers of encirclements +1,3,5... are not possible by construction of the NDF.

References

[1] J.G. Linville and L.G. Schimpf, "The Design of Tetrode Transistor Amplifiers", Bell System Technical Journal, Vol 35, July 1956, pp. 813-840.

[2] J.M. Rollett, "Stability and Power-Gain Invariants of Linear Two-Ports", IRE Transactions on Circuit Theory, Vol CT-9, March 1962, pp. 29-32.

[3] H. Nyquist, "Regeneration Theory", Bell System Technical Journal, Vol 11, January1932, pp. 126-147.

[4] H.W. Bode, "Network Analysis and Feedback Amplifier Design", D. Van Nostrand Co. Inc., New York, 1945.

[5] E.J. Routh, "Dynamics of a System of Rigid Bodies", 3rd Edition, Macmillan, London, 1877.

[6] A. Platzker, W. Struble, and K. Hetzler, "Instabilities Diagnosis and the Role of K in Microwave Circuits", IEEE MTT-S International Microwave Symposium Digest, 1993, pp. 1185-1188.

[7] W. Struble and A. Platzker, "A Rigorous Yet Simple Method for Determining Stability of Linear N-Port Networks", GaAs IC Symposium Digest, 1993, pp. 251-254.

[8] A. Platzker and W. Struble, "Rigorous Determination of the Stability of Linear N-Node Circuits From Network Determinants and the Appropriate Role of the Stability Factor K of Their Reduced Two-Ports", 3rd International Workshop on Integrated Nonlinear Microwave and Millimeter-wave Circuits, University of Duisberg, Germany, Oct. 1994, pp. 93-107.

Detailed Analysis of a High Temperature Superconducting Filter

— With Special Emphasis on Accuracy —

James C. Rautio

Sonnet Software, Inc.
Email: info@sonnetusa.com
WWW: http://www.sonnetusa.com

Two Kinds of Meshing

Volume Meshing

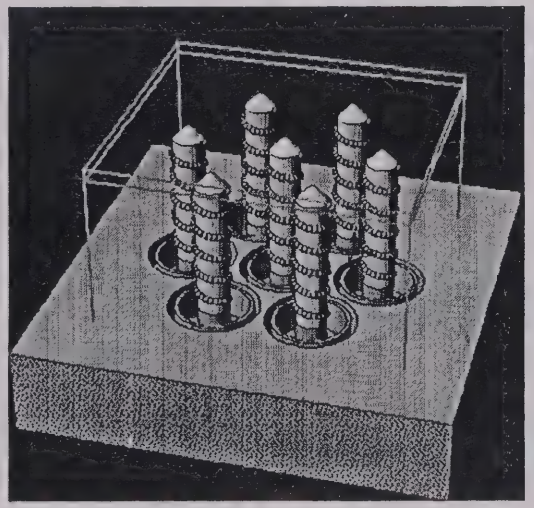

Surface Meshing

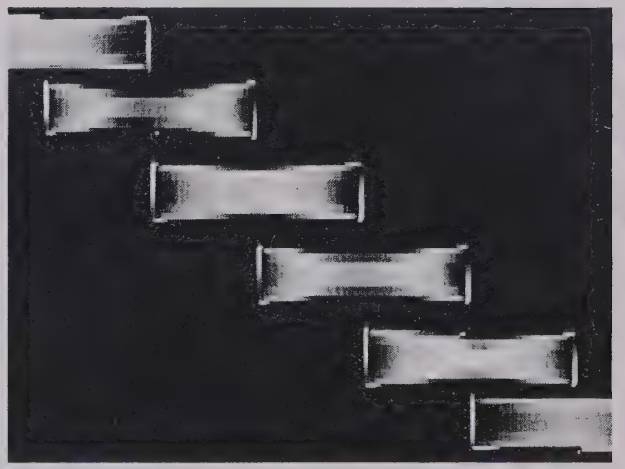

Volume Meshing

- Best for 3-D arbitrary structures
- Finite Elements (tetrahedral mesh)
  - Best established.
  - Ideal for frequency domain.
- FDTD and TLM (rectangular mesh)
  - Well established technology, but only recently introduced commercially.
  - Best for radiation, fast rise time pulse response, and wide band frequency domain.

Surface Mesh

- Best for 3-D planar circuits.
- Open environment
  - Rectangles and triangles on arbitrary mesh size, but requires numerical integration.
  - Best for fast analysis with large subsections.
- Shielded environment
  - Rectangles and triangles on FFT snap grid, but no numerical integration.
  - Best for high accuracy, esp., with convergence analysis.

Diverse Tool Set Required

- The fully equipped microwave engineer will need 4 to 5 different electromagnetic tools.
- One or two tools is not enough.
- The designer must know the trade-offs between different tools very well.
- Designer must use the best tool for a given task in order to beat the competition.

Area of Influence

1) Estimate subsection-to-subsection coupling based on cell-to-cell coupling.
2) Estimate error in estimate of coupling.
3) Then, if error is small enough, use estimated coupling.

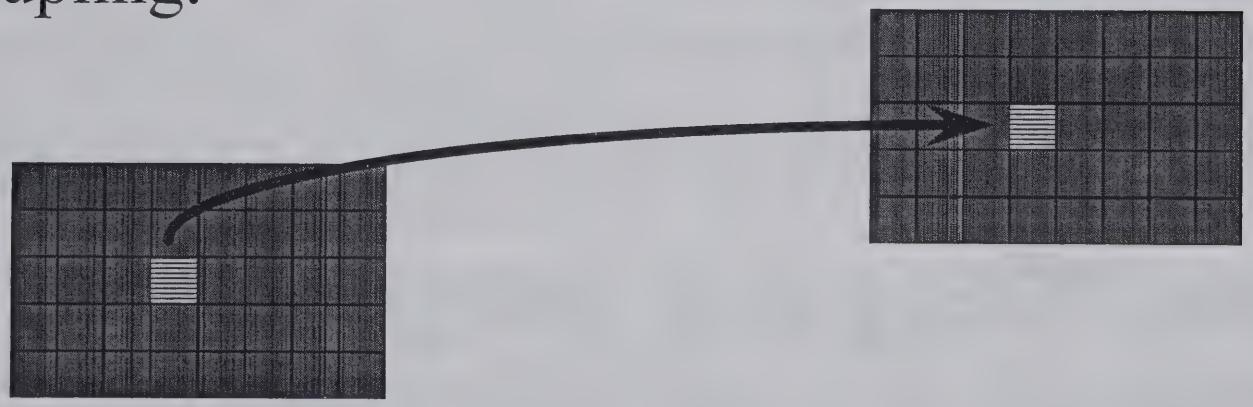

Area of Influence

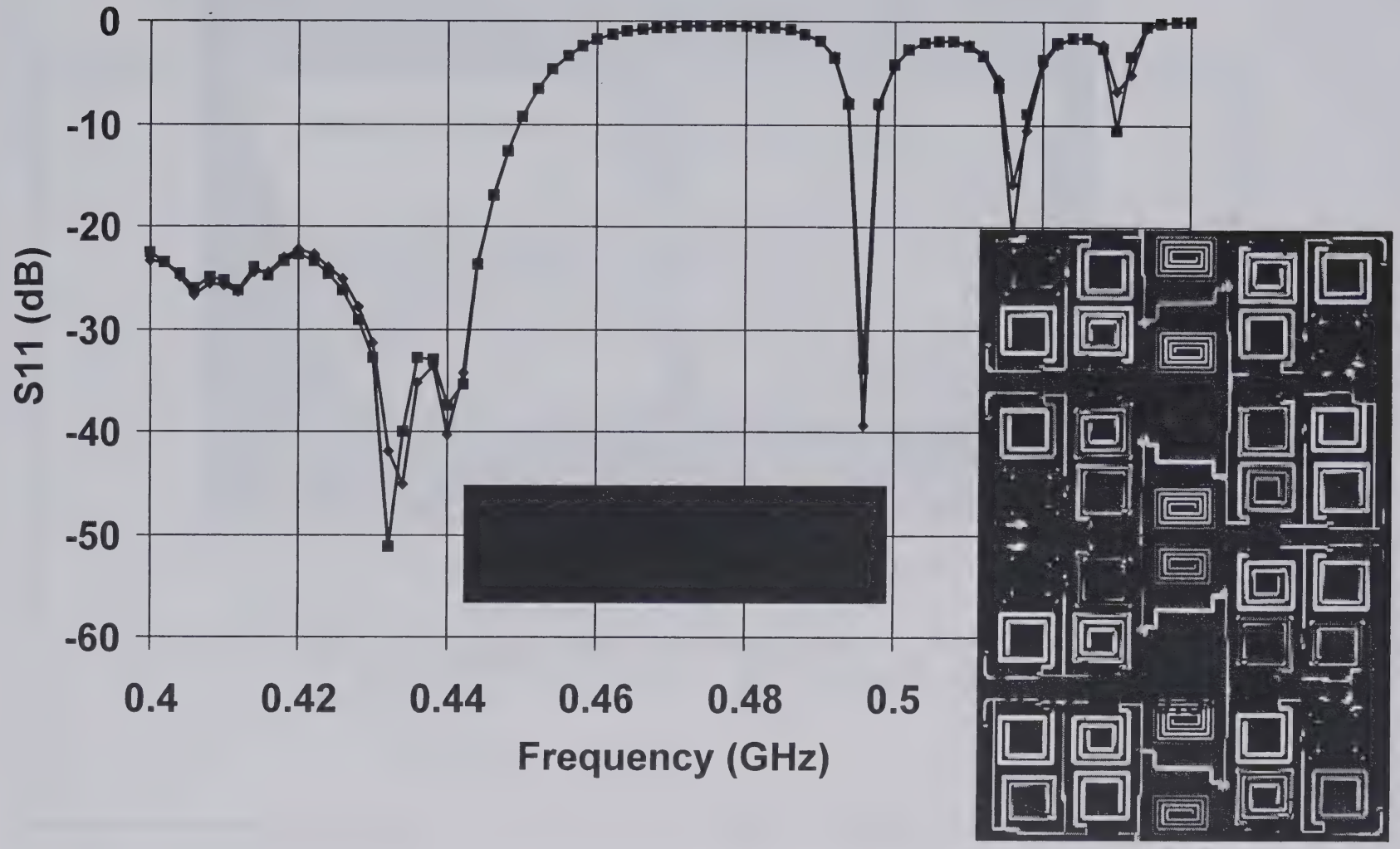

SONNET ®

Dielectric Bricks

Non-planar dielectric

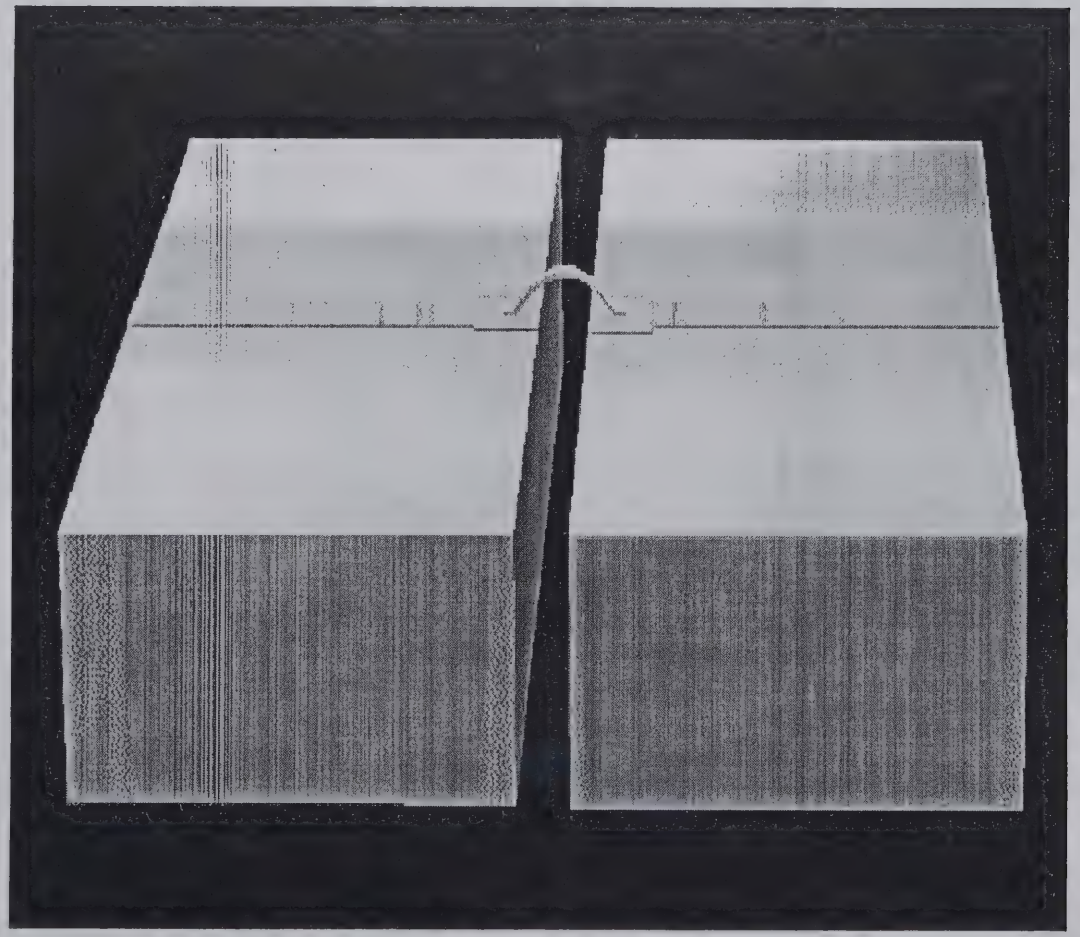

Design Example

Measurement ≠ calculation. Why?

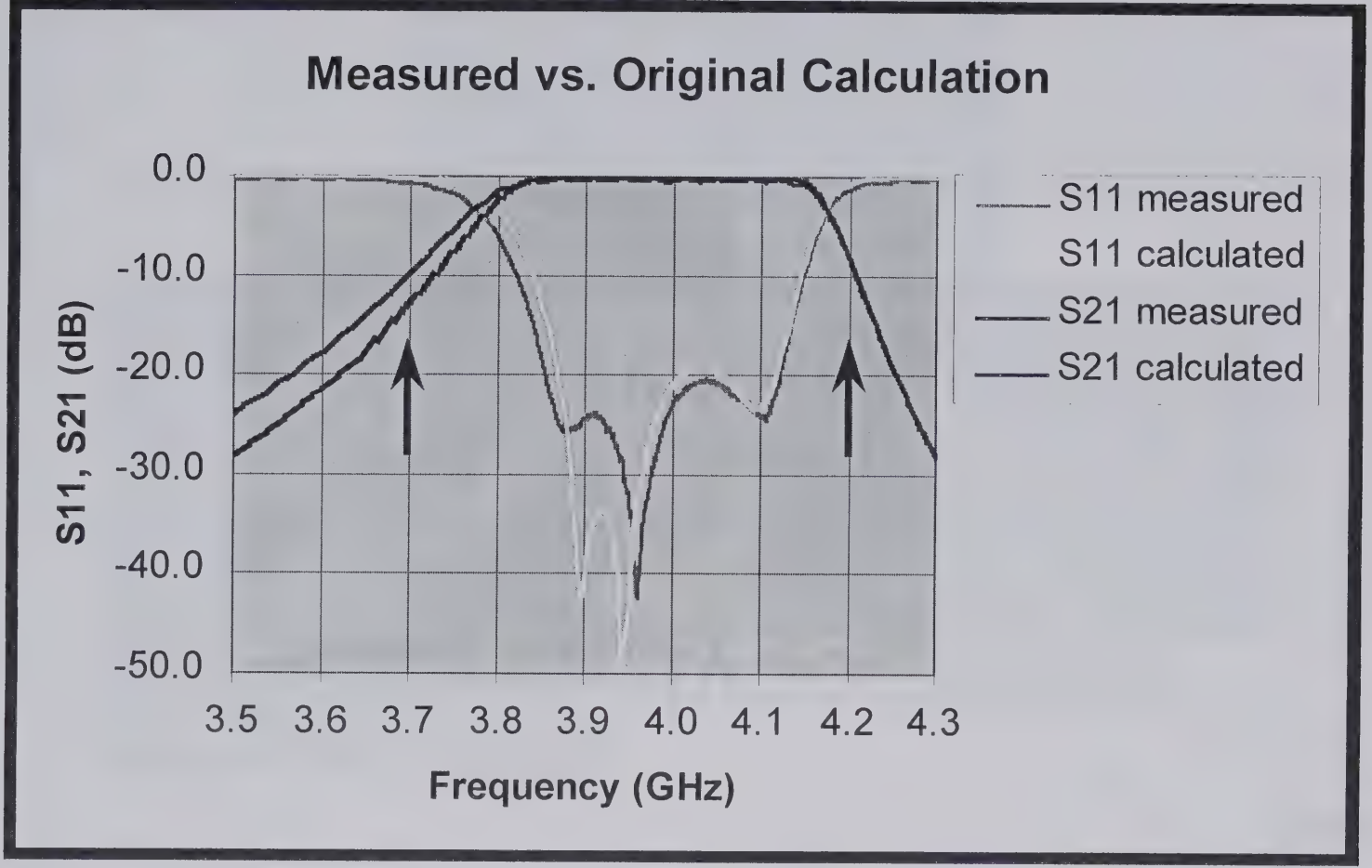

SONNET ®

Testing Hypotheses

Check sensitivity of error sources

Error due to cell size

Cell Size (mm)	S21(dB) (8.7GHz)
0.0500	-12.88
0.0250	-12.34
0.0125	-12.11
0.0000	-11.88
Measured	-9.78

SONNET ®

Testing Hypotheses

Check sensitivity of error sources

Error due to metal thickness and loss

Thickness (microns)	S21(dB) (3.7GHz)
0.0	-12.8
1.0	-12.9
10.0	-13.0
100.0	-13.3
Measured	-9.8

Loss (Ohms/sqr)	S21(dB) (3.7GHz)
0.00	-12.8
0.01	-13.2
Measured	-9.8

SONNET ®

Testing Hypotheses

Check sensitivity of error sources

Error due to box size (dimensions: A x B)

Box A Dim. (mm)	Box B Dim. (mm)	S21(dB) (3.7GHz)	S21(dB) (4.2GHz)
12.8	25.6	-12.8	-8.3
25.6	25.6	-11.9	-8.3
25.6	51.2	-9.6	-8.2
	Measured	-9.8	-8.3

Design Example

Now, good agreement, but ...

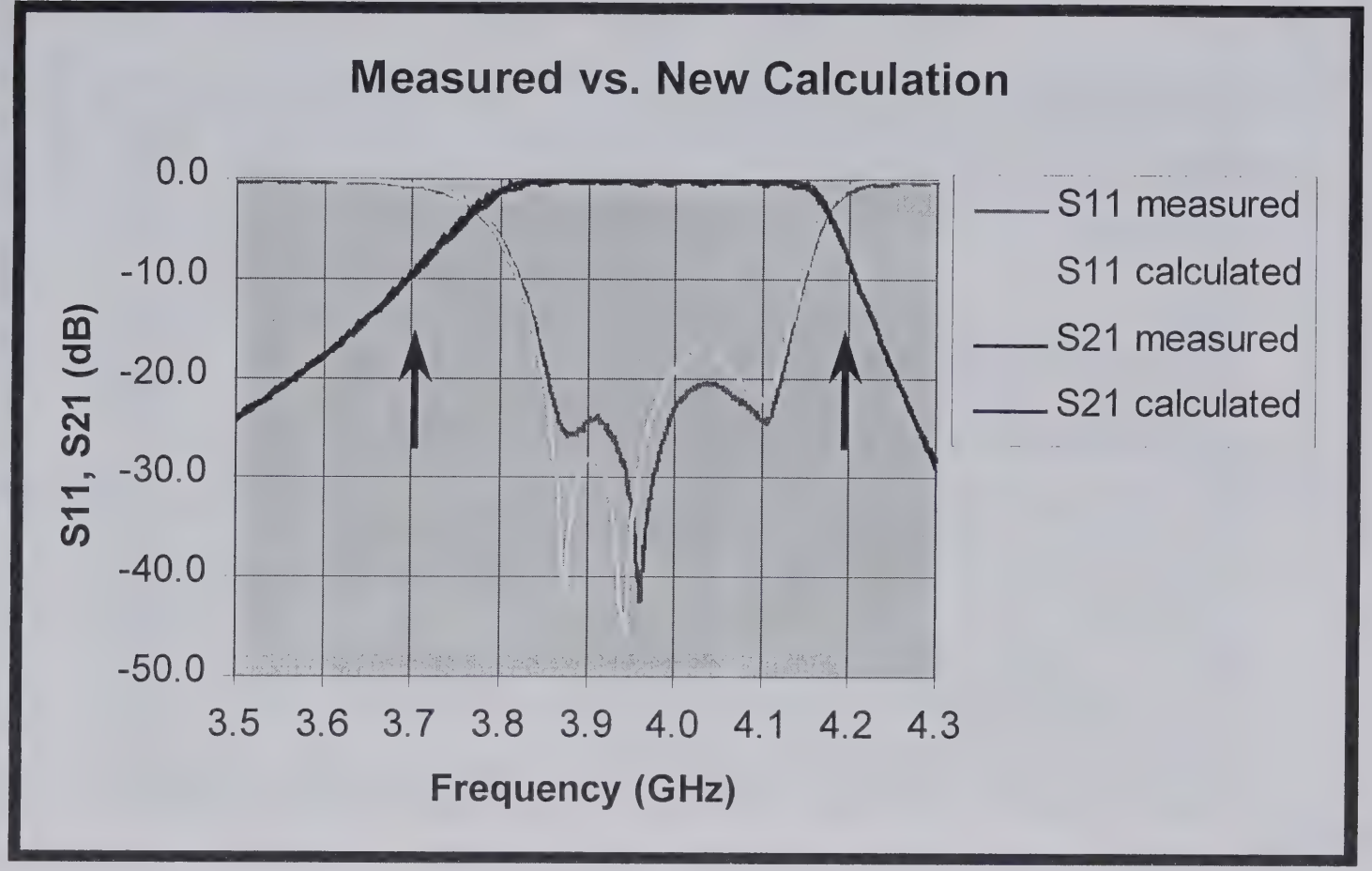

Design Example

Convergence Check

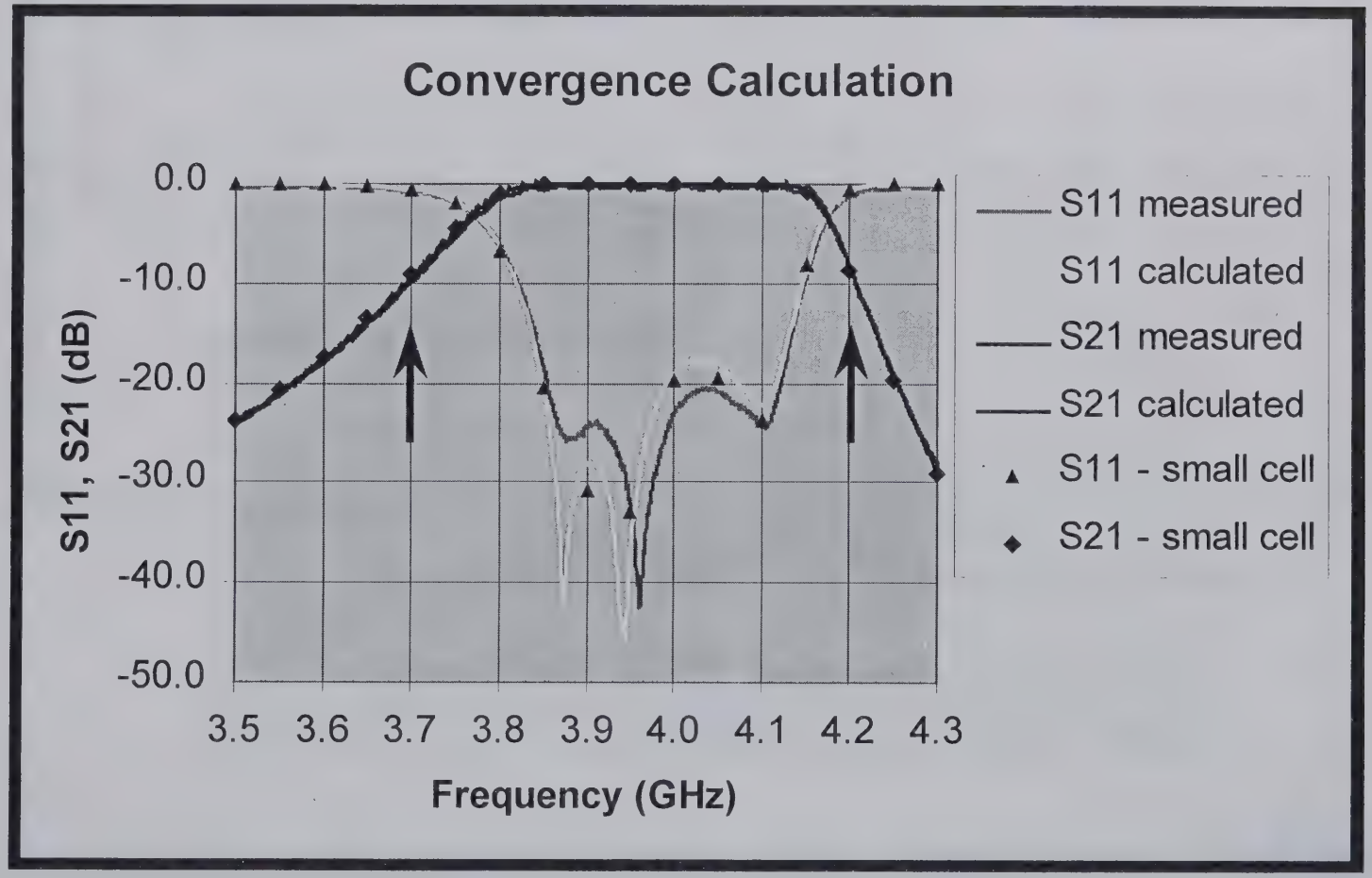

A Different Approach

Make box as small as possible and break the filter into pieces

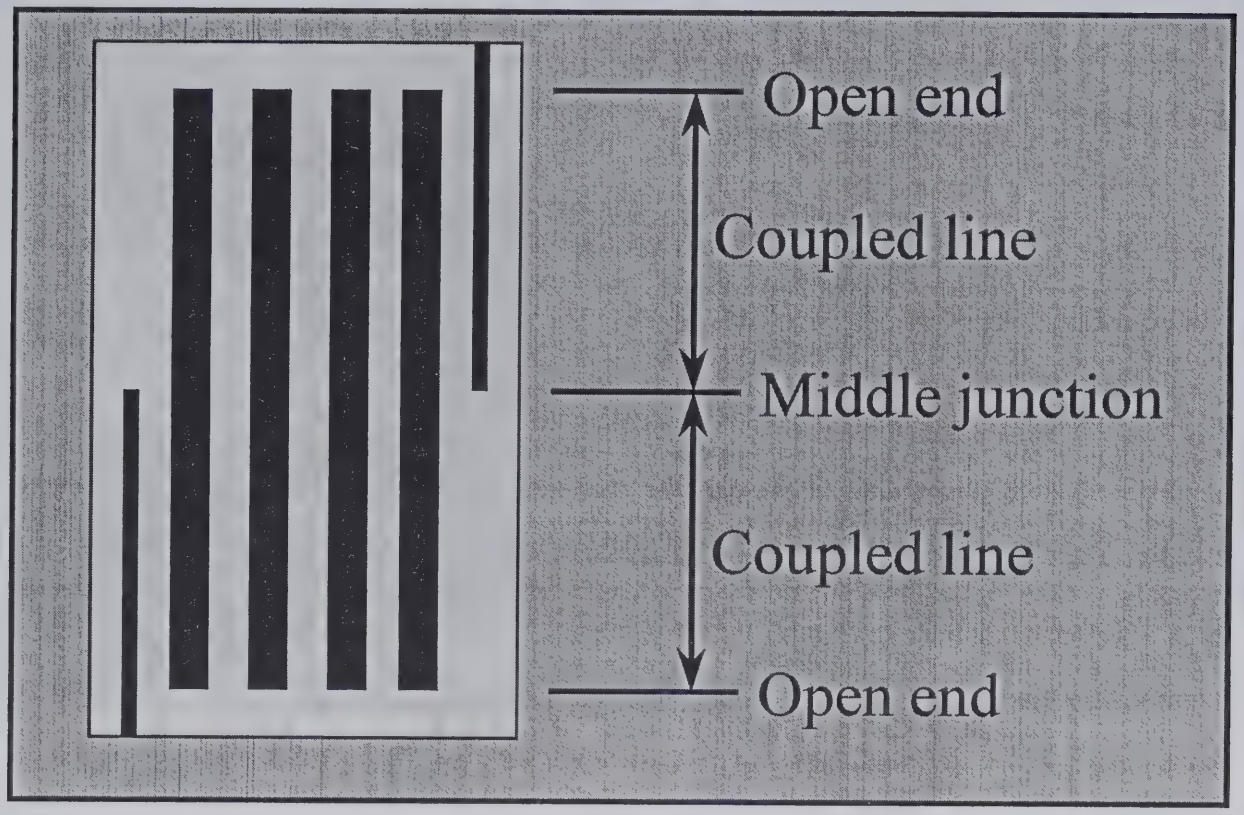

Two Stage Analysis

1) Divide circuit into pieces and analyze each piece at a few frequencies across the band of interest.
   - Each piece is small and analyzes quickly.
   - The result for each piece varies slowly with frequency.
2) Interpolate result from each piece to many frequencies and connect the pieces together with a nodal analysis.

Both steps done automatically with a Sonnet ".net" file.

The Sonnet ".net" File

```
CKT
  GEO 1 2 3 4 5 6 end.geo OPT=mvd CTL=complete.an                          ! Open end
  GEO 2 3 4 5 6 7 8 9 10 11 long.geo OPT=mvd CTL=complete.an               ! 7.15 mm section
  GEO 7 8 9 10 11 12 13 14 15 16 short.geo OPT=mvd CTL=complete.an         ! 0.05 mm section
  GEO 12 13 14 15 16 17 18 19 20 21 middle.geo OPT=mvd CTL=complete.an     ! Middle section
  GEO 21 20 19 18 17 26 25 24 23 22 long.geo OPT=mvd CTL=complete.an       ! 7.15 mm section
  GEO 27 26 25 24 23 22 end.geo OPT=mvd CTL=complete.an                    ! Open end

  DEF2P 1 27     COMPLETE                    ! Complete filter

FILEOUT
  COMPLETE TOUCH complete.s2p S MA R 50

FREQ
  SWEEP 3.5 4.3 .01
```

Sonnet Two Stage Analysis

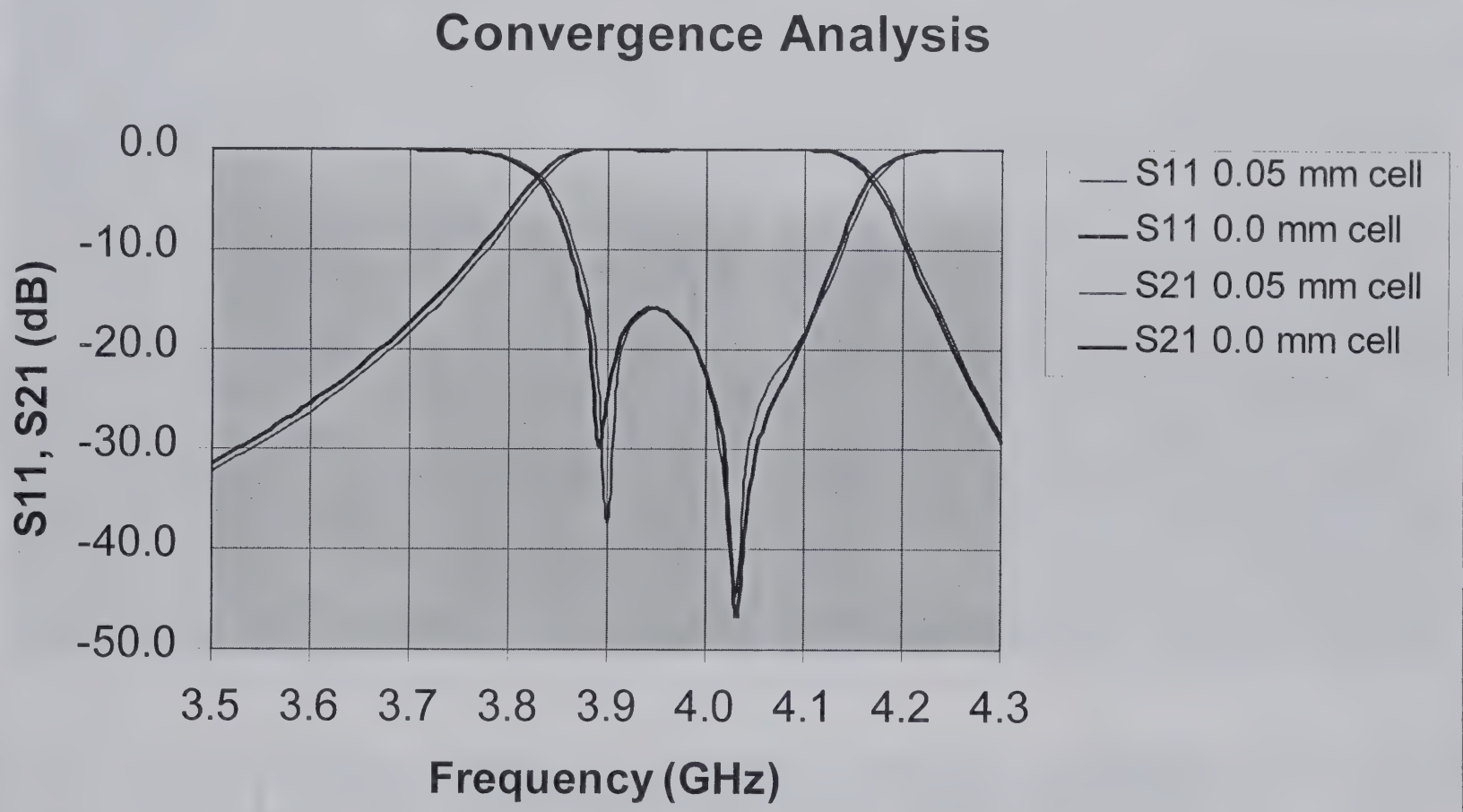

Zero mm cell size estimated from 0.050 mm and 0.025 mm cell size.

SONNET ®

Comparison of Timings

		ge (sec/freq)
0.050	196	12
0.025	858	45

Timings for two stage analysis includes analysis of each piece at four frequencies with final result at 81 frequencies. All analyses performed on a 266 MHz Pentium II.

Effect of Box Size

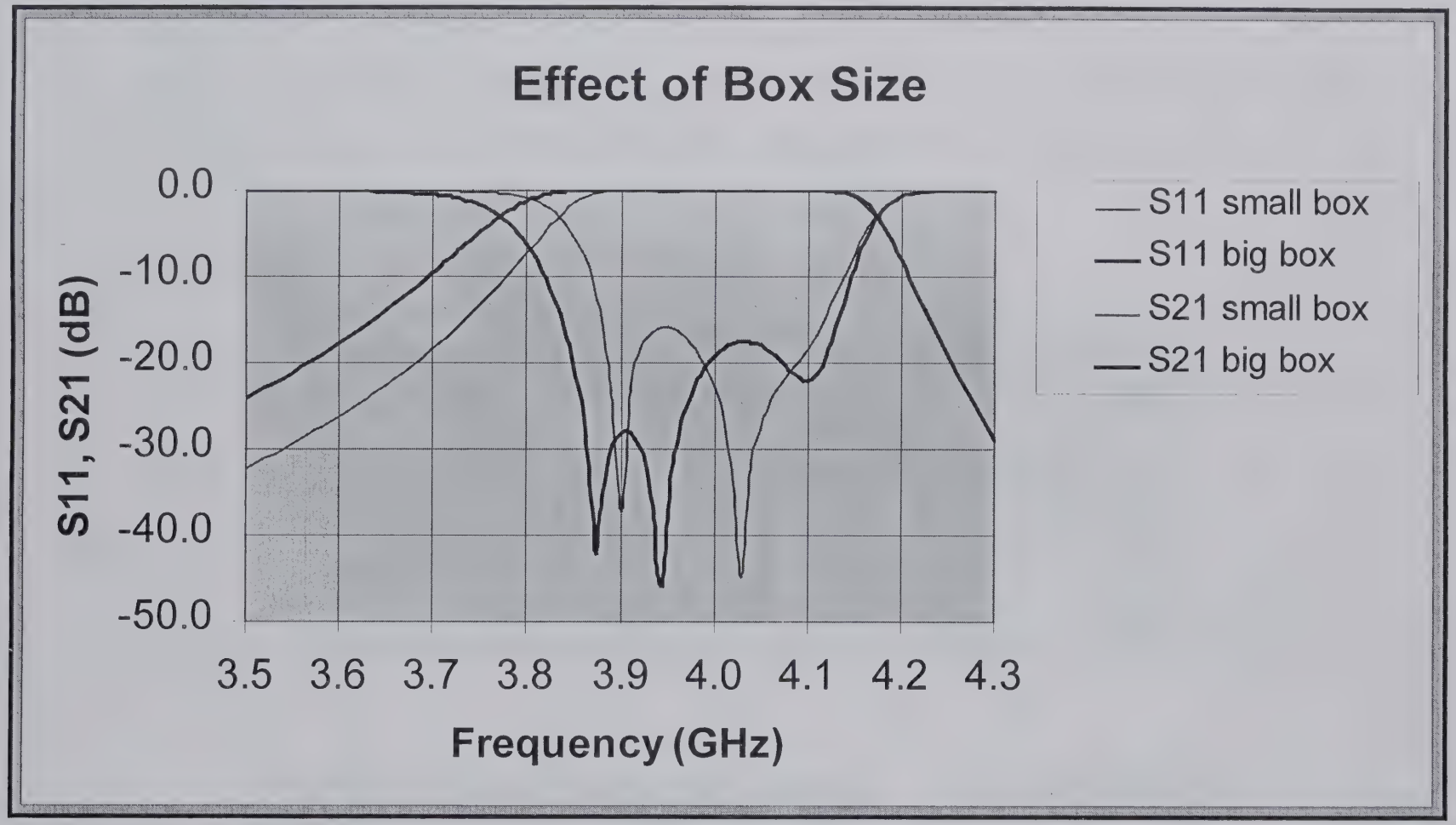

Small box: 8 mm x 16 mm.

Big box: 25.6 mm x 51.2 mm.

Antenna Analysis

Best for certain kinds of antennas.

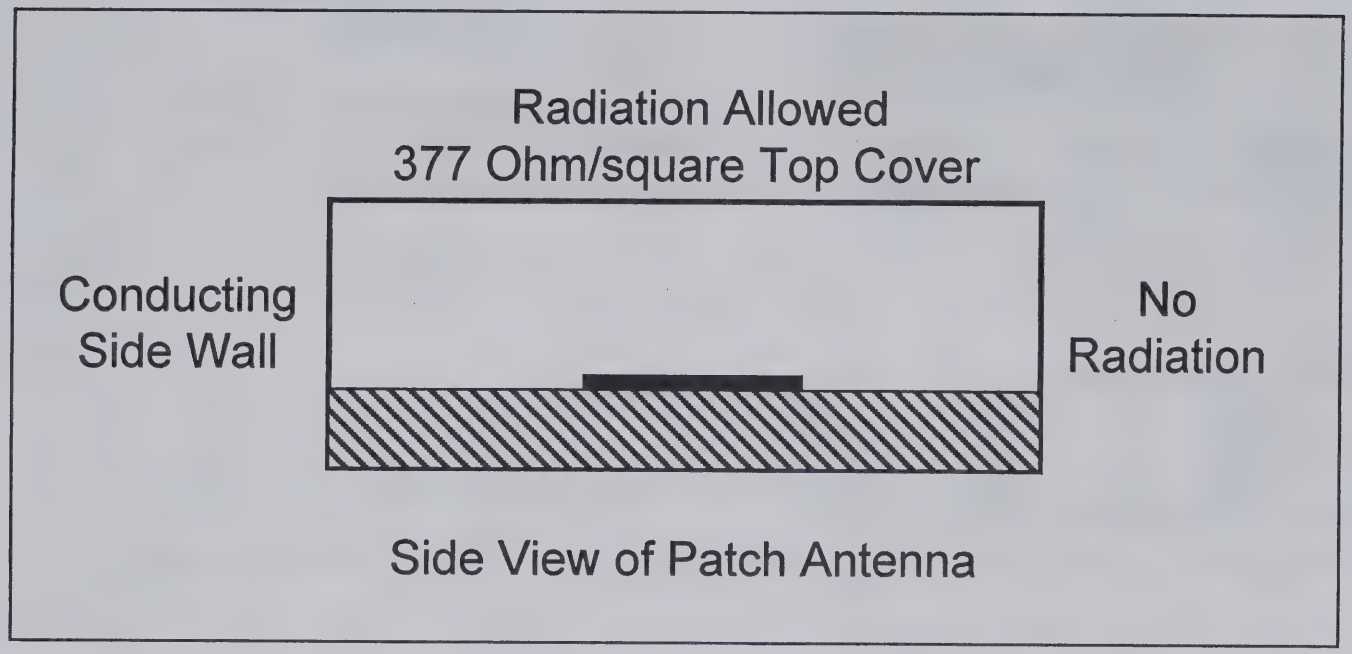

Patch Antenna

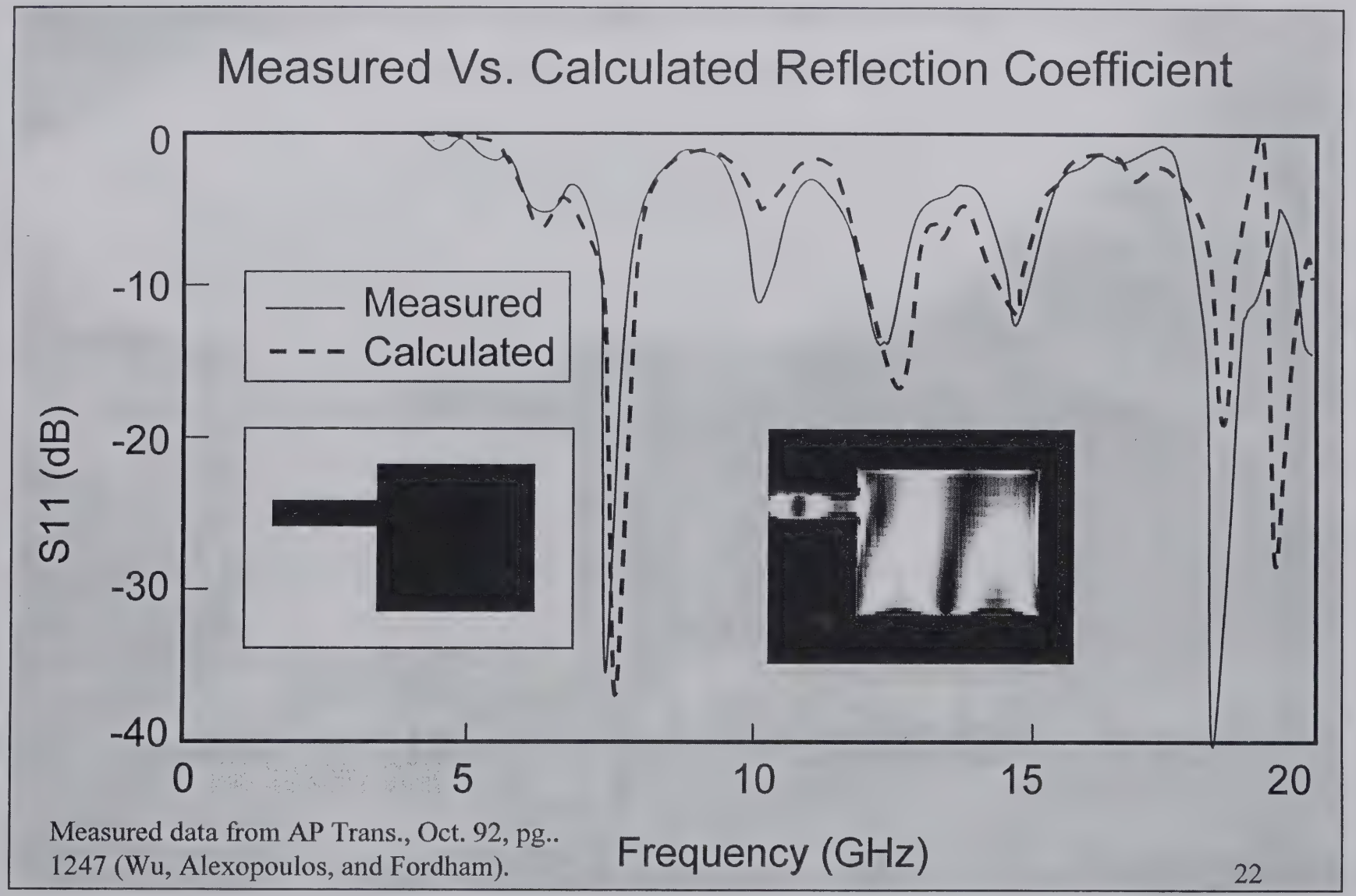

Measured data from AP Trans., Oct. 92, pg.. 1247 (Wu, Alexopoulos, and Fordham).

Triple Patch Antenna

Measured Vs. Calculated Reflection Coefficient

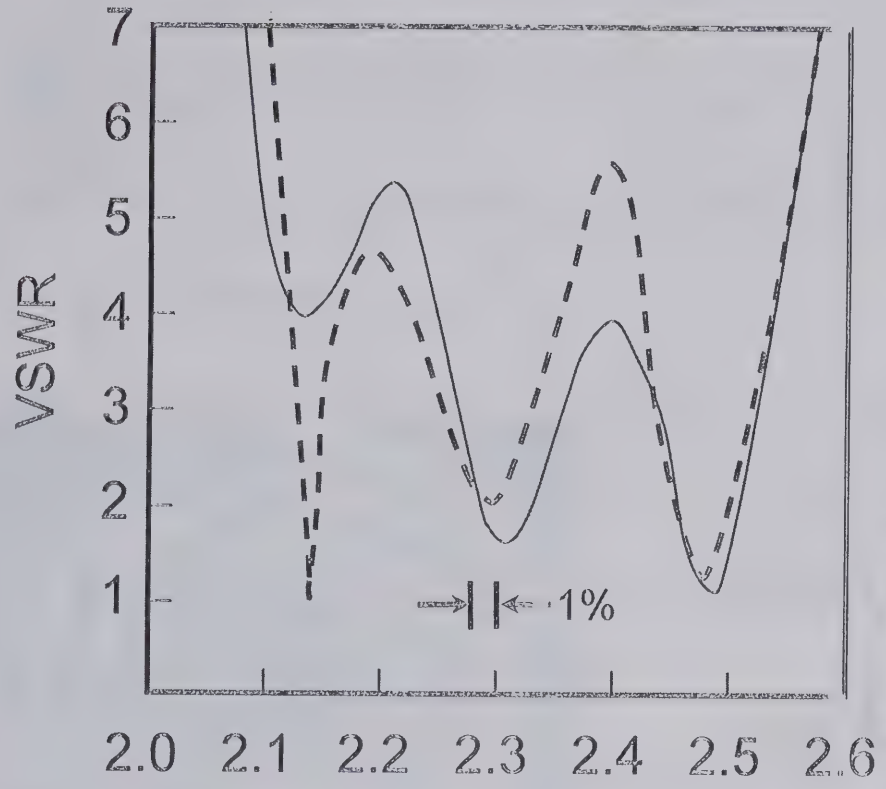

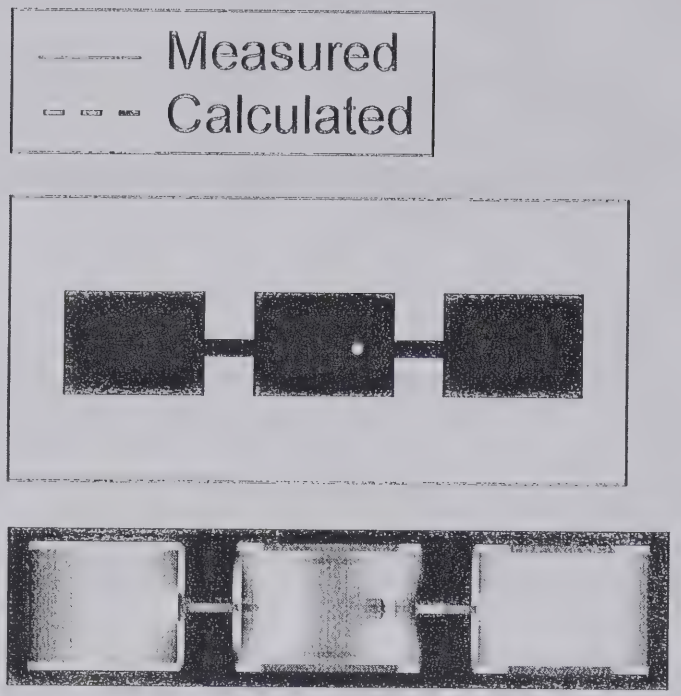

Measured data from Matra Defense,
Antennas & Stealthiness Dept., France.

SONNET ®

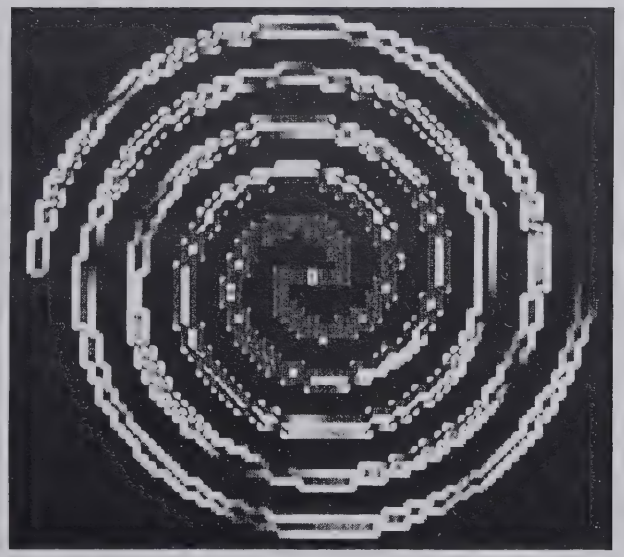

Spiral Antenna

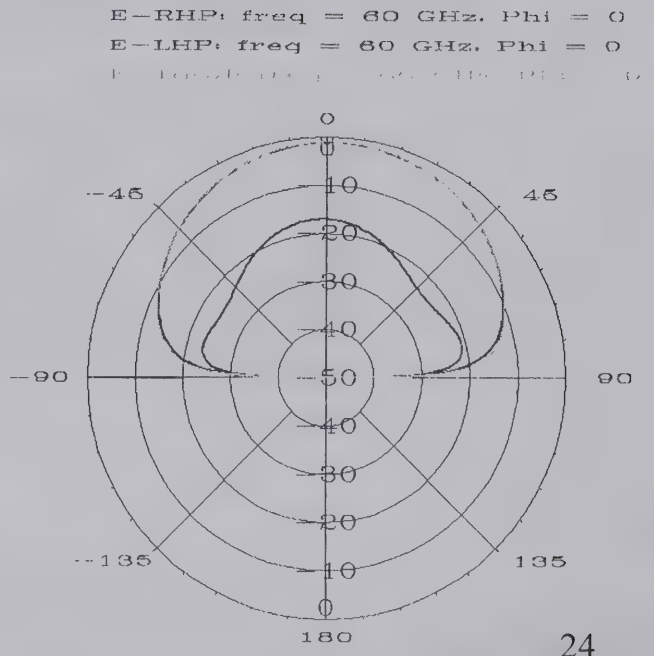

Conclusion

- Many different kinds of electromagnetic analyses.
- Very important to select the right kind for a given problem.
- There is some overlap between different kinds of analyses.
- When high accuracy is required, convergence analysis is needed.
- Careful evaluation of error sources can lead to new understandings of how a circuit operates.

Broadband Planar Monolithic Balanced Mixers and Frequency Multipliers

Stephen Maas

Nonlinear Technologies, Inc.

PO Box 7284, Long Beach, CA 90807 USA

310-426-1639

Email s.maas@ieee.org

Planar Diode Mixers

The Problem:

- We wish to fabricate mixers as GaAs monolithic circuits (MMICs)
- Most conventional types of mixer baluns are not suitable for MMICs
  - * These use coupled-line baluns, that depend on high even-mode characteristic impedances.
  - * Low even-mode characteristic impedance allows an even mode to propagate on the balun.
  - * The result is poor isolation, poor spurious-response rejection.

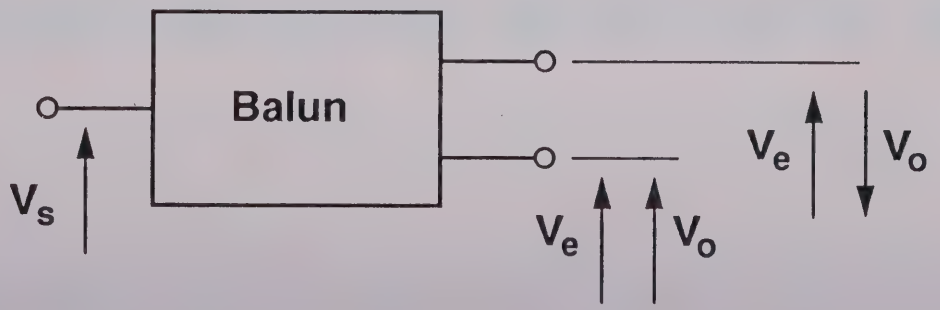

Even and Odd Modes

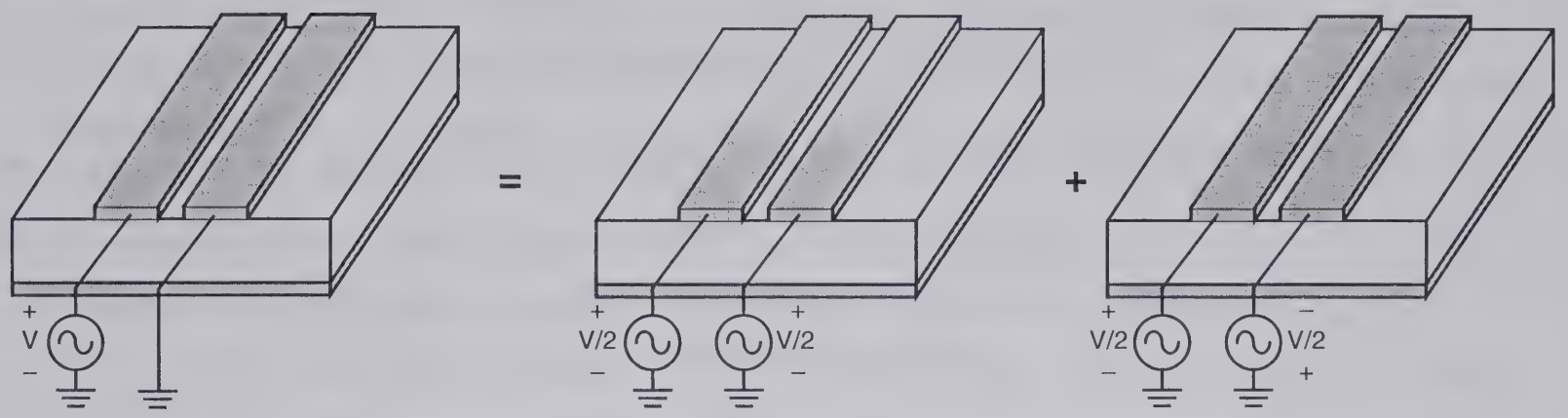

Balun **Even Mode** **Odd Mode**

- **Ideally we want a purely odd mode on the balun.**
- **The even mode contributes imbalance; we must suppress it.**

Diode-Mixer Baluns

The Even-Mode Problem

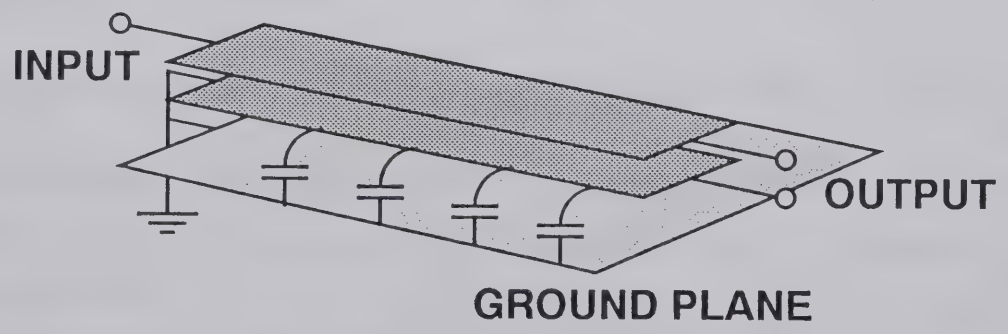

- Capacitance between the conductors and the ground plane supports an even mode.
  - * Degrades many of the characteristics of a balanced mixer:
    - ◆ Port-to-port isolation;
    - ◆ Even-order spurious-response rejection.
- Simple coupled-line baluns require a suspended substrate; they cannot be used in monolithic circuits.

The Even-Mode Problem

- In a parallel-strip balun, there are two ways to eliminate the even mode:
  - Make the even-mode characteristic impedance very high: on the order of 1000 ohms.
  - Don't generate the even mode in the first place.
- Most hybrid mixers use a combination of both techniques:
  - Suspended substrate minimizes capacitance to ground → maximizes Z_{0e}.
  - Coax-to-microstrip transition and a tapered ground plane → minimizes even mode generation.
- If the even mode is suppressed, the coupled lines behave as a floating, balanced transmission line having $Z_0 = 2\ Z_{0o}$.
- If even modes are well suppressed, a balun connected as a power divider have an equal power split at its output and 180-degree phase difference.

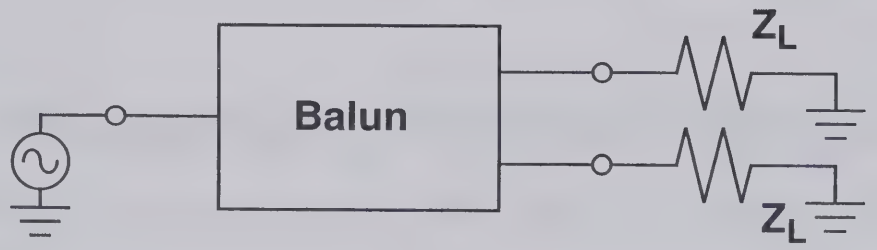

Suspended-Substrate Balun

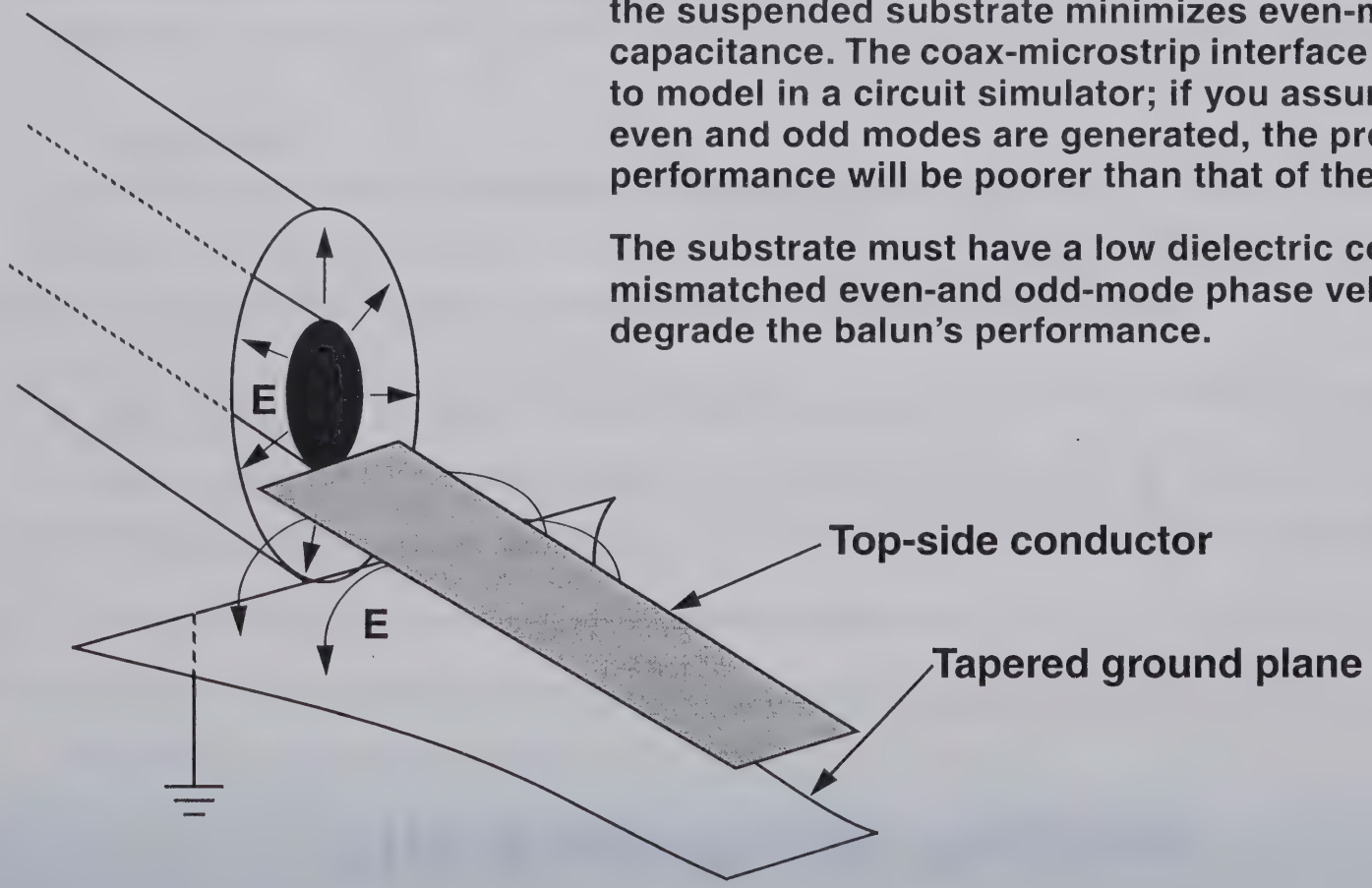

This is a typical balun used in a hybrid mixer. The geometry of the coax-microstrip interface excites more of an odd mode than an even mode, and the air gap around the suspended substrate minimizes even-mode capacitance. The coax-microstrip interface is very difficult to model in a circuit simulator; if you assume that equal even and odd modes are generated, the predicted performance will be poorer than that of the real circuit.

The substrate must have a low dielectric constant, or the mismatched even-and odd-mode phase velocities will degrade the balun's performance.

Planar Diode Mixers

GaAs MMIC Circuits

Possible Solutions:

- Maximize the even-mode impedance by minimizing stray capacitance
  - * Thick substrates and thin conductors.
  - * This just doesn't work!
    - ◆ Even with 600-μm substrates and conductor widths below 4 μm, the even-mode impedance is too low.
- Use baluns that tolerate low even-mode impedance
  - * Hybrids.
    - ◆ OK for some designs.
    - ◆ Not very broadband.
  - * Marchand balun and related types of baluns.
  - * Bifilar spiral balun.

Marchand Balun

Classical Coaxial Form

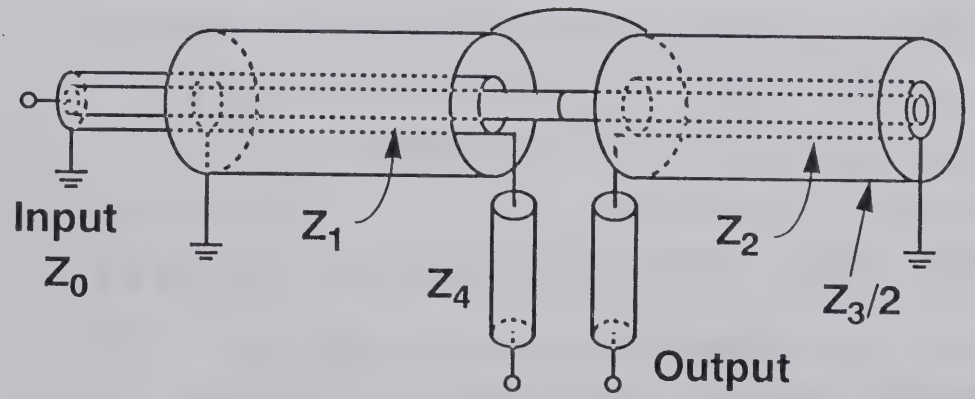

Coaxial Balun

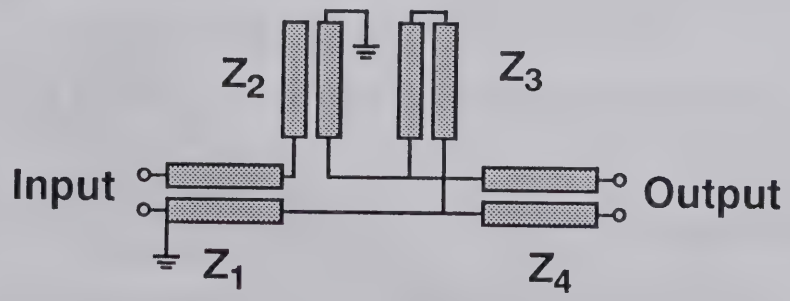

Equivalent Circuit

* A coaxial balun is well described by the transmission-line equivalent circuit
* Theoretical bandwidth: 10:1 with 15 dB return loss! (Chebyshev characteristic)
* Planar realizations are not well described by this equivalent circuit, because it doesn't account for capacitance between the center conductor and ground, or between the Z_4 conductors and ground.

Planar Marchand Balun

A Coupled-Line Balun

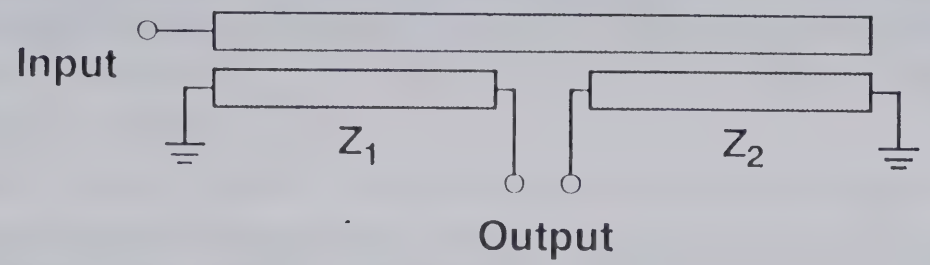

- The output section (Z_4) is eliminated (impractical in certain types of mixers).
- Z_3 is realized by the even-mode characteristic impedance (usually we want $Z_3 \rightarrow \infty$).
- With $Z_1 = Z_2$ ($= 2\,Z_{0o}$) $= (Z_s\,Z_L)^{0.5}$ ~2:1 bandwidth can be achieved.
- Much better bandwidth results from $Z_1 = (Z_s\,Z_L)^{0.5}$ and Z_2 as low as can be achieved in practice.
- Design and analysis *must* include the full capacitance matrices of the coupled lines; a transmission-line model is inadequate!

Planar Marchand Baluns

- It is difficult to achieve ~25 Ω Z_{0o} with two edge-coupled strips, and four strips results in a low Z_{0e}.
  - ~25 Ω Z_{0o} can be achieved with broadside coupling. However, the capacitance matrix of the coupled lines is strongly asymmetrical. This may affect balance.
  - We use three-strip structures for our baluns. These are especially practical for star mixers.
  - Width and spacings are adjusted to achieve desired amplitude balance in "power-divider" configuration (phase balance is always nearly perfect.)

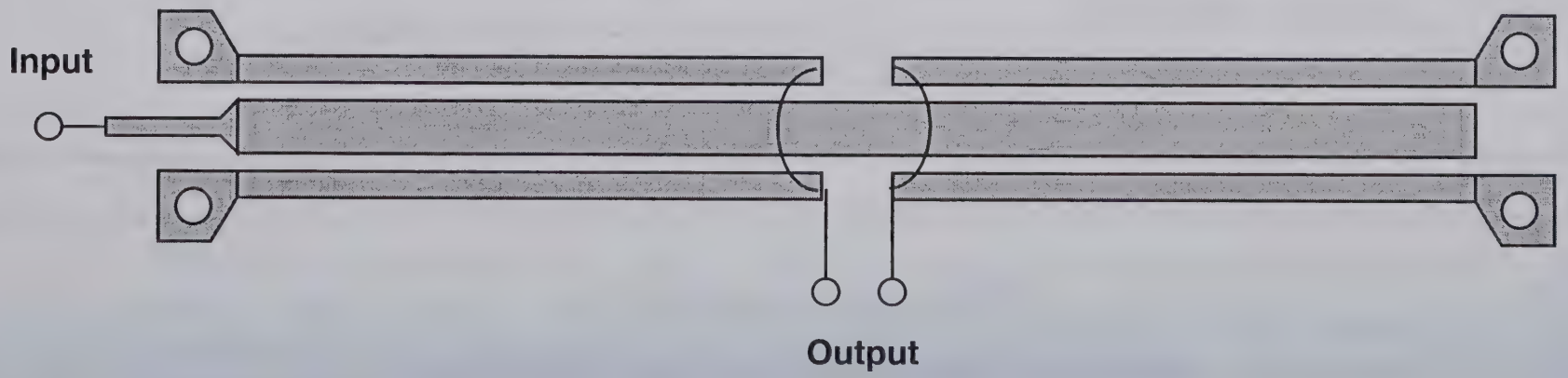

Some Complications

- We need a general analysis of coupled lines
  - * Usually we want Z_{0o} ~ 25 ohms or less. This requires multiple coupled lines ("Lange" couplers).
  - * Certain types of mixers require an odd number of coupled lines.
  - * Sometimes symmetrical coupled lines are not optimum: asymmetrical coupled lines give more freedom to optimize the circuit.
- Method:
  - * Use electromagnetic analysis software to obtain the modal voltage and current matrices, and propagation constants, of the structure.
  - * Import these directly into a circuit simulator.
  - * Calculate the nodal admittance matrix of the coupled-line structure directly from the modal characteristics.
  - * The n-coupled-line section becomes a 2n-terminal circuit element.
- For EM analysis we use LINPAR by Djordjevic et. al.
  - * Quasistatic moment method.
  - * GaAs circuits are small enough that dispersion is rarely significant below 100 GHz.

LINPAR

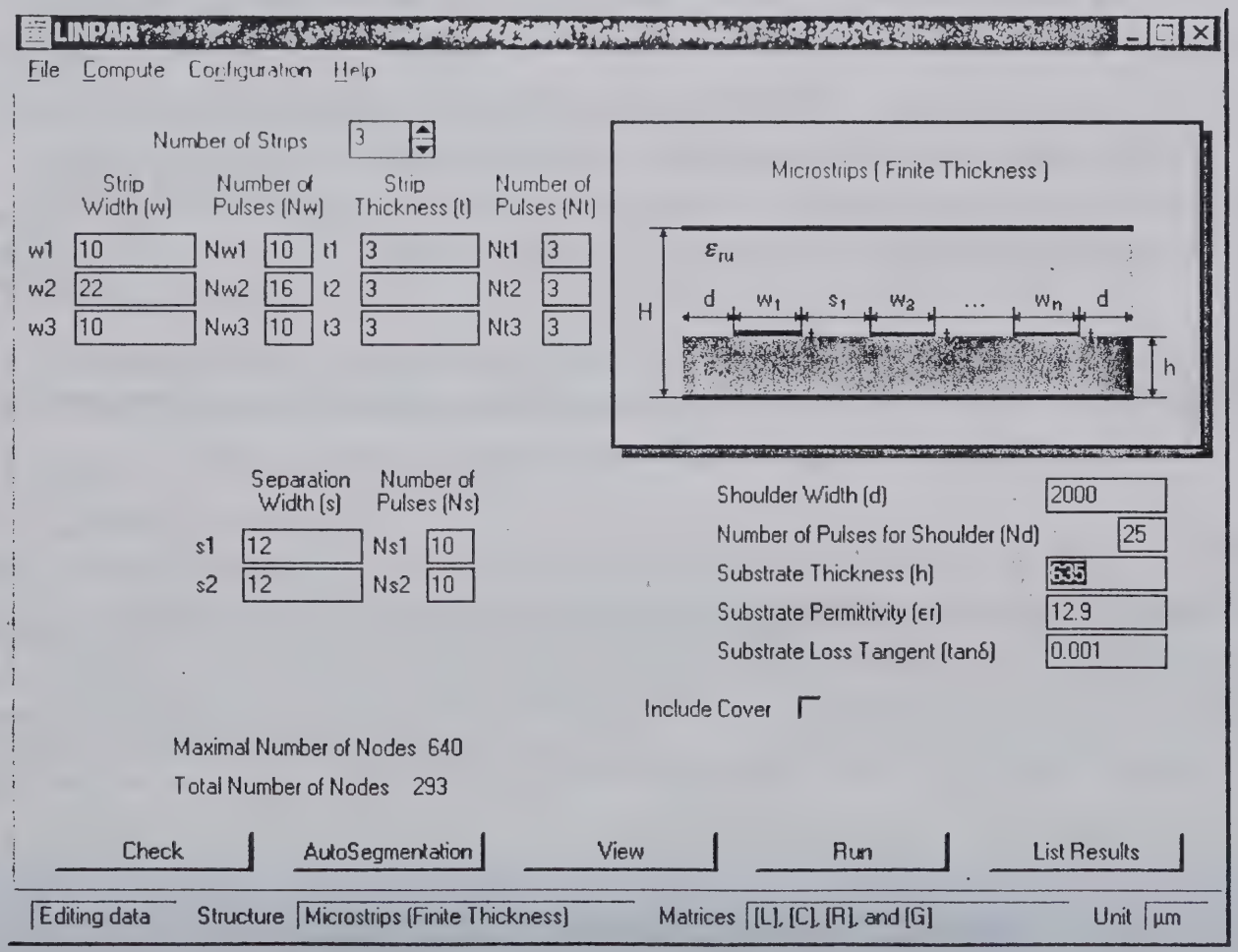
LINPAR
File Compute Configuration Help
Number of Strips 3
Strip Width (w) Number of Pulses (Nw) Strip Thickness (t) Number of Pulses (Nt)
w1 10 Nw1 10 t1 3 Nt1 3
w2 22 Nw2 16 t2 3 Nt2 3
w3 10 Nw3 10 t3 3 Nt3 3
Microstrips (Finite Thickness)
H
d w1 s1 w2 ... wn d
h
Separation Width (s) Number of Pulses (Ns)
s1 12 Ns1 10
s2 12 Ns2 10
Shoulder Width (d) 2000
Number of Pulses for Shoulder (Nd) 25
Substrate Thickness (h) 635
Substrate Permittivity (εr) 12.9
Substrate Loss Tangent (tanδ) 0.001
Include Cover
Maximal Number of Nodes 640
Total Number of Nodes 293
Check
AutoSegmentation
View
Run
List Results
Editing data
Structure Microstrips (Finite Thickness)
Matrices [L], [C], [R], and [G]
Unit µm

LINPAR Analysis

- LINPAR calculates L, C, R and G matrices for multiple coupled lines of arbitrary cross-sectional geometry. It also produces modal matrices and propagation constants.

- LINPAR performs a *quasistatic analysis*. It does not include the effects of dispersion from non-TEM modes, but it does include dispersion from finite metal conductivity.

- Is this good enough for monolithic circuit design?
  - In monolithic circuits, quasistatic analysis is adequate to well into the millimeter-wave region.
  - Metal thickness is much more significant than dispersion in most MMICs.
  - Most available coupled-line models were designed for hybrid circuits. These do not account for metal thickness accurately.
  - In many coupled-line models, the range of dimensions over which the analysis is accurate is not appropriate for MMICs.
  - By accounting for metalization thickness, but not dispersion, we have analyzed 40-GHz Lange couplers accurately.

Analysis of Coupled-Line Baluns

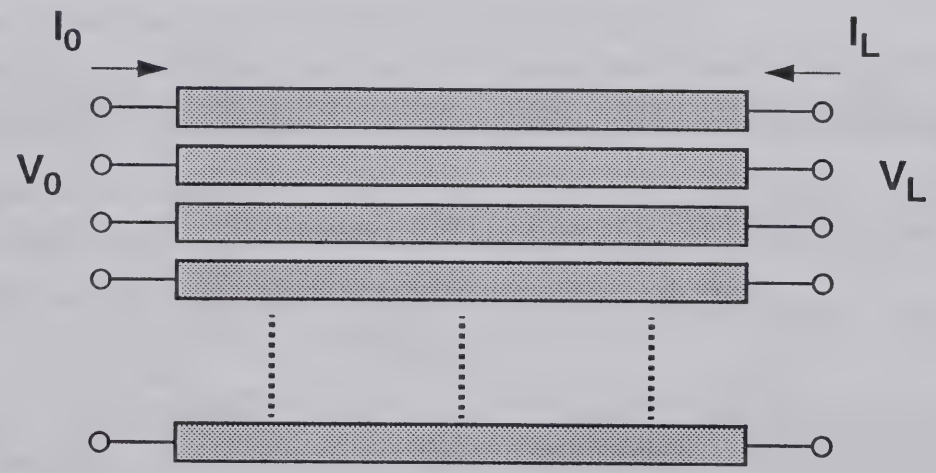

$$I_0 = S_I(1+\Gamma_{2L})(1-\Gamma_{2L})^{-1}S_V^{-1}V_0$$

$$I_L = -2S_I\Gamma_L(1-\Gamma_{2L})^{-1}S_V^{-1}V_0$$

$$\begin{bmatrix} I_0 \\ I_L \end{bmatrix} = \begin{bmatrix} Y_{0,0} & Y_{0,L} \\ Y_{L,0} & Y_{L,L} \end{bmatrix} \begin{bmatrix} V_0 \\ V_L \end{bmatrix}$$

* This gives half the Y matrix ($Y_{0,0}$ and $Y_{L,0}$). The other half is obtained through symmetries.

Modal Matrices

- **Complex magnitudes of the current and voltage modes:**

$$S_I = \begin{bmatrix} I_{1,1} & I_{2,1} & \cdots & I_{N,1} \\ I_{2,1} & I_{2,2} & \cdots & I_{N,2} \\ \cdots & \cdots & \cdots & \cdots \\ I_{N,1} & I_{N,2} & \cdots & I_{N,N} \end{bmatrix}$$

$$S_V = \begin{bmatrix} V_{1,1} & V_{2,1} & \cdots & V_{N,1} \\ V_{2,1} & V_{2,2} & \cdots & V_{N,2} \\ \cdots & \cdots & \cdots & \cdots \\ V_{N,1} & V_{N,2} & \cdots & V_{N,N} \end{bmatrix}$$

- **Propagation constants:**

$$\Gamma_L = \begin{bmatrix} \exp(\Gamma_1 L) & 0 & \cdots & 0 \\ 0 & \exp(\Gamma_2 L) & \cdots & 0 \\ \cdots & \cdots & \cdots & \cdots \\ 0 & 0 & \cdots & \exp(\Gamma_N L) \end{bmatrix}$$

Modeling and Design

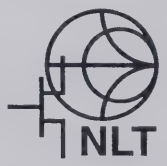

- Don't set $Z_{0e} \rightarrow \infty$ to create an ideal balun. Often the IF must propagate on the balun in an even mode, so this may open-circuit the IF.

- If the even mode is suppressed, the balun is equivalent to a floating transmission line of impedance 2 Z_{0o}. Therefore, its length is not determined by the odd mode.

- The balun behaves approximately as a shorted stub to the even mode. Therefore, it must be long enough so the even-mode output impedance is large compared to the load impedance. Thus, we have

$$Z_{0e} \tan(\beta_e l) >> Z_L$$

  Where Z_L is the load impedance, β_e is the even-mode phase-shift constant, and l is the length. This sets the minimum length of the balun, or for a given length, the minimum operating frequency.

- When $\beta_e l \rightarrow \pi$, the balun's even-mode output impedance will again be low. This establishes the upper frequency limit.

Modeling and Design
(Continued)

- The tapered coax-to-suspended substrate balun is difficult to model.
  - * Clearly, the coaxial line does not excite equal even and odd modes (virtually all even- and odd-mode analysis assumes equal mode excitation.
  - * It is difficult to say how much of each mode is excited; this is essential for modeling the transition.
  - * FEM analysis may be necessary to model this transition adequately.
  - * Assuming equal even and odd modes causes predicted performance to be *much worse* than actual performance! In this case, performance of the real circuit is *better* than the theoretical prediction.

- A microstrip-to-parallel strip transition excites equal even and odd modes. This is one reason why the microstrip version of this balun is much worse than the suspended-substrate version.

Star Mixer

Conventional suspended-Substrate Circuit

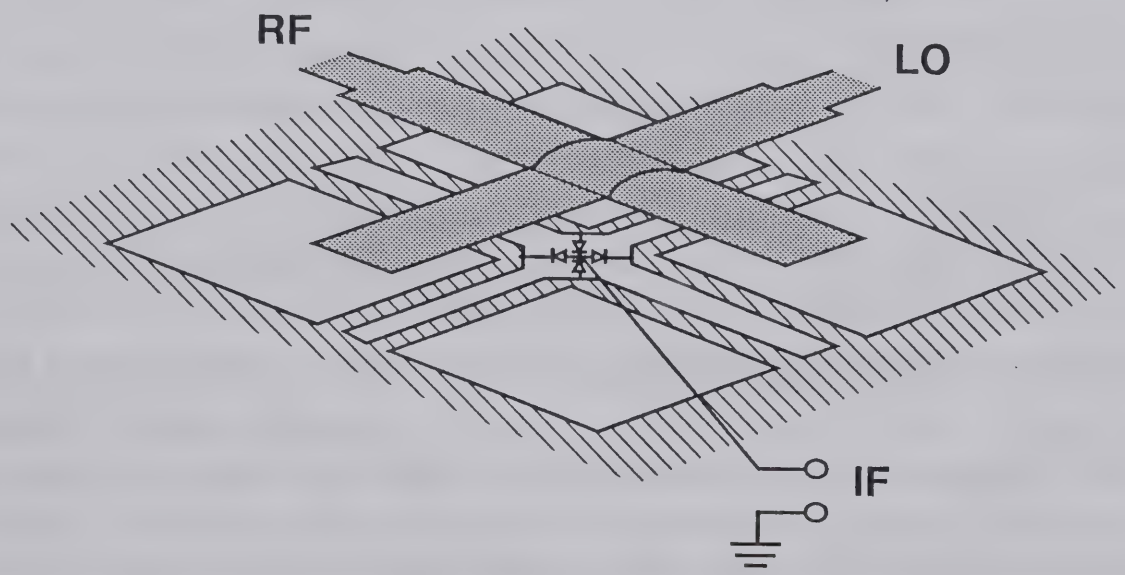

* Invariably realized on a composite ("Duroid") suspended substrate.
* Doesn't work well if a high-ε_r substrate is used; mismatched phase velocities causes poor balun performance.
* IF is on the opposite side from the RF & LO; sometimes a practical difficulty.
* There are no commercial star diode quads; must use two "tee" diodes.

Microstrip Star Mixer

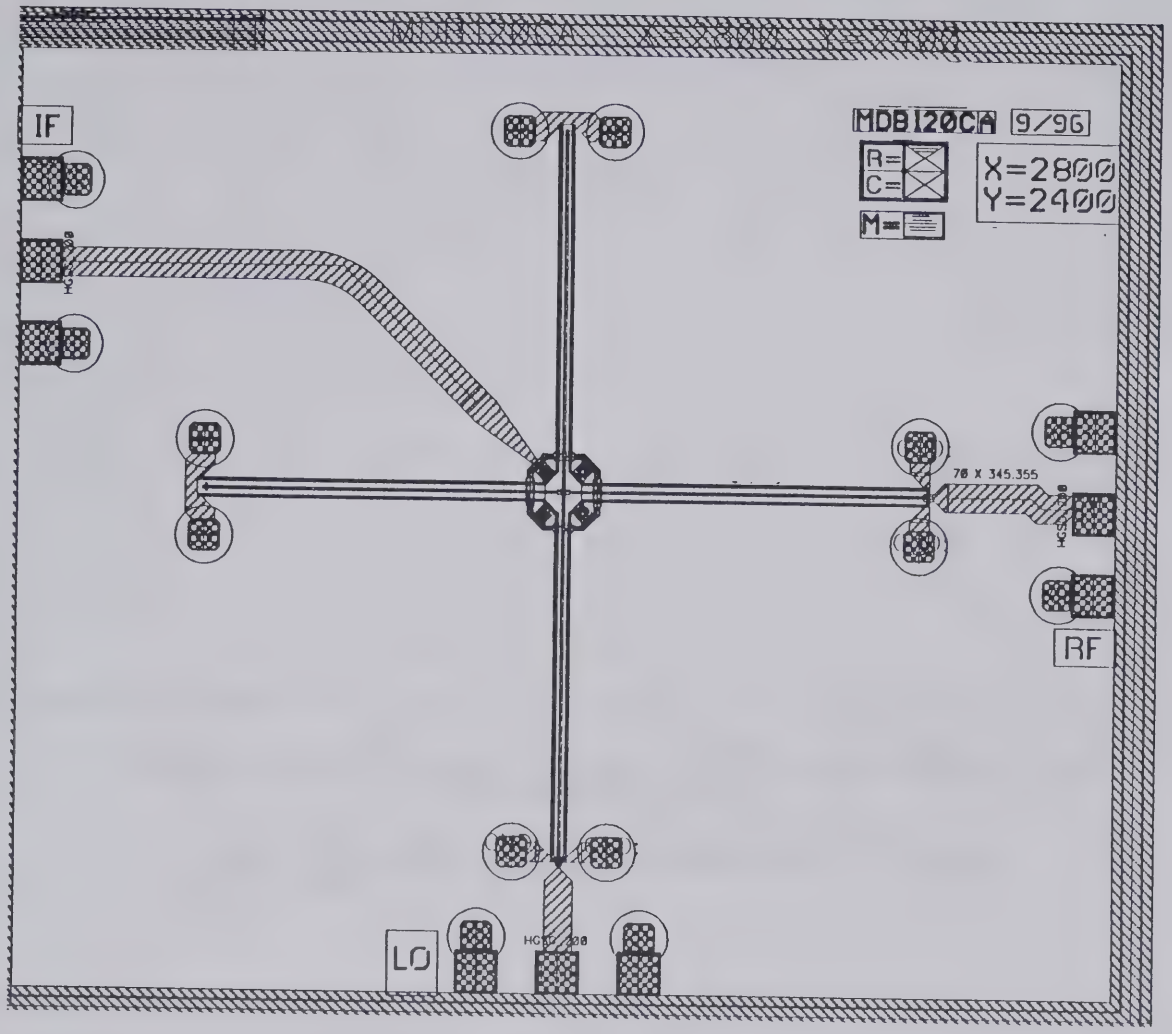

Star Mixer Conversion Loss

LSB Upconverter; IF=28 GHz, LO=29-46 GHz

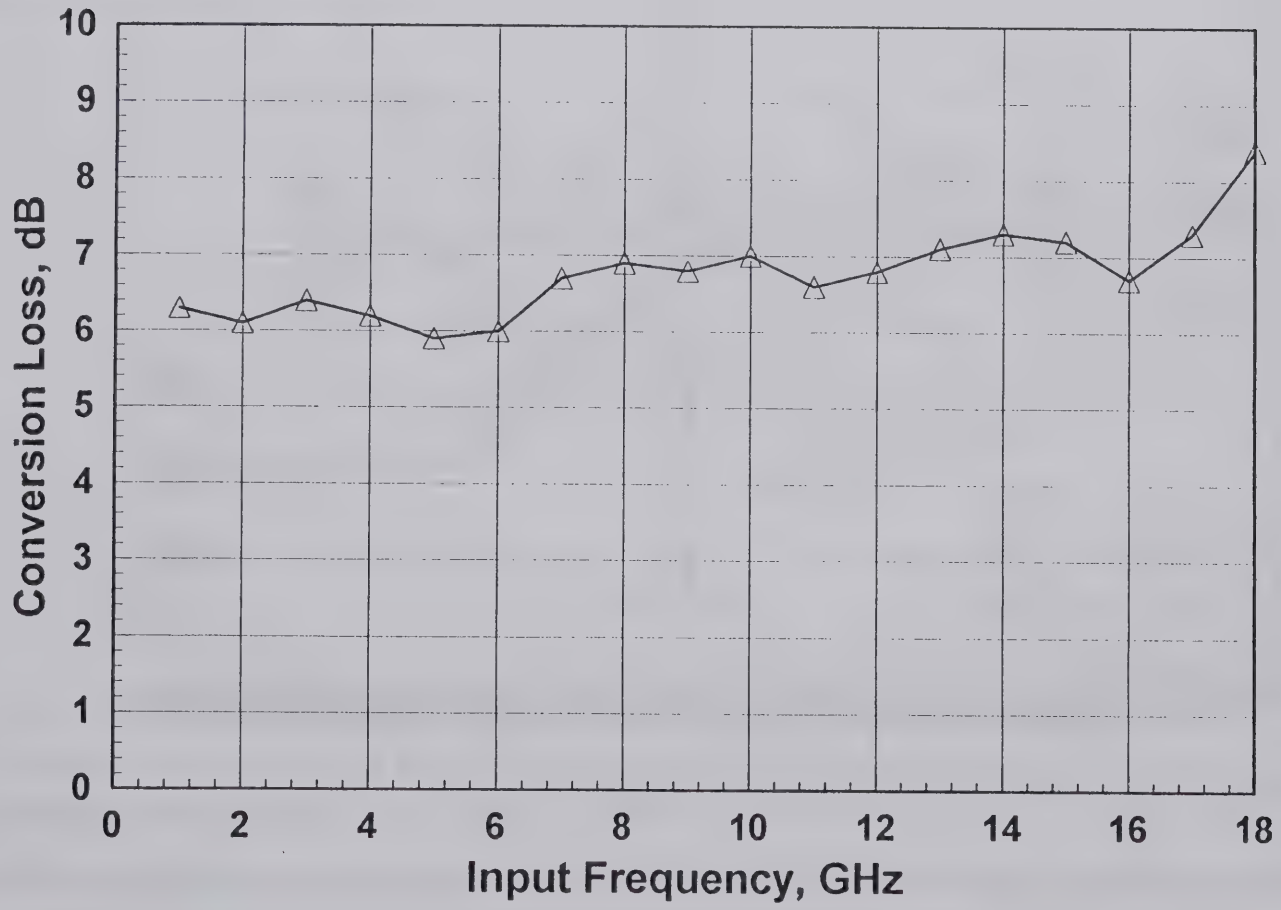

Star Mixer LO-to-RF Isolation

P_{LO} = +16 dBm

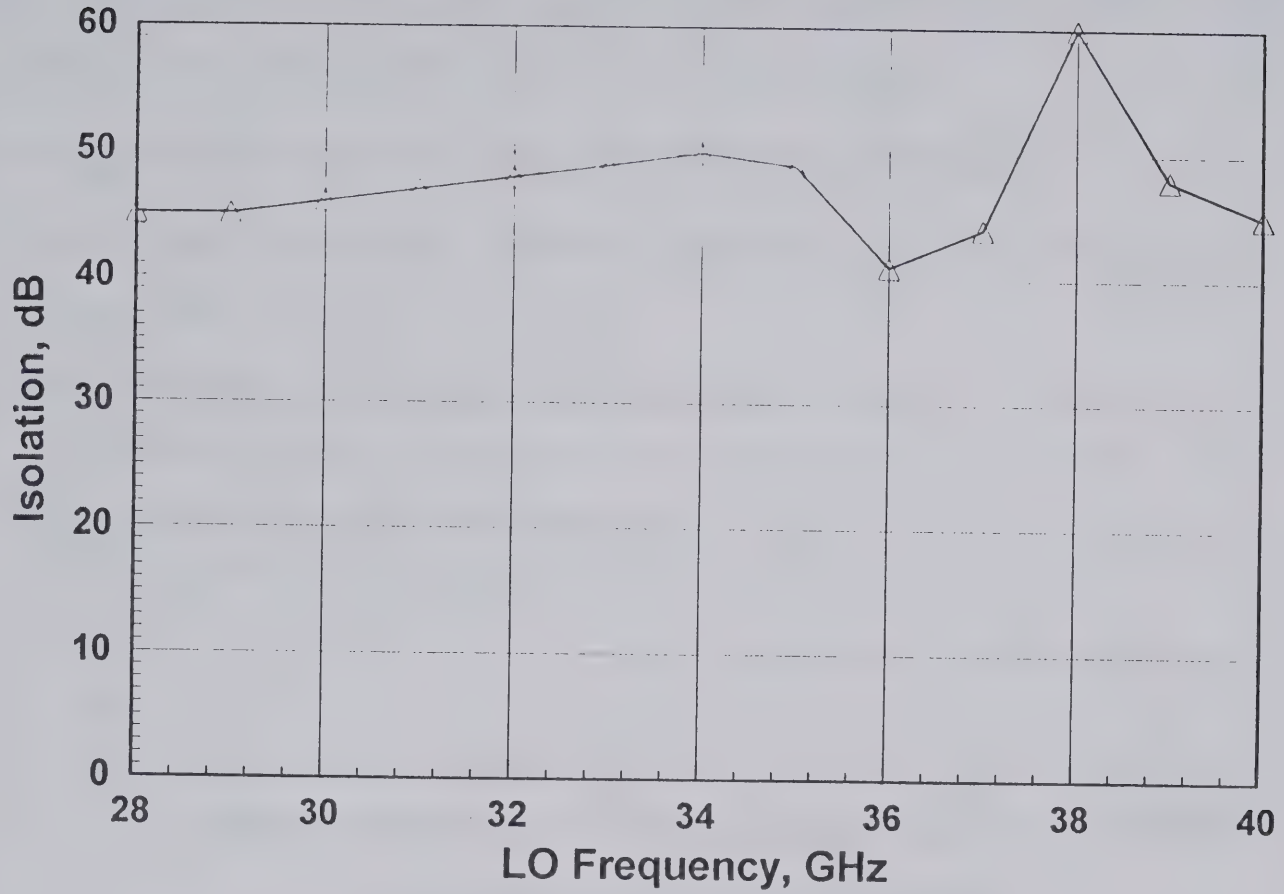

Star Mixer Output IP3

LSB Upconverter, f_{out}=22.1 GHz, P_{LO} = +16 dBm

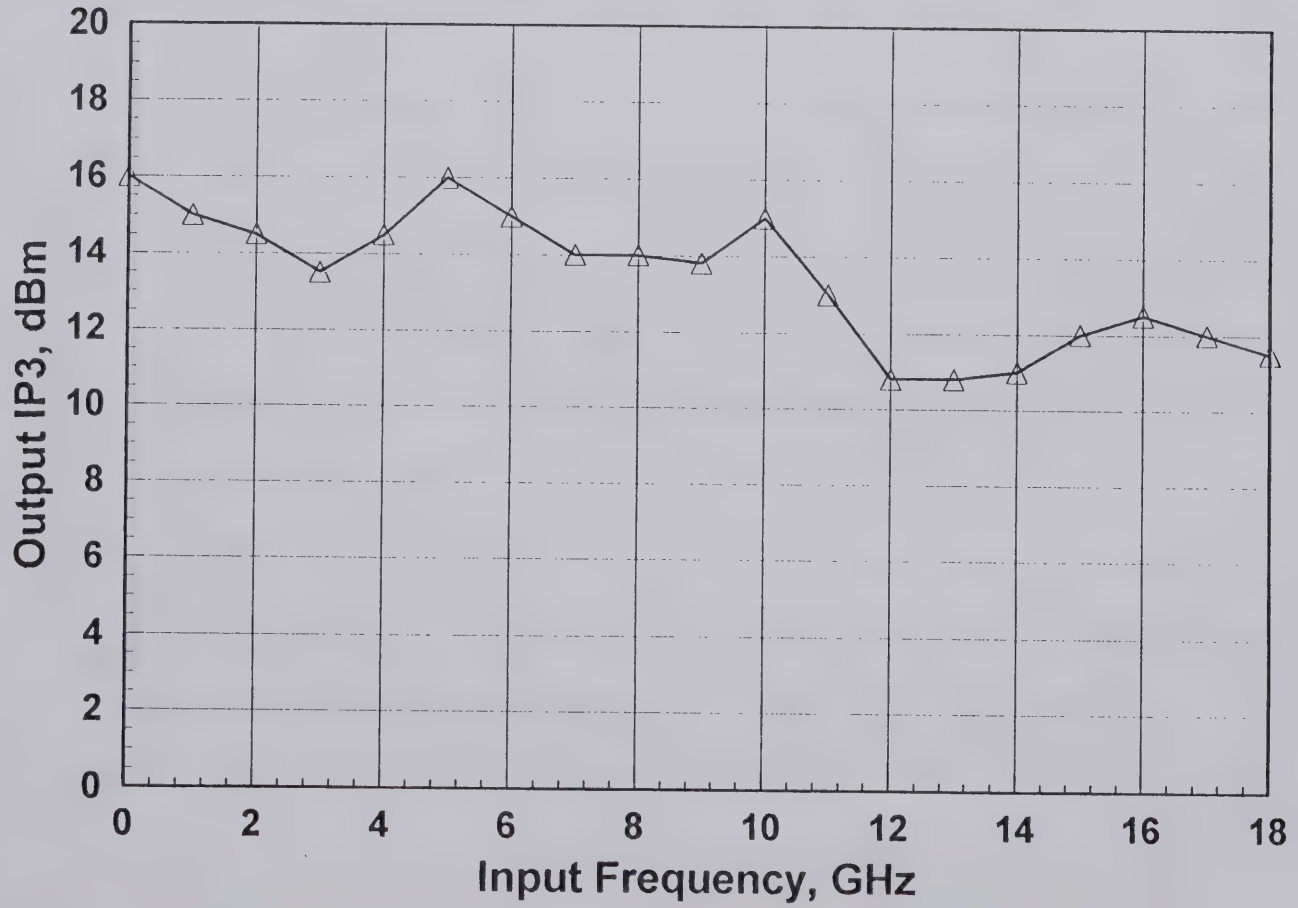

Diodes

- Diodes are not as critical as one might think.
- We have done surprisingly well with poor devices.
- First 26-40 GHz mixers used FET gate-to-channel junctions.
  - * f_c ~ 250 GHz.
- Most mixers now use an "HBT" diode.
  - * Schottky diode fabricated on the collector mesa of an HBT.
  - * f_c ~ 1500 GHz (RF measurement).
  - * Still not optimum: collector doping is quite light.

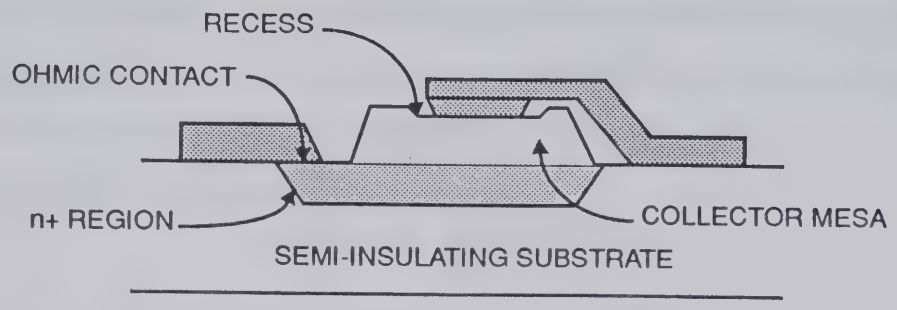

New Balun

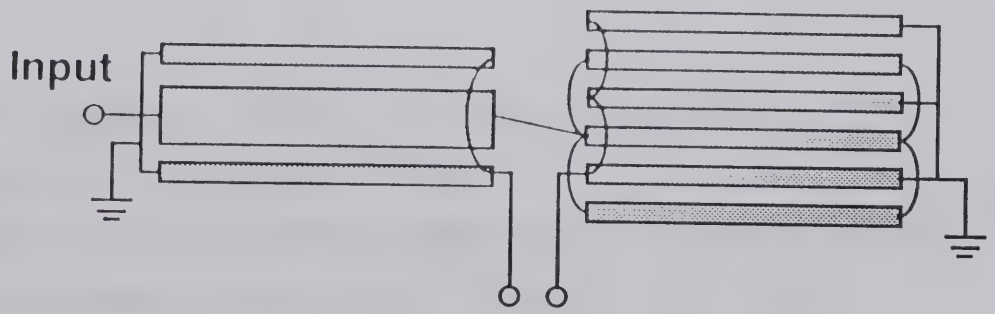

- Input section is similar to the earlier design
- Second section has 6 strips, equal width and spacing.
  - * Z_{0o} = 11 Ω, Z_{0e} = 95 Ω
- Losses in the coupled lines:
  - * Measure transmission-line sections with an automated network analyzer.
  - * Determine the conductivity from transmission-line loss.
  - * Use this value of conductivity in the analysis.

Ring Mixer

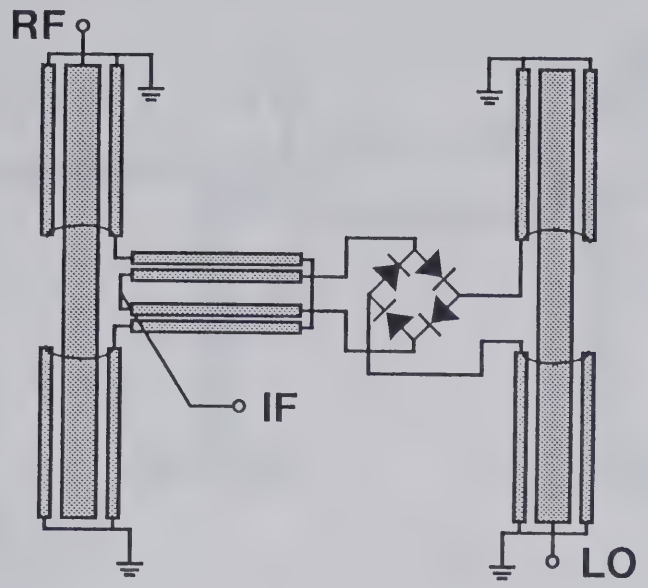

* This circuit is similar in concept to commercial, suspended-substrate mixers.
* Additional section in the RF balun improves the balance and provides an IF output.
* In practice we use multiple coupled lines throughout.
* LO and RF baluns can have different center frequencies
* IF band can overlap the RF band somewhat.

Ring Mixer

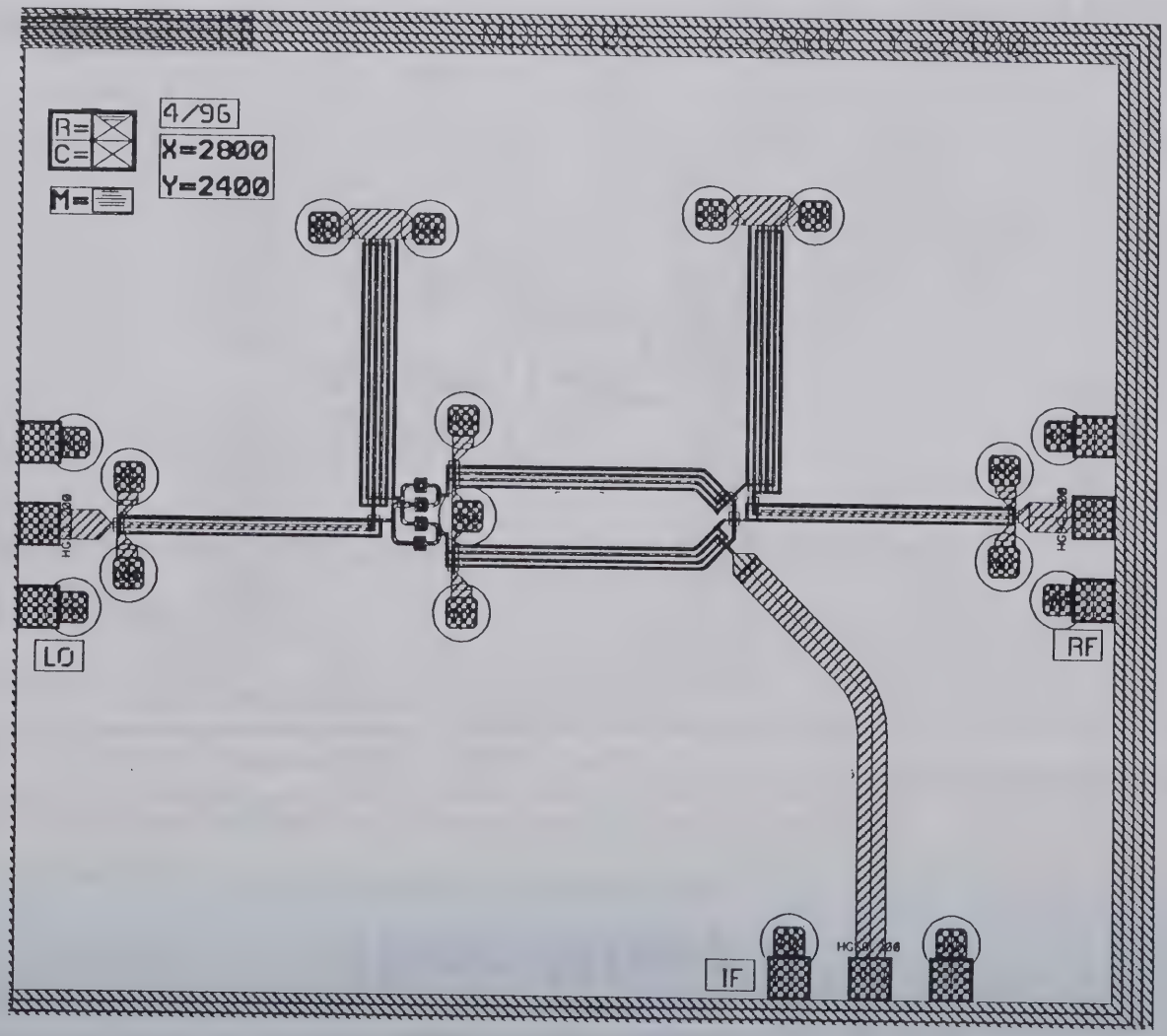

Calculated Balun Performance

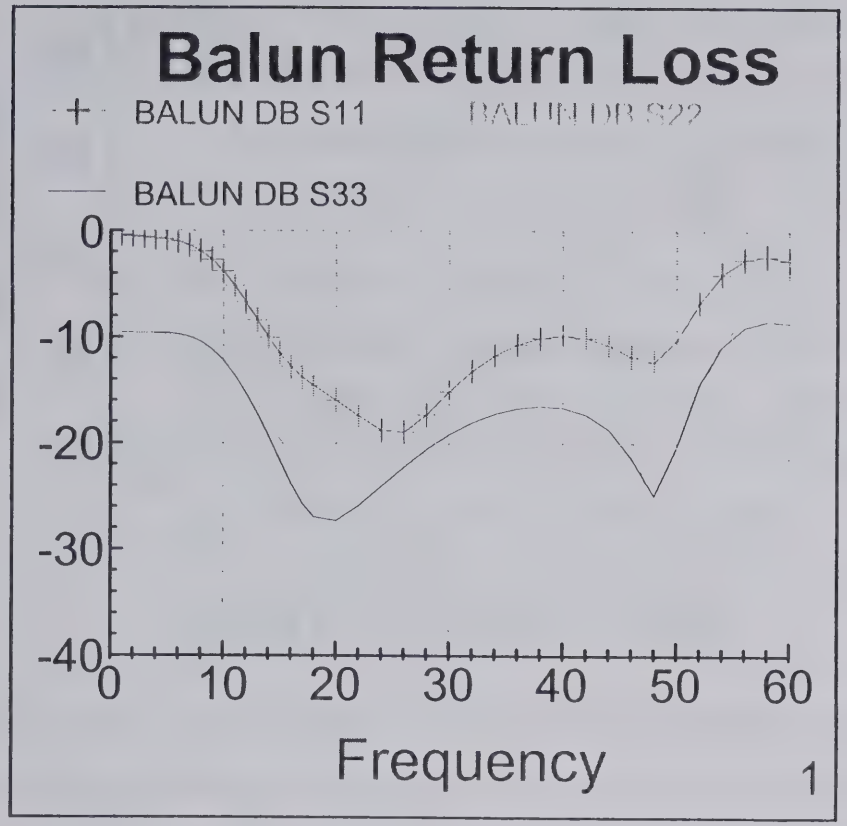

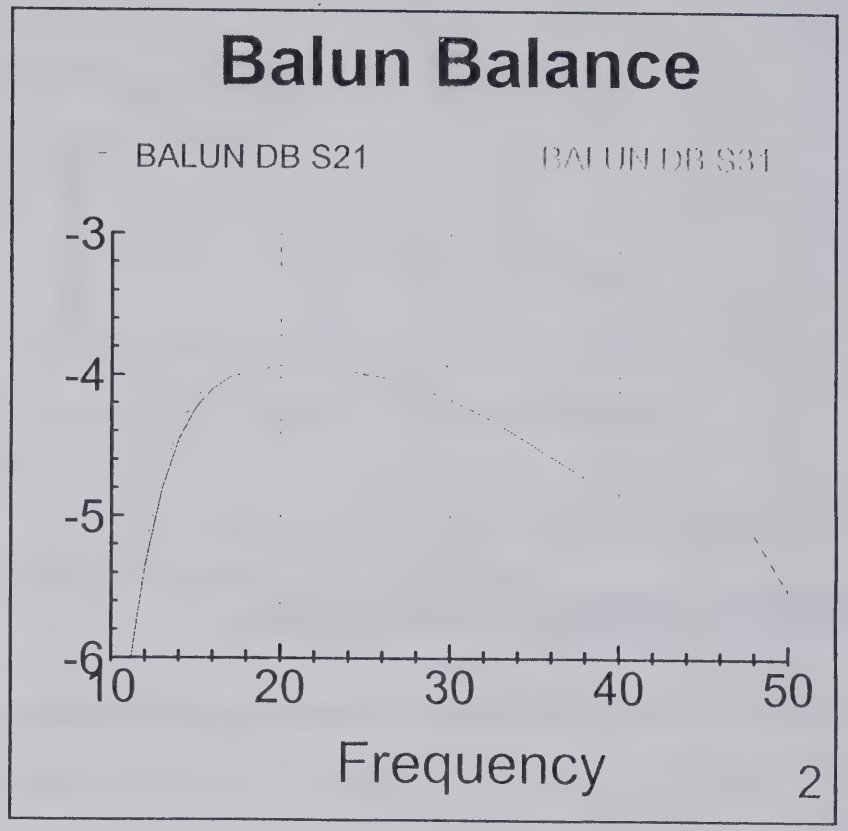

Measured Balun Performance

Port Return Loss

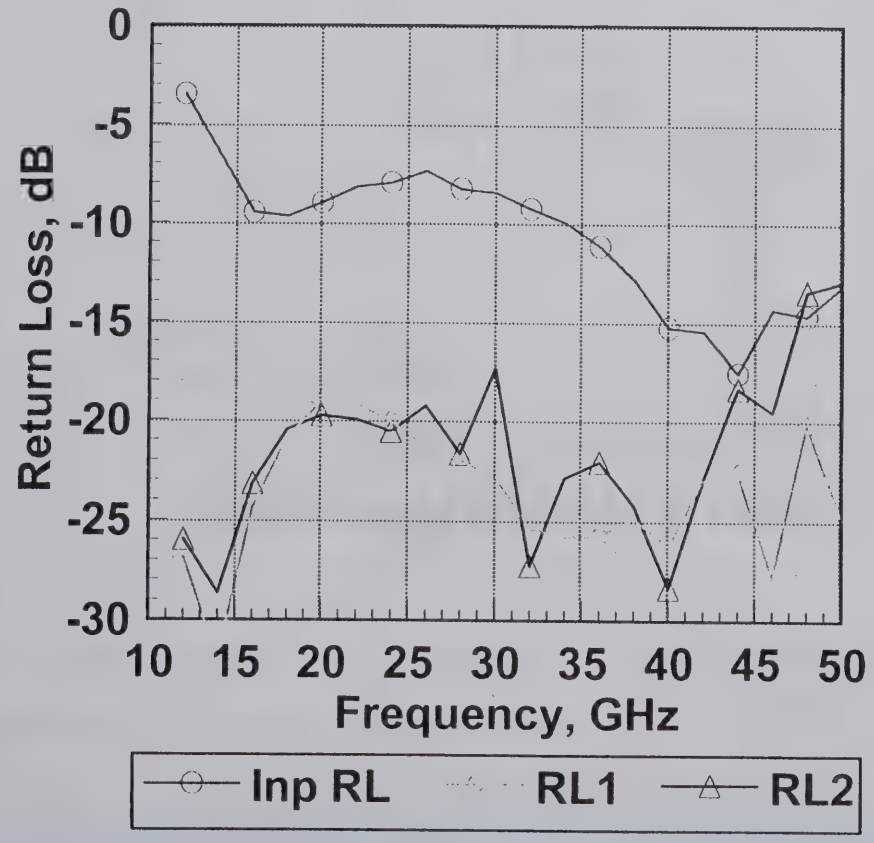

Input-to-Output Loss

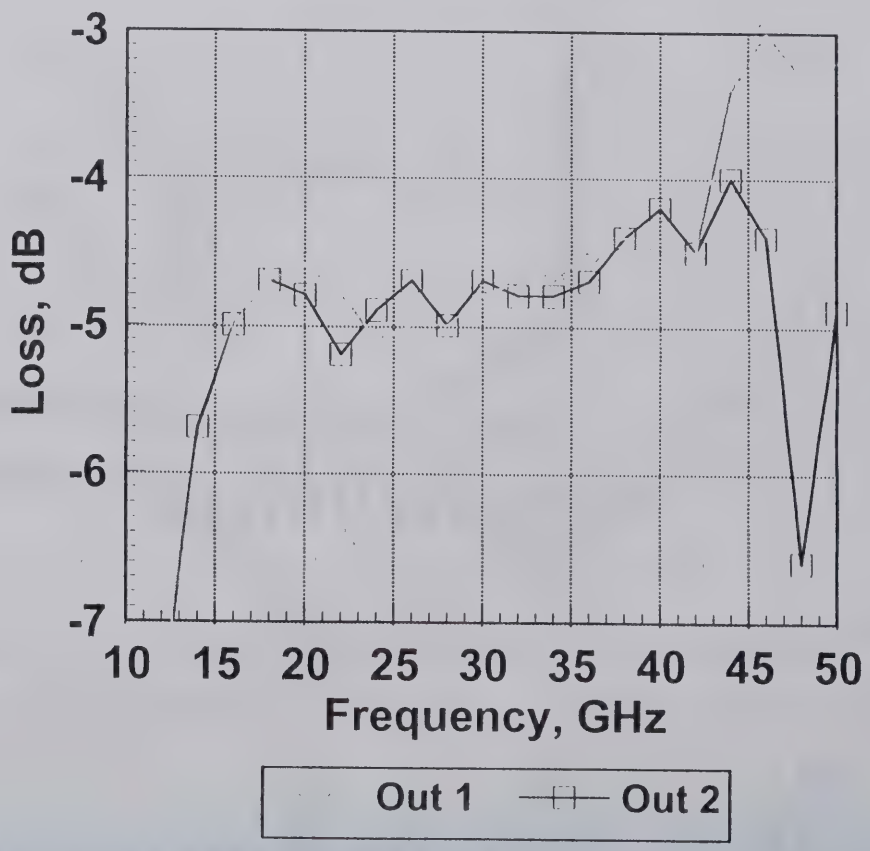

Mixer Simulation

- C/NL2: Microwave circuit simulator
  - * Runs on Intel platforms under Windows 95, Windows NT, and Win32s
  - * Includes linear analysis and static Volterra series
  - * Published by Artech House
- C/NL2 Harmonic-balance version
  - * Runs on Sun Sparcstations under Solaris 2.5 (Open Look).
  - * Includes all capabilities of the Windows version, plus harmonic-balance analysis and time-varying Volterra analysis.
  - * Conversion-loss analysis uses incremental ("conversion matrix") methods.
  - * Capabilities include analysis of mixer intermodulation distortion.

Incremental Methods

- In a mixer, we usually have a large signal (LO) and one or more small RF excitations.
- The system is *incrementally* nonlinear; i.e., the deviation from the large-signal response, at any instant, is a small signal.
  - * This characteristic can be used to simplify the problem enormously.
- Example: Diode Voltage

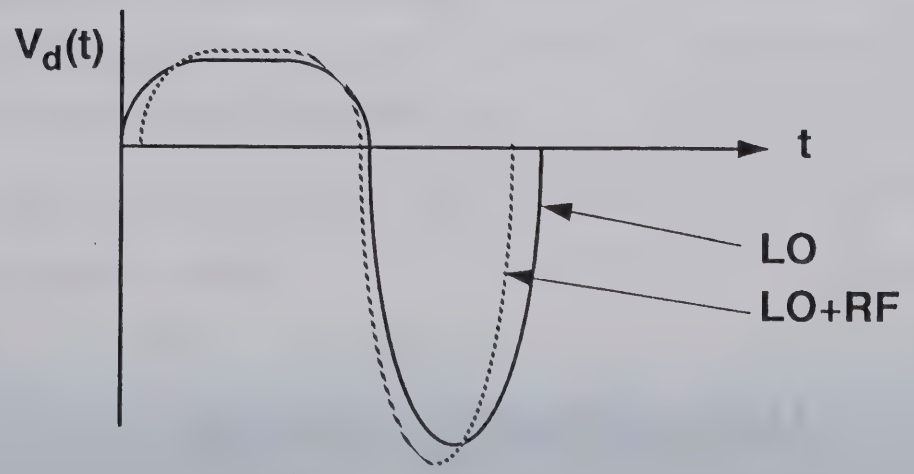

Single-Diode Mixer

Two-Tone IM; 16 LO Harmonics

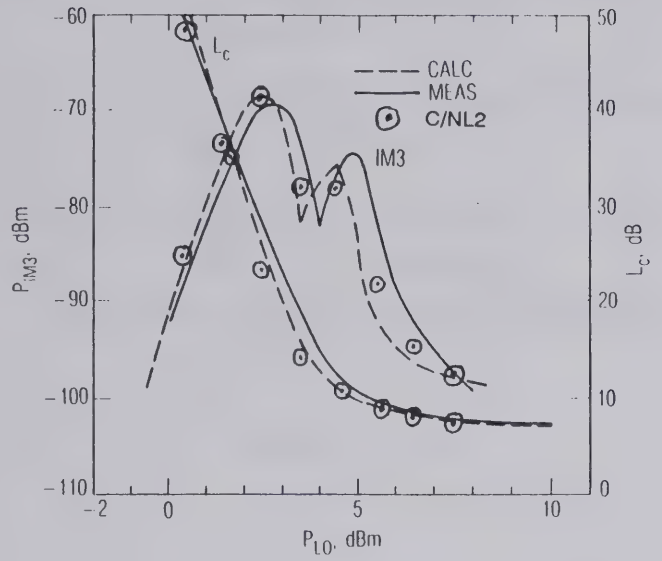

Third order ($2f_2$-f_1) and L_c

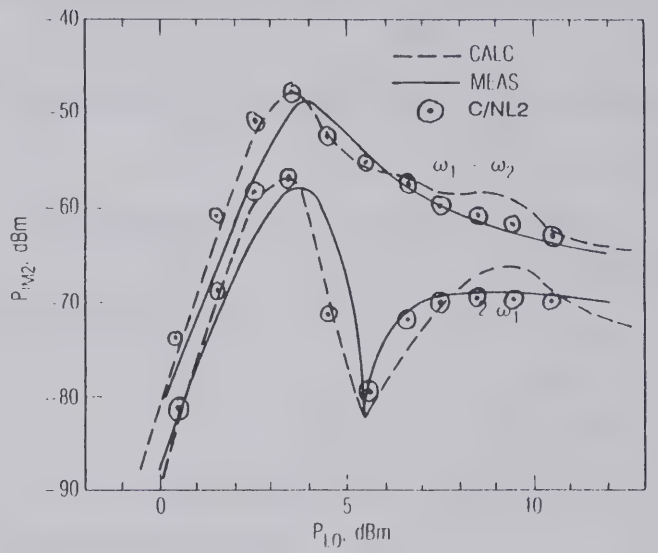

Second Order

Star Mixer Lc & IP3H

PLO = +16; USB Downconverter

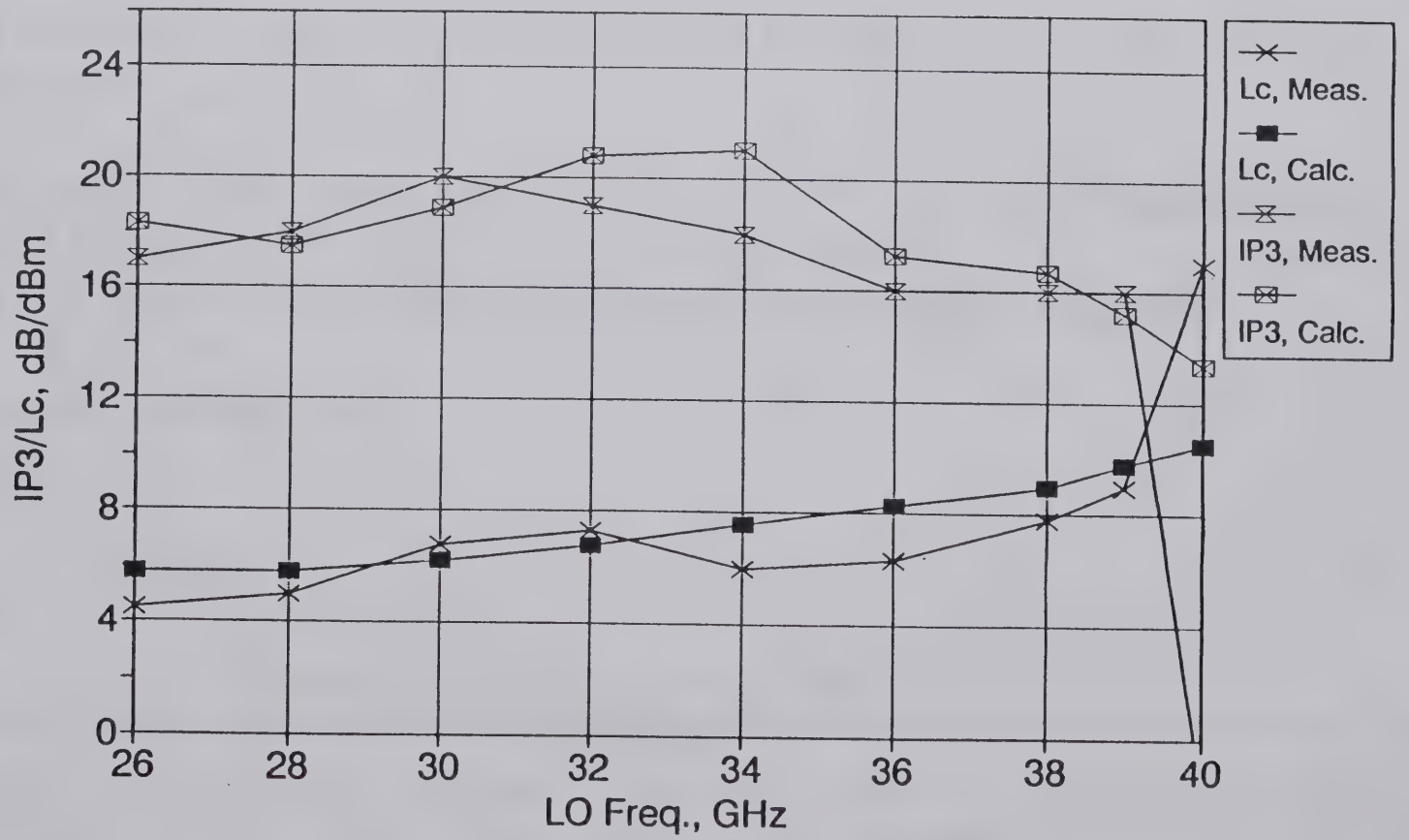

Conclusions

- Balun design is the key to successful broadband mixer design.
- Two approaches have been successful:
  - * Marchand baluns: tolerant of low even-mode impedance in the coupled-line sections.
  - * Spiral baluns: achieve high even-mode impedance through high even-mode inductance.
- High-performance octave-band mixers have been fabricated on GaAs.
- Two-octave bandwidths are theoretically possible.

Behavioral Analysis Methods Applied To The Design & Simulation of Linear Power Amplifiers

Joe Staudinger

Motorola

Semiconductor Products Sector

Tempe, AZ 85284

August 9, 1998

Acknowledgments

George Norris

Richard Sherman

Gary Sadowniczak

Monica C de Baca

Steve Shaw

Bill Knappenberger

Outline

1) Overview
   - Why The Interest In Behavioral Modeling & Simulation
2) Behavioral Model
   - Description & Implementation
   - Issues: Representing Transfer Function via Series Expansion
     Choice of Basis Functions, How Many Terms
     Source/Load Harmonic Terminations, Sub-Harmonics
   - Single Stage PA Excited W/ 2 Tone Sinusoidal Stimulus
     HB Simulated am-am & am-pm Response For Behavioral Model
3) Validation Studies - Comparison of Measurements to Behavioral Model Predictions
   - HEMT Based Power Amplifier
     Use Measured am-am & am-pm Response For Behavioral Model
     Stimuli: 2 Tone Sinusoidal,
     $\pi/4$ DQPSK Stimulus Compliant to NADC
     O-QPSK Stimulus Compliant to CDMA
4) Conclusions

Overview

- 2nd Generation Cellular and PCS

  Digital Modulation in 2 G systems, e.g., PDC, NADC, CDMA, ... π/4 DQPSK, O-QPSK

  Amplitude of Modulated Envelope Is Not Constant

  Require Linear PAs Rather Than Saturated Ones

  Optimal PA Performance ➜ Battery Life, Longer Talk Time, Lighter, Smaller ...

  Harmonic Balance & SPICE Are Ill Suited For Digitally Modulated Signals

  Spice: ➜ Very large number of time samples to represent even small data sequence

  HB: ➜ Large number of frequency components

  Conventional Simulation Tools ➜ Intermodulation Distortion w/ 2 Tone Signal

  Two Tone Signal Is Different Than a Digitally Modulated Signal

  Correlation Between IMD & ACPR Are Difficult Is Best

Behavioral Model

- Behavior Modeling Approach
  - ➜ Transfer Function Representation Of Non-Linearity
    - Quadrature Model - - - Many Advantages
    - Common To Communications Systems Analysis
    - Accommodates Sinusoidal & Digitally Modulated Signals
    - Effective PA Design Tool, Computationally Efficient
    - Prediction: Output Power, Distortion Components
      - Efficiency, Gate & Drain current

- Assumptions/Requirements
  - Narrowband Signals (Signal BW, Carrier Freq, I/O Matching Circuitry)
  - Circuit/Device Non-Linearity is Memoryless

Behavioral Model

(Based on the work of Kaye *et at.*, [1])

Consider a Narrowband Signal

$$v_{in}(t) = V(t)\cos(\omega_o\ t + \Theta(t))$$

where ω_o is the carrier frequency
V(t) is the low pass envelope voltage (amplitude modulation)
Θ(t) describes phase characteristics (phase modulation)

Alternatively, the signal can be expressed in I/Q format

$$v_{in}(t) = \mathrm{Re}\left[(V_i(t) + jV_q(t))e^{j\omega_o t}\right]$$

where *Vi*(t) is the in-phase voltage component of the envelope
Vq(t) is the quadrate-phase voltage component of the envelope

[1] A. R. Kaye, D. A George, M. J. Eric, "Analysis and Compensation of Band pass Non-linearities," IEEE Transactions on Communications, vol. COM-19, October 1972, pp. 965-972.

[2] Jeruchim, Balaban, Shanmugan, Simulation of Communication Systems, Plenum Press, 1992

Behavioral Model

Assumptions:

1st zonal components (Bandpass)

Non-linearity - Memoryless - Time invariant - Frequency independent

$$v_{out}(t) = \mathrm{Re}\left\{ G(V(t))\ e^{j\{\Theta(t) + \varphi(V(t)) + \omega_o t}\right\}$$

G(V(t)) ➜ input-output envelope voltage
φ(V(t)) ➜ phase characteristics

Or in Quadrature Form:

$$v_{out}(t) = \mathrm{Re}\left\{ \left[G_i[V(t)] \langle V_i(t) + jV_q(t) \rangle + jG_q[V(t)] \langle V_i(t) + jV_q(t) \rangle \right] e^{j\omega_o t} \right\}$$

$$\left.\begin{aligned} G_i(V) &= G(V)\cos(\varphi(V)) \\ G_q(V) &= G(V)\sin(\varphi(V)) \end{aligned}\right\}$$ **Amplitude Only Transfer Functions**

Behavioral Model - Implementation

- Functional Representation of Transfer functions G_i, G_q, G_d, & G_g

  Consider series expansions of Bessel & Polynomial Basis Functions

  Bessel expansion:

$$G_i(A) = \sum_{k=odd}^{2M+1} a_k J1(k A \xi) \qquad G_q(A) = \sum_{k=odd}^{2M+1} b_k J1(k A \xi) \qquad G_d(|A|) = \sum^{M} b_k (|A| \xi)^k$$

  Polynomial expansion

$$G_i(A) = \sum_{k=odd}^{2M+1} a_k (A \xi)^k \qquad G_q(A) = \sum_{k=odd}^{2M+1} b_k (A \xi)^k \qquad G_d(|A|) = \sum^{M} c_k (|A| \xi)^k$$

- G_i & G_q are odd functions
- Coefficients can be extracted via least squares methods

  various methods, e.g, orthogonal equation, Q/R, SVD, ...

  Some methods are more robust than others

Behavioral Model - Issues

Issues:

- What Type of Series Basis Functions Should Be Used
- How Many Terms Are Needed

Example:

- Consider PA am-am & am-pm Response (Via Harmonic Balance Simulations)

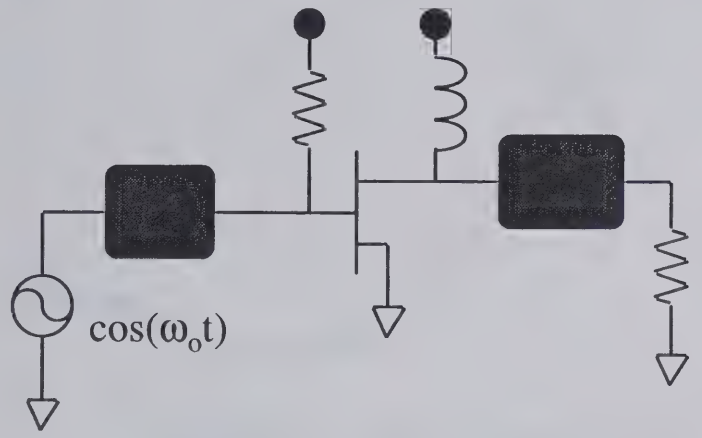

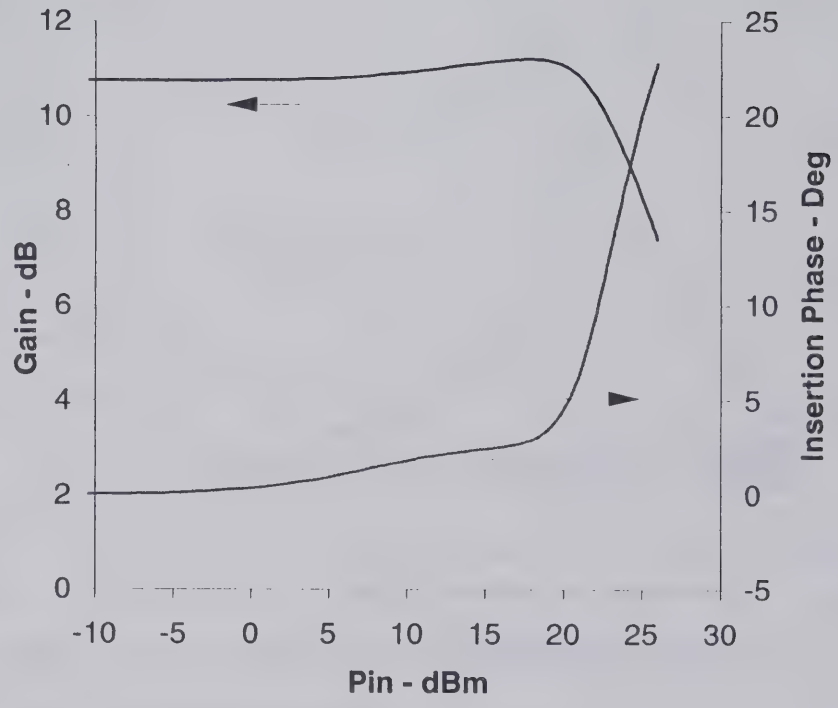

Behavioral Model - Issues

(Type of series basis function & how many terms are needed)

- Consider Odd Order Series Expansions of Bessel & Polynomial Functions
- M=5, i.e., 6 term series, a_1,a_3, a_5, a_7, a_9, a_{11}

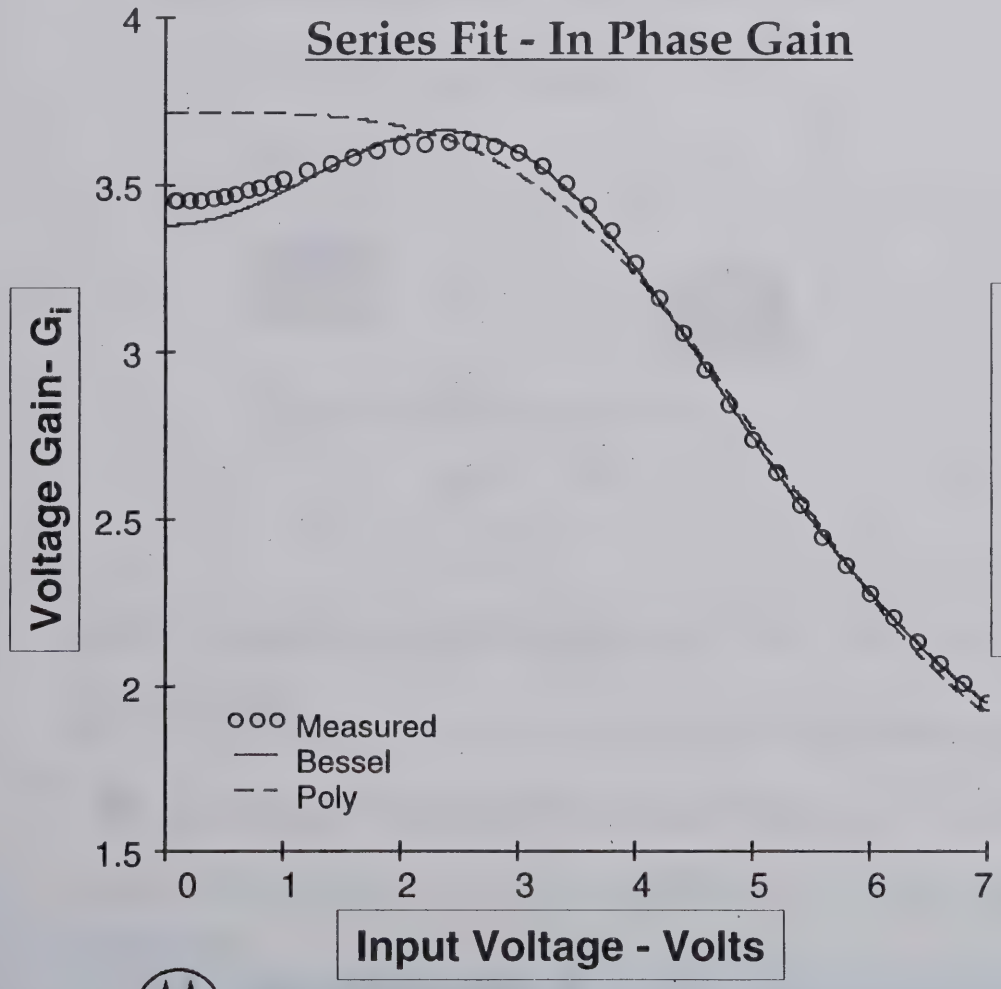

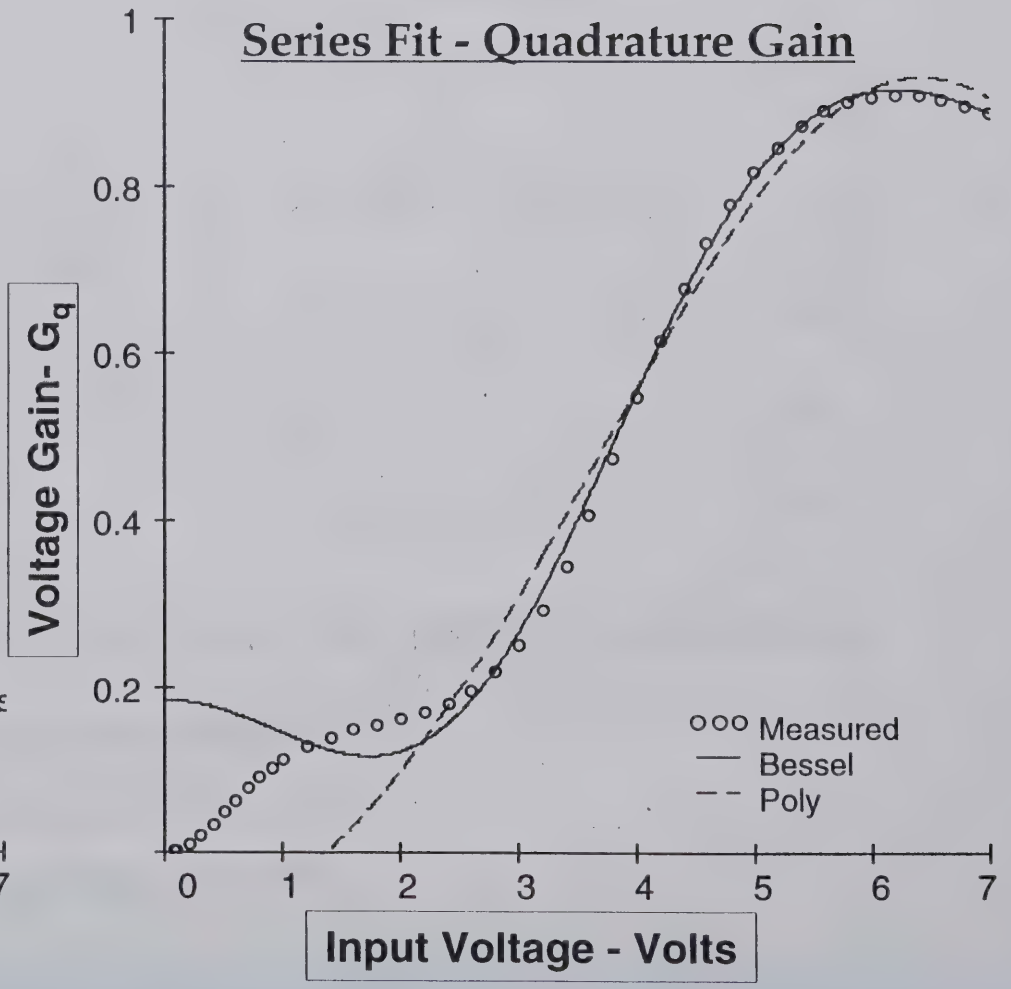

Behavioral Model - Issues

(Type of series basis function & how many terms are needed)

- Higher Order Series Generally Fit Data Better
- M=15, i.e., 16 terms, $a_1, a_3, a_5 \ldots . a_{31}$

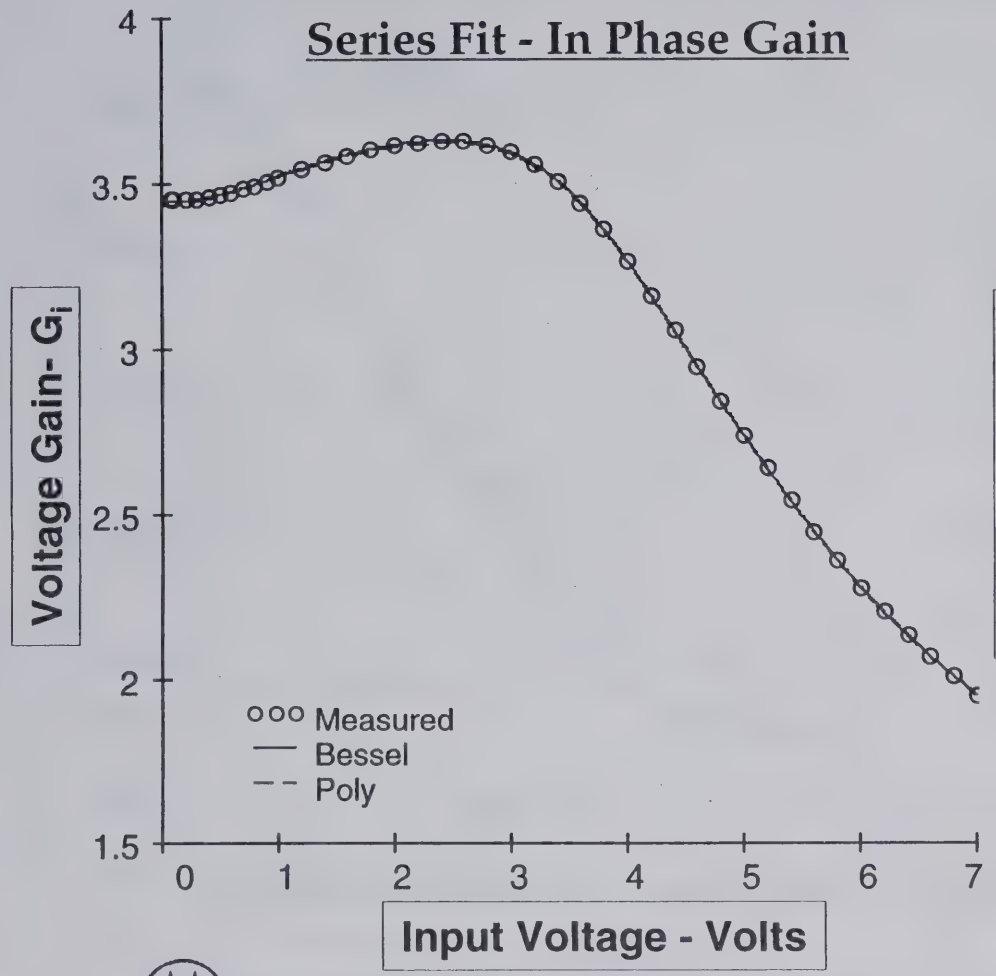

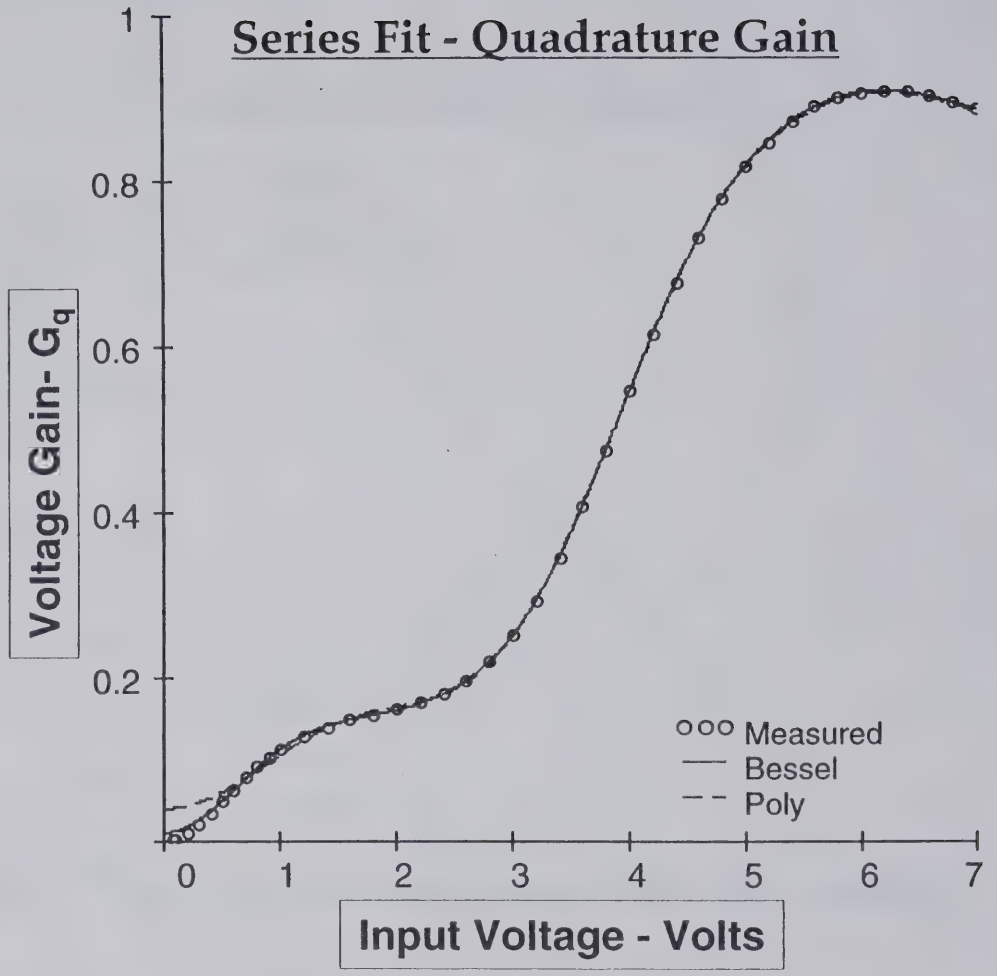

Behavioral Model - Issues

(Type of series basis function & how many terms are needed)

- Series expansion for supply current

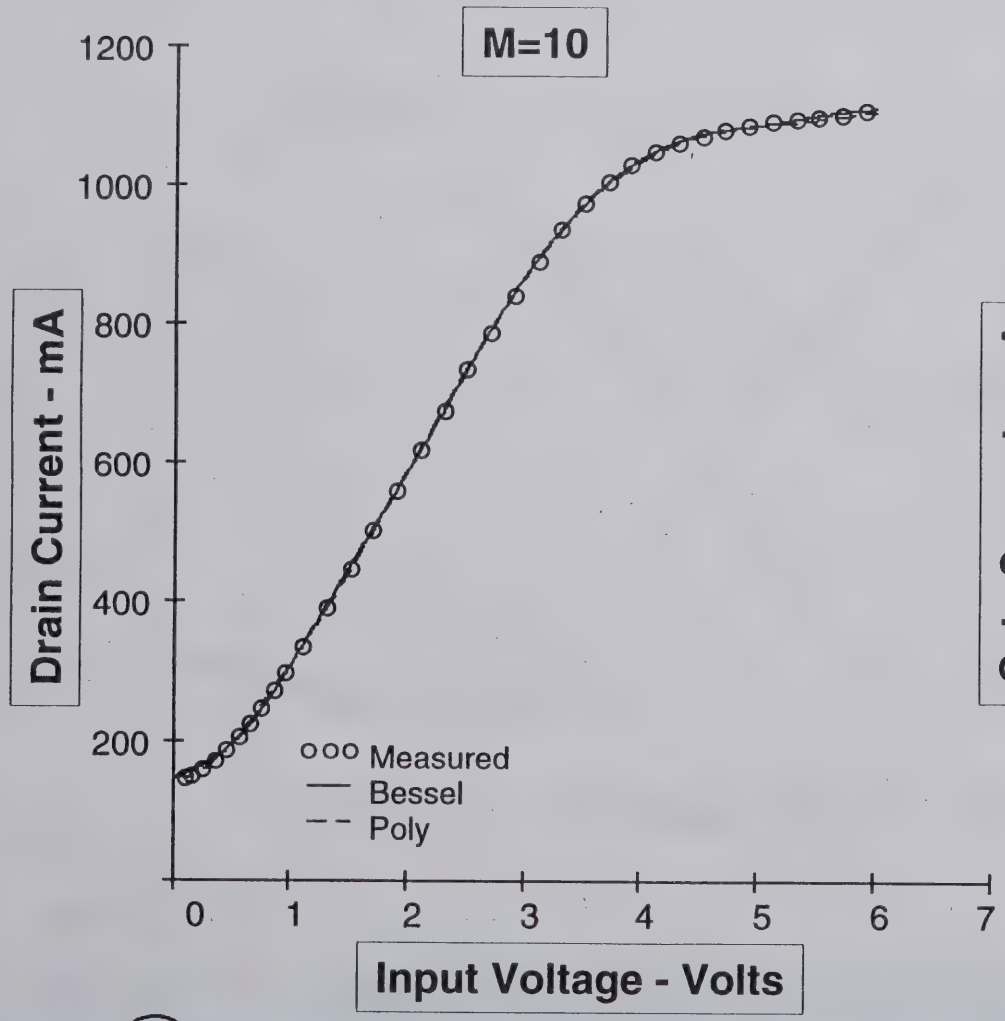

- Splines work well for gate current

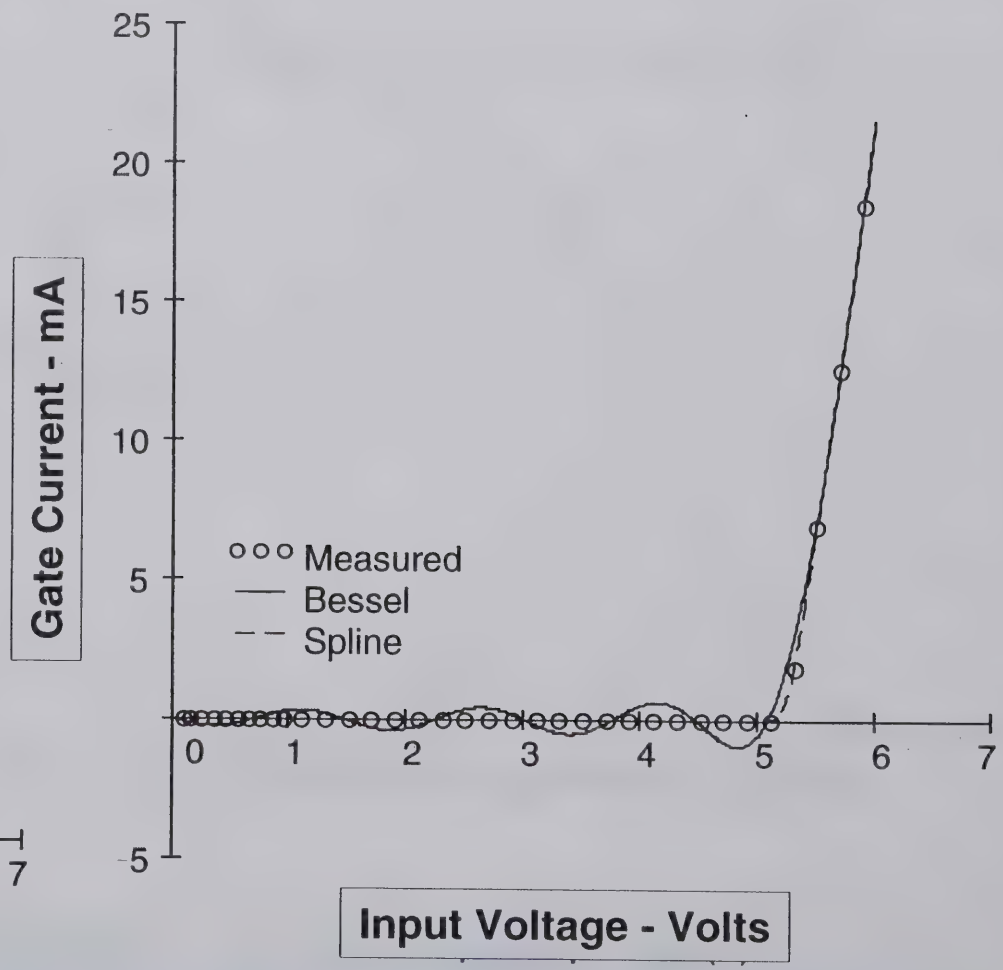

Behavioral Model - Issues

(Type of series basis function & how many terms are needed)

Residuals Resulting From Fitting Series Expansion

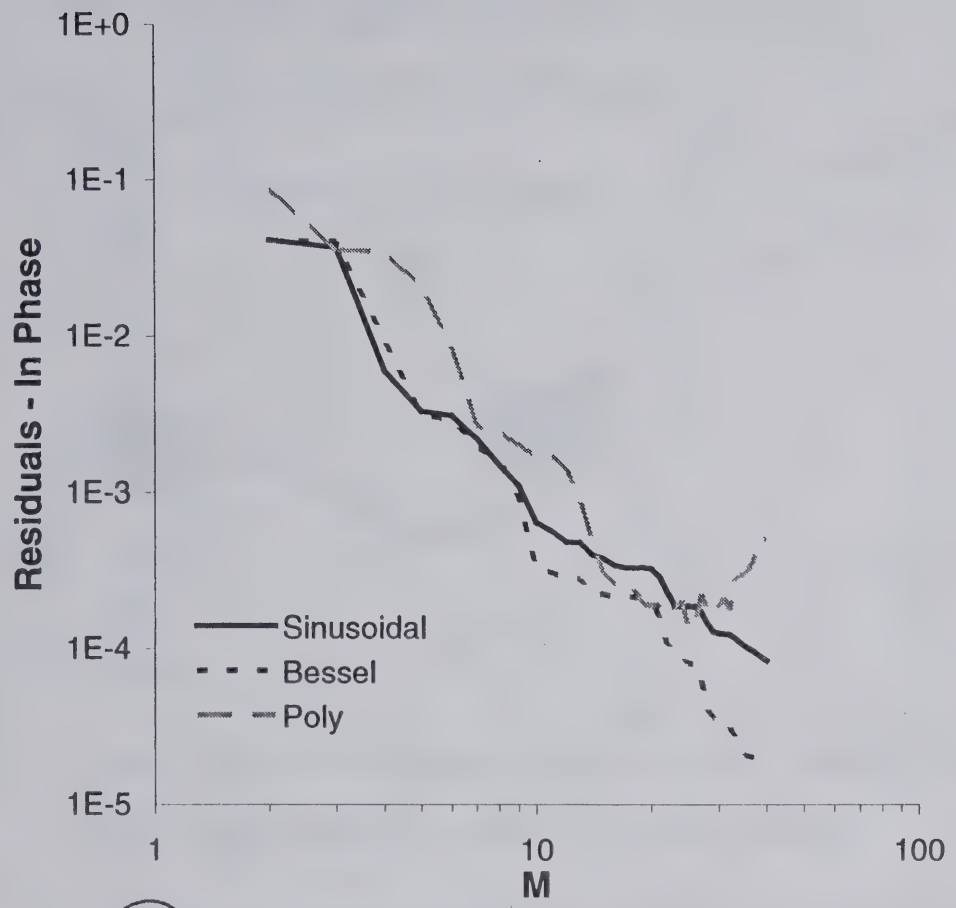

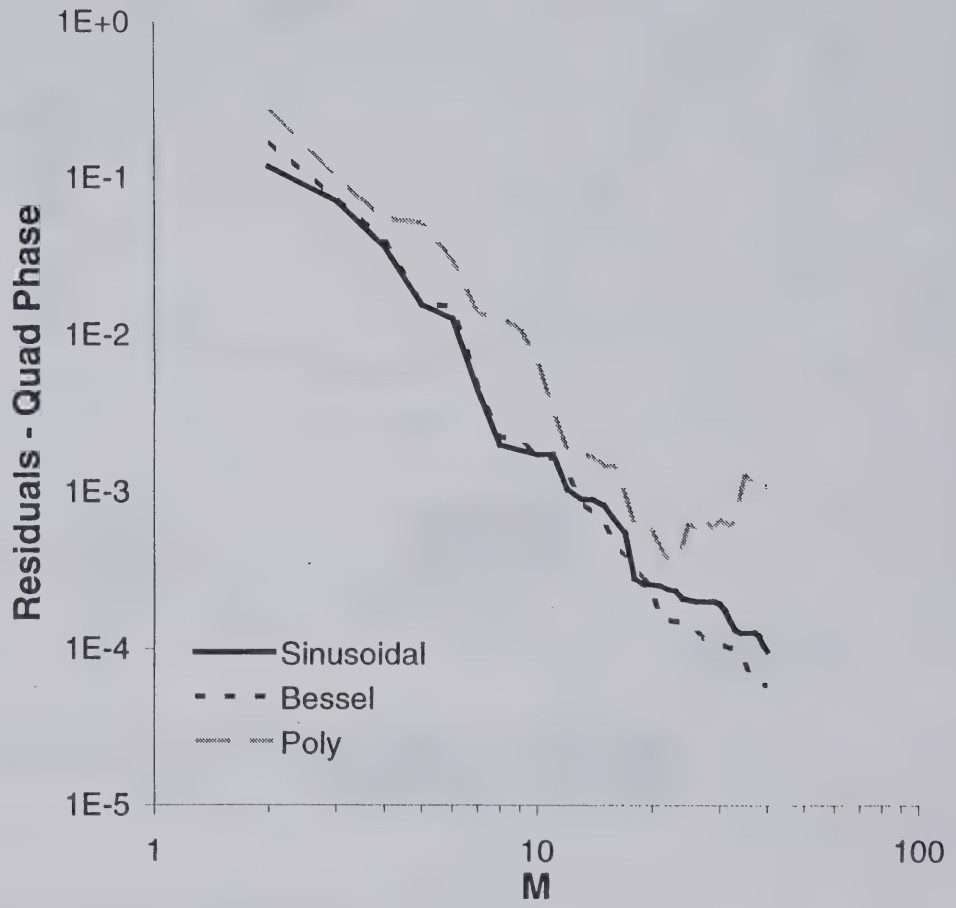

Behavioral Model - Issues

- Robustness of fitting algorithm
- High condition matrix - e.g., with increasing M values

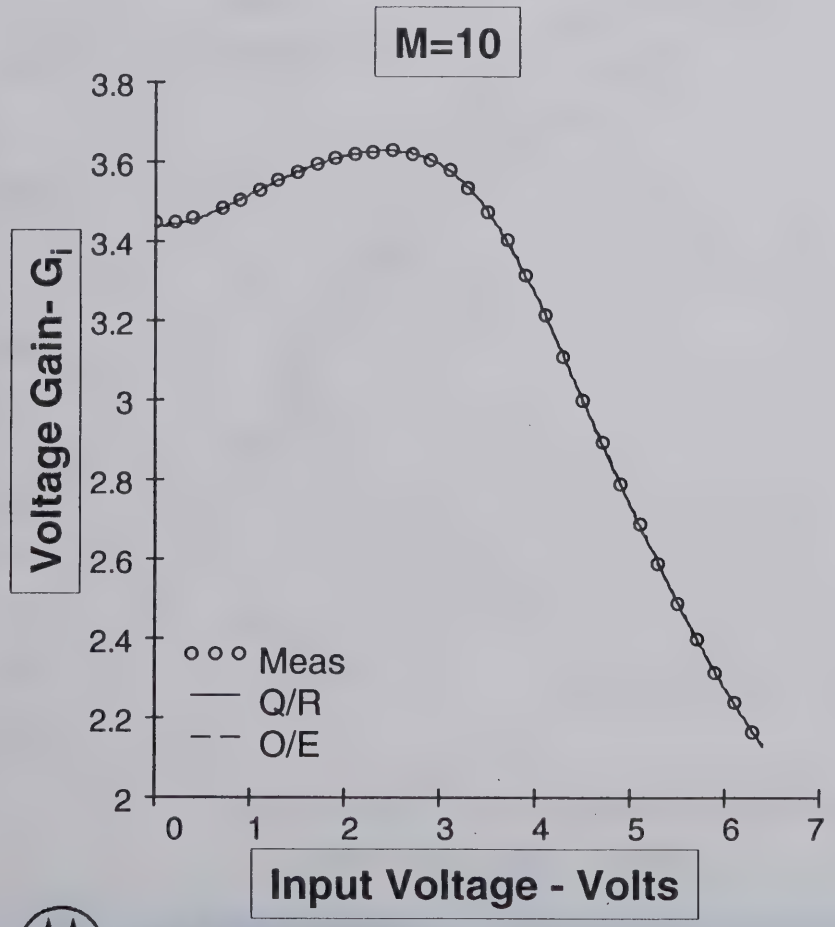

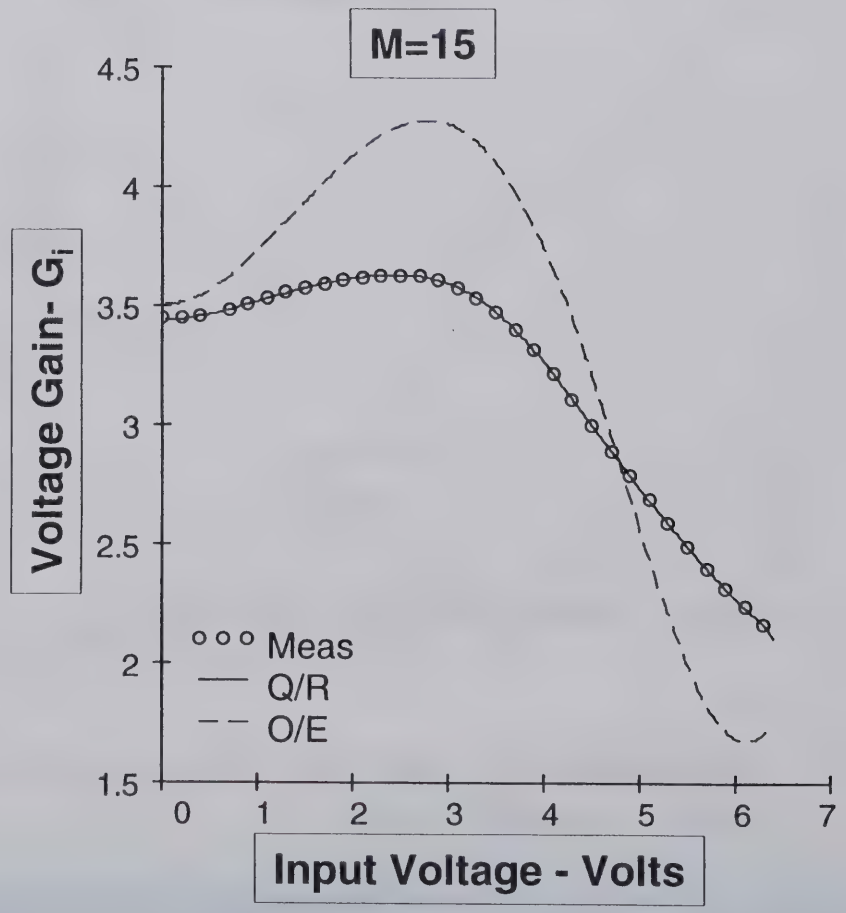

Issues:

- What Type of Series Basis Functions Should Be Used
- How Many Terms Are Needed

Example:

- Compare Behavioral Model to HB
  2 tone sinusoidal stimulus

Harmonic Balance

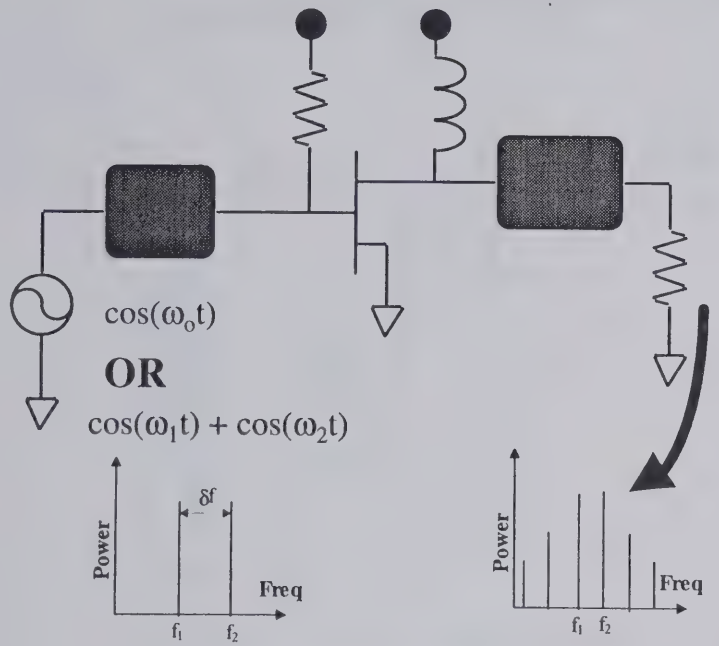

Single Tone

Behavioral Method

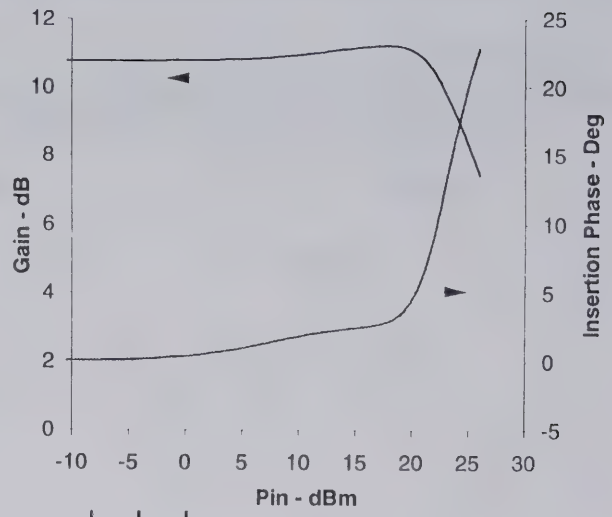

2 Tone Stimulus

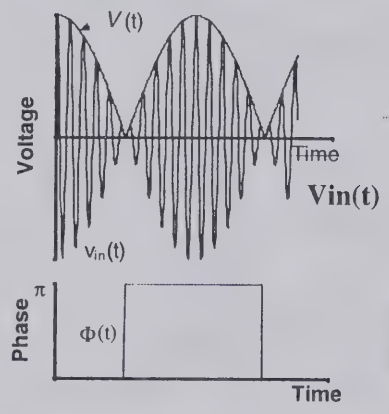

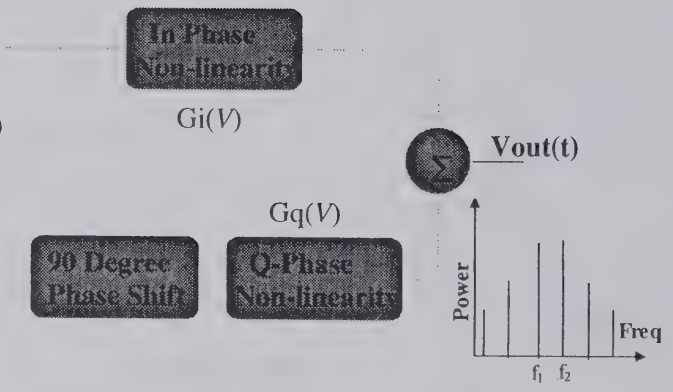

Intermodulation Distortion

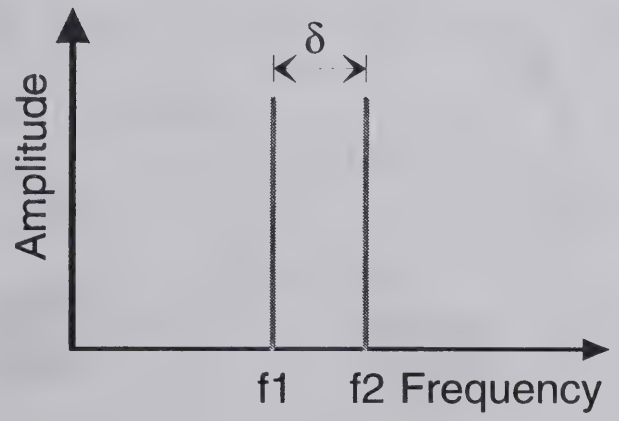

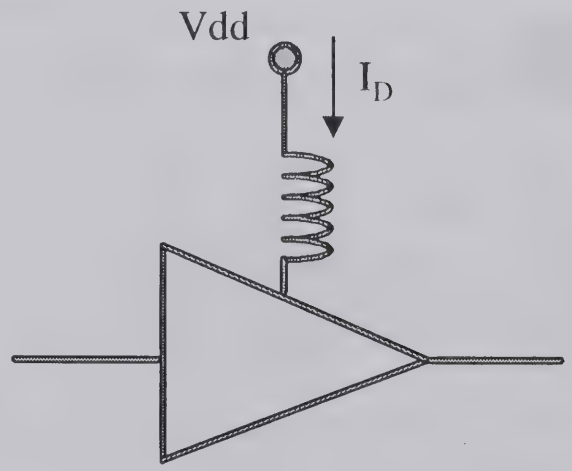

IM3: $2f_1 - f_2$, $2f_2 - f_1$

IM5: $3f_1 - 2f_2$, $3f_2 - 2f_1$

IM7: $4f_1 - 3f_2$, $4f_2 - 3f_1$

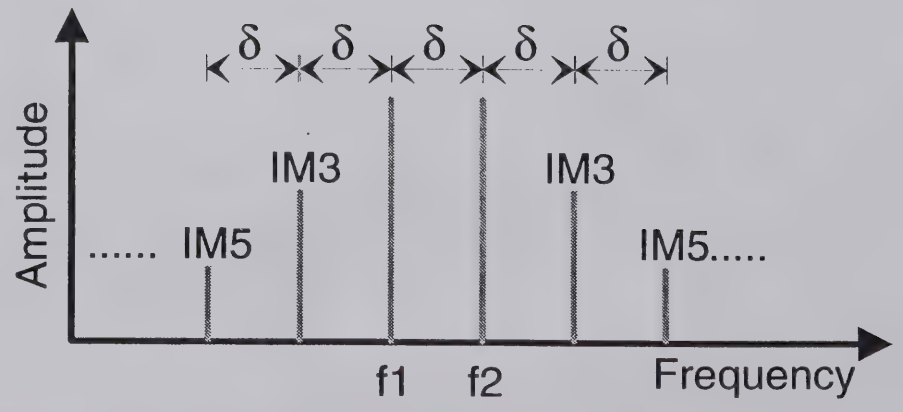

Comparison Of Quadrature Model To Harmonic Balance

- Relatively Low Order Series Generally Work Well for Gain & Average Drain Current

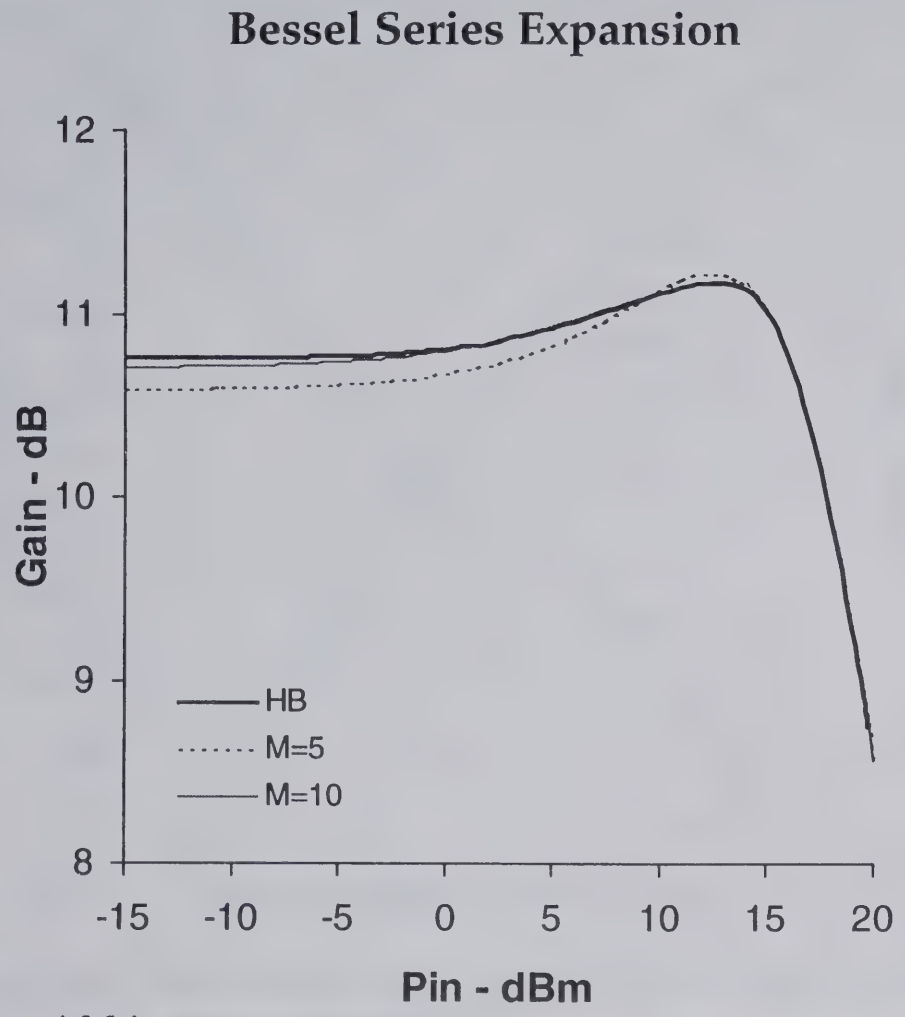

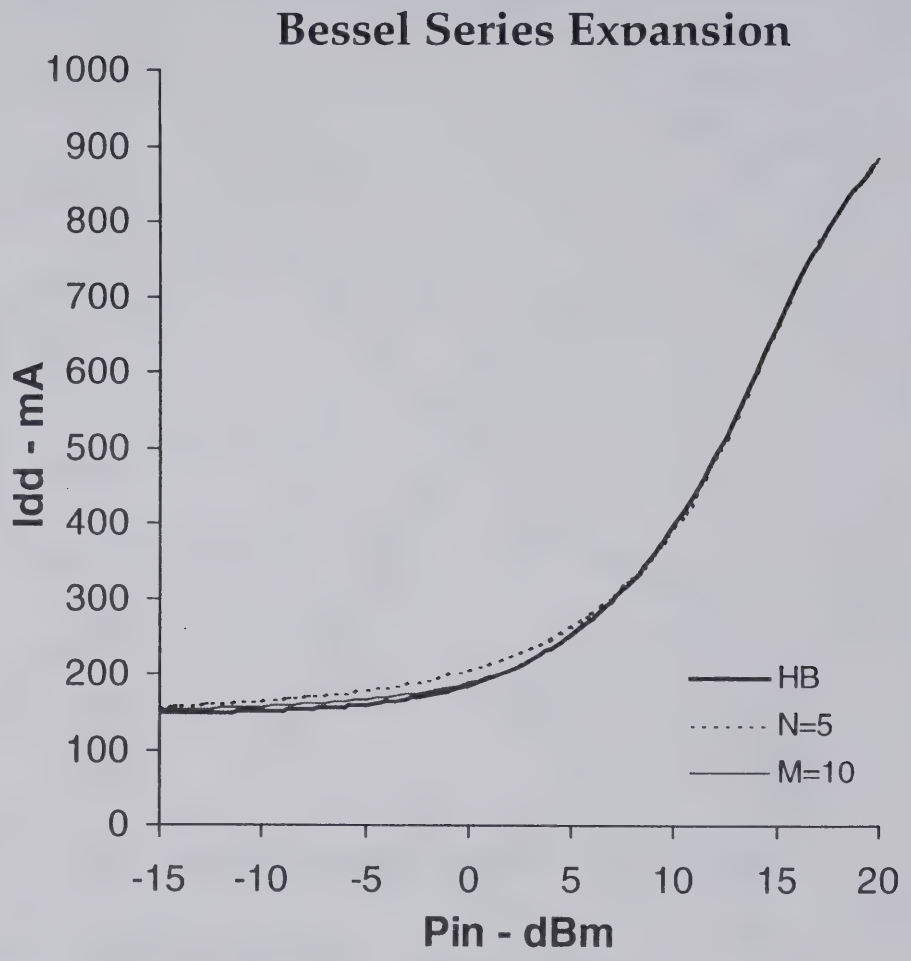

Comparison Of Quadrature Model To Harmonic Balance

- Relatively Low Order Series Generally Work Well for IM3

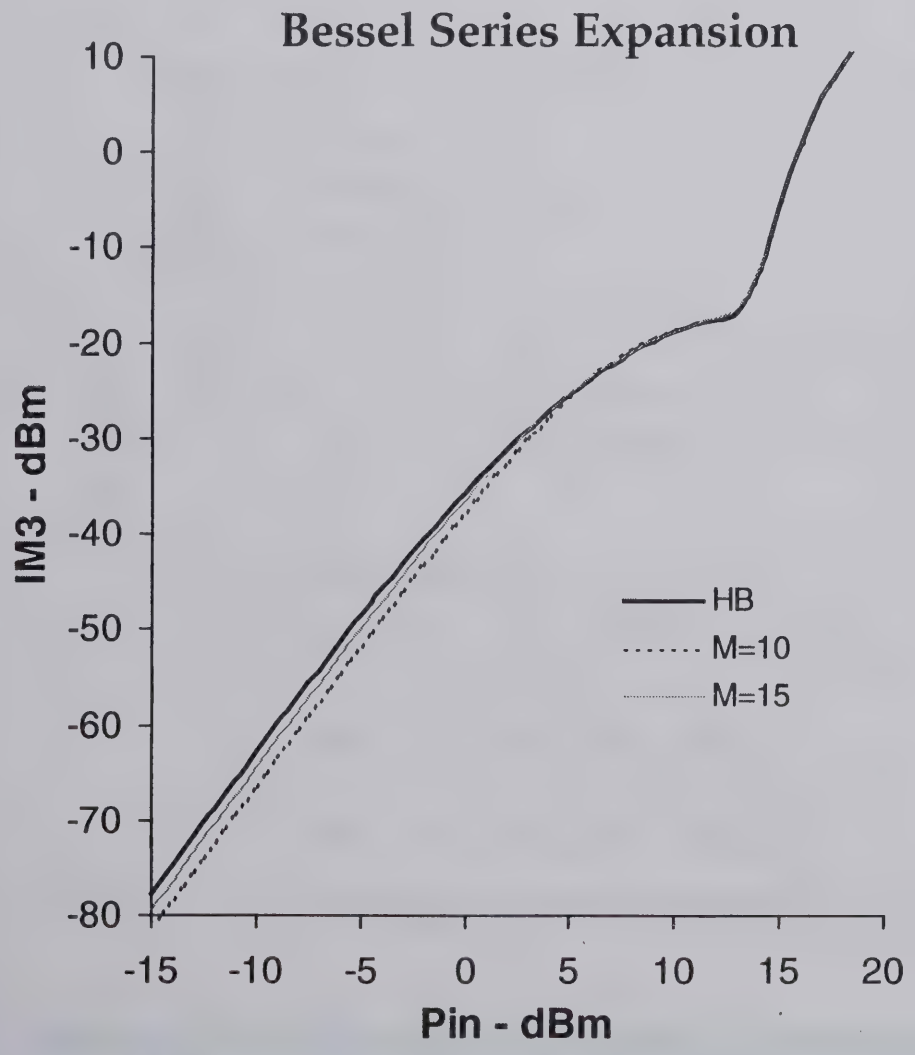

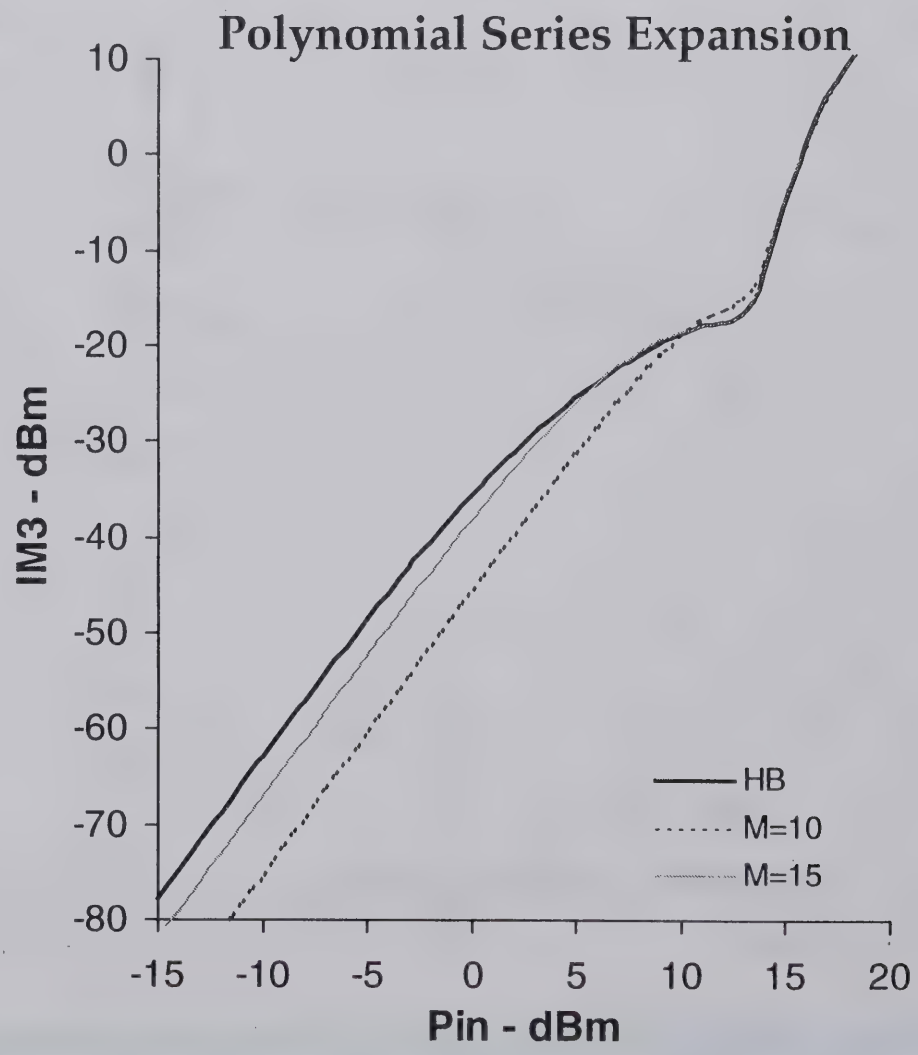

Comparison Of Quadrature Model To Harmonic Balance

- Higher Order For Higher Order IM Products

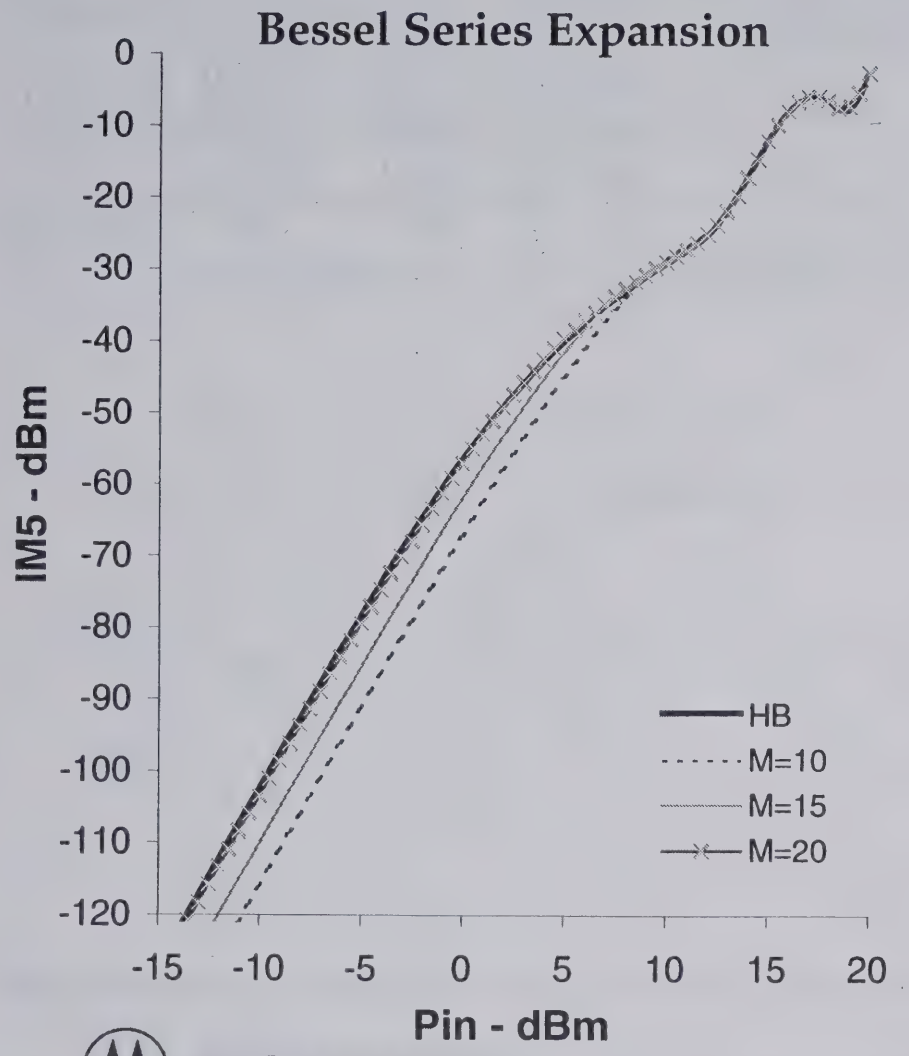

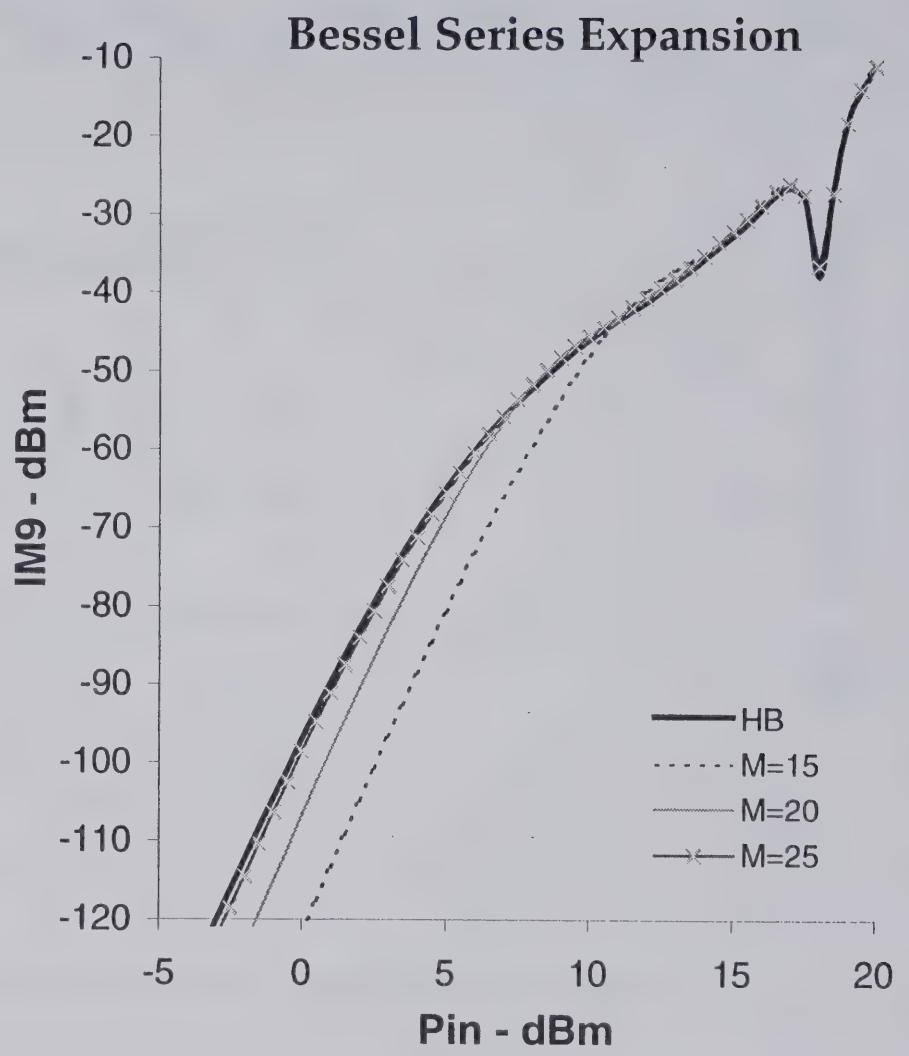

Behavioral Model - Issues

- Harmonic Load/Source Terminations (Alters am-am & am-pm Response)

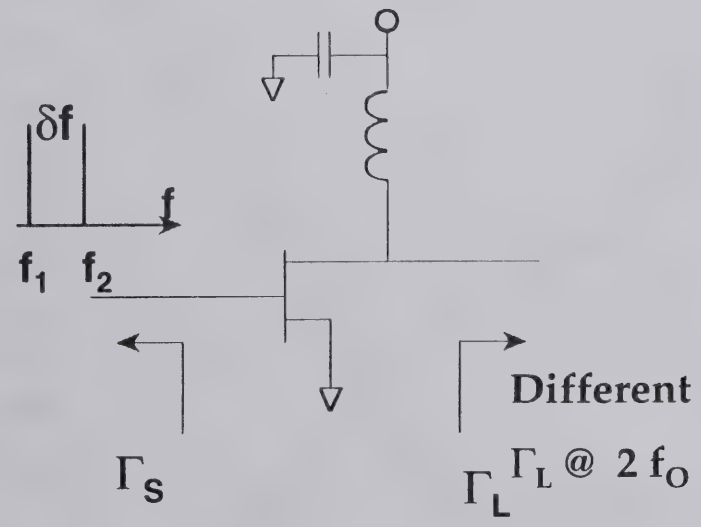

Freq	Load Network A |ΓL|	Load Network A < ΓL	Load Network B | ΓL |	Load Network B < ΓL
f_O	0.940	-174.6	0.940	-174.6
2 f_O	0.985	-172.8	0.970	177.1
3 f_O	0.980	161.4	0.980	131.3
4 f_O	0.940	-177.9	0.940	-177.9
5 f_O	0.940	-178.1	0.940	-178.1

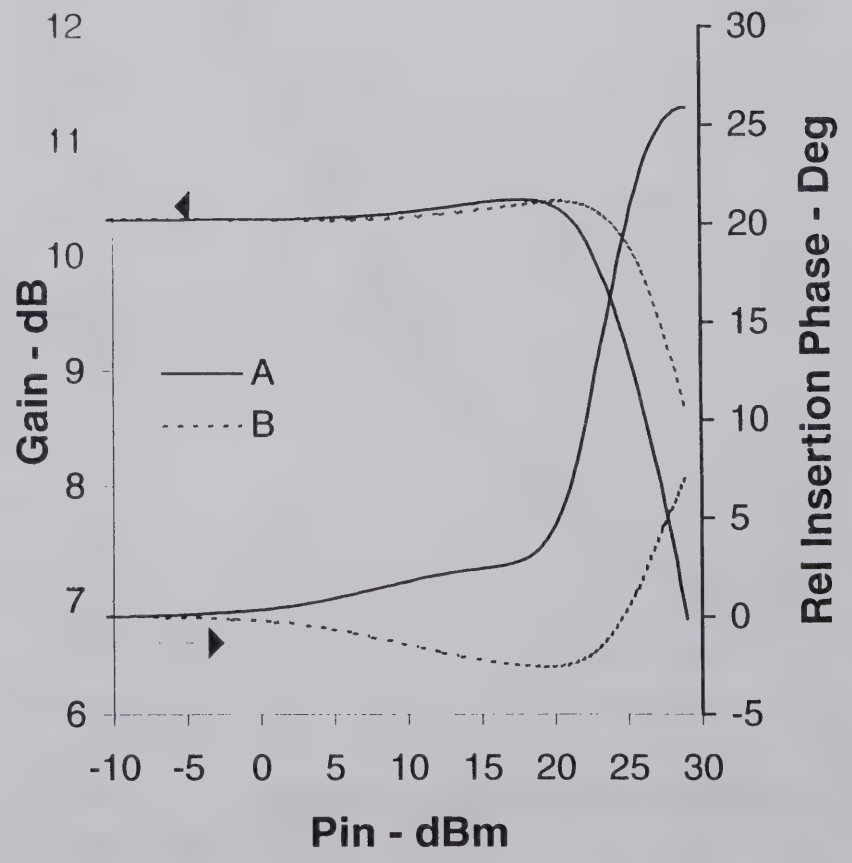

Behavioral Model - Issues

- Effects Due To Bias Decoupling Network, e.g., Drain Bias Inductance
- Consider a two tone sinusoidal excitation w/ tone spacings of 10 KHz & 1 MHz

Power Amplifier Circuit

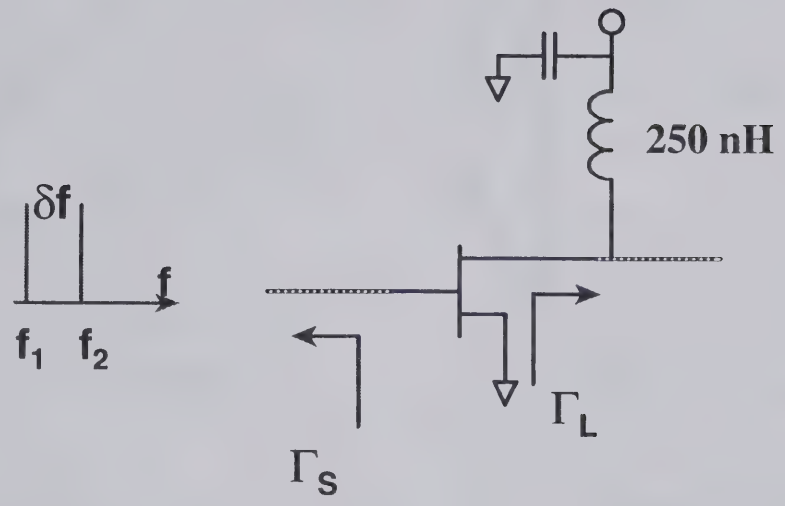

Behavioral Model - Issues

- Effects Due To Bias Decoupling Network, e.g., Drain Bias Inductance

Power Amplifier Circuit

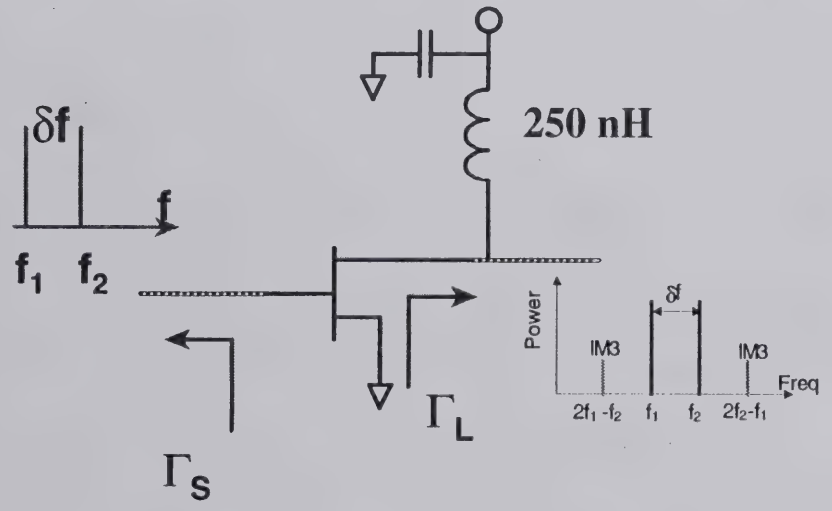

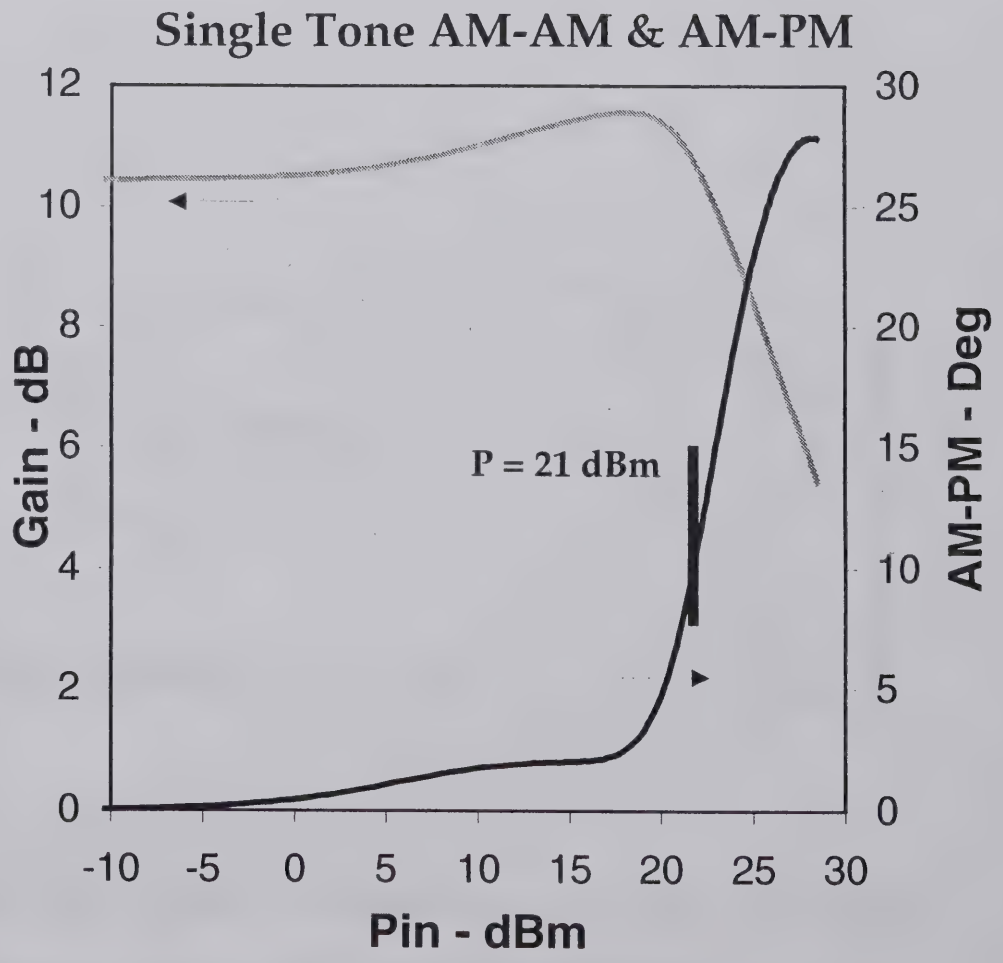

Example:

- 2 Tone Sinusoidal Stimulus
- Sweep Pin_{AVG}
- Vary tone spacing δf = 10 KHz, 1 MHz
- Compare HB to Behavioral Analysis

Comparison of Behavioral Method to Harmonic Balance

- $\delta F = 10$ KHz
- Good agreement between HB and behavioral analysis

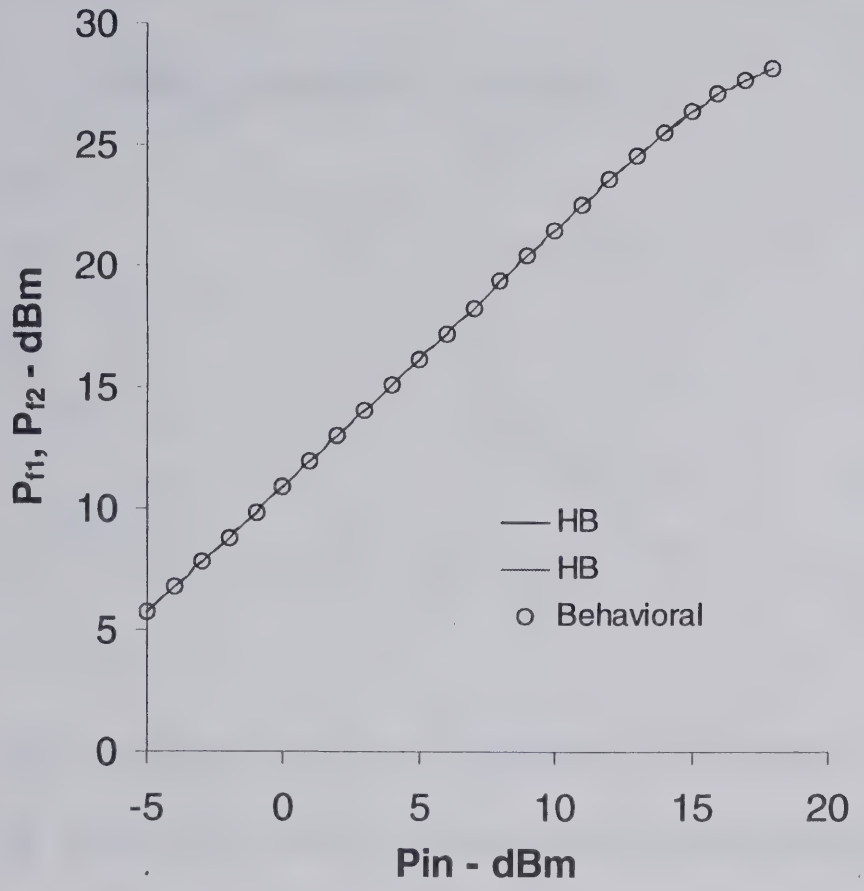

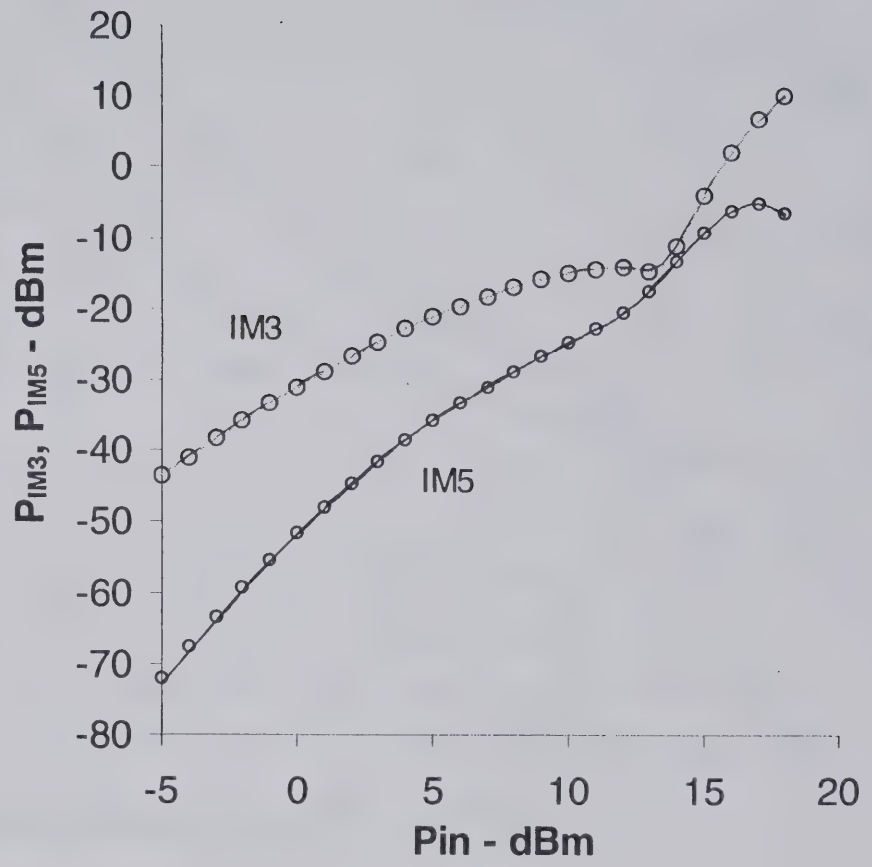

Comparison of Behavioral Method to Harmonic Balance

- $\delta F = 1$ MHz
- Poor agreement between HB and behavioral analysis!!
- Spectral tones are unequal in power!!

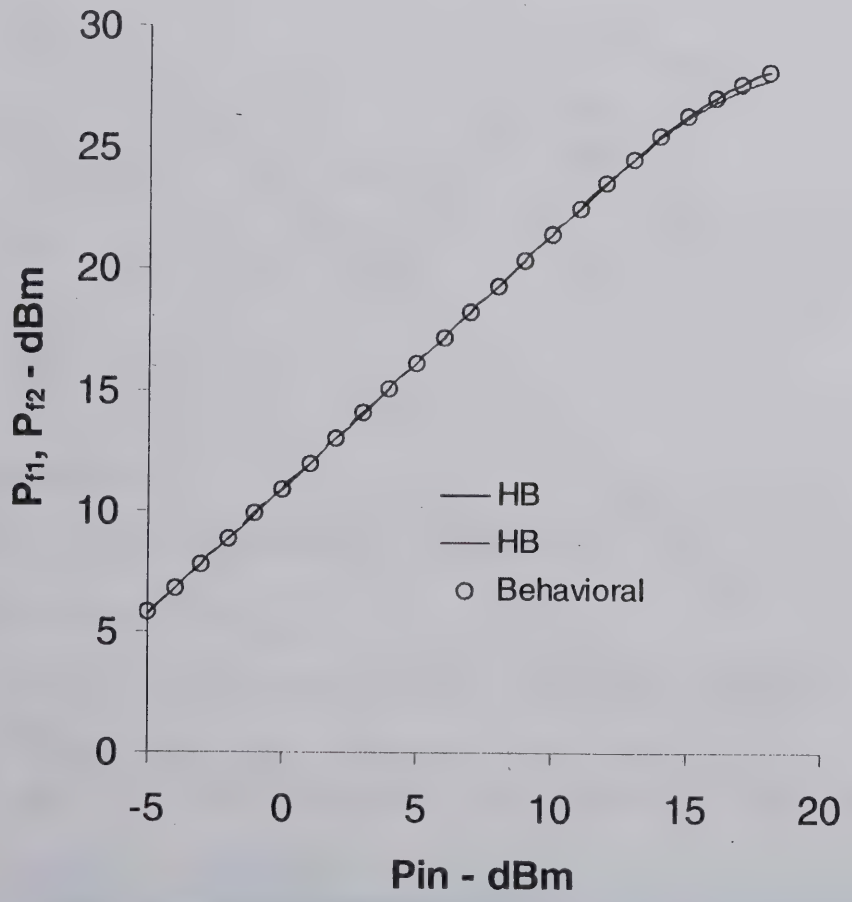

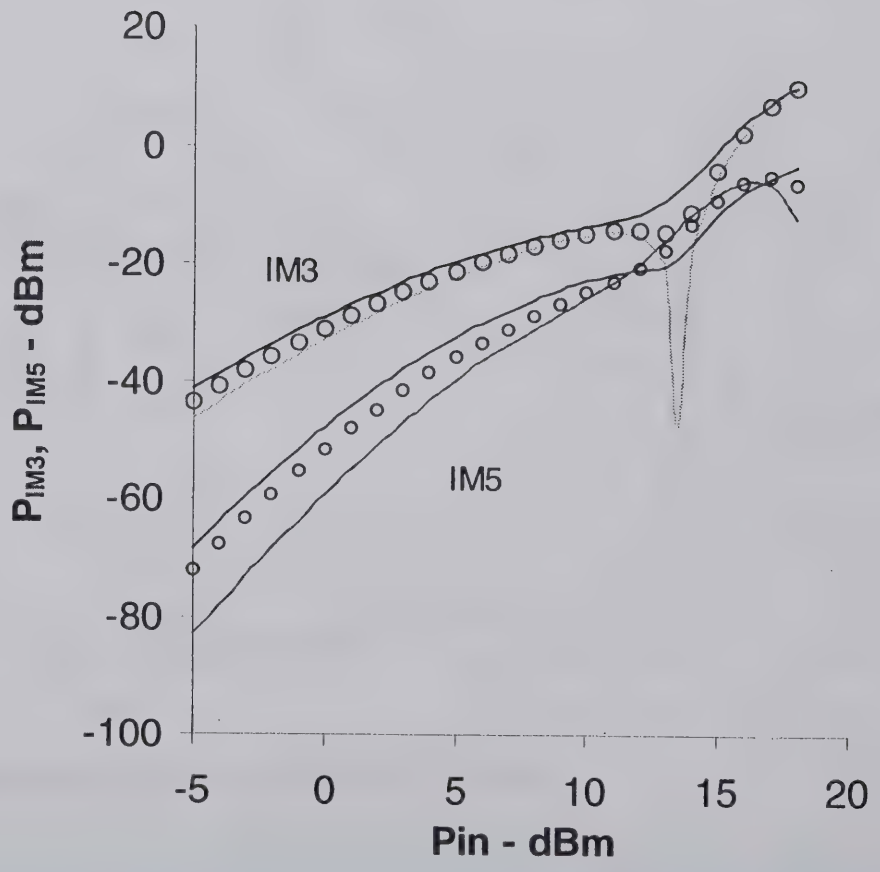

Revise Drain Bias Network

- Set $\Gamma_L = 0, 180^o$ @ n $f_{envelope}$, n=1, 2, 3 …
- Γ_L is unaffected at all other frequencies

Power Amplifier Circuit

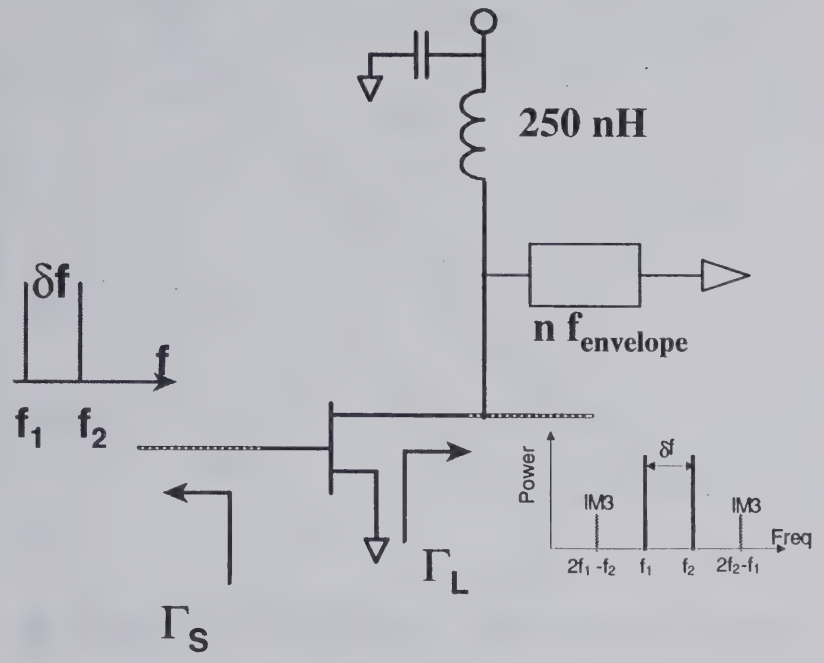

Single Tone AM-AM & AM-PM

Response has not changed!!

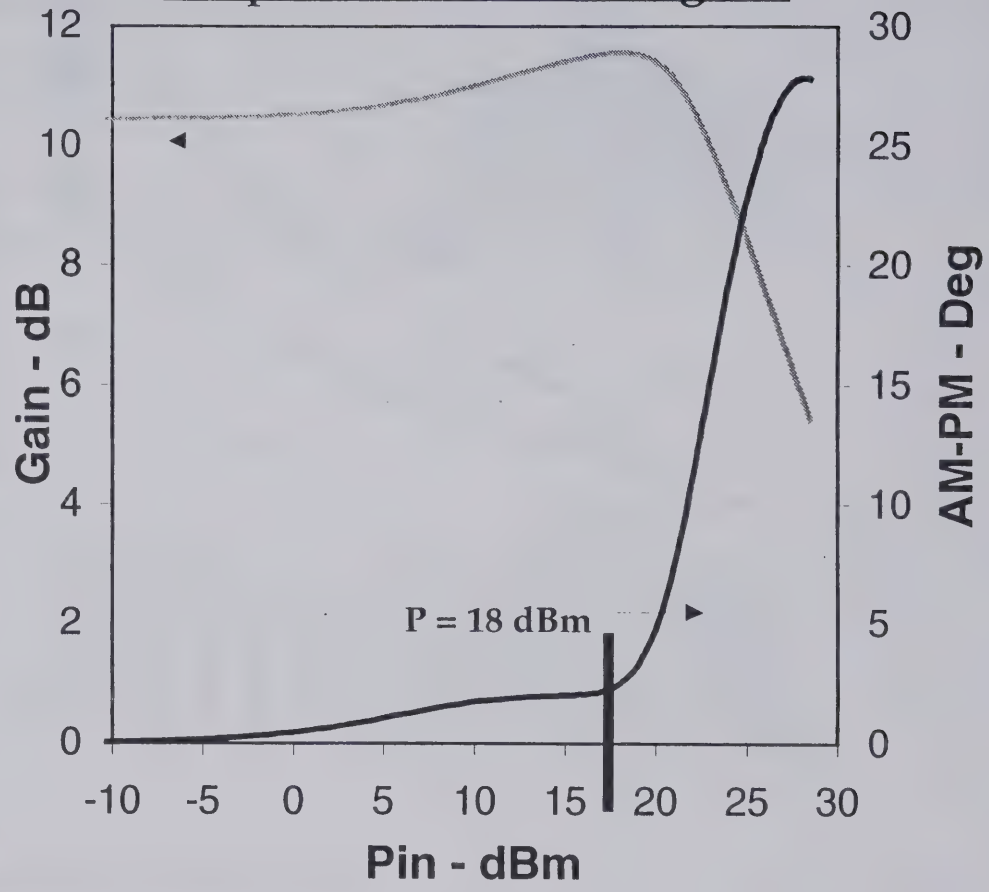

Revised Drain Bias Network

- δF = 1 MHz
- Good agreement between HB and behavioral analysis!!
- Spectral tones are equal in power!!

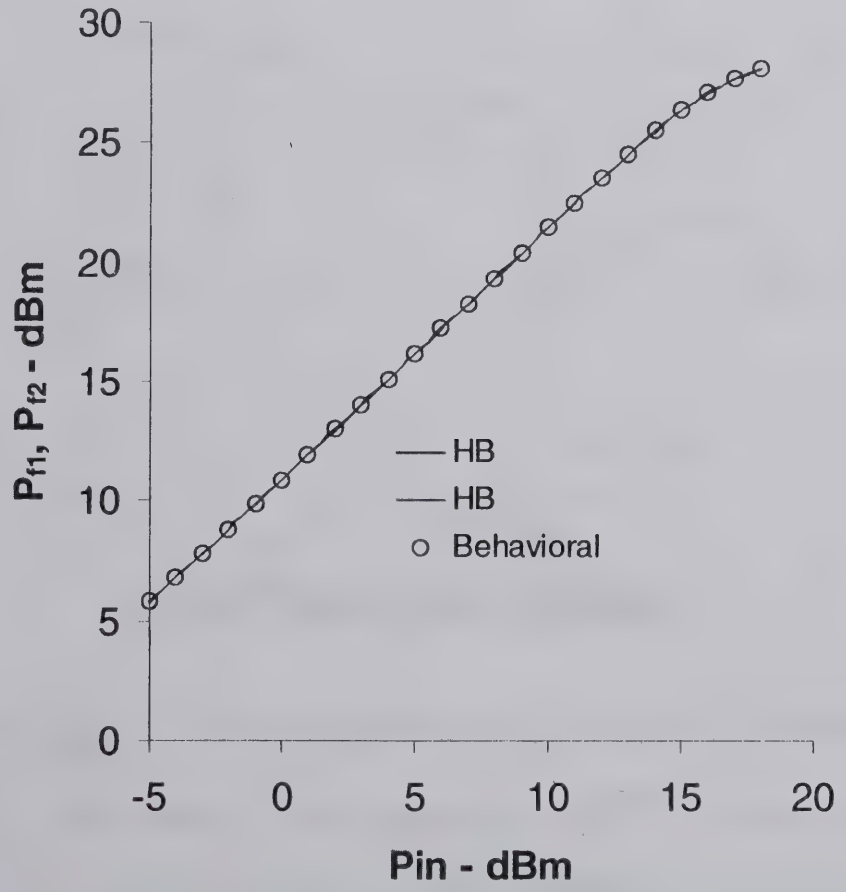

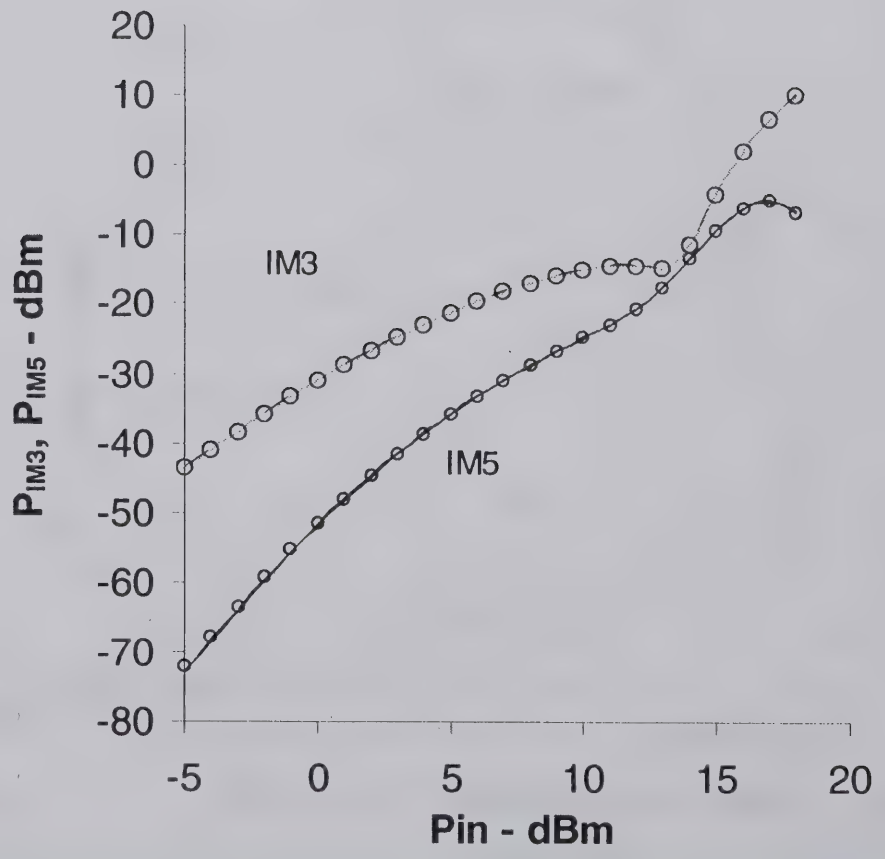

- $\delta F = 1$ MHz

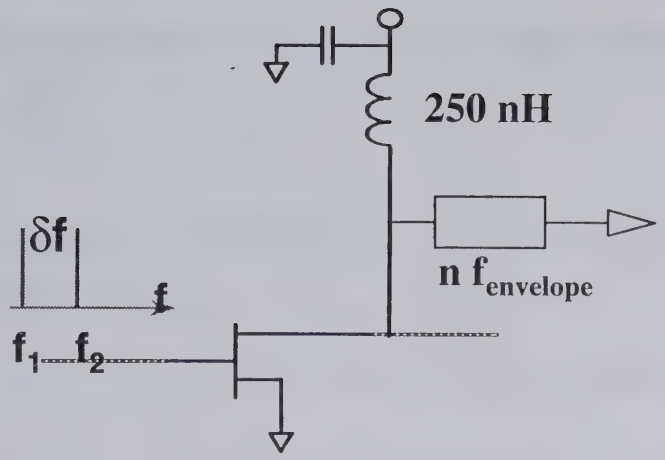
250 nH
δf
f
n f envelope
f1 f2

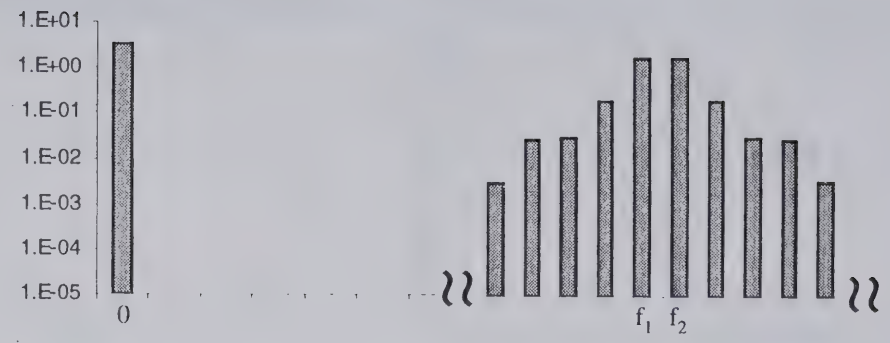
1.E+01
1.E+00
1.E-01
1.E-02
1.E-03
1.E-04
1.E-05
0
f1 f2

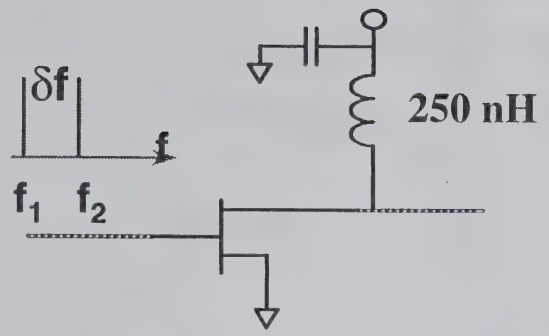
250 nH
δf
f
f1 f2

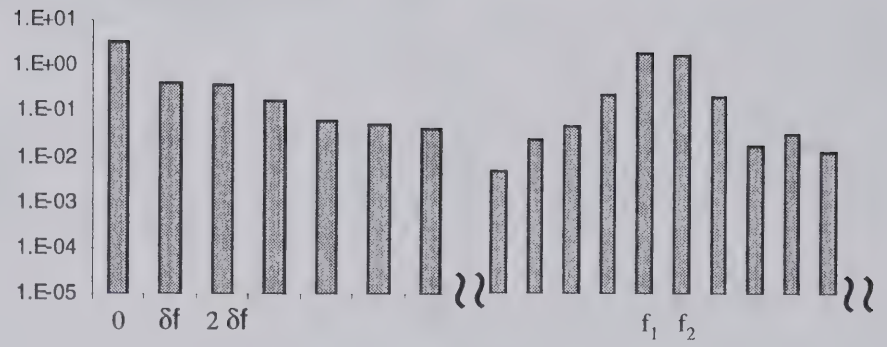
1.E+01
1.E+00
1.E-01
1.E-02
1.E-03
1.E-04
1.E-05
0 δf 2 δf
f1 f2

- $\delta F = 1$ MHz

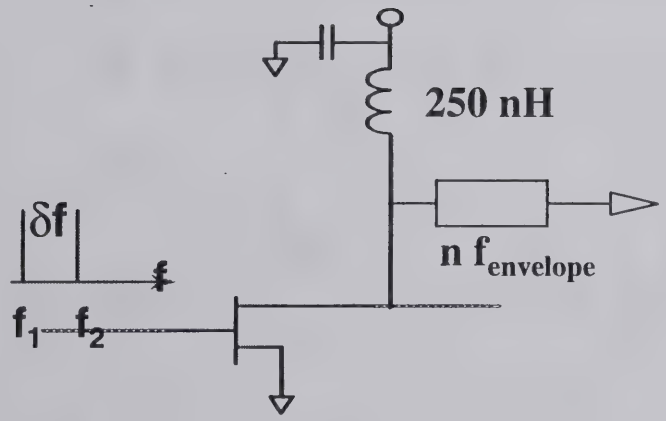

RF Envelope

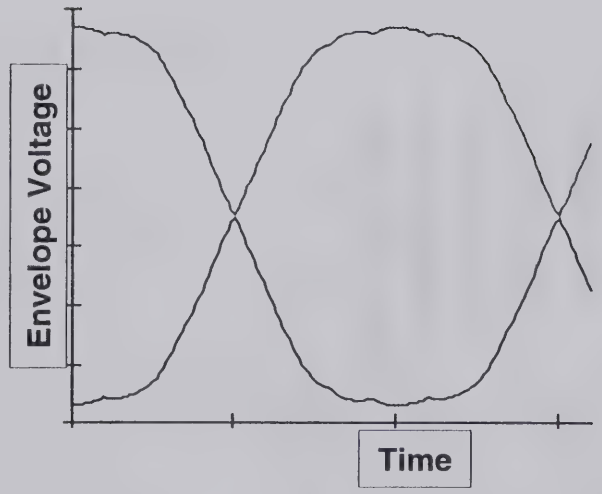

RF Envelope
1st Spectral Zone Only

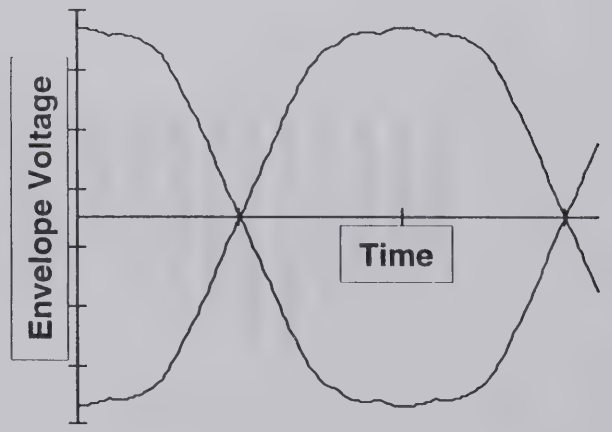

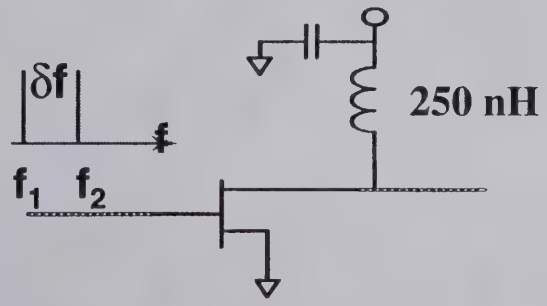

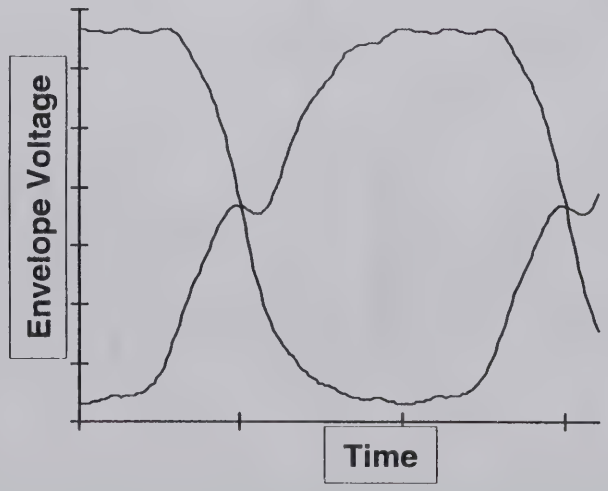

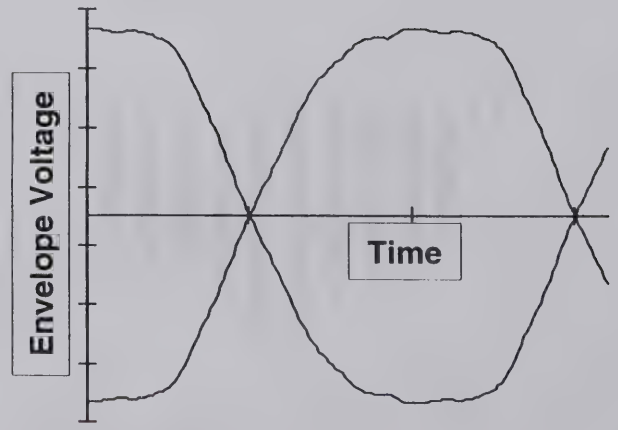

Behavioral Model Validation Studies

- **Compare Measurements of a PHEMT Based PA to Behavior Technique**

Technique - Measure PA Response:

PHEMT based power amplifier

Sweep P_{IN} from small signal conditions to several dB of gain compression

Stimuli: single tone sinusoid >> extract behavioral model parameters

Compare behavioral model to measurements

2 tone sinusoid

$\pi/4$ DQPSK stimulus compliant w/ NADC

O-QPSK stimulus compliant w/ CDMA

Behavioral Model Validation Studies

<u>Measurements:</u>

Single Tone Sinusoidal Stimulus:

am-am, am-pm, Idd, Igg

2 Tone Sinusoidal Stimulus

Gain, IM3, IM5, IM7, Idd, Igg

π/4 DQPSK Stimuli

Gain, adj. & alt. ACPR, Idd, Igg

<u>Behavioral Model:</u>

Use measured data to determine transfer function coefficients

i.e, $G_i(A)$, $G_q(A)$, $G_d(A)$, $G_g(A)$

<u>Compare Behavioral Method to Measured Results</u>

2 tone signal: gain, IM3, IM5, IM7, drain current, gate current

π/4 DQPSK & O-QPSK stimulus:

gain, adjacent & alternate channel power ratios, avg drain current

Generating an NADC Compliant π/4 DQPSK Stimulus

- **IS-136 Digital Cellular Standard**

Data rate:	48.6 Kb/s
Symbol rate:	24.3 Kb/s
Modulation:	π/4 DQPSK
Base band filtering:	root raised cosine w/ α = 0.35

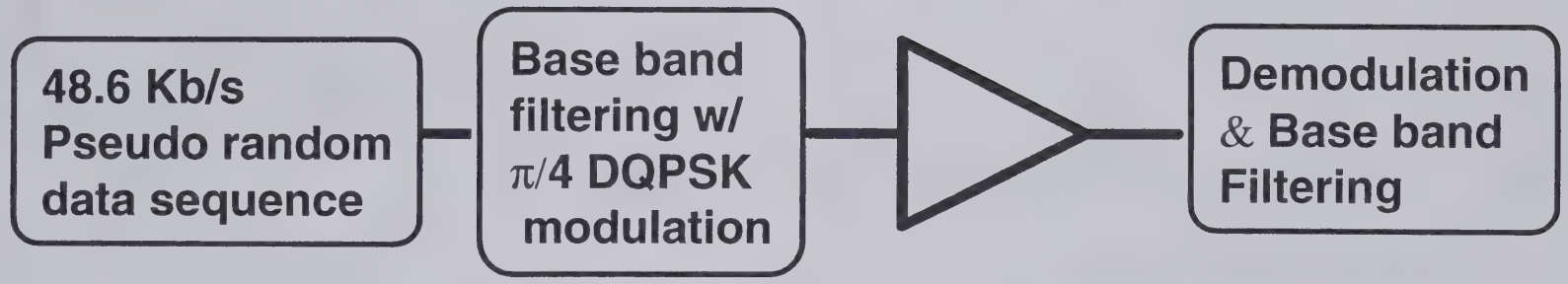

Generating an NADC Compliant π/4 DQPSK Stimulus

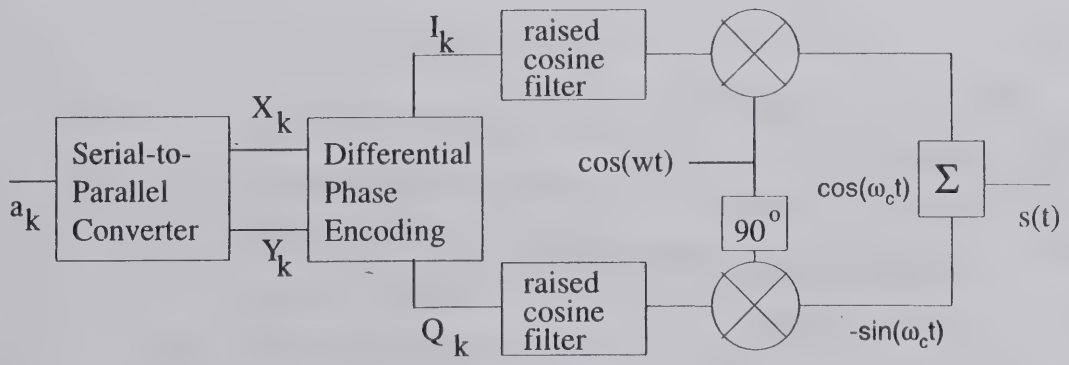

$$S(t) = \sum_n g(t - n\,T)\cos(\phi_n)\cos(\omega_c t) - \sum_n g(t - n\,T)\sin(\phi_n)\sin(\omega_c t)$$
$$= I(t)\cos(\omega_c t) - Q(t)\sin(\omega_c t)$$
$$= \mathrm{Re}\left\{\left[I(t) + j\,Q(t)\right]e^{j\omega_c t}\right\}$$

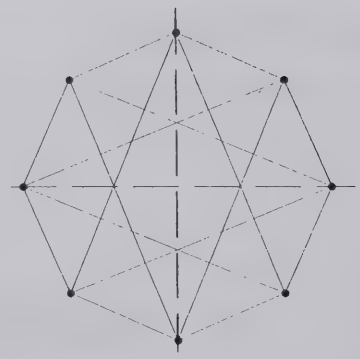

Data Sequence

X_K	Y_K	Δϕ
1	1	-3π/4
0	1	3π/4
0	0	π/4
1	0	-π/4

Encoding

$$I_K + jQ_K = (I_{K-1} + jQ_{K-1})e^{j\,\Delta\phi_K}$$

RRC Filter

$$H(f) = \begin{cases} 1 \\ \sqrt{\frac{1}{2}\left\{1 - \sin\left(\frac{\pi\,(2fT - 1)}{2\alpha}\right)\right\}} \\ 0 \end{cases} \quad \begin{cases} 0 \le \frac{(1-\alpha)}{2T} \\ \frac{(1-\alpha)}{2T} \le f \le \frac{(1+\alpha)}{2T} \\ f \ge \frac{(1+\alpha)}{2T} \end{cases}$$

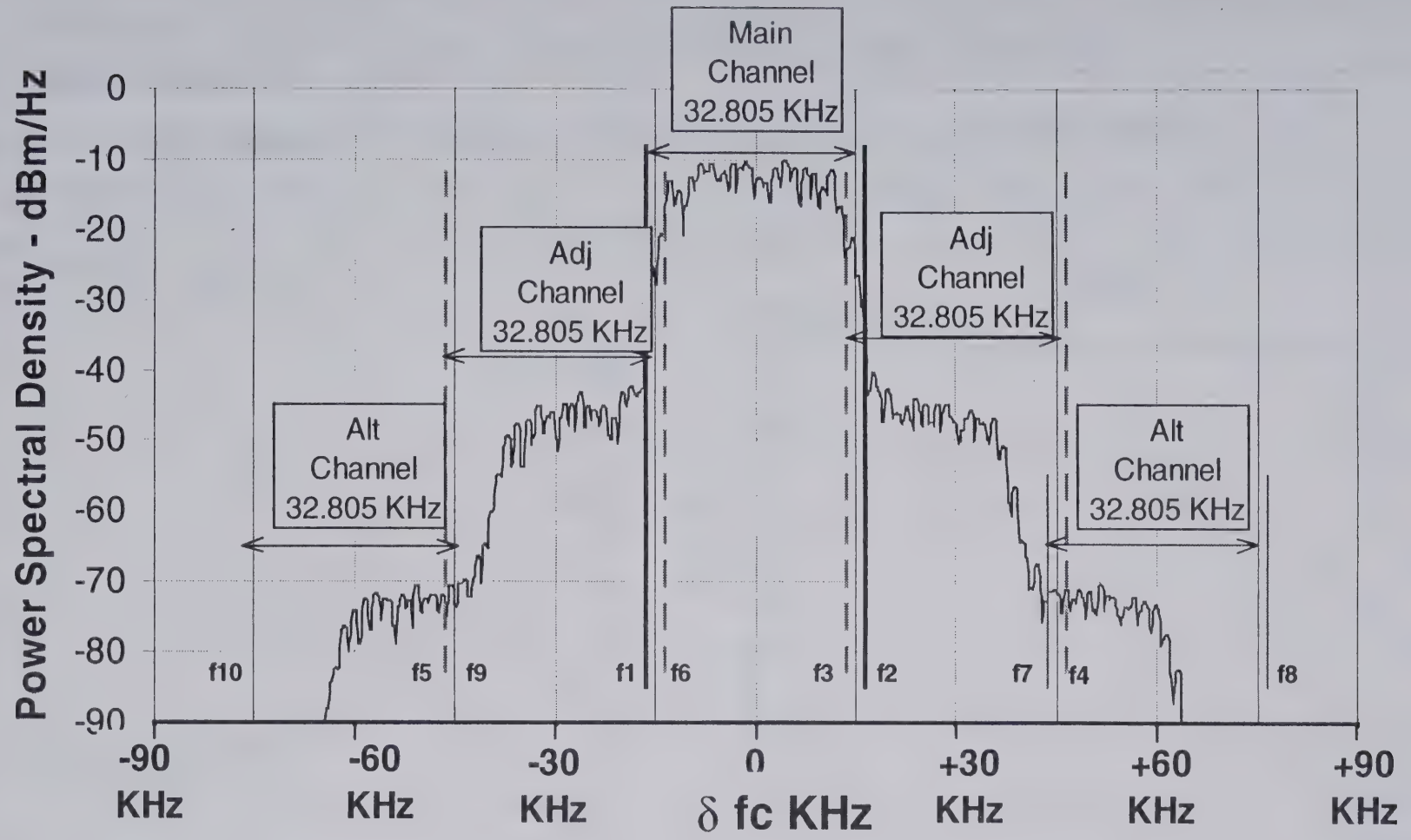

Adjacent Channel

$$ACPR_{Lower} = \frac{\int_{f5}^{f6} |H(\alpha,T_c)|^2 S(f)\,df}{\int_{f1}^{f2} |H(\alpha,T_c)|^2 S(f)\,df} \qquad ACPR_{Upper} = \frac{\int_{f3}^{f4} |H(\alpha,T_c)|^2 S(f)\,df}{\int_{f1}^{f2} |H(\alpha,T_c)|^2 S(f)\,df}$$

Alternate Channel

$$ACPR_{Lower} = \frac{\int_{f9}^{f10} |H(\alpha,T_c)|^2 S(f)\,df}{\int_{f1}^{f2} |H(\alpha,T_c)|^2 S(f)\,df} \qquad ACPR_{Upper} = \frac{\int_{f7}^{f8} |H(\alpha,T_c)|^2 S(f)\,df}{\int_{f1}^{f2} |H(\alpha,T_c)|^2 S(f)\,df}$$

Behavioral Model Validation Studies

- **Measured Single Tone Response**

Gain/Insertion Phase

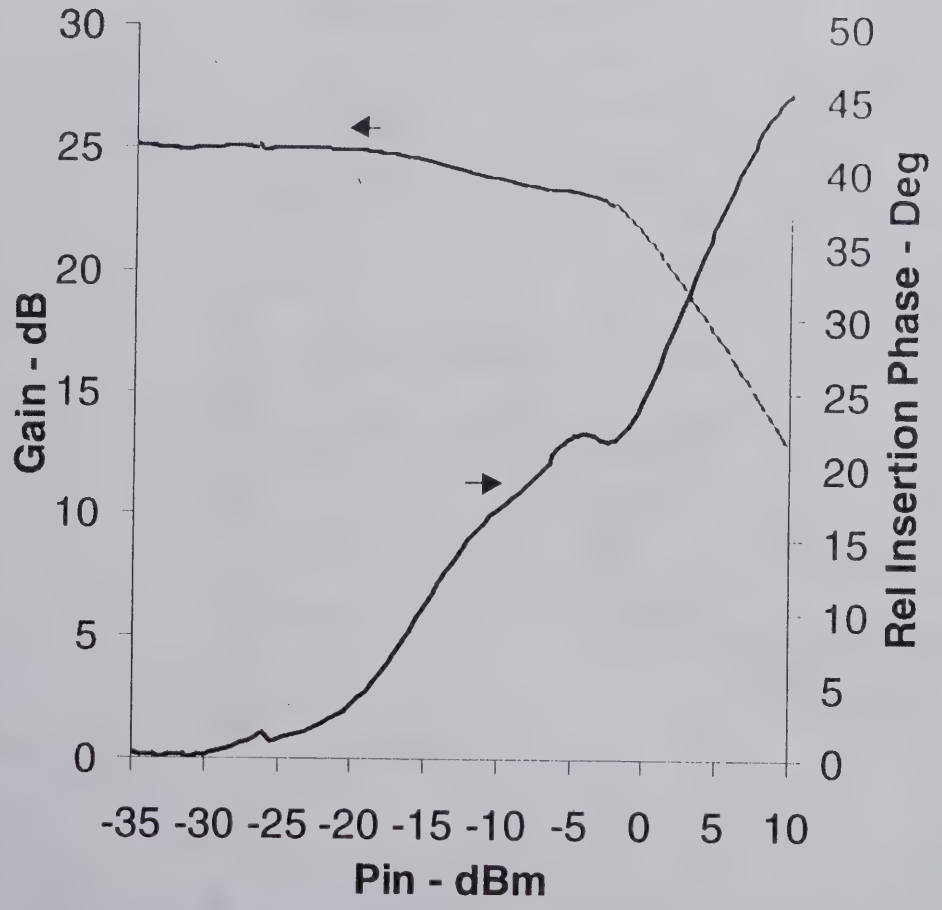

Current

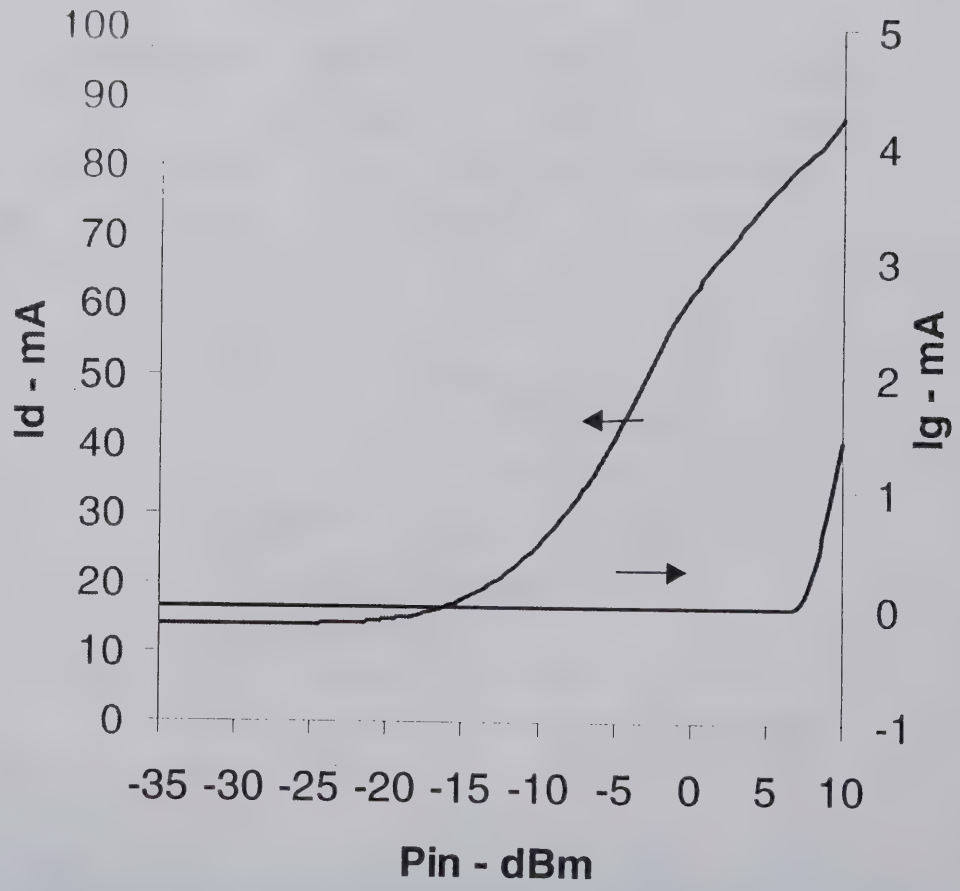

Behavioral Model Validation Studies

- **Comparison of Measured & Modeled 2 Tone Response Using Behavioral Analysis**

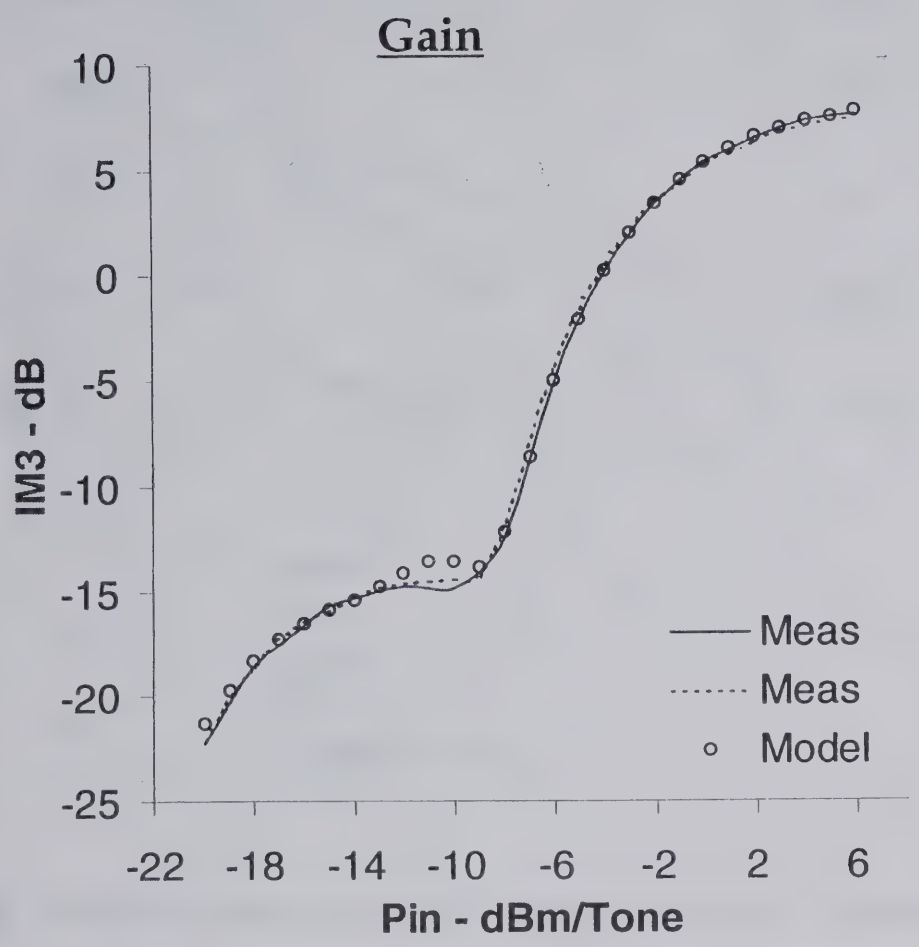

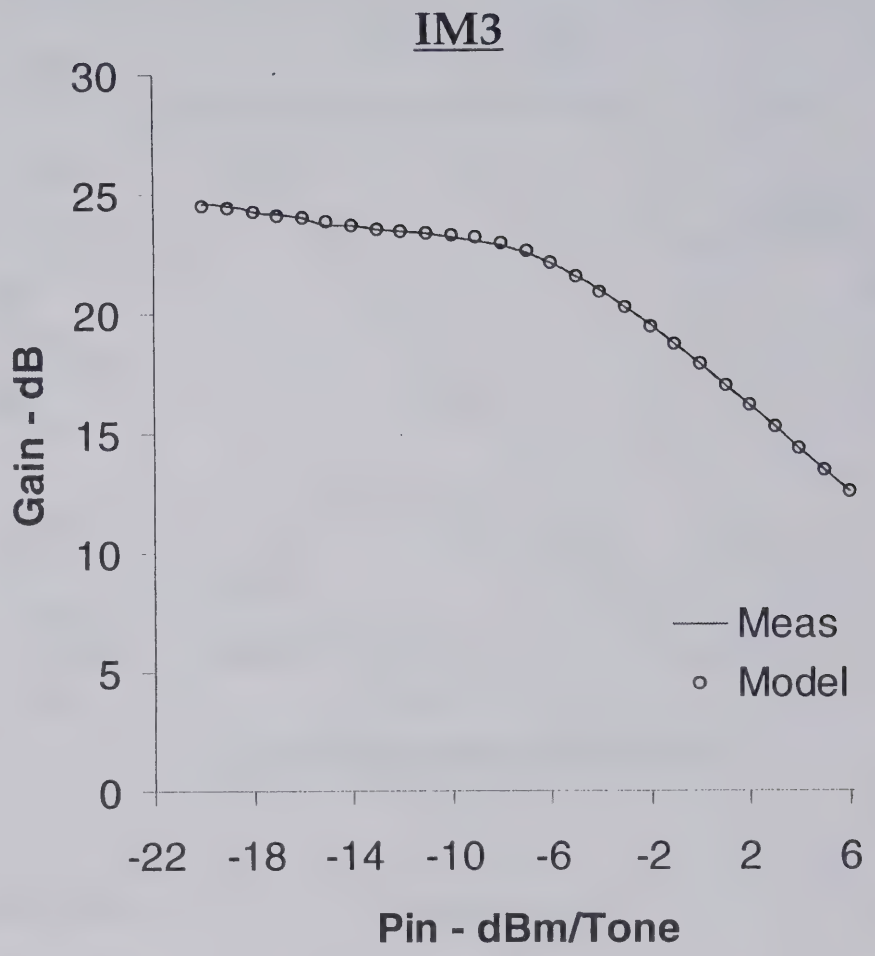

Behavioral Model Validation Studies

- **Comparison of Measured & Modeled 2 Tone Response**

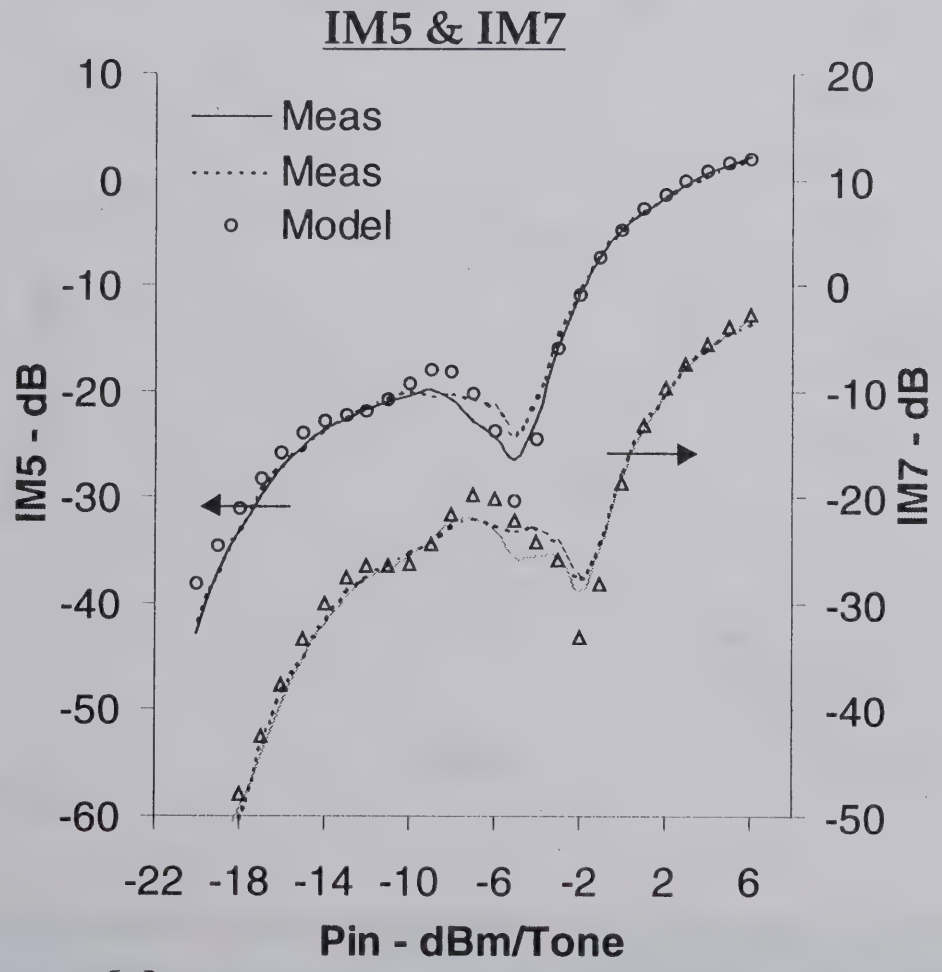

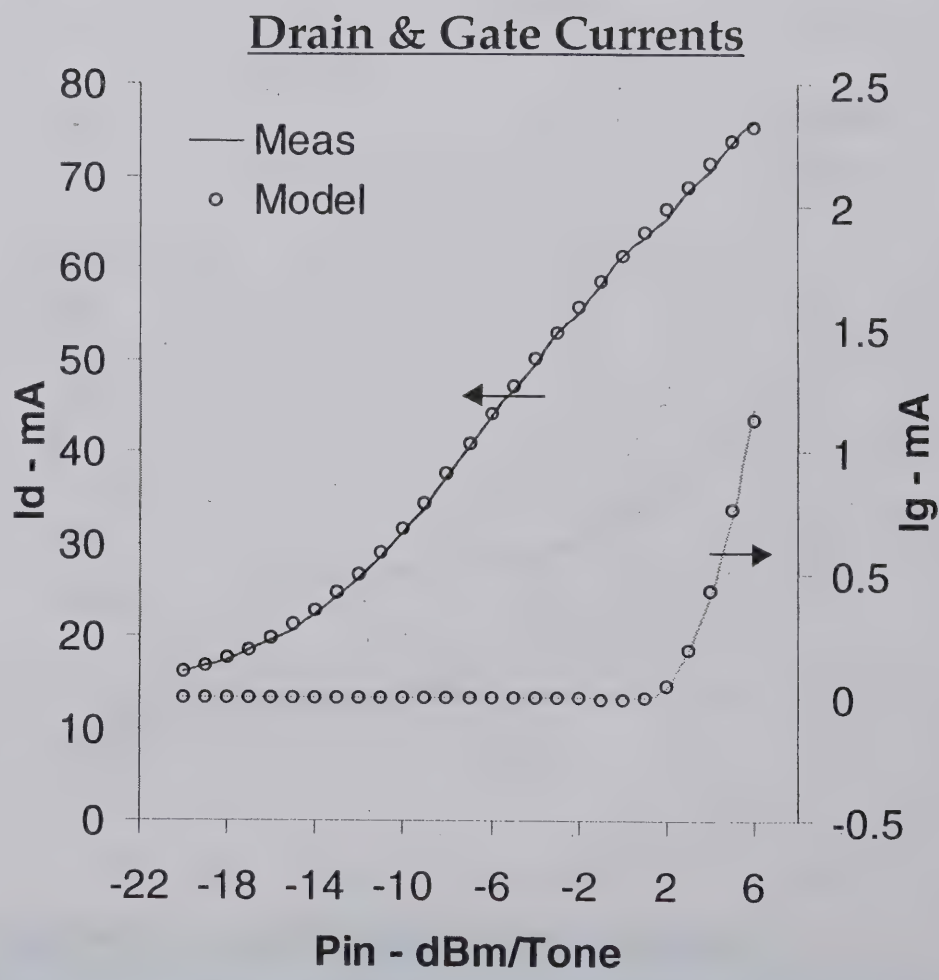

Behavioral Model Validation Studies

- **Comparison of Measured & Modeled - π/4 DQPSK NADC Compliant Stimulus**

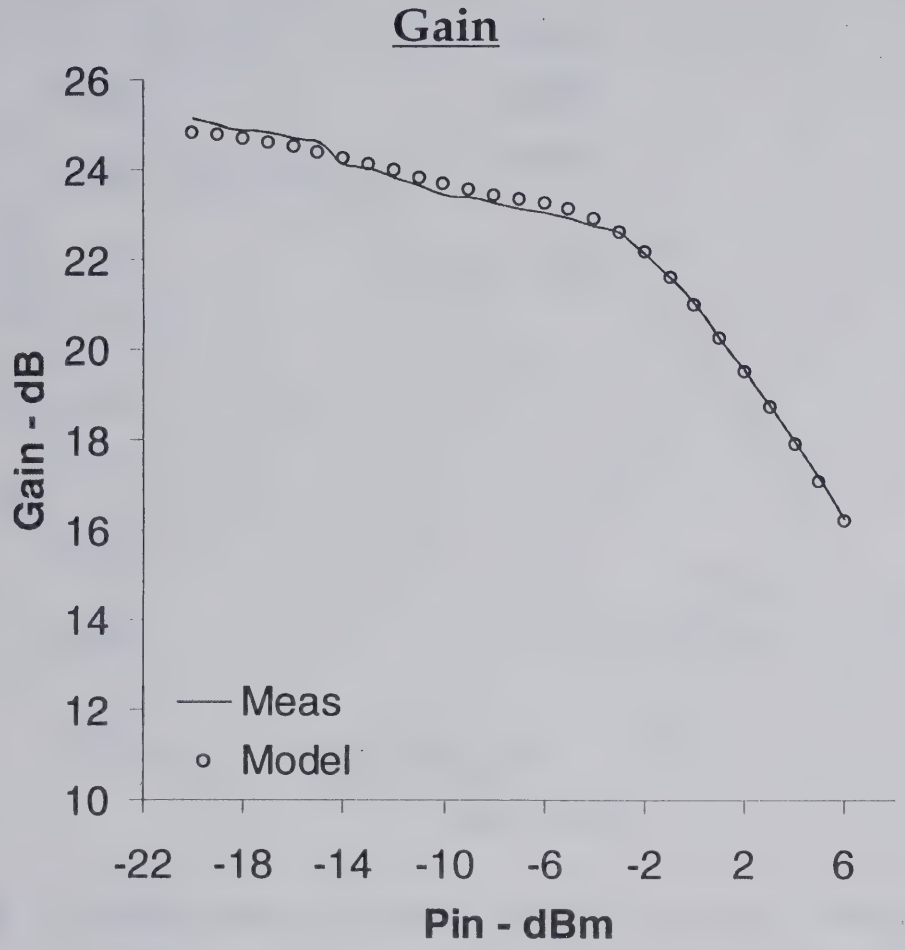

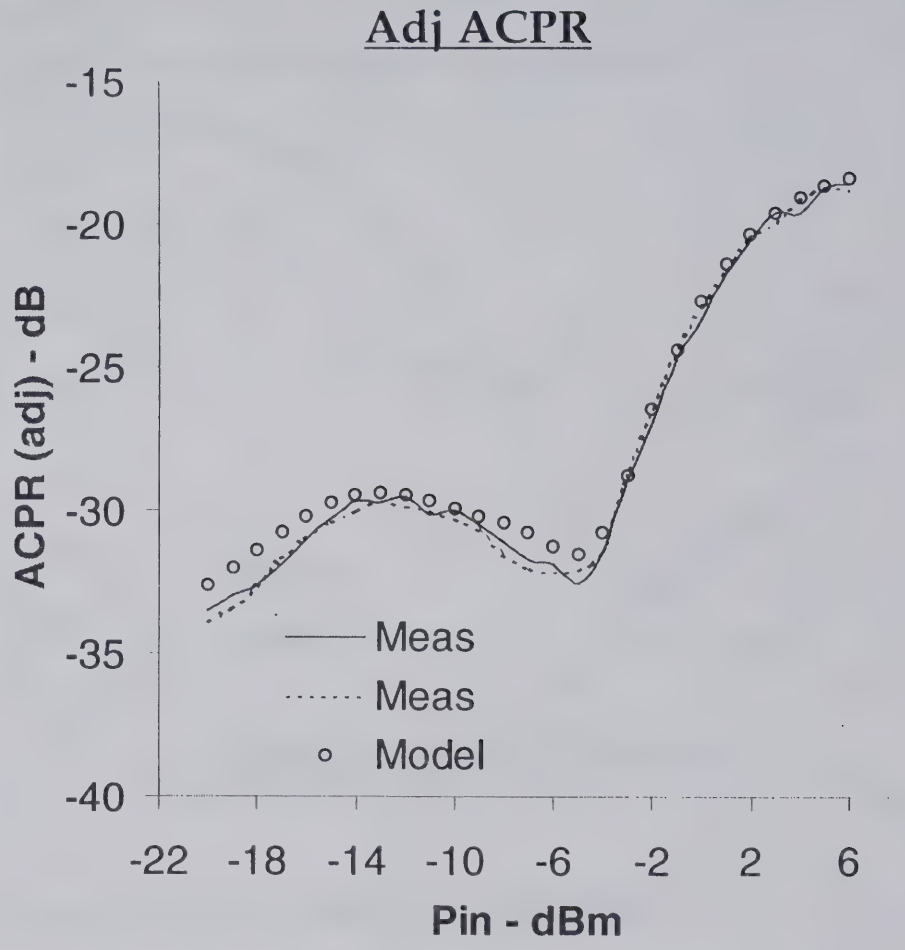

Behavioral Model Validation Studies

- **Comparison of Measured & Modeled - π/4 DQPSK NADC Compliant Stimulus**

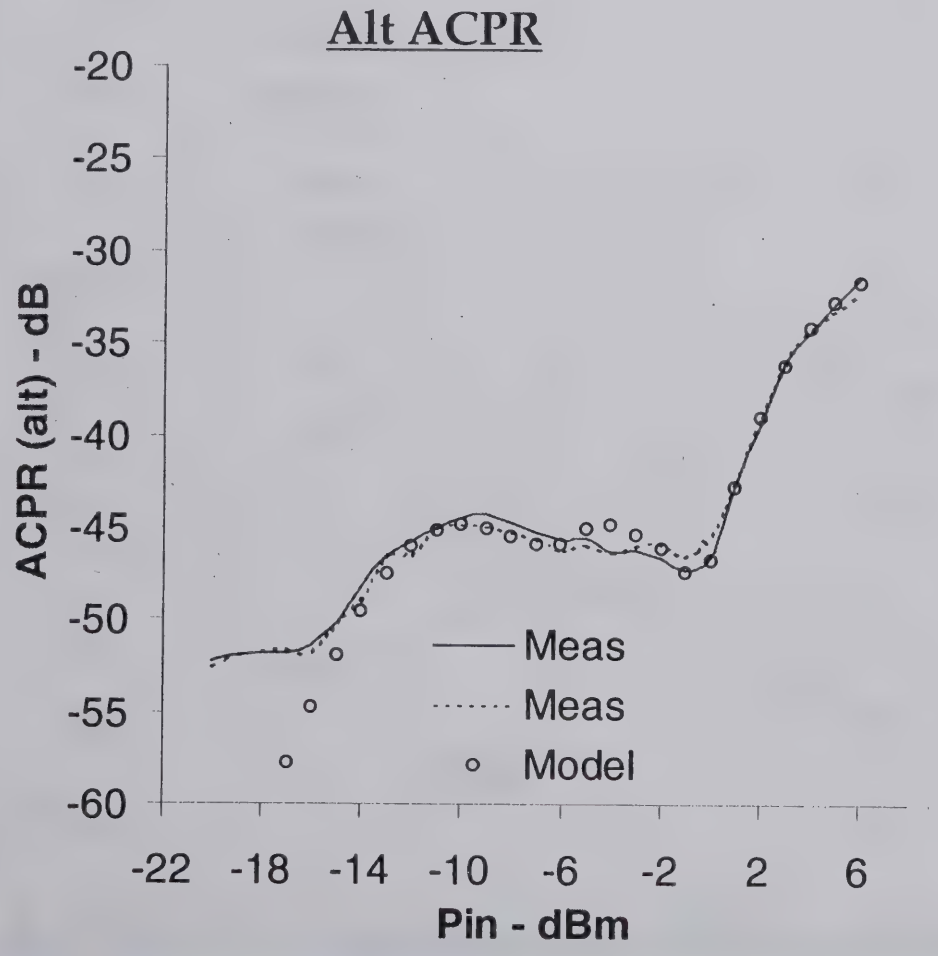

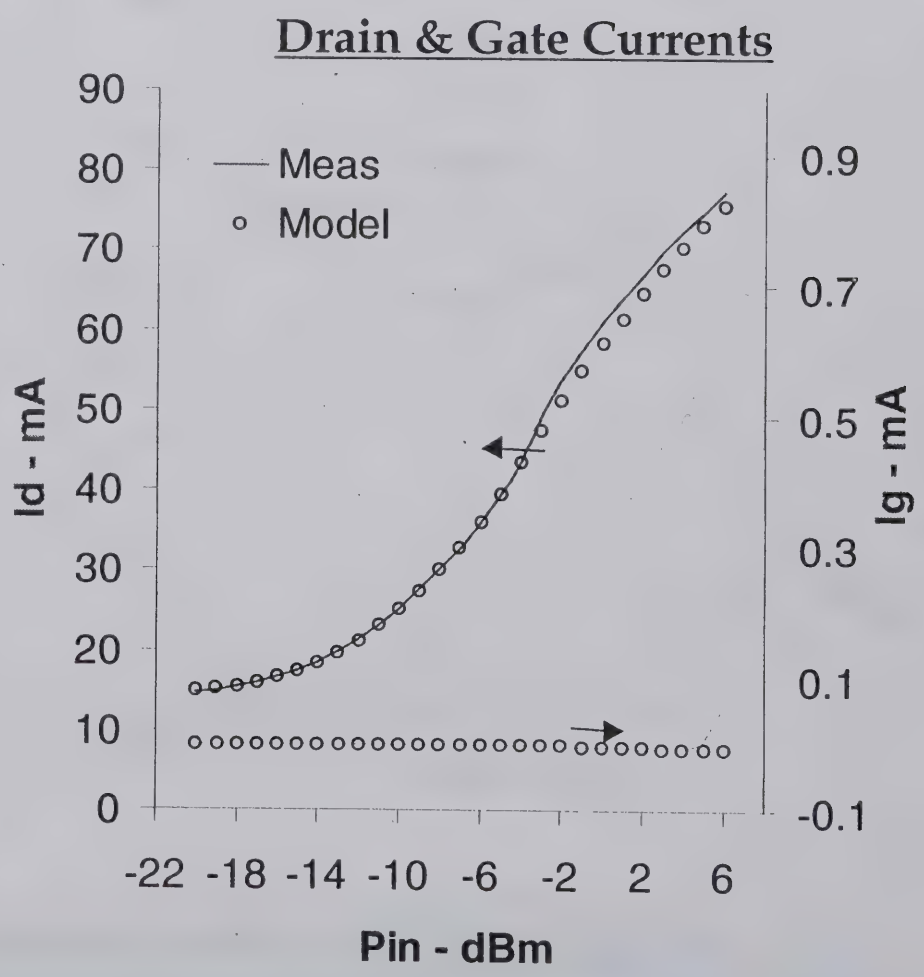

Behavioral Model Validation Studies

- **Comparison of Measured & Modeled Results**
  O-QPSK CDMA Compliant Stimulus

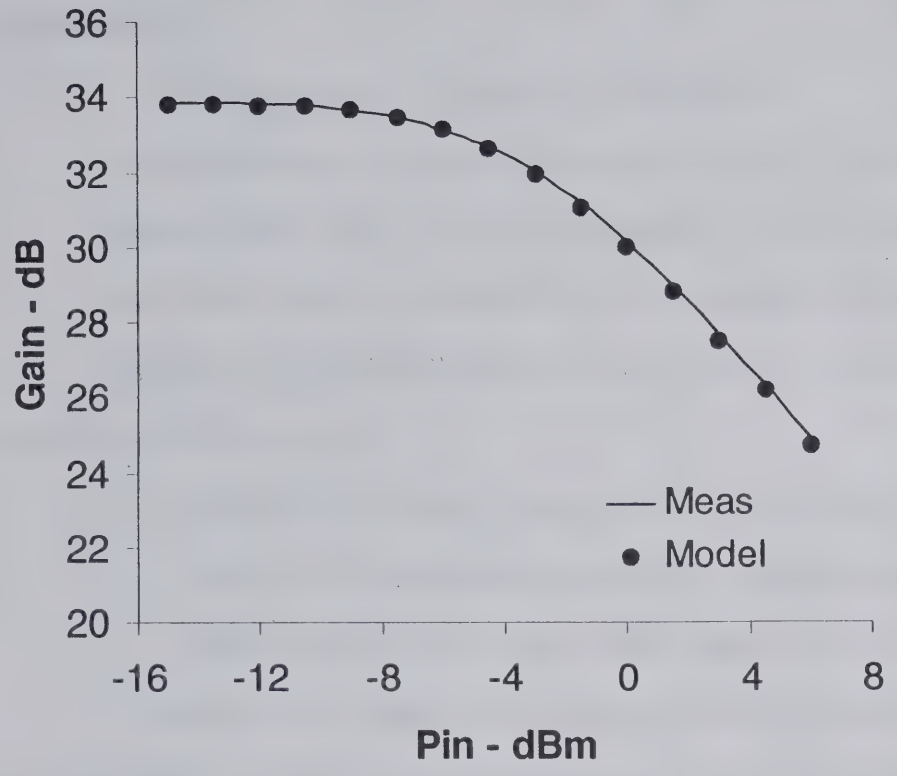

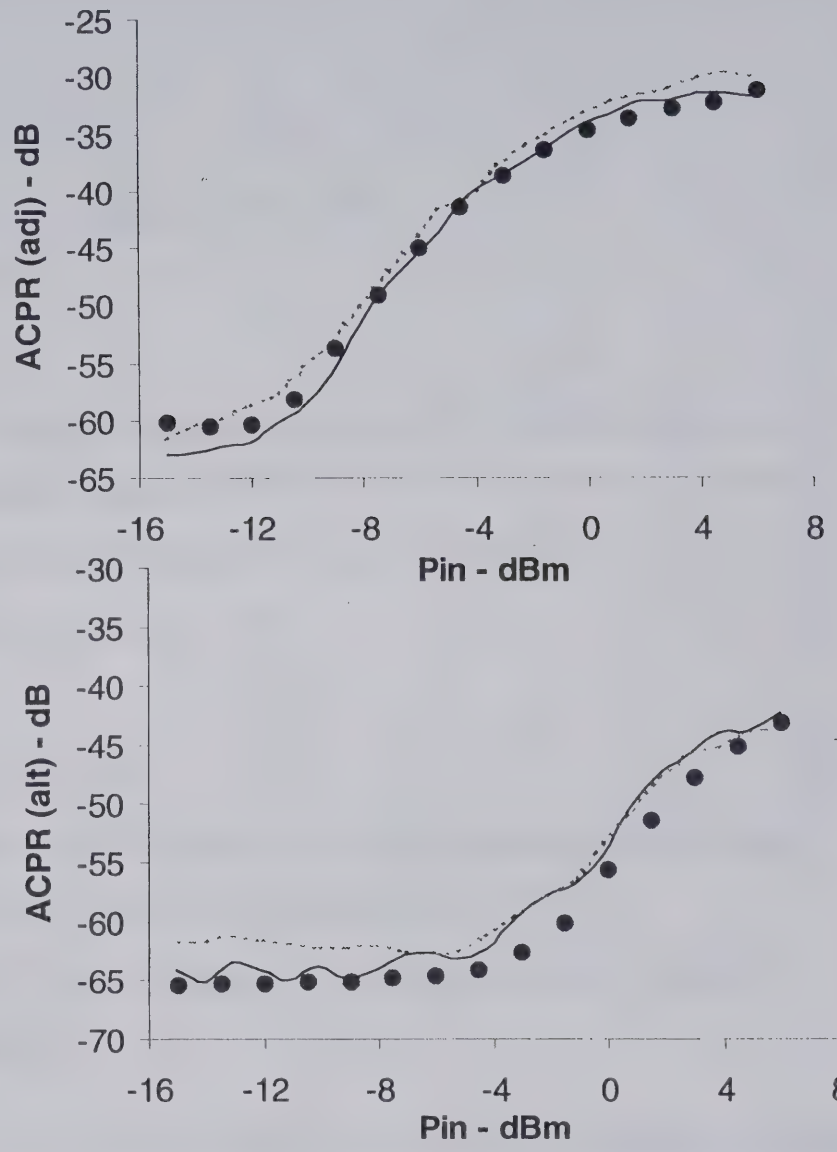

Summary

- ➜ The Behavioral Method Can Be An Effective Design & Analysis Tool For Certain Problems
- ➜ Accurate Predictions Shown For Various Signal
  - 2 tone sinusoidal, $\pi/4$ DQPSK stimuli compliant w/ NADC, O-QPSK CDMA Signal
    - Gain, Efficiency, IM3, IM5, IM7, Adj. & Alt. Channel Pwr Ratios, I_{DD}, I_{GG}
    - Results Compare Closely w/ Measurements & Results From Other Simulations
    - Computationally Efficient - 3 Seconds (2 tone)
- ➜ Some Limitations
  - Signal & Circuit Must Be Bandpass & Memoryless
  - May Be More Problematic for Wider Bandwidth Signals, E.G., W-CDMA
  - GaAs Devices Tend To Exhibit Some Memory Effects
  - Sub-harmonic Terminations Are Not Considered With a CW Single Tone Derived
    - AM-AM and AM-PM Response
- ➜ Issues
  - Number Of Terms Used in Series Expansion Affect Accuracy
  - Series Basis Functions

Behavioral Analysis Methods Applied To The Design & Simulation of Linear Power Amplifiers

J. Staudinger
Motorola, Semiconductor Products Sector
2100 E. Elliot Road, MS EL-712, Tempe, AZ 85284

Abstract

This work examines some of the issues and limitations of applying behavioral analysis methods to the design and simulation of linear power amplifiers driven by digitally modulated signals, such as for example, those applied in digital cellular handsets. Compared to other analysis techniques, this method offers the advantages of computational efficiency and a high degree of accuracy when certain criteria are satisfied. Such criteria are examined and illustrations are included comparing the results obtained from this method to measured amplifier data as well as to results obtained by other simulation techniques.

Introduction

Generally, the usual RF design/simulation tools such as SPICE and conventional harmonic balance are poorly suited for predicting the non-linear performance of power amplifiers driven by digitally modulated stimuli. In second generation digital cellular systems, the modulation bandwidth is small in comparison to the carrier frequency. For SPICE based analysis, time samples are taken at a fraction of the period of the carrier signal which then requires an extraordinarily high number of time samples (and simulation time) to represent even a short data sequence. The difficulty with conventional harmonic balance lies with high numbers of frequency components needed to describe such a waveform. Several alternatives to SPICE and conventional harmonic balance can be applied to this problem. One alternative is a behavioral analysis approach which is the topic of this paper [1-4]. Numerous behavioral models have been suggested and a substantial amount of work has been published in this area. The focus of this work, however, is to review a number of basic issues which affect the success of this method when it is applied to predict key power amplifier performance parameters, such as adjacent channel power ratio (ACPR), output power, and efficiency.

Behavioral Analysis

To begin, the bandwidth of the modulated carrier is assumed narrow (with respect to the carrier frequency) and as such the signal can be written as:

$$v_{in}(t) = V(t)\cos(\omega_o t + \Theta(t)) \tag{1}$$

or alternatively in an I/Q format as

$$v_{in}(t) = \mathrm{Re}\left[(V_i(t) + jV_q(t))e^{j\omega_o t}\right] \tag{2}$$

where $V(t)$ is the modulation envelope,
ω_o is the carrier, and
$\Theta(t)$ describes phase characteristics.

Assuming the amplifier non-linearity can be represented as a memoryless and bandpass non-linearity, and restricting the output voltage to the first spectral zone, the output voltage takes the form:

$$v_{out}(t) = \mathrm{Re}\left\{G(V(t))e^{j\{\Theta(t)+\varphi(V(t))+\omega_o t\}}\right\} \tag{3}$$

Where G(V) and ϕ(V) describe amplitude and phase characteristics of the amplifier as a function of input envelope voltage (V). Alternatively, the voltage can be expressed in an I/Q format which takes the following form:

$$v_{out}(t) = \mathrm{Re}\left\{\left[\begin{array}{l} G_i[V(t)](Vi(t) + jVq(t)) + \\ jG_q[V(t)](Vi(t) + jVq(t)) \end{array}\right] e^{j\omega_o t}\right\} \tag{4}$$

Where G_i and G_q are in- and quadrature-phase amplitude (only) gain transfer functions expressed as

$$G_i(V) = G(V)\cos(\varphi(V)) \tag{5}$$

and

$$G_q(V) = G(V)\sin(\varphi(V)) \tag{6}$$

In the above equation which describes the output voltage around the first spectral zone, the low pass nature of the signal is evident. However, it is important to emphasize two underlying assumptions, 1) the non-linearity & stimuli/circuit must be bandpass and 2) the non-linearity must be memoryless. The first requires that the frequency-dependence of the amplitude and phase characteristics be negligible over several x the modulation bandwidth centered around the carrier and harmonic frequencies. To a large extent, this is often the case for power amplifiers designed for second generation cellular systems since the modulation bandwidth is small in comparison to the carrier

frequency. In addition, circuit aspects of the amplifier, such as input & output matching networks applied around the device, generally exhibit a wide band response (relative to the modulation frequency) thereby providing a near constant impedance to the device over several x the modulation bandwidth. One exception is possible sub-harmonic frequency termination effects occurring near the zero'th spectral zone, such as those due to drain bias decoupling networks [6,7]. The second assumption dealing with memory is often violated to some extent due to thermal effects and other device memory behavior (e.g., time constants due to surface traps).

Previous work has shown that the behavior model can also be utilized to predict both supply current Idd(t) (from bias supply V_{DD}) and power added efficiency [7]. Similar to Eq. 4, supply current can be expressed as a function of the magnitude of the input envelope voltage. The time averaged value of Idd(t) along with the known supply voltage allows computing the dc power supplied to the amplifier (P_{DC}).

In general, the amplitude and phase transfer functions describing the non-linearity ($G_i V$ and $\theta(V)$) can be obtained either by measurement or simulation (such as harmonic balance or SPICE) using a single tone CW stimulus. In the latter case, the active device must be represented with an appropriate large signal model, and passive circuitry such as the input and output matching networks, must be adequately described over a broad frequency range to obtain an accurate determination of the non-linear gain/phase transfer function.

Issue 1 - Non Linear Transfer Functions

In general, the transfer functions G_i and G_q are often represented as a convergent series (odd functions) of sufficient order to accurately represent the measured am-am and am-pm response. The coefficients of the series expansion can easily be computed using least square techniques.

An example illustrating the am-am & am-pm response of a power amplifier obtained via harmonic methods based on a single tone CW stimulus is shown in Figure 1. Consider representing G_i as a series expansion of Bessel and Polynomial functions taking the form:

$$G_i = \sum_{k=odd}^{2M+1} a_k J1(kA\xi) \qquad (7)$$

and

$$G_i = \sum_{k=odd}^{2M+1} b_k (A\xi)^k \qquad (8)$$

where A is the amplitude of the signal envelope and ξ is a normalizing function. The residuals from fitting G_i to the am-am & am-pm data for values of M ranging from 2 to 40 is shown in Figure 2. A Q/R matrix factorization method based on a least squares method was applied to extract series coefficients. Clearly, as the order of the series increases, the residuals decrease and the series expansion more closely represents the data. An exception is noted for the Polynomial series at high orders (M>20) where the residuals begin to increase due to high condition of the matrix. It is also noted that for a given value of M, the residuals are generally smaller for the Bessel series. Although not shown, the results for the quadrature gain transfer function (G_q) exhibit similar behavior.

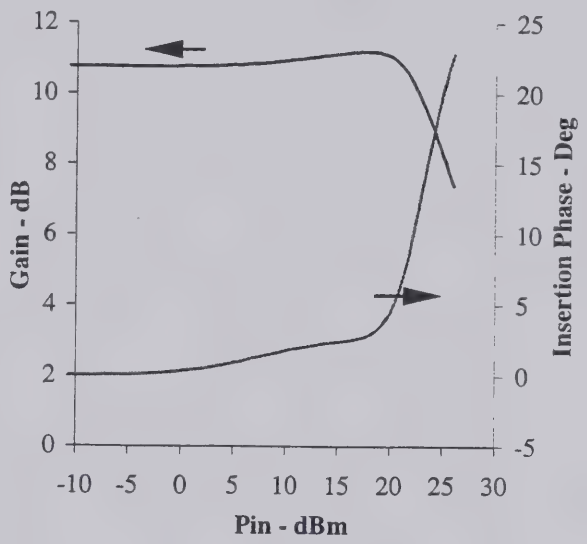

Figure 1 Am-am & am-pm response of power amplifier.

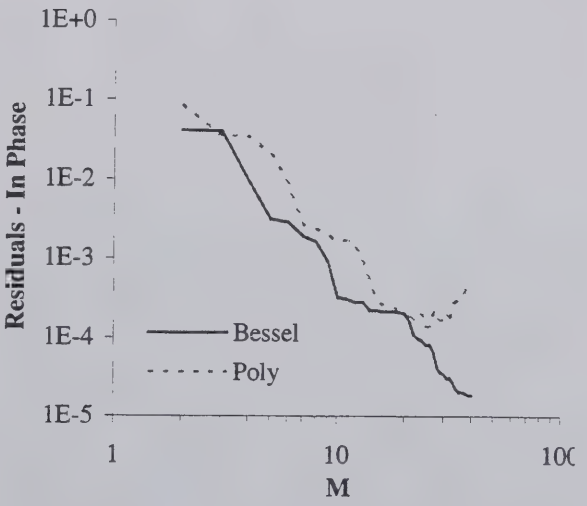

Figure 2 Residuals from fitting G_i to series expansions of Bessel and Polynomial functions.

A comparison of the amplifier's IM3 performance computed using harmonic balance contrasted to that obtained by behavioral analysis methods is illustrated in Figure 3. An inspection of Figure 3 suggest that in applying behavioral analysis techniques, the results obtained with transfer functions G_i and G_q expressed with Bessel functions result in more accurate predictions of IM3 compared to Polynomial expansions. It is also noted from an inspection of Figure 2, at M values of 10 and 15 the former series expansion has significantly smaller residuals than the latter. The results also suggest that for increasing values of M, the behavioral model predictions become more accurate. This trend is in agreement with previously reported results [6,7].

Issue 2 - Sub-harmonic Terminations

Previous results [5,6] have shown that sub-harmonic frequency terminations on the active device's gate & drain terminals on or around the frequency of the modulation envelope can significantly effect linearity performance of the amplifier. This effect is illustrated by way of example. Consider a 1 W power amplifier as illustrated by the partial schematic shown in Figure 4 where a 250 nH inductor is utilized for drain biasing. The IM response of the amplifier when driven by a two tone sinusoidal signal with tone spacing of 10 kHz and 1 MHz is calculated using harmonic balance methods and is illustrated in Figure 5. In addition, the amplifier am-am & am-pm response is calculated using harmonic balance by sweeping the power of a single tone CW stimulus. Both in-phase and quadrature-phase transfer functions are then calculated and the behavioral analysis method is exercised to determine the amplifier's IM3 performance for the above mentioned two tone sinusoidal stimulus at the two tone spacings. These results are also shown in Figure 5. The amplifier's IM3 performance computed using the two analysis methods are nearly identical for the 10 KHz tone spacing. However, at the higher tone spacing of 1 MHz, the two analysis methods differ substantially over the entire power range. It is also observed that the upper and lower frequency IM frequency products (including 3rd, 5th, and 7th) are unequal in amplitude. It is also observed, that the behavioral analysis results do not change with tone spacing.

For this case, it will be shown that these differences are due to device sub-harmonic termination effects related to the 250 nH drain bias inductor. At envelope frequencies of 10 kHz and 1 MHz, the 250 nH inductor presents an impedance at the drain terminal of .016 and 1.6 ohms, respectively – both of which are a relatively small value.

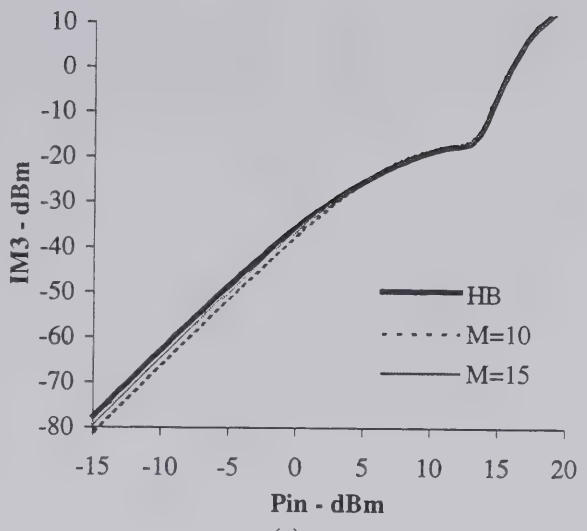

(a)

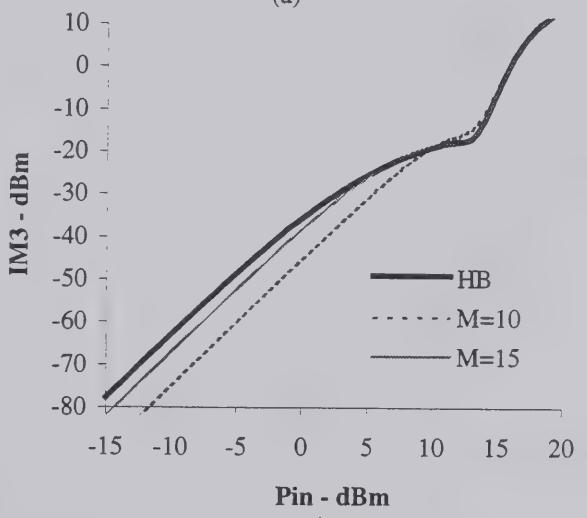

(b)

Figure 3. Amplifier IM3 response computed using harmonic balance (HB) compared to behavioral model predictions a) w/ G_i and G_q expressed as series expansion of Bessel functions, and b) w/ G_i and G_q expressed as series expansion of Polynomials.

The amplifier is now modified as shown in Figure 6 by including series resonant circuits connected at the device's intrinsic drain terminal. The resonant frequency of these circuits are set to coincide with the fundamental and harmonics of the envelope frequency, at n $f_{envelope}$, n=1, 2, 3 ... (e.g., 1, 2, 3 ... MHz). It is noted that these resonant circuits have no influence at the carrier frequency and harmonics of it. The amplifier's single tone am-am and am-pm response remains unchanged. The IM performance is recalculated using harmonic balance methods and the results are found to be nearly identical to those shown in

Figure 5, matching the results for the 10 KHz tone spacing and agreeing very well with behavioral analysis predictions.

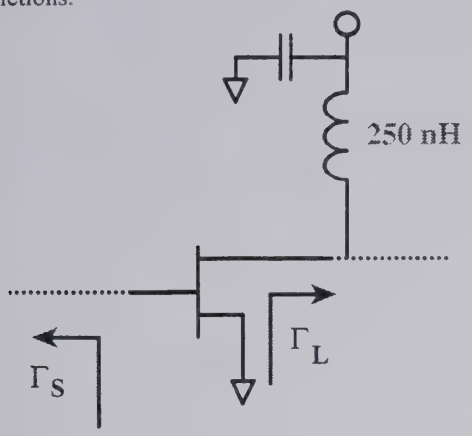

Figure 4 Partial schematic of a 1 W power amplifier where a 250 nH inductor is utilized for drain bias de-coupling.

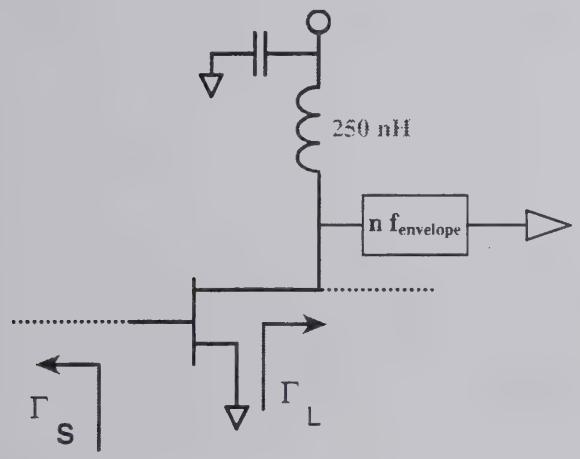

Figure 6 The amplifier is modified by including series resonant circuits connected at the device's drain terminal with the resonant frequency set to coincide with the fundamental and harmonics of the envelope frequency thereby presenting a zero ohm termination to these frequencies components.

This effect is investigated further by examining the envelope signal at the outputs of both amplifiers around the first spectral zone (Figure 7). The envelope signal corresponding to amplifier using a 250 nH drain bias inductor (Fig. 4) exhibits an envelope signal which is asymmetrical wrt to time with the asymmetry due to envelope signal contributions. The envelope signal has the appearance of a memory effect even though the large signal model utilized in the simulation is ideal in that it is memoryless (i.e., the instantaneous drain current does not depend on prior gate-source and drain-source voltages) The other amplifier configuration (Fig. 6) exhibits an envelope signal which is highly symmetrical wrt to time.

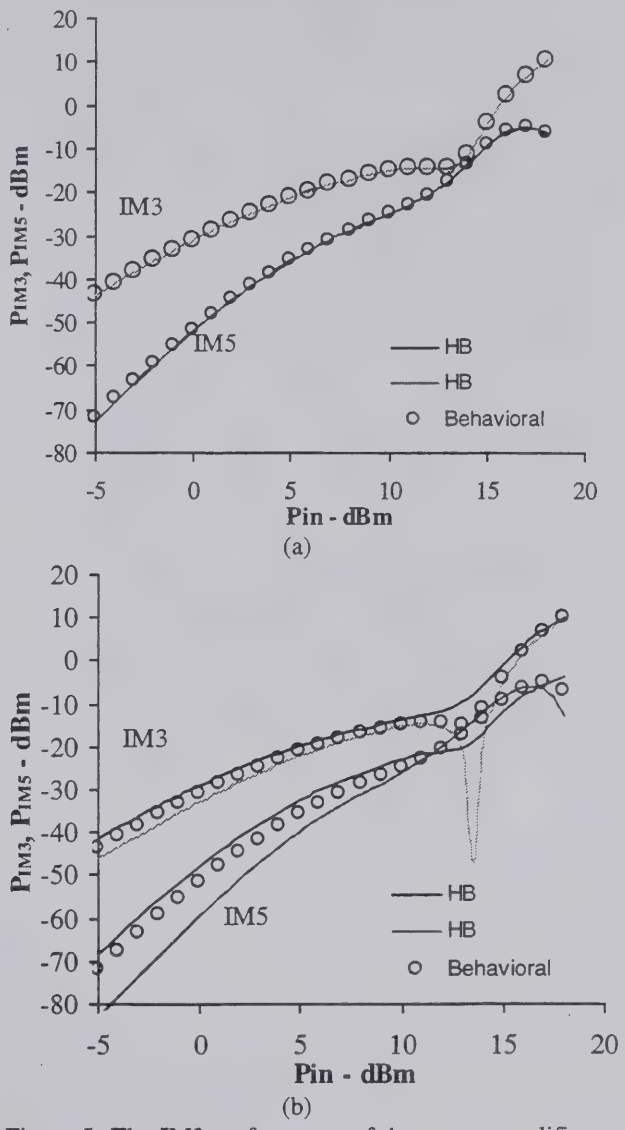

Figure 5 The IM3 performance of the power amplifier is simulated using harmonic balance (HB) and behavioral analysis methods for an input two-tone sinusoidal signal with tone separations of 10 KHz and 1 MHz. a) 10 KHz tone spacing, and b) 1 MHz tone separation.

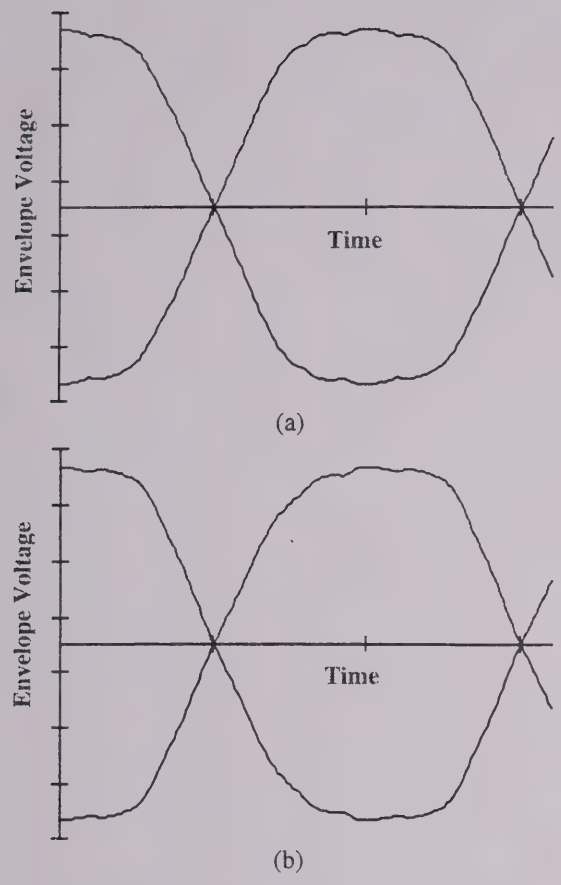

Figure 7 The envelope signal at the amplifier's output terminal around the first spectral zone. a) Envelope signal corresponding to amplifier configuration of Fig. 4, and b) Envelope signal corresponding to amplifier configuration of Fig. 6.

Summary

Behavioral analysis methods can accurately predict distortion characteristics, output power, and efficiency of power amplifiers driven by multi-tone sinusoids and digitally modulated signals when certain underlying criteria are satisfied. In general, model accuracy improves by representing the gain transfer functions with series expansions of increasing order. It is shown that sub-harmonic frequency terminations, such as those related to drain bias networks, can significantly effect the linearity performance of the amplifier. Such effects are not modeled by the behavioral analysis methods presented in this work.

References

[1] A. R. Kaye, D. A George, M. J. Eric, "Analysis and Compensation of Band pass Non-linearities," *IEEE Transactions on Communications,* vol. COM-19, October 1972, pp. 965-972.

[2] J. Jeruchim, P. Balaban, K. Shanmugan, *Simulation of Communication Systems,* Plenum Press, 1992

[3] M. Eric, "IMD Analysis of Non-linear Devices for Multiple-Carrier Inputs", CRC Report No. 1234, Communications Research Center, Department of Communications, Canada, 1972

[4] T. Takagi, S. Ogura, Y. Ikeda, N. Suematsu, "Intermodulation and Noise Power Ratio Analysis of Multiple-Carrier Amplifiers Using Discrete Fourier Transform", Trans. IEICE, Vol. E77-C, No 6, pp. 935-941, June 1994

[5] J. Sevic, K. Burger, M. Steer, "A Novel Envelope-Termination Load-Pull Method for ACPR Optimization of RF/Micorwave Power Amplifiers", 1998 IEEE International Microwave Symposium, June, 1998

[6] J. Staudinger, "The Importance Of Sub-Harmonic Frequency Terminations In Modeling Spectral Regrowth From CW AM-AM and AM-PM Derived Non-Linearities", Wireless Communications Conference, Boulder, CO, 8/12/97 pp 121-125

[7] J. Staudinger, "Applying the Quadrature Modeling Technique to Wireless Power Amplifiers", Microwave Journal, Nov., 1997 pp 66-86

Elements of Measurement-Based Large-signal Device Modeling

David E. Root
Hewlett Packard Company
Microwave Technology Center
Santa Rosa, CA 95403

Outline

- Conservation laws and their consequences
- Remarks on intermodulation
- Pulsed characterization and modeling of GaAs PHEMTs

Introduction: Physics to Equivalent Circuit

Shockley: field-independent mobility, gradual channel approximation, etc.:

Derive *terminal dynamics* and *constitutive relations*:

$$I_D(t) = I_D^{DC}(Vgs(t), Vds(t)) - C(Vgd(t))\frac{d}{dt}Vgd = I_D^{DC}(Vgs(t), Vds(t)) - \frac{d}{dt}Q(Vgd(t))$$

$$I_G(t) = C(Vgs(t))\frac{d}{dt}Vgs + C(Vgd(t))\frac{d}{dt}Vgd = \frac{d}{dt}Q(Vgs(t)) + \frac{d}{dt}Q(Vgd(t)) = \frac{d}{dt}Q_G(Vgs(t), Vgd(t))$$

$$I_D^{DC}(Vgs, Vds) = \frac{W\mu qN_D a}{\varepsilon L}\cdot\left[V_{ds} - \frac{2}{3}\sqrt{\frac{2\varepsilon}{qN_D a^2}}[[V_{ds}+\phi-V_{gs}]^{3/2} - [\phi - V_{gs}]^{3/2}]\right]$$

$$C(V) = WL\sqrt{\frac{q\varepsilon N_D}{2(\phi - V)}} \qquad C_{GS} = C(V_{GS})$$

$$Q(V) = -WL\sqrt{2q\varepsilon N_D(\phi - V)} \qquad C_{GD} = C(V_{GD})$$

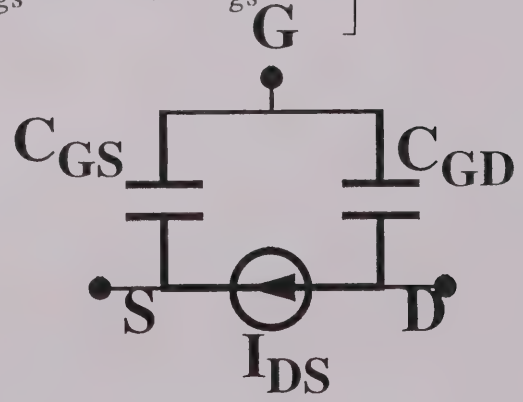

Physically-based *large-signal* equivalent circuit model

Voltage-controlled current source and two 2-terminal nonlinear capacitors

$C(V)\frac{dV}{dt} = \frac{d}{dt}Q(V)$ for any 2-terminal capacitor

Shockley -> C_{GS} *depends only on* V_{GS} ; C_{GD} *depends only on* V_{GD}

Capacitance Data parameterized by bias:

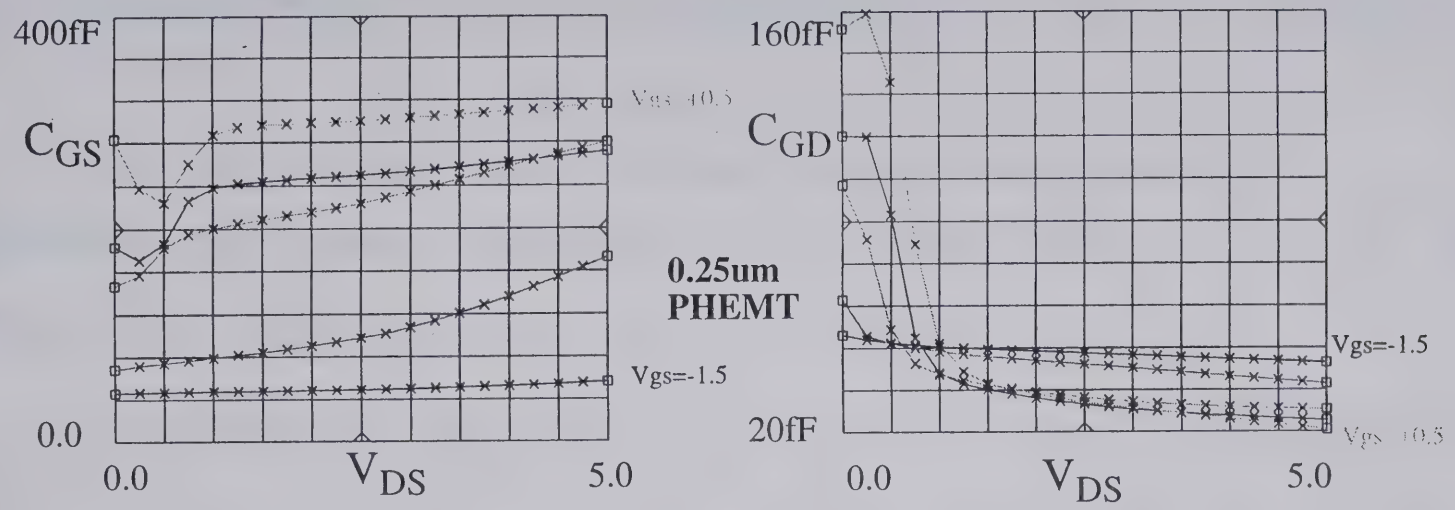

Extract Branch Elements from Port (nodal) data by:

$$\begin{bmatrix} C_{GS}+C_{GD} & -C_{GD} \\ C_{11} & C_{12} \end{bmatrix} \equiv \frac{\mathrm{Im}}{\omega}\left(\begin{bmatrix} Y_{11}^{data}(V_{GS}, V_{DS}, \omega) & Y_{12}^{data}(V_{GS}, V_{DS}, \omega) \end{bmatrix}\right)$$

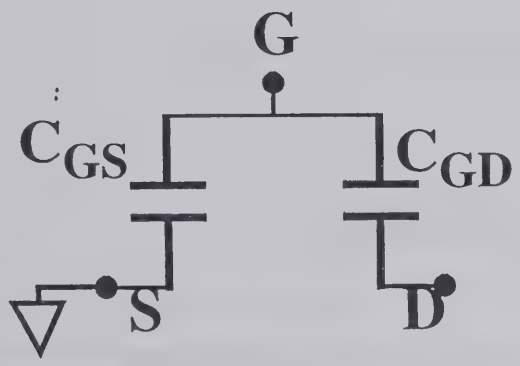

- C_{GS} and C_{GD} depend on *both* V_{GS} and V_{GD}
- C_{GD} at pinch-off < C_{GD} open channel
- C_{GS} and C_{GD} are not two-terminal capacitors
- Data requires reinterpretation of equivalent circuit

Multi-terminal capacitances

Proposal: The time-domain gate current can be written:

$$I_G(t) = C_{GS}(V_{GS}(t), V_{DS}(t))\frac{d}{dt}V_{GS}(t) + C_{GD}(V_{GS}(t), V_{DS}(t))\frac{d}{dt}V_{GD}(t)$$

Question: Is this a good way to model "displacement current even though it will agree *exactly* with bias-dependent linear data?"

Answer: Probably Not!

Reason: This will produce a *DC component* of $I_G(t)$, which increases as the frequency of the fundamental increases

Can always implement above ODEs in simulators such as MDS or ADS (see later on)

Example

Expand capacitances about a fixed operating point, say $V_{GS}^{op} = -1$ $V_{DS}^{op} = 2.5$

$$C_{GS} = C_{GS0} + \lambda_{11} v_{GS} + \lambda_{12} v_{DS} + O(v_{GS}^2, v_{DS}^2, v_{GS} v_{DS})$$

$$C_{GD} = C_{GD0} + \lambda_{21} v_{GS} + \lambda_{22} v_{DS} + O(v_{GS}^2, v_{DS}^2, v_{GS} v_{DS})$$

Assume terminal voltages vary according to: $v_{GS}(t) = A\cos(\omega t)$ $v_{DS}(t) = A\sin(\omega t)$

Substitute into:

$$I_G(t) = C_{GS}(V_{GS}(t), V_{DS}(t))\frac{d}{dt}V_{GS}(t) + C_{GD}(V_{GS}(t), V_{DS}(t))\frac{d}{dt}V_{GD}(t)$$

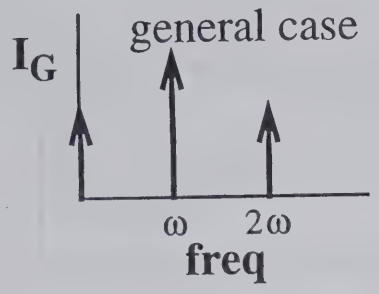

$$\overline{I_G(t)} = -\frac{A^2\omega}{2}(\lambda_{12} + \lambda_{21} + \lambda_{22})$$

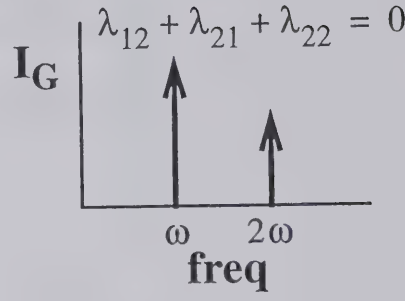

Notice, for this example:

$$\frac{\partial}{\partial v_{DS}}(C_{GS} + C_{GD}) = \lambda_{12} + \lambda_{22} \qquad \frac{\partial C_{GD}}{\partial v_{GS}} = \lambda_{21}$$

To avoid non-physical DC components, we can write:

$$\frac{\partial}{\partial V_{DS}}(C_G) - \frac{\partial}{\partial V_{GS}}(-C_{GD}) = 0 \qquad \text{where } C_G \equiv C_{GS} + C_{GD}$$

This constraint on the model capacitances is *general*

One *can not independently fit capacitances* directly from bias-dependent

Terminal Charge Conservation Law

Rewrite previous equation as: $\nabla \times C = 0$

with $\nabla = \hat{V}_{GS}\frac{\partial}{\partial V_{GS}} + \hat{V}_{DS}\frac{\partial}{\partial V_{DS}}$ and $C = \begin{bmatrix} C_G \\ C_{GD} \end{bmatrix}$

$\Rightarrow \exists Q_G$ such that

$$C_G^{model}(V_{GS}, V_{DS}) \equiv \frac{\partial}{\partial V_{GS}} Q_G^{model}(V_{GS}, V_{DS})$$

$$C_{GD}^{model}(V_{GS}, V_{DS}) \equiv -\frac{\partial}{\partial V_{DS}} Q_G^{model}(V_{GS}, V_{DS})$$

$$I_G(t) = \frac{d}{dt} Q_G^{model}(V_{GS}, V_{DS})$$

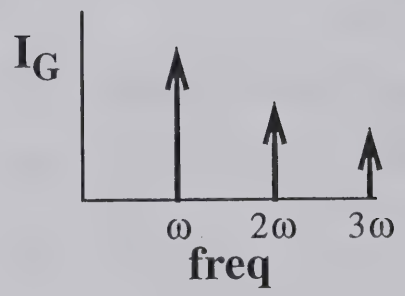

- C_G and C_{GD} are said to "conserve terminal charge at the gate" or "conserve gate charge"
- C_G and C_{GD} form a *two-dimensional conservative vector field* in voltage space
- Constraints must be consistent with bias-dependence of measured linear (small-signal) parameters. This is testable *independent of any functional form* of the model constitutive relations
- Q_G can be constructed by path-independent contour integration
- *Two independent model functions*, C_{GS} and C_{GD}, now *replaced by a single model function*, Q_G
- Constraints may cause non-exact model simulation of measured bias-dependence of S-parameters

Charge can be calculated, for conserving capacitances

$$C_G(V_{GS},V_{DS}) \equiv \frac{\text{Im } Y_{11} \quad (V_{GS},V_{DS},\omega)}{\omega} \qquad C_{GD}(V_{GS},V_{DS}) \equiv \frac{-\text{Im } Y_{12} \quad (V_{GS},V_{DS},\omega)}{\omega}$$

$$Q_G(V_{GS},V_{DS}) = \oint [C_G(V'_{GS},V'_{DS})dV'_{GS} - C_{GD}(V'_{GS},V'_{DS})\,dV'_{DS}]$$

- The contour integrals are path independent

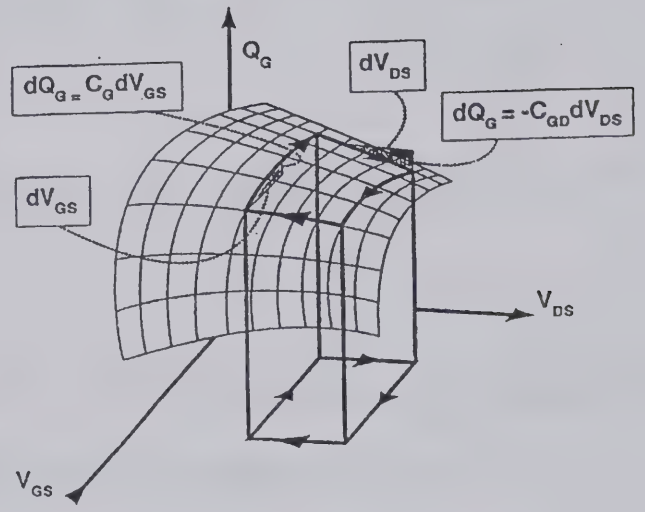

Experimental Validation

Gate Charge QG (VGS, VDS)
(Computed Along Two Different Contours

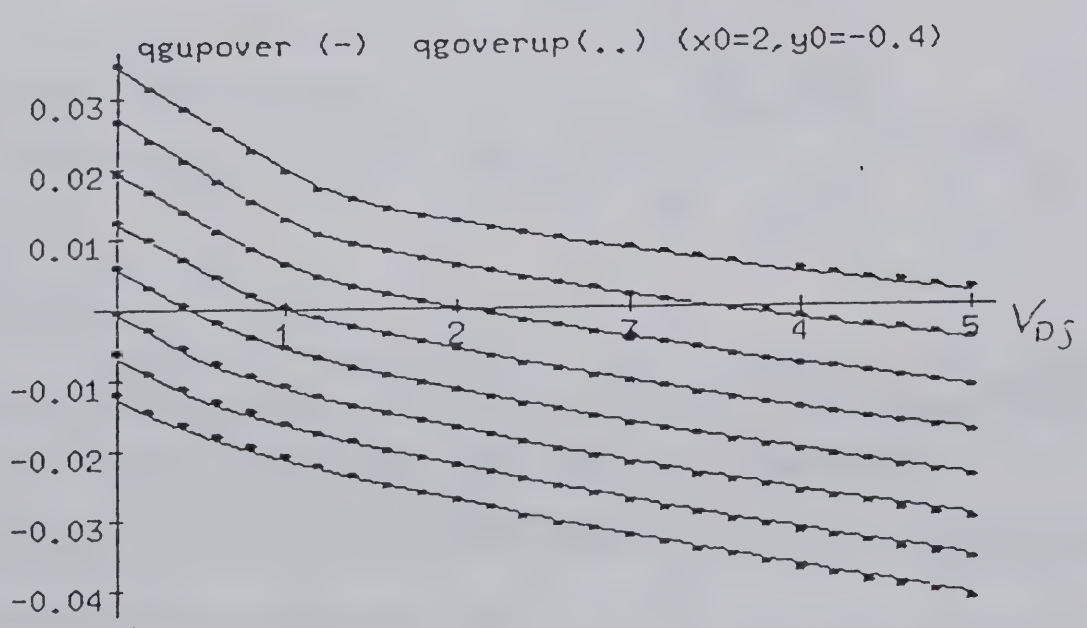

$$-1.4V \leq V_{GS} \leq 0V$$

Full Two-Port Capacitance Model

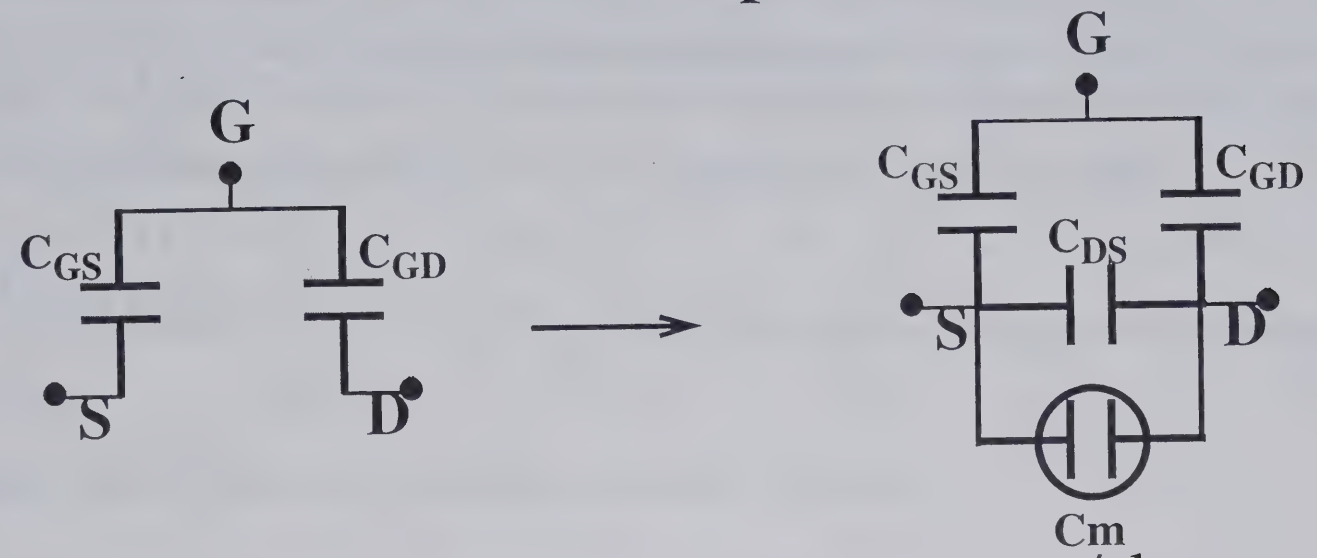

Four "independent" capacitance measurements/elements

$$\begin{bmatrix} C_{GS}+C_{GD} & -C_{GD} \\ C_m - C_{GD} & C_{DS}+C_{GD} \end{bmatrix} \equiv \frac{\mathrm{Im}}{\omega}\left(\begin{bmatrix} Y_{11}^{data}(V_{GS}, V_{DS}, \omega) & Y_{12}^{data}(V_{GS}, V_{DS}, \omega) \\ Y_{21}^{data}(V_{GS}, V_{DS}, \omega) & Y_{22}^{data}(V_{GS}, V_{DS}, \omega) \end{bmatrix} \right)$$

Transcapacitance C_m comes from linear equivalent circuit model with delay

$$g_m e^{-j\omega\tau} \approx g_m(1 - j\omega\tau) = g_m + j\omega C_m$$

$$C_m \approx -\, g_m \tau$$

C_m can be comparable to C_{GD}

Two-port Charge-Based Model

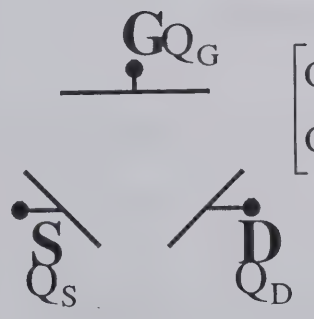

$$\begin{bmatrix} C_{11} & C_{12} \\ C_{21} & C_{22} \end{bmatrix} \equiv \begin{bmatrix} C_{GS}+C_{GD} & -C_{GD} \\ C_m - C_{GD} & C_{DS}+C_{GD} \end{bmatrix} \equiv \begin{bmatrix} \frac{\partial Q_G}{\partial V_{GS}} & \frac{\partial Q_G}{\partial V_{DS}} \\ \frac{\partial Q_D}{\partial V_{GS}} & \frac{\partial Q_D}{\partial V_{DS}} \end{bmatrix} \equiv \frac{\mathrm{Im}}{\omega}\left(\begin{bmatrix} Y_{11}^{model} & Y_{12}^{model} \\ Y_{21}^{model} & Y_{22}^{model} \end{bmatrix} \right)$$

$$I_i(t) = \frac{d}{dt} Q_i(V_{GS}, V_{DS}) \quad i = G, D, S$$

Still have four, unequal capacitance matrix elements

KCL is *not terminal charge conservation*, but rather global charge conservation

$$Q_G + Q_D + Q_S = 0 \quad (KCL)$$

***Four* capacitances derivable from *two* independent node charges**

Question: Is this a good way to model an active device charge storage, even though it guarantees no dc components to generated currents?

Answer: Probably Not

Reason: Non-reciprocal capacitances (transcapacitances) imply energy is not conserved!

Energy Conservation

Energy constrains charges as charge constrains capacitances

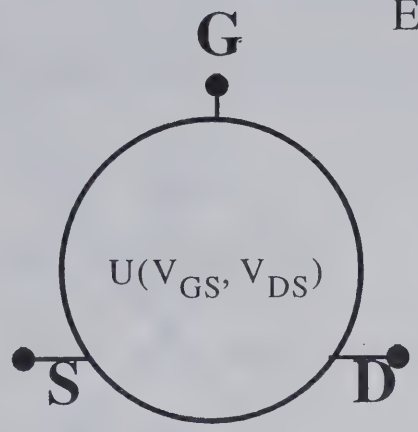

$$\nabla \times Q = 0 \qquad Q = \begin{bmatrix} Q_G \\ Q_D \end{bmatrix} \qquad \nabla = \hat{V_{GS}} \frac{\partial}{\partial V_{GS}} + \hat{V_{DS}} \frac{\partial}{\partial V_{DS}}$$

$$Q_G \equiv \frac{\partial U}{\partial V_{GS}} \qquad Q_D \equiv \frac{\partial U}{\partial V_{DS}} \qquad \frac{\partial Q_D}{\partial V_{GS}} = C_{21} = C_{12} = \frac{\partial Q_G}{\partial V_{DS}}$$

$$\begin{bmatrix} C_{GS}+C_{GD} & -C_{GD} \\ -C_{GD} & C_{DS}+C_{GD} \end{bmatrix} \equiv \begin{bmatrix} \frac{\partial^2 U}{\partial V_{GS}^2} & \frac{\partial^2 U}{\partial V_{GS}\partial V_{DS}} \\ \frac{\partial^2 U}{\partial V_{GS}\partial V_{DS}} & \frac{\partial^2 U}{\partial V_{DS}^2} \end{bmatrix} \equiv \frac{\mathrm{Im}}{\omega}\left(\begin{bmatrix} Y_{11}^{\mathrm{model}} & Y_{12}^{\mathrm{model}} \\ Y_{21}^{\mathrm{model}} & Y_{22}^{\mathrm{model}} \end{bmatrix} \right)$$

Down to *one* independent model function, U, for reactive model

Frequency Dispersion in GaAs FETs

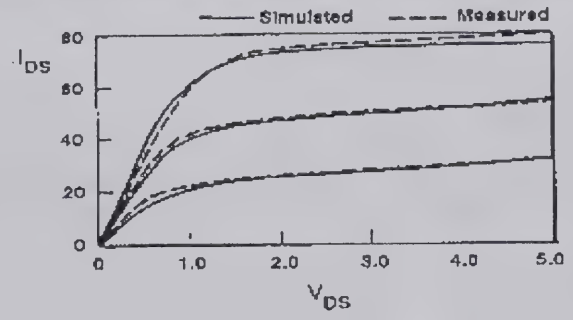

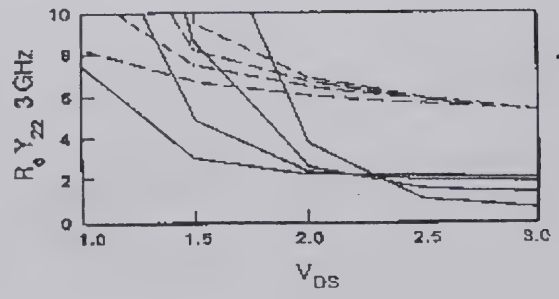

1. Fit Transfer Curves → 2. Model RF g_{DS} Doesn't Fit

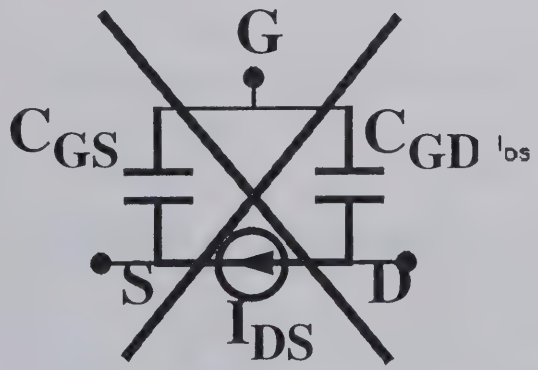

3. Fit RF g_{DS} → 4. Now Model Transfer Curves Don't Fit

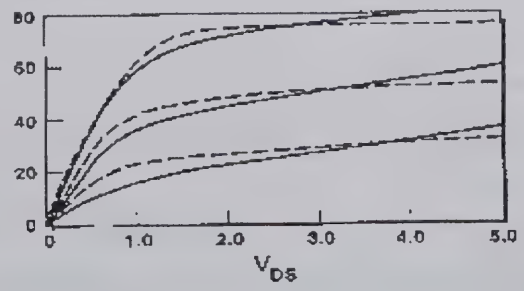

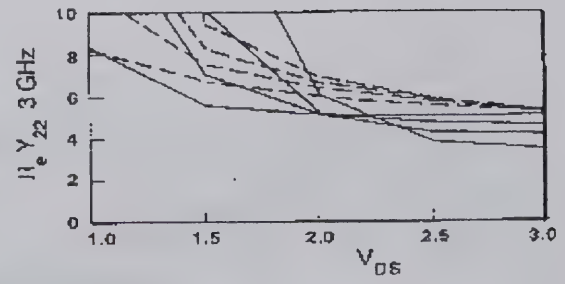

$$g_m(\vec{V}, \omega) \equiv \mathrm{Re}(Y_{21}(\vec{V}, \omega)) \neq \frac{\partial}{\partial V_1} I_D^{DC}(\vec{V})$$

$$g_{DS}(\vec{V}, \omega) \equiv \mathrm{Re}(Y_{22}(\vec{V}, \omega)) \neq \frac{\partial}{\partial V_2} I_D^{DC}(\vec{V})$$

Simple text book relations don't hold!

Can't simultaneously fit DC and bias-dependent small-signal admittances with a single I-V transfer function

Is There Another Conservation Law Here?

$$\nabla \times g = 0 \; ? \quad g = \begin{bmatrix} g_m^{ac} \\ g_{DS}^{ac} \end{bmatrix} = \begin{bmatrix} \mathrm{Re}(Y_{21}(\vec{V}, \omega)) \\ \mathrm{Re}(Y_{22}(\vec{V}, \omega)) \end{bmatrix} \Rightarrow \quad g_m^{ac} = \frac{\partial I_D^{high}}{\partial V_{GS}} \qquad g_{DS}^{ac} \equiv \frac{\partial I_D^{high}}{\partial V_{DS}}$$

- Not as well-satisfied as terminal charge conservation conditions
  I_D^{high} is path-dependent
- Probable Causes: Thermal (self-heating) and trapping effects
- Consequence of imposing this constraint is that S21 and S22 can not simultaneously fit, vs. bias, exactly over the entire operating space

Vd=5V
Vg=-0.5

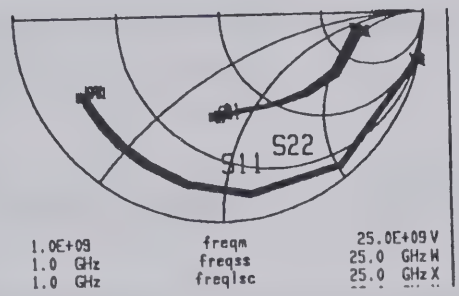

Vd=2.5V
Vg=+0.5

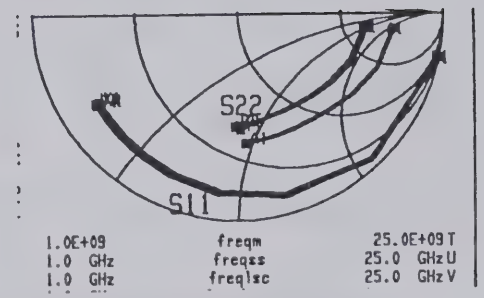

State Functions: High Frequency Curents

High Frequency Drain Current $I_D^{High}(Vgs, Vds) \simeq \oint g_m^{ac} \cdot dV_{GS} + g_{ds}^{ac} \cdot dV_{DS}$
computed along two different contours

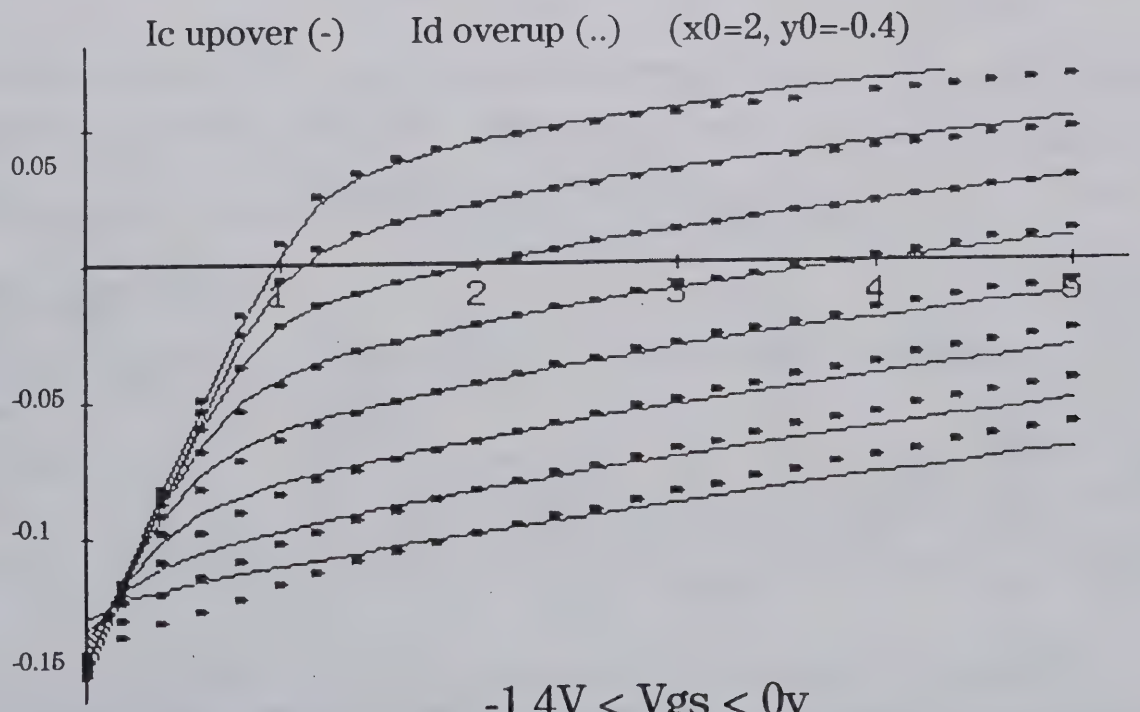

$-1.4V \leq Vgs \leq 0v$

From ReY21(Vgs, Vds) & ReY22(Vgs, Vds)

Large-signal Model with Qg, Qd, and Id-high

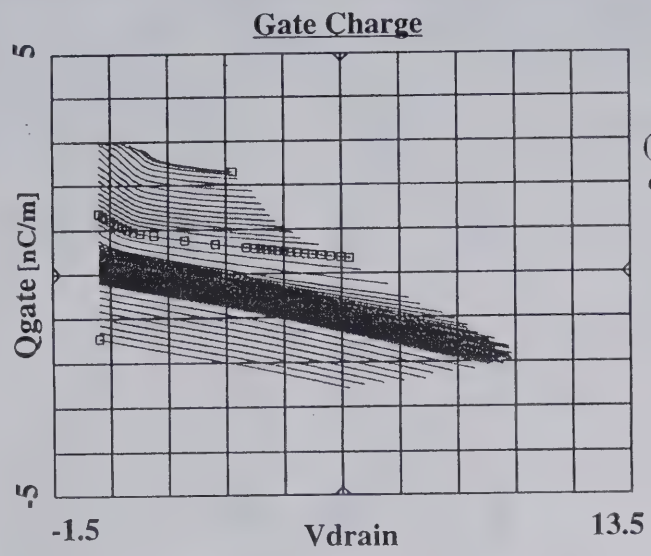

(Red points correspond to Vgate=-0.2V)

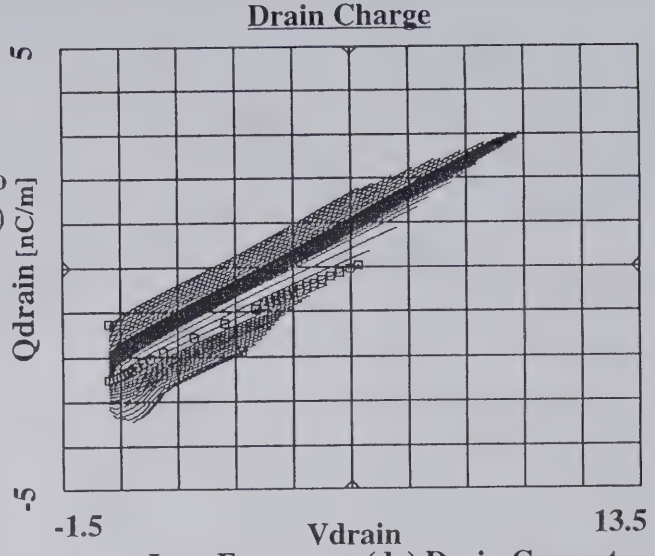

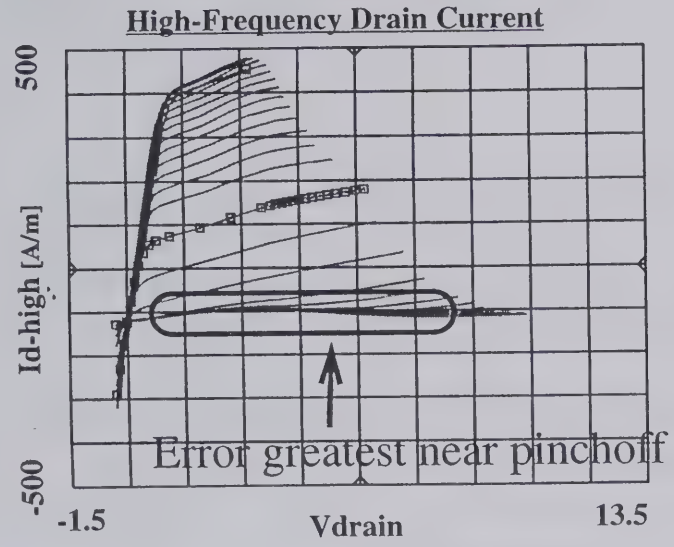

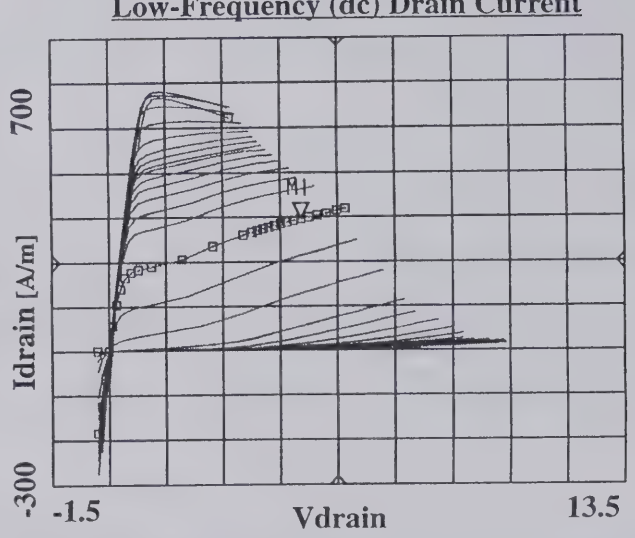

Effect of Transcapacitance + Conservation Constraints

Data to 25 GHz
Simulations to 50 GHz

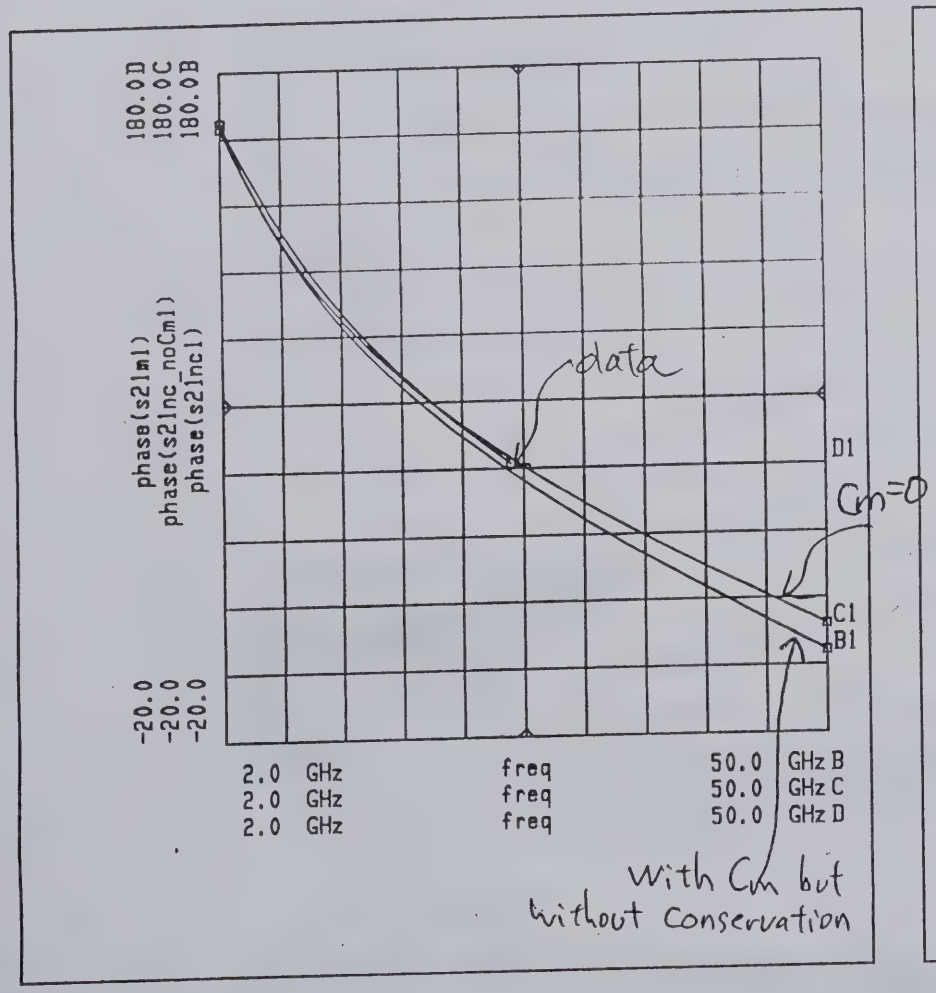

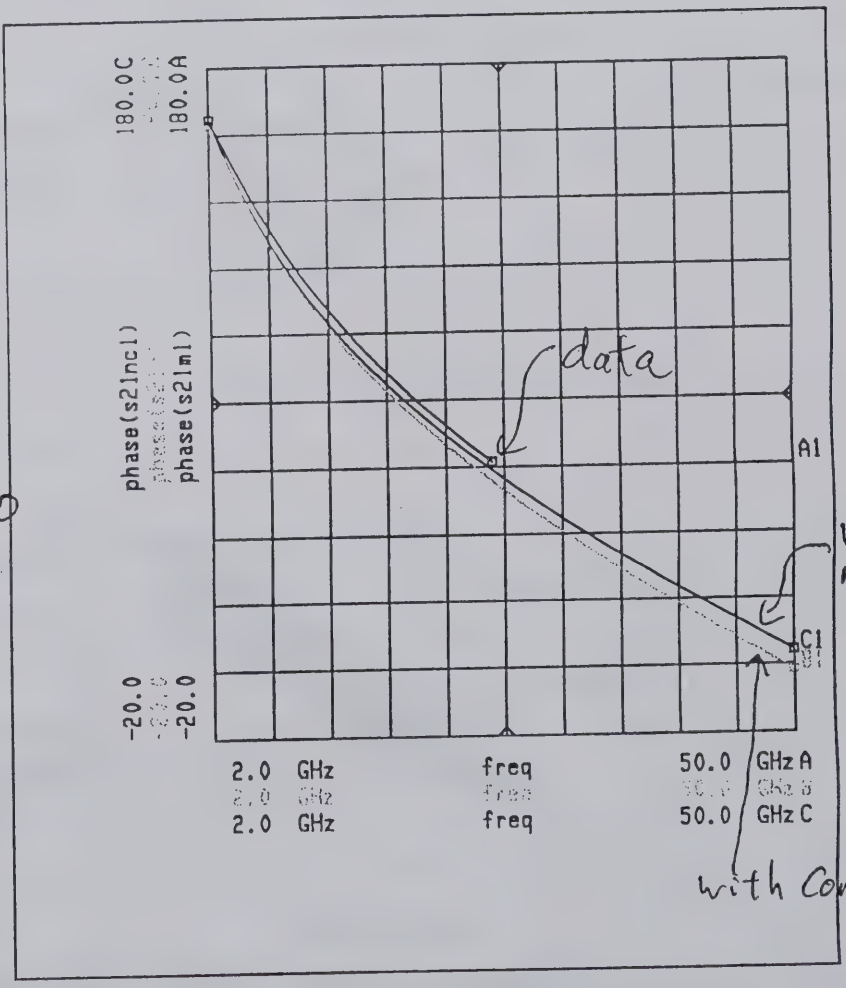

Intermodulation and Table-Based Models; Splines

Si NJFET

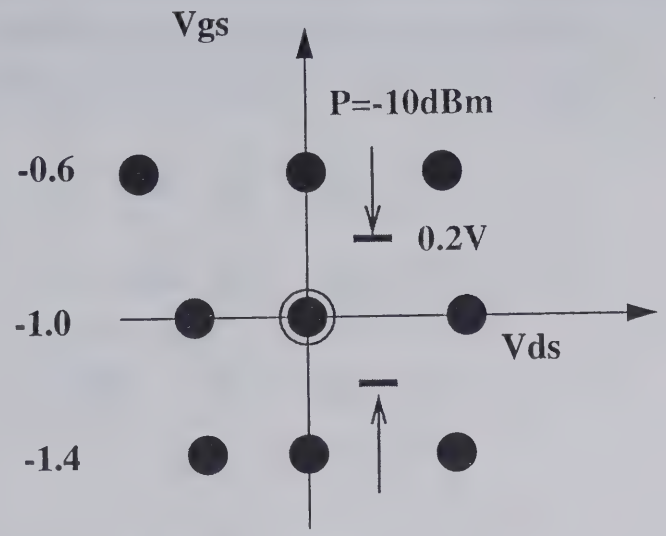

2-tones @ 100MHz (+1MHz)

(a) Vg=-1V Power=-10dBm

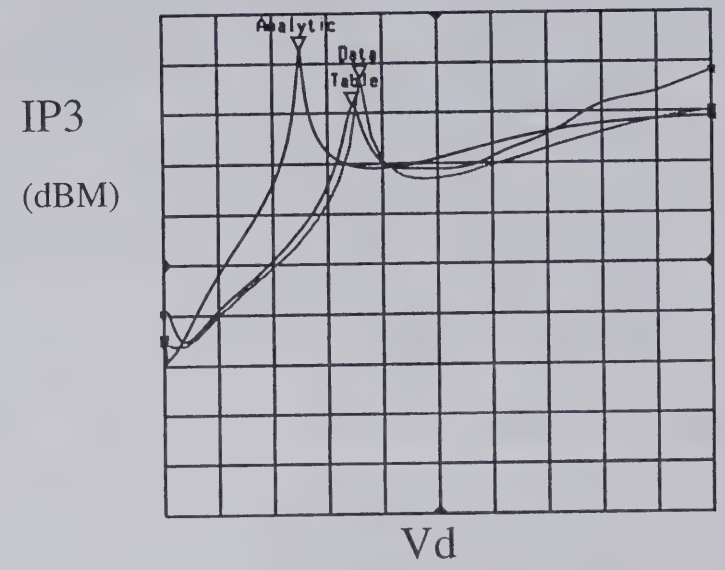

- Scales unlabeled for confidentiality
- Results from Spline-based models can depend on *interpolant* rather than *data* for small-amplitude signals (for some spline schemes, at some biases).
- When signal voltage swings become comparable to the distance between data points, model accuracy is acceptable.

Consequences of Spline Behavior

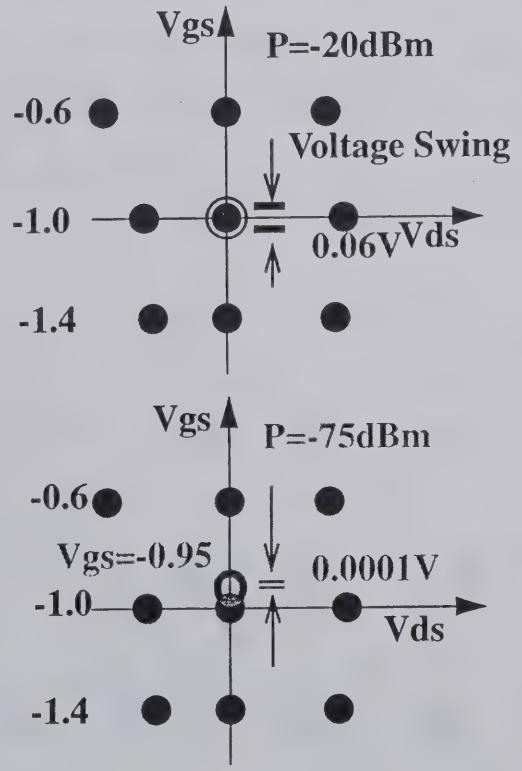

(b) Vg=-1V Power=-20dBm

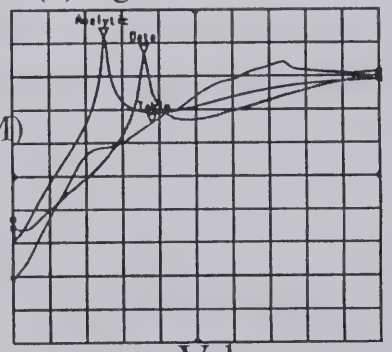

(c) Vg=-0.95V Power=-75dBm

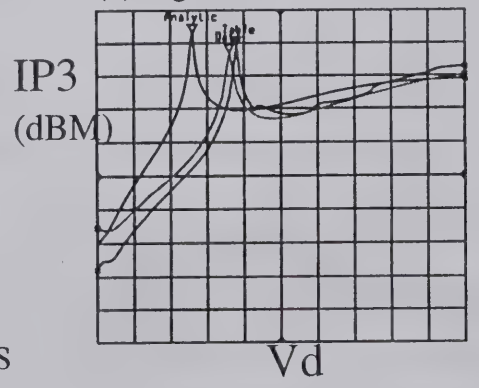

- Results can depend on *interpolant* at low amplitudes
- Watch out for spline symmetry pts!
- Want multi-dimensional approximation (constrained splines). Generally hard.
- Want highly differentiable constitutive relations & correct dynamical models
- Intermods and harmonics are not just derivatives of transfer functions

Diode Model Simulated and Measured [15]

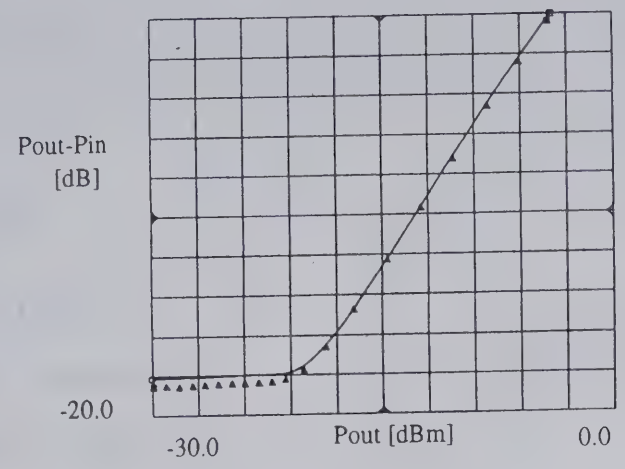

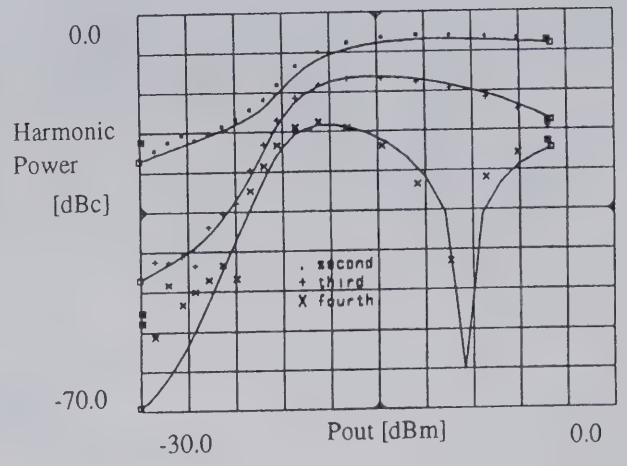

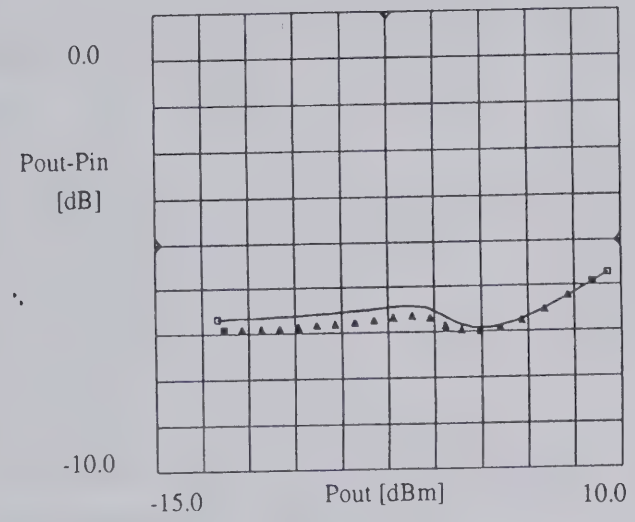

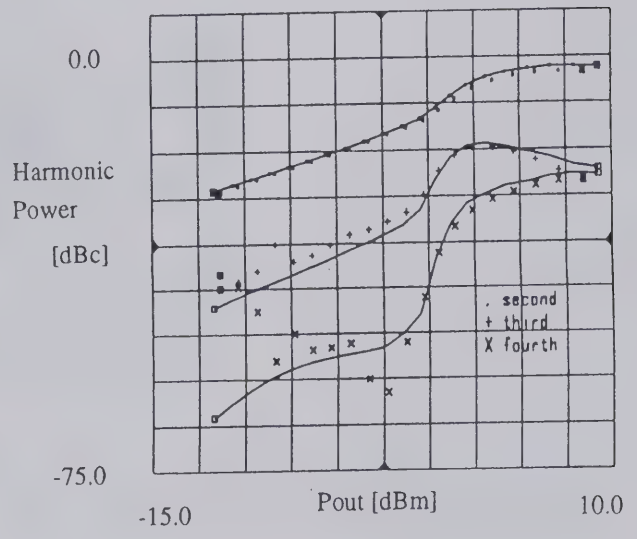

0-6 GHz HEMT Feedback Amplifier

- Another example of excellent agreement between measured and modeled power and harmonics

(Matt Borg)

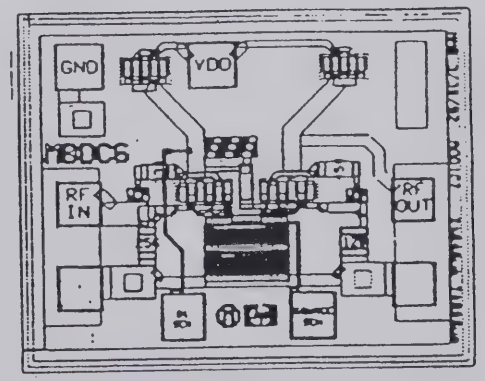

chip size : 640 x 800 μm^2

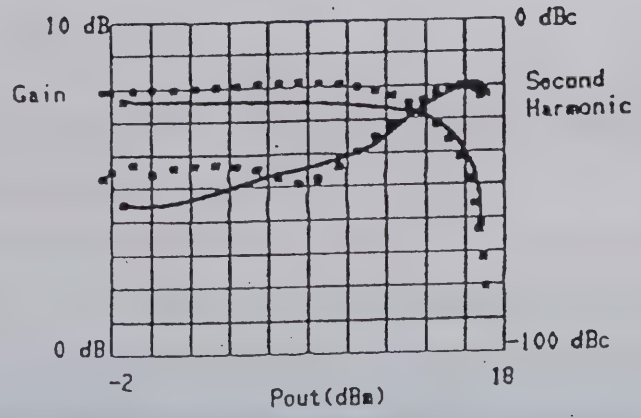

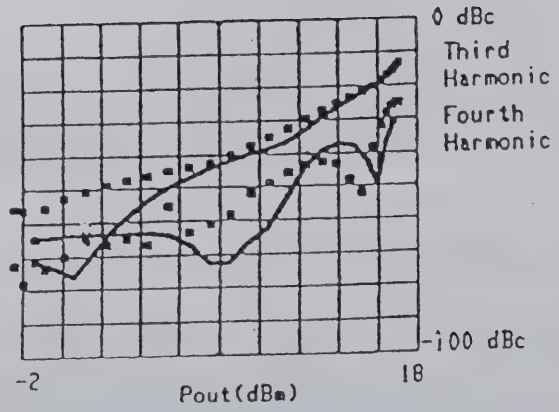

Reasons for Pulsed Data Acquisition

- Extends device characterization into regions where the device operates but where dc and small-signal measurements can not be made

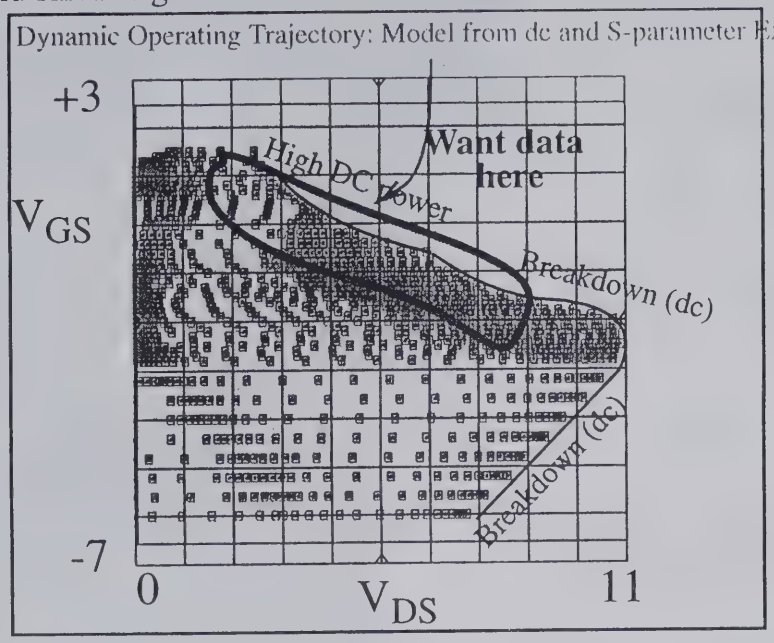

- Makes possible the ability to *accurately simulate and design*, including thermal and trapping dependences which cause of dispersion
- System provides device data under closer-to-use conditions
- Significantly reduces stress on device in extreme regions of operation
- System is FAST! (100 times faster than commercial alternatives)
- Large-signal characteristics can **not** be inferred only from dc & small-signal data

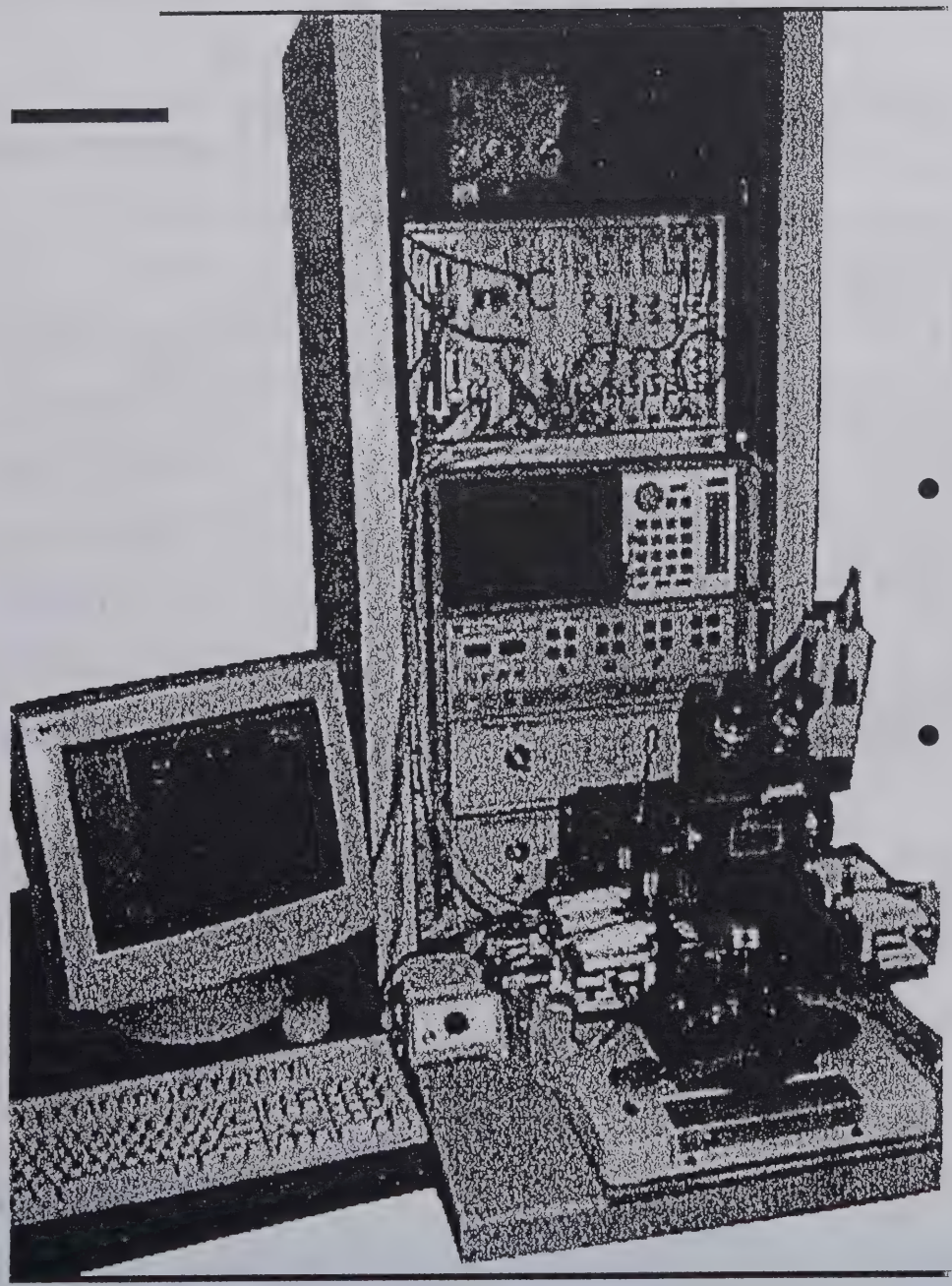

MWTD Installation

- APSPA in VXI
  - 400 ns Pulsed-I/V
- HP 85108A
  - 2 - 50 GHz
    Pulsed S-parameter

Pulsed Characterization of PHEMTs

APSPA
Arbitrary Pulsed Semiconductor Parameter Analyzer

- Low-cost Pulsed-bias measurements
- Fast, suitable for production testing
- Experiment over all regions of bias
- Measure over all operating points

- Hold DUT at constant bias (10 ms)
- Measure I-V characteristics with short pulsed (< 500 ns)
- DUT does not heat up
- Traps don't have time to change

DC Measurement

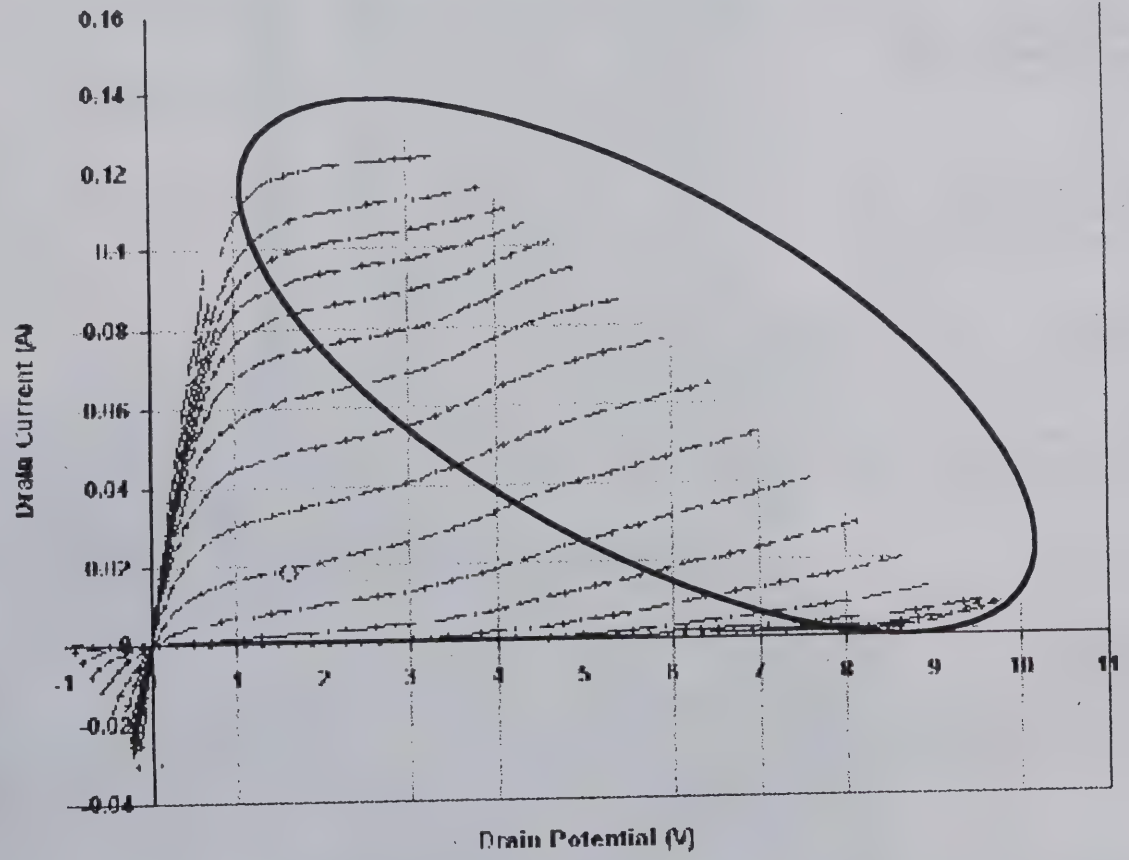

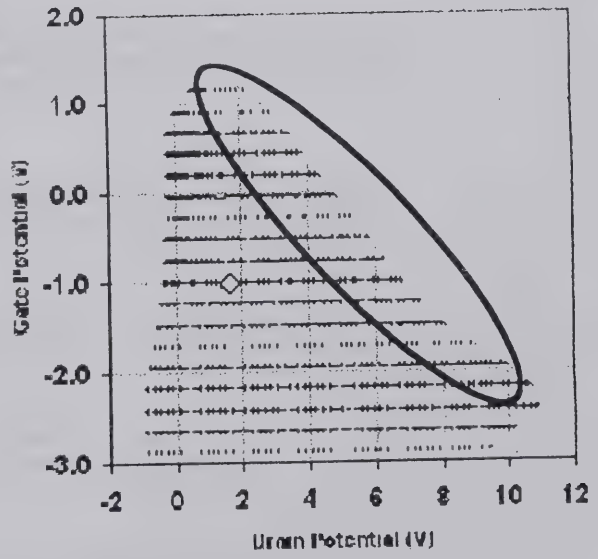

I/V Characteristics

Voltage Plane

Pulse All Operating Points

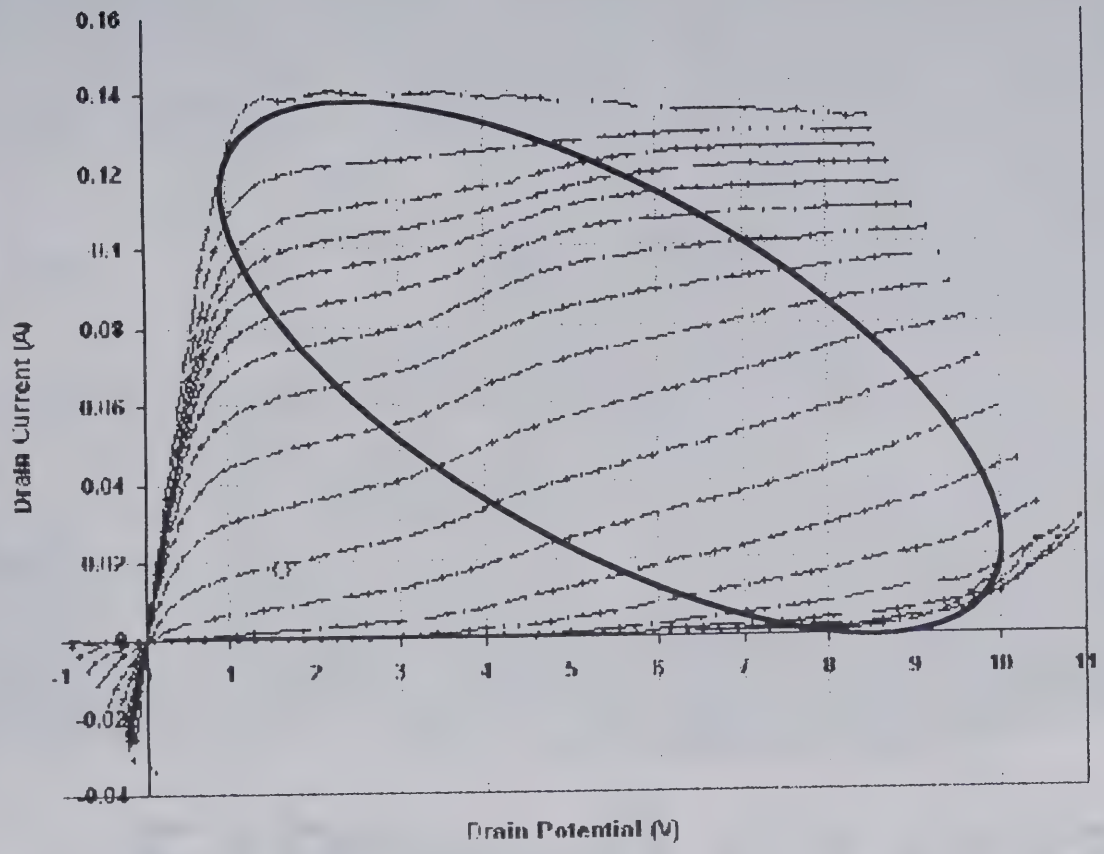

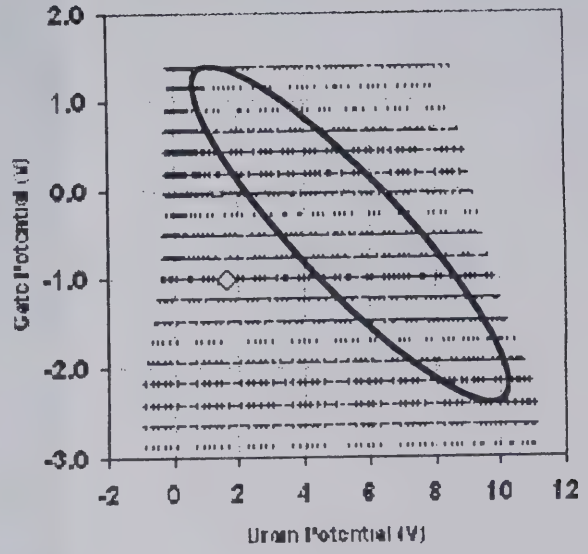

Pulse Characteristics

Pulse Points

Exploring All Bias Points

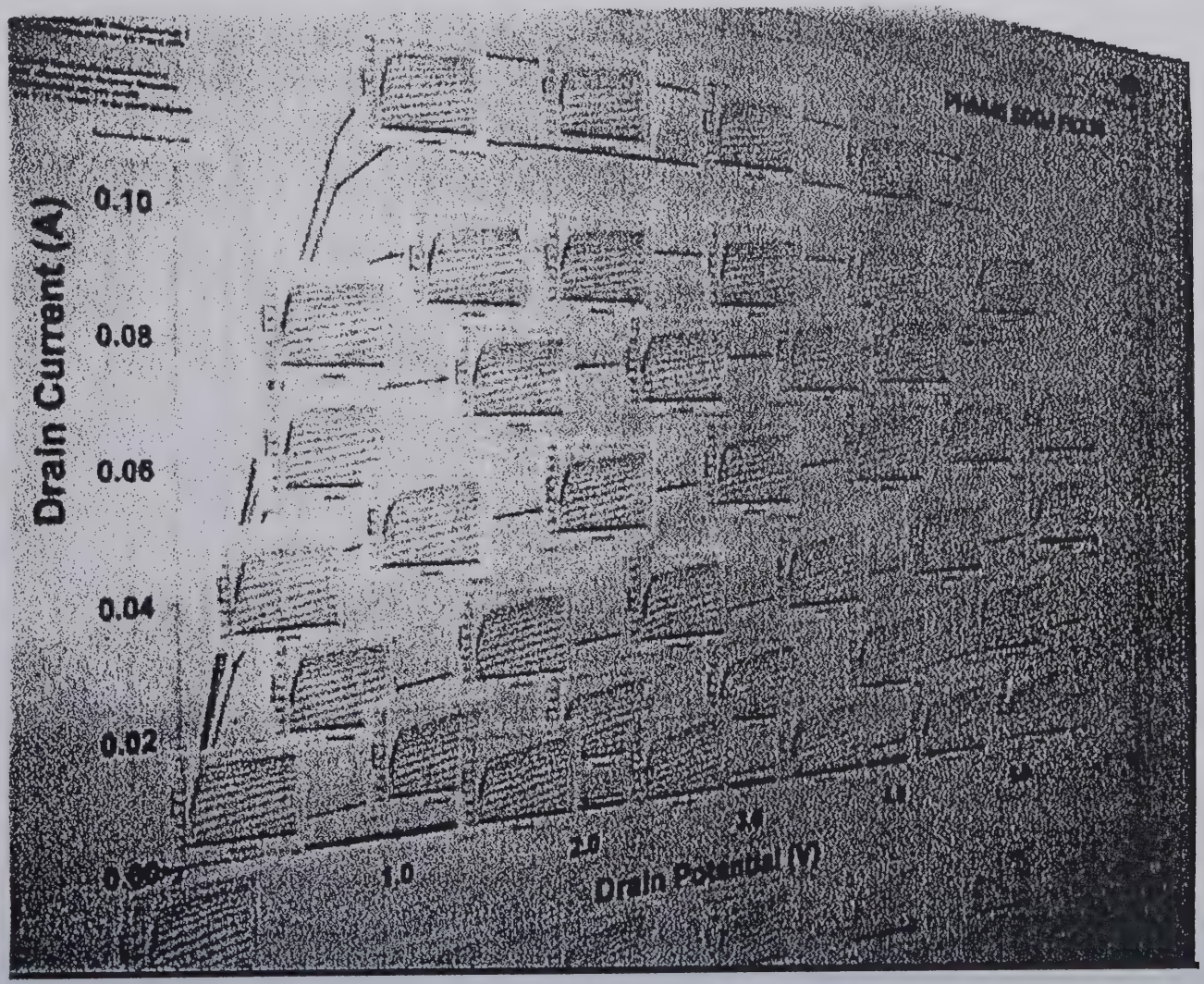

Two Modes

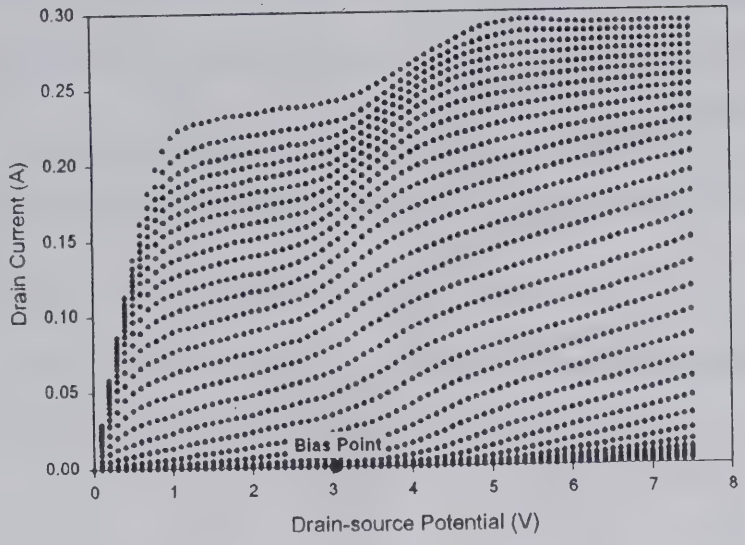

Region 1

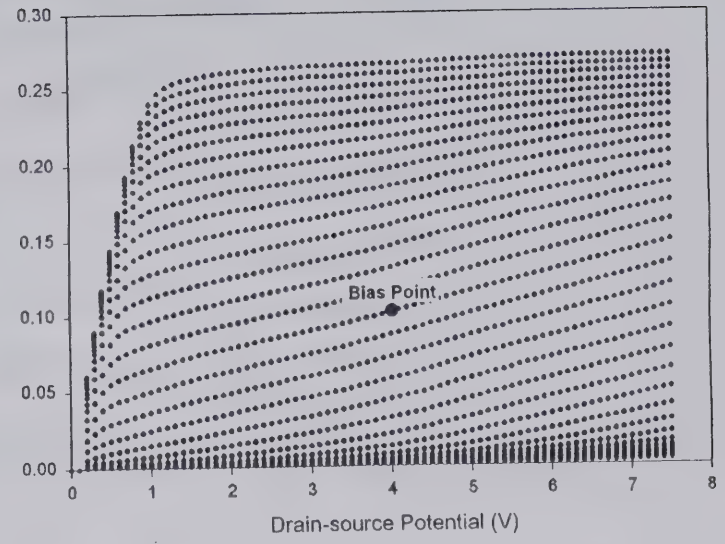

Region 2

New PHEMT Measurement-based model

- Model is rich enough to reproduce major dynamical effects
  Can't just substitute pulsed data for static data in previous models
- Dynamic self-heating included: Model calculates power dynamically
- Model includes fast and slow dynamical effects.
  Transfer functions depend on temperature, and "slowly varying" bias
- Includes gate-lag effect
- Uses iso-dynamic data
  based on pulsed I-Vs over extended region
  rather than spliced-together static and small-signal data

Raw Data

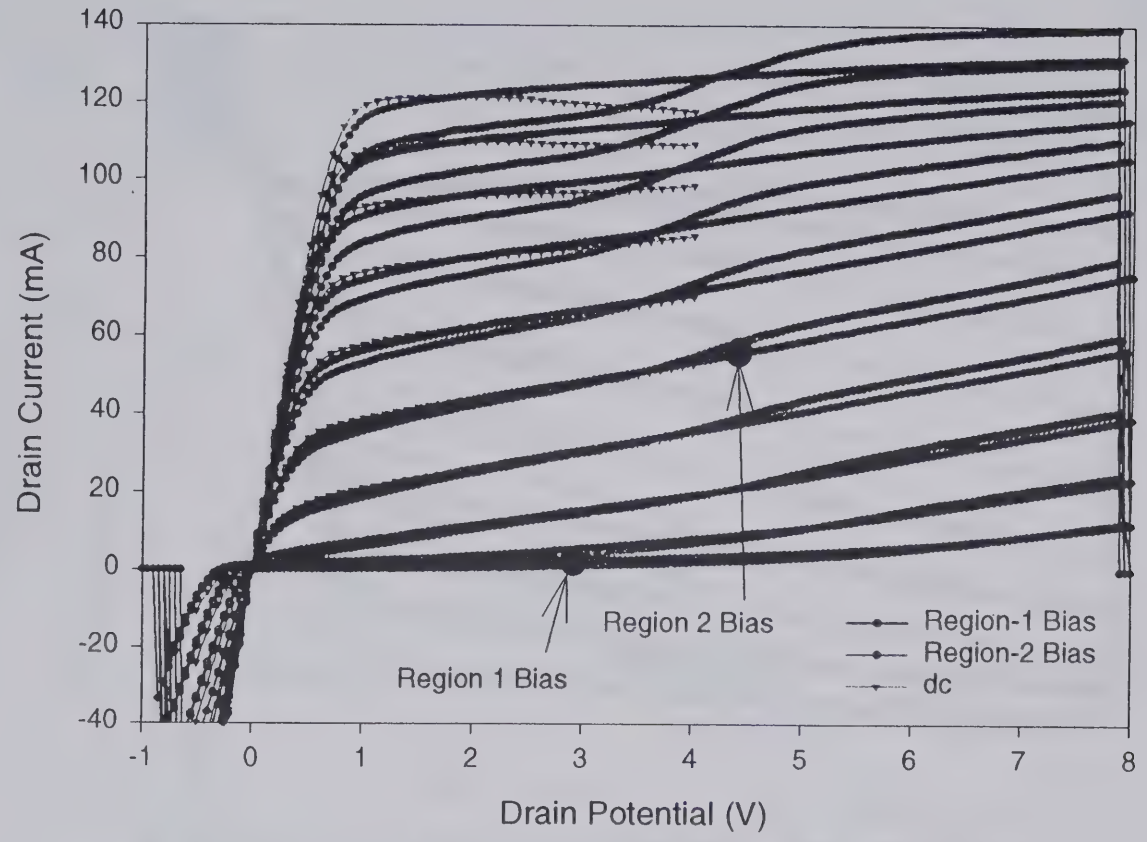

PH9A045 F8X30

Normalized Data

(to temperature of Quiescent Point)

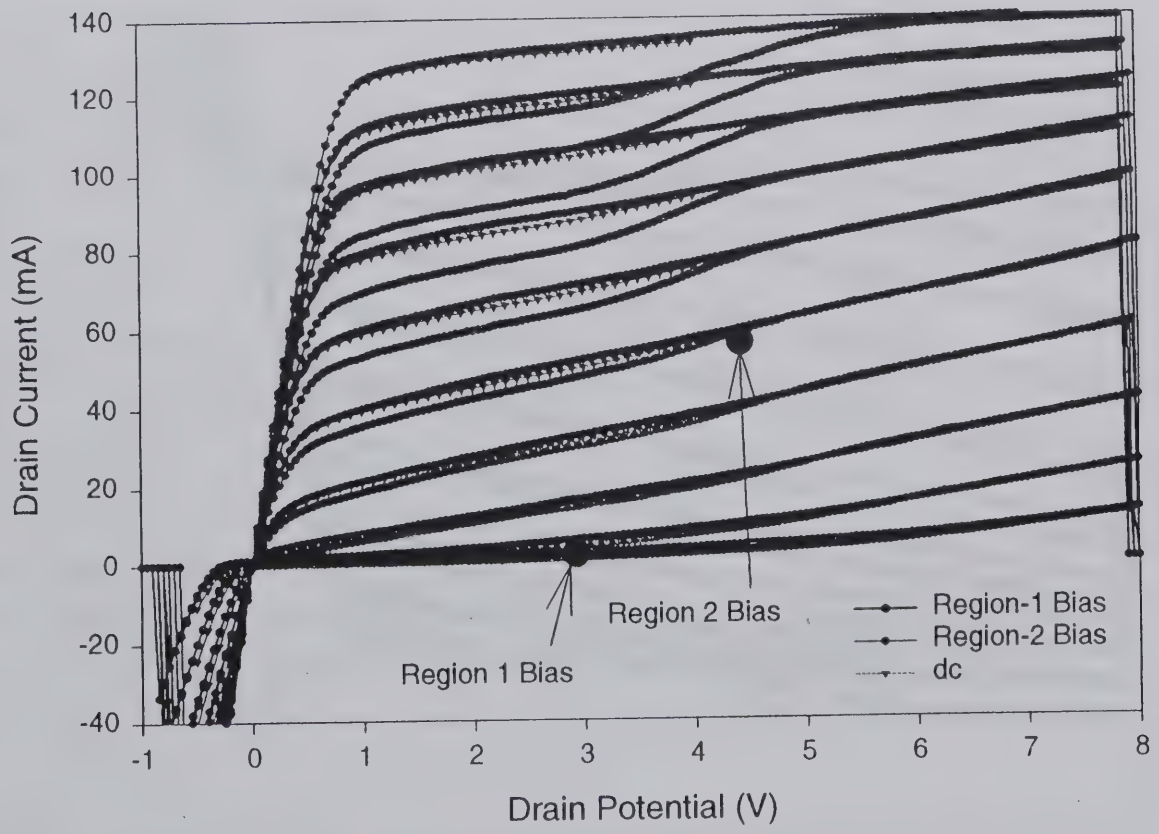

PH9A045 F8X30 $\delta = 0.25$

Dynamic Load-line

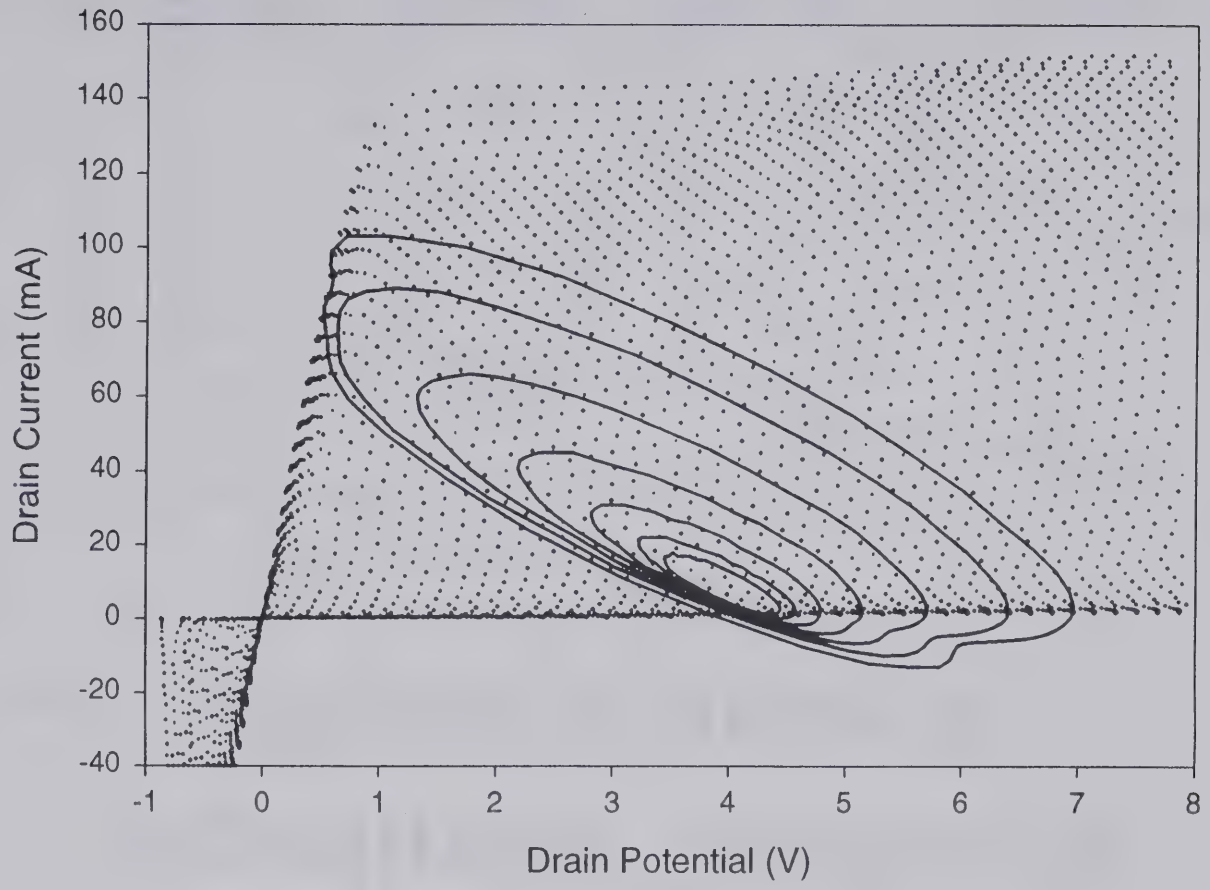

Nonlinear Network Measurement

Model Validation

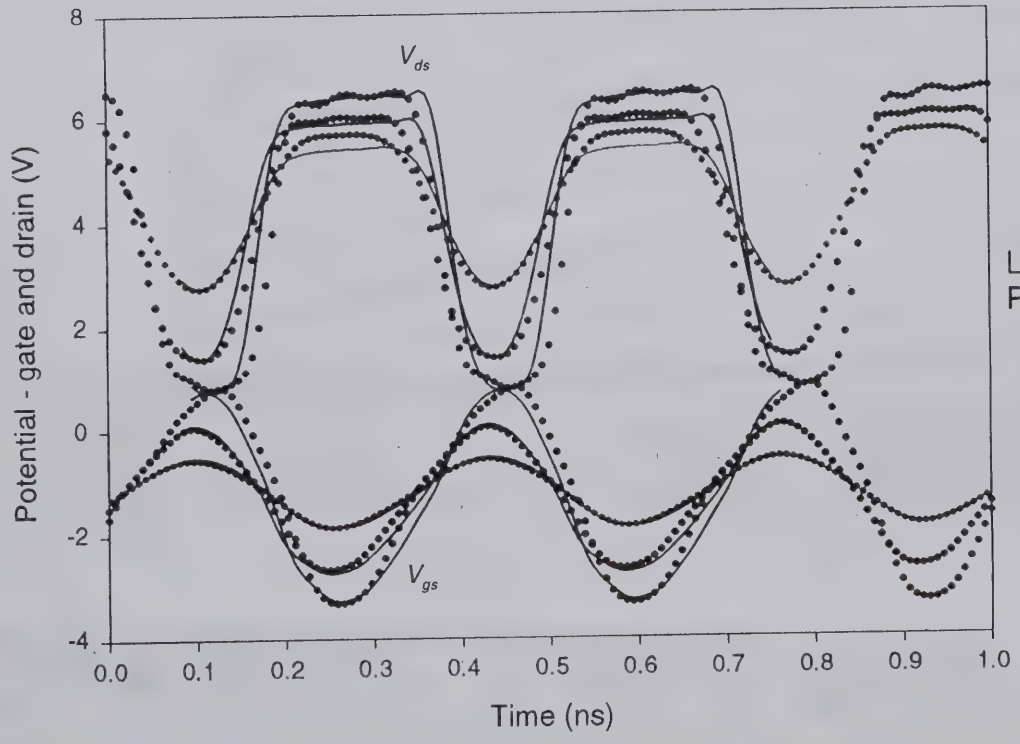

Lines - measured
Points - model

Simulated vs Measured

Transient from Region 1 Pinch-off to $V_{gs} = 0$

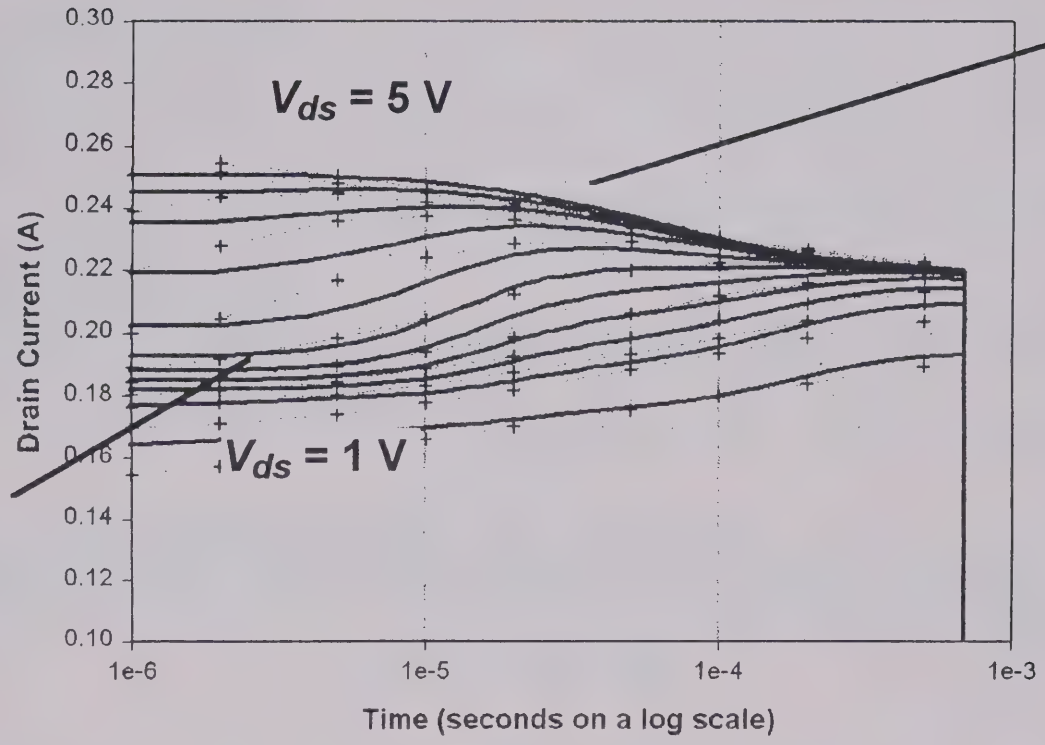

Drain *OVERSHOOT*

(dynamic heating)

Gate *LAG*

Acknowledgments

The author is grateful to Professor Anthony Parker, who brought up the pulsed modeling system and developed the new pulsed model while on sabbatical at HP Microwave Technology Division from Macquarie University, Australia. Thanks also to Dr. John Wood for simulations using various Microwave Technology Division FET models. Alex Cognata provided significant technical assistance with the pulsed system. Finally, the author thanks HP management for support of this work.

References

[1] D.E.Root, **Measurement-Based Mathematical Device Modeling for Nonlinear Circuit Simulation,** to be published by Kluwer Academic Press, 1998 or early 1999

[2] D.E.Root, "On Table-Based Device Models," in *1997 IEEE MTT-S Nonlinear Measurements and Modeling Workshop,* Denver, CO,

[3] A.E.Paker and D.E.Root "Pulse Measurements Quantify Dispersion in PHEMTs," to be presented at ISSSE, Pisa, Italy, September, 1998.

[4] D.E.Root, "Foundations of Measurement-Based Modeling for Nonlinear Circuit Simulation," in *1996 IEEE MTT-S Workshop on New Directions in Nonlinear RF and Microwave Characterization*, San Francisco, CA

[5] "Pulsed-device Measurements and Applications," *IEEE Trans. MTT,* 44(12), Dec. 1996

[6] "Determining Timing for Isothermal Pulsed-bias S-parameter Measurements," IEEE MTT-S, San Francisco, June 17-24, 1996.

[7] "Method for determining correct timing for pulsed-I/V measurement of GaAs FETs," Electronics Letters, 31(19), pp. 1697-1698, Sept. 14, 1995.

[8] "Trends in device characterization: A pulsed semiconductor parameter analyzer system for III-V FETs," J. of Electrical and Electronics Eng., Australia, 14(3), pp. 196-205, Sept. 1994

[9] "Nonlinear Network Measurement System: Technology Update," Hewlett-Packard Co. Santa Rosa Systems Division, Revision 1.0, December, 1997

[10] G.B.Norris, "IC Technologies for Wireless Applications Beyond 2000," in *1997 GaAs IC Symposium Workshop*

[11] F.Filicore et al "Empirical Modeling of Low-Frequency Dispersive Effects Due to Traps and Thermal Phenomena in III-V FETs," *IEEE Trans. Microwave Theory Tech.* Vol 43, No. 12, Dec., 1995, pp.2972-2981

[12] F.Filicore, G.Vannini, and V.A.Monaco, "A nonlinear integral model of electron devices for HB circuit analysis," *IEEE Trans. Microwave Theory Tech.*, vol. 42, pp. 1088-1091, 1992.

[13] D.McGinty, D.E.Root, and J.Perdomo, "A production FET modeling and library generation system," in *1997 MANTECH Conference Technical Digest*

[14] D.E.Root, D.McGinty, and B.Hughes, "Statistical Circuit Simulation with Measurement-Based Active Device models: Implications for Process Control and IC Manufacturability," *1995 GaAs IC Symposium Technical Digest*, San Diego, pp. 124-127

[15] Root, D.E., Pirola, M., Fan, S., Anklam, W.J., & Cognata, A, "Measurement-Based Large-Signal Microwave Diode Model for Circuit and Device Design", *IEEE Transactions on Microwave Theory and Techniques*, December, 1993 pp. 2211-2217.

[16] D.E. Root, "Measurement-Based Active Device Modeling for Circuit Simulation", Advanced Microwave Devices, Characterization, and Modelling Workshop, *European Microwave Conference*, Madrid, Spain, September, 1993

[17] Meyer, J., Root, D.E., and Poulton, K., "Dynamic Electro-Thermal Modeling", Thermal Workshop at *1993 International Microwave Symposium*, Atlanta, Georgia, June, 1993

[18] Root, D.E. and Fan, S., "Experimental Evaluation of Large-Signal Modeling Assumptions Based On Vector Analysis of Bias-Dependent S-Parameter Data from MESFETs and HEMTs", *1992 IEEE MTT-S International Microwave Symposium Technical Digest*, pp.255-259.

[19] Root, D.E., Fan, S., and Meyer, J. "Technology-Independent Large-Signal FET Models: A Measurement-Based Approach to Active Device Modeling", *Proc. 15th ARMMS Conference*, Bath, England, September, 1991

[20] W.M.Coughran, W.Fichtner, E.Grosse, "Extracting Transistor Charges from Device Simulations by Gradient Fitting," 1989, IEEE *Trans. Computer-Aided Design CAD-8*: 4 pp 380-394.

[21] R.Anlholt, **Electrical and Thermal Characterization of MESFETs, HEMTs, and HBTs,** Artech House, 1995

HEWLETT PACKARD

David E. Root

Microwave Technology Division

RAWCON'98 - SUNDAY WORKSHOP

High-Frequency CAD - The Key to Success in Wireless Design

Thomas J. Brazil

Department of Electronic and Electrical Engineering
University College Dublin
Ireland
tom.brazil@ucd.ie

Summary

- Overview and Context
- Non-linear Device Modelling
- Circuit Simulation Techniques
- Systems-Level Simulation
- Future Challenges

UMTS
(Universal Mobile Telecommunications System)
IMT- 2000
(International Mobile Telecommunications - 2000)

- UMTS is the term commonly used within Europe to describe the next generation of wireless, wideband digital communication systems with enhanced characteristics such as full-motion video, graphics-intensive Internet, flexible service provision, universal coverage, and support for data rates up to 144kb/sec (wide-area) or up to 2Mb/sec (indoor/local);
- At a global level, UMTS represents Europe's input to the effort by ITU-R to standardise third generation wireless systems, known as IMT-2000 , previously referred to as FPLMTS. The '2000' signifies both the approximate frequency band (2000MHz or 2GHz), as well as the approximate initial date for deployment.

Evolution Towards UMTS

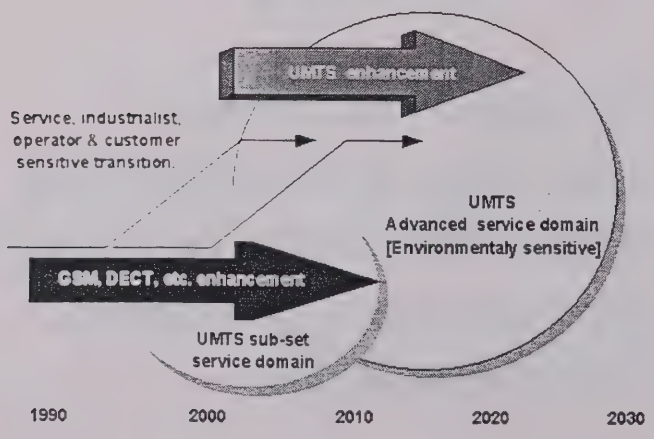

Standardisation of Air Interface for UMTS

- In January 1998, ETSI agreed a critical milestone for the future development of UMTS, namely, definition of a single standard for the air interface, hoping to allow Europe to build on its GSM success;
- The chosen concept uses WCDMA for wide-area applications and TD/CDMA for low-mobility high-capacity indoor applications, and will be jointly promoted by leading telecommunications suppliers, including significant support from Japan;
- The WCDMA decision was strongly supported by operators who will not need new cites or cell structures - they can simply overlay existing GSM networks in migrating to the new WCDMA hardware, which will operate to open standards;
- The standard will support basic speech as well as flexible high speed data (circuit-switched - e.g. ISDN and packet e.g. TCP/IP), with possible multiple simultaneous services.

Some Technology Features of UMTS

- Use of adaptive antennas (on MS and BS);
- Integrated satellite component (S-UMTS) for very-wide area operation on a global scale, ultimately maybe linked to GPS;
- Extensive use of IN concepts
- 'Software radios' may permit highly flexible terminals, self customising to local standards or capable of down-loading upgrades, new features etc.

Emerging MM-Wave Markets

- The characteristics of mm-wave which make it problematic for traditional microwave relay applications, actually make it ideal for short distance links, using cellular-type concepts;
- Multiple frequency re-use becomes possible over very short distances (e.g. indoor broadband wireless, pico-cell concept at 60GHz, taking advantage of strong absorption in this range);
- New volume markets are under development in LMDS around 29GHz, MVDS (42GHz), broadband wireless LAN's, satellite links, MBS (60GHz), automobile ACC-CW/CA (77GHz) etc.

From Cordless to Mobile Broadband (MBS)

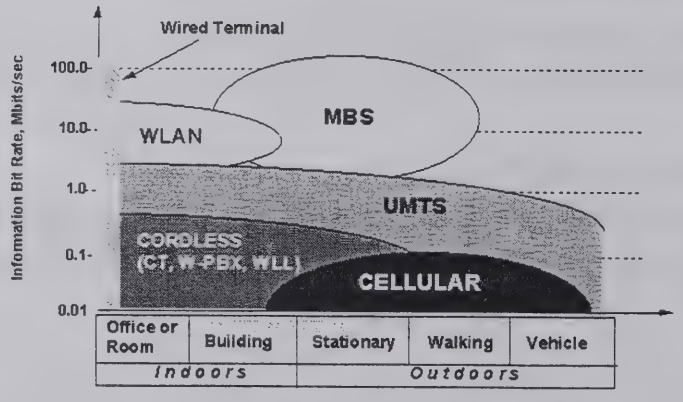

Device/MMIC Technologies

Silicon:

- bipolar junction transistor (BJT);
- MOS-based (LDMOS, RF CMOS..);

Silicon Alloys:

- SiGe Heterojunction Bipolar Transistor (HBT).

Compound Semiconductors:

- GaAs FET (MESFET);
- High Electron Mobility Transistor (HFET/HEMT);
- Pseudomorphic HEMT (PHEMT);
- GaAs-based HBT's;
- InP-based FET's.

Block Diagram, Typical Multi-Technology RF Transceiver

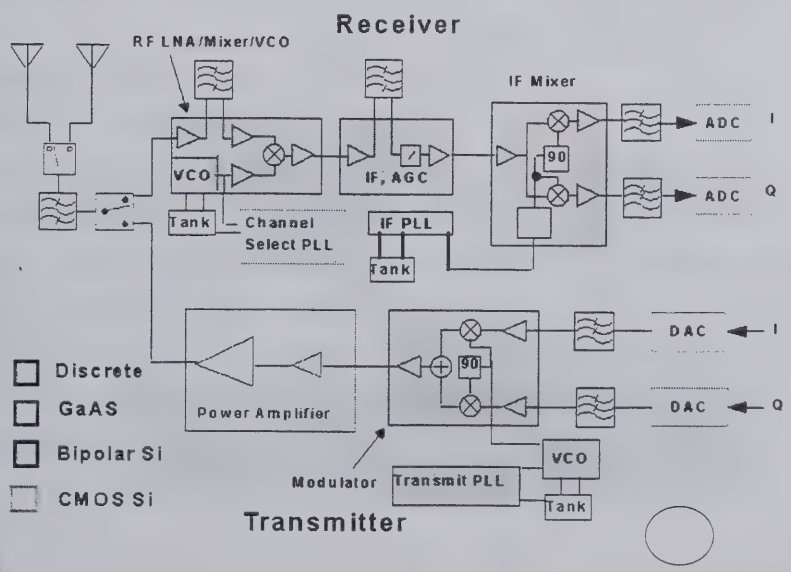

Technology Speed Figure of Merit vs Time

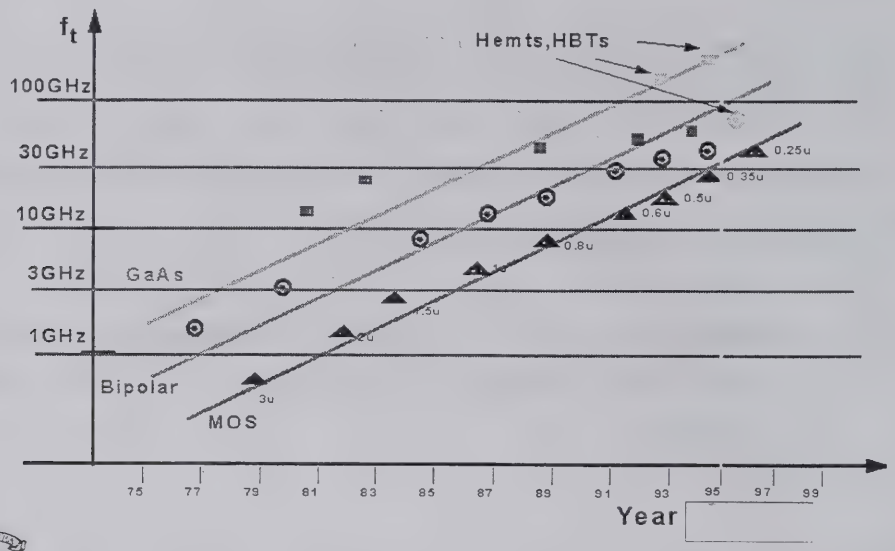

GaAs-Based Technology Trends

Breakdown of MMIC Designs by Technology

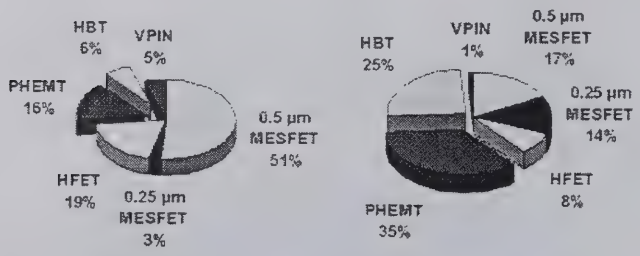

Figure 2
The MDE Consortium's view of the increasing usage of PHEMT and HBT circuits in MMICs, indicating that they will likely dominate the field by the year 2000. In response, the MDE project is focusing on improving microwave and millimeter wave non-linear region modeling.

High-Frequency CAD

- CAD is now a critical enabling technology across almost every aspect of microwave and RF applications, but especially in MMIC design;
- CAD may be applied at many different levels, e.g.:
  - *Process Simulation:* predicting distributions of dopants, layer structures... from given growth conditions;
  - *Physics-Based Device Modelling:* predicting/optimising performance (and ideally yield) from doping, geometry and materials information;
  - *Electromagnetic Solvers:* analysing or even synthesising complex physical geometries with Maxwell's equations;
  - *Circuit-Level CAD:* Analysis/design of linear/non-linear microwave sub-systems for gain, noise, efficiency, linearity, output power etc.;
  - *Systems-Level CAD:* predicting the performance of complete microwave systems, possibly studying trade-offs between baseband/DSP solutions and RF techniques;

General Trends in High Frequency CAD

- shift from military to commercial markets;
- shift from Workstation to PC;
- increased complexity of CAD tools/interfaces - role of vendors in contract design;
- high cost of ownership of mainstream CAD environments but these are then often 'under-used';
- CAD a strategic technology (e.g. for UMTS/IMT-2000);
- Internet as a means for sales, marketing and support;
- links between high-frequency, DSP, optoelectronics..

Some Technical Trends in High-Frequency CAD

- increasingly stringent system specs. placing severe demands on existing CAD tools;
- volume exploitation of mm-wave markets (LMDS, MVDS ..) requiring better mm-wave models, yield analysis tools, EM/physics-based simulation...;
- users need more *synthesis* tools as well as tools for *analysis*: increasing interest in 'design assistant' software;
- sub-micron CMOS an increasingly competitive RF technology at the lower frequencies;

The European EDGE Project

EDGE 

- EDGE is a project part-funded under the European Commission ESPRIT programme, in the area of high-frequency analog CAD;
- It is about 2 years in duration and due to finish during 1998;
- The total buget for the project is 2.8 Mecu of which the EC contribution is 1.6 Mecu, representing a total work effort of about 27.5 Person-Years;
- The project consortium consists of a mixture of software developers/vendors (5) and users/component manufacturers (3).

The EDGE Consortium

- *Co-ordinator:* University College Dublin *(UCD - IRL)*
  (National University of Ireland, Dublin)
- *Partners:* Barnard Microsystems Ltd. *(BML - UK)*
  Dassault Electronique *(DE - F)*
  GaAsCode Ltd *(GC - UK)*
  GEC-Marconi Materials Technology *(GMMT - UK)*
  Jansen Microwave GmbH *(JMG - D)*
  Philips Microwave Limeil *(PML - F)*
- *Ass. Partner:* Universita di Roma II 'Tor Vergata' *(UR - I)*

[vendor/developer] [user/manufacturer]

Specific Objectives of EDGE Project

- Provide Improved Working Links between Commercial European CAD Tools;
- Provide Useful Links between European Tools/Models and US-vendor software;
- Support Advanced User Interface Development for MMIC Design and Evolution of a Common User Interface Style;
- Integration of Time-Domain, EM analysis and Yield Enhancement CAD tools for MMIC Design;
- Provision of a Standardised Advanced Non-linear European FET Foundry Model (the *COBRA* model);
- Develop a future collaborative business structure for commercial exploitation of European CAD expertise both within EDGE and outside (e.g. from universities/institutes).

Three Main Axes of Technical Development

- Semiconductor device characterisation, modelling and parameter extraction;
- Passive component modelling and electromagnetic simulation;
- Simulation/optimisation engines and solution strategies and algorithms.

'from Gate recess depth to Bit Error Rate'

• Nonlinear Device Modelling

- ✶ Physics-based non-linear models;
- ✶ Equivalent Circuit Based device models;
- ✶ Table-Based Models, other approaches ...

Physics-Oriented Nonlinear Modelling

- In this approach, the physical behaviour of the non-linear device is encapsulated in a set of equations, which assume a knowledge of basic material parameters for the device material, and full geometrical and process information for the device under study;
- The potential advantages are clear:- clear physical insight into behaviour, potential for process optimisation for performance and improved yield; no need for fitting large numbers of parameters to empirical models; automatic consistency over operating regions and predictive capability;
- Advances in computing power at low cost are bringing this kind of simulation more-and-more within the reach of circuit designers;

Hydrodynamic Equations

- the standard drift-diffusion equations of semiconductor physics are inadequate to describe hot-electron transport and velocity overshoot in short-dimensional structures;
- carrier transit times in such structures are of the same order as the energy and momentum relaxation times, and the standard local models of mobility break down;
- in such cases, a more rigorous solution is required based on the Boltzmann transport equation, applying conservation of particle number, momentum and energy, as the zeroth-, first- and second-order moments of this equation, respectively;

Basic formulation of hydrodynamic equations:

*(n = electron concentration; **p** = momentum; W= energy density; **u** = heat flux; subscript 'c' indicates collision contributions)*

$$\frac{\partial n}{\partial t} + \nabla \cdot (n\bar{v}) = \left(\frac{\partial n}{\partial t}\right)_c$$

$$\frac{\partial \bar{p}}{\partial t} + \bar{v}\nabla \cdot \bar{p} + \bar{p} \cdot \nabla \bar{v} = -qn\bar{E} - \nabla(nT) + \left(\frac{\partial \bar{p}}{\partial t}\right)_c$$

$$\frac{\partial W}{\partial t} + \nabla \cdot (\bar{v}W) = -qn\bar{v} \cdot \bar{E} - \nabla \cdot (\bar{v}nT) - \nabla \cdot \bar{u} + \left(\frac{\partial W}{\partial t}\right)_c$$

$$\nabla \cdot (\varepsilon \bar{E}) = q[N_d - N_a - n]$$

Constitutive Relations (parabolic energy bands):

(κ = thermal conductivity of electron gas)

$$\bar{u} = -\kappa \nabla T \qquad \bar{p} = m n \bar{v} \qquad W = \frac{3}{2} n T + \frac{m}{2} n |\bar{v}|^2$$

Heat Flow:

*(T_L = lattice temperature; **c** = specific heat; ρ = density; κ_l = lattice thermal conductivity)*

$$c\rho \frac{\partial T_L}{\partial t} = \nabla \cdot (\kappa_l \nabla T_L) + \bar{J} . \bar{E} + q E_g \left(\frac{\partial n}{\partial t}\right)_c$$

Some Issues in Hydrodynamic Analysis

- There are many possible variations in the physical equations, depending on effects considered or assumptions made (cf. electromagnetic analysis where the equations to be solved, Maxwell's Equations, are much better defined);
- Non-parabolicity of the energy bands is probably necessary but introduces much additional complexity and uncertainty;
- In devices involving quantum wells etc., the equations can be extended to include modes arising from solutions to Schrodinger equation at the cost of extra complexity ('quantum hydrodynamics')
- Determining values the basic physical parameters may be problematic over the wide range of parameters required and ordinary users do not usually have access to detailed process data;
- Numerical analysis of such equations under large drive conditions is a non-trivial problem and still time-consuming

Non-Linear Equivalent Circuit Modelling

- This is generally the most popular and well-understood approach among designers;
- It is customary to divide the model into an *extrinsic* part, representing the electrical (and possibly thermal) environment between the active part of the semiconductor and the accessible outside terminals, and an *intrinsic* part, describing the core device behaviour;
- While broadly justifiable on the basis of physics, the usual intrinsic model formats represent a major simplification of what is a much more complex underlying behaviour at microwave frequencies - e.g. the conducting channel may behave in reality more as a distributed, active R-C line, device fingers are themselves distributed lines at high frequencies etc. ;
- The extrinsic network is dominated by parasitic elements, and may become complicated with element values which are hard to determine, especially over broad operating bandwidths ($\sim f_T$) and if the device is packaged;

Topology and Parasitics

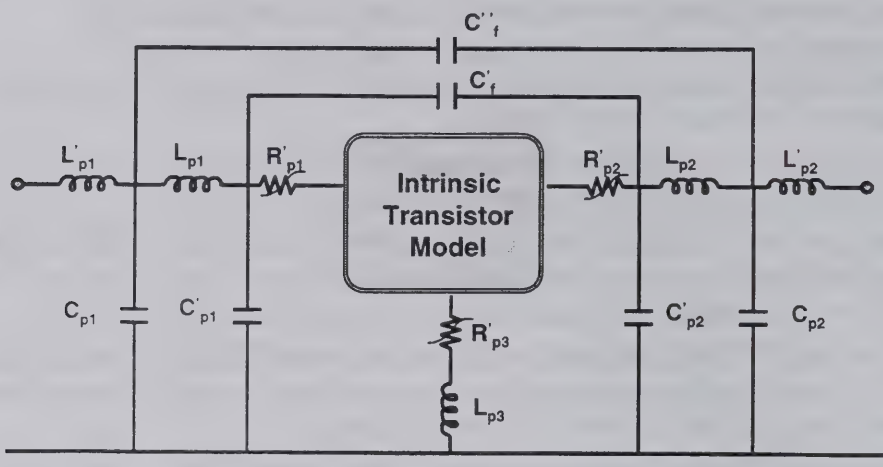

accurate extraction of parasitics is critical!

Some Issues in Non-linear FET Modelling

- Continuity and high-derivative accuracy of model equations;
- Charge-conservation and non-quasi-static behaviour of capacitance;
- Dispersion / non-quasi-static behaviour of drain current / bias-dependent delay/ current lag effects;
- Scalability up to very large device sizes;
- Subthreshold, avalanche breakdown, behaviour around origin and into third quadrant;
- Thermal effects and self-heating;
- Distributed behaviour at very high frequencies;
- Parameter extraction and measurements;
- Implementation in CAD environments;
- Model Validation.

COBRA Model

$$I_{ds}(V_{GS},V_{DS}) = \beta \cdot V_{eff}^{\frac{\lambda}{1+\mu \cdot V_{DS}^2+\xi \cdot V_{eff}}} \cdot \tanh[\alpha V_{DS} \cdot (1+\zeta \cdot V_{eff})]$$

$$V_{eff} = \frac{1}{2}\left(V_{gst} + \sqrt{V_{gst}^2 + \delta^2}\right)$$

$$V_{gst} = V_{GS} - \left(1+\beta_r^2\right)V_{T0} + \gamma \cdot V_{DS}$$

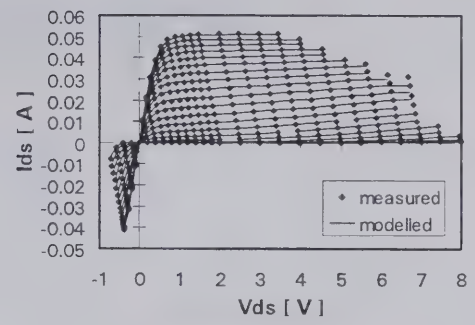

Modified Materka Model

$$I_{ds}(V_{GS},V_{DS}) = I_{dss} \cdot \left(1 - \frac{V_{gs}}{V_{T0} + \gamma \cdot V_{ds}}\right)^{ec + ke \cdot V_{gs}} \cdot \left(1 + \frac{\lambda \cdot V_{ds}}{I_{dss}}\right) \cdot \tanh\left[\frac{\alpha \cdot V_{DS}}{I_{dss} \cdot (1 - k_g \cdot V_{gs})}\right]$$

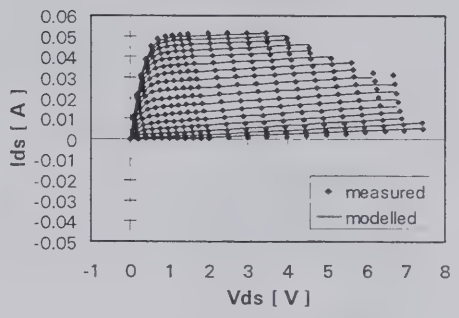

University College Dublin

Calculated derivatives of the drain current model function
(0.2x120µm PHEMT: *Vpo = -1.0V; Vds = 3.0V*)

COBRA Model

Modif. Materka Model

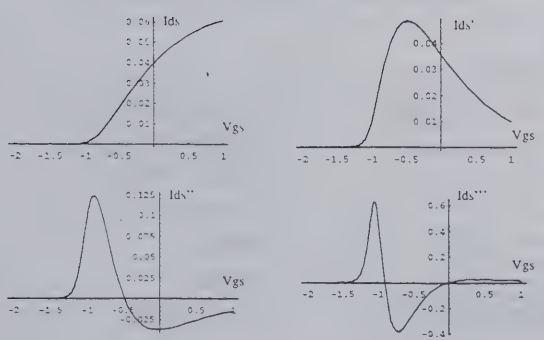

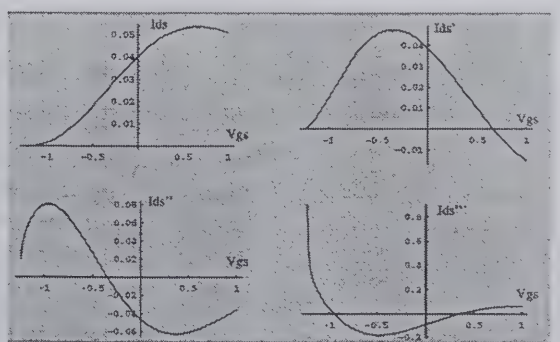

University College Dublin

Calculated derivatives of the gate-capacitance model function
(0.2x120μm PHEMT: *Vpo = -1.0V; Vds = 3.0V*)

$\frac{\partial Q_g}{\partial V_{gs}}$ $\frac{\partial^2 Q_g}{\partial V_{gs}^2}$ $\frac{\partial^3 Q_g}{\partial V_{gs}^3}$

COBRA Model

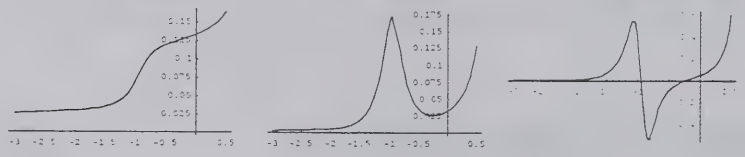

Modified Materka Model

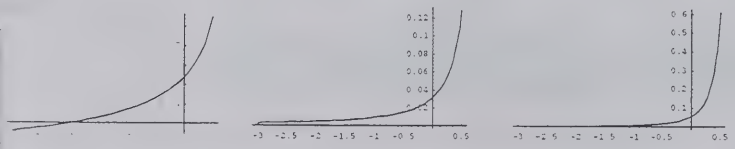

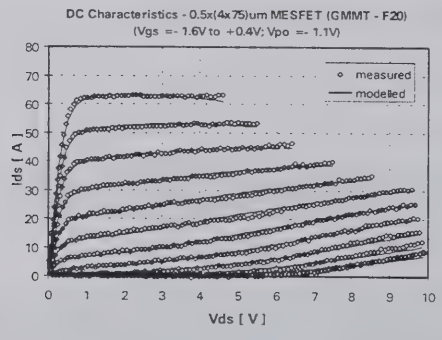

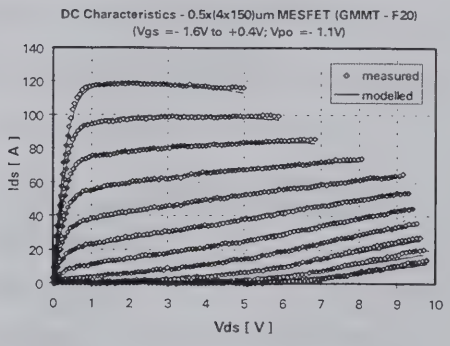

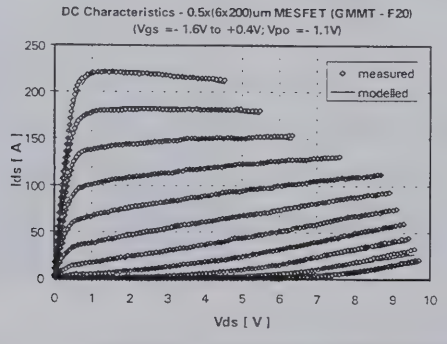

DC Scaling Tests for EDGE Non-Linear FET/ PHEMT model *(COBRA)*

Simple FET Capacitance Model

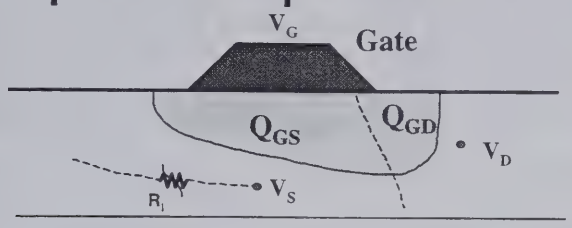

Total static Gate charge (partition line assumed bias-independent):

$$Q_G(V_{GS}, V_{GD}) = Q_{GS}(V_{GS}) + Q_{GD}(V_{GD})$$

This leads to a simple (quasi-static) capacitance model, as used in the early Curtice model etc. E.g.:

$$C_{gs}(V_{gs}) = \frac{C_{gso}}{[1 - V_{gs}/\phi_i]^m}; \quad C_{gd}(V_{gd}) = \frac{C_{gdo}}{[1 - V_{gd}/\phi_i]^m}$$

Charge Conservation

- Experimental results and physical intuition suggest that the simple model is inadequate, as C_{gs} and C_{gd} will depend significantly on *both* bias values, especially below the 'knee' or in the ohmic region of the drain characteristics;
- Many simulators then require use of quasi-static partitioned charge formulations of the form:

$$Q_{GS}(V_{gs}(t), V_{ds}(t)) \text{ and } Q_{GD}(V_{gs}(t), V_{ds}(t))$$

- Each of these is assumed to be a state variable which *conserves charge*, in the sense of returning to the same initial condition after having been cycled through an arbitrary closed dynamic path in the V_{ds}, V_{gs} plane:

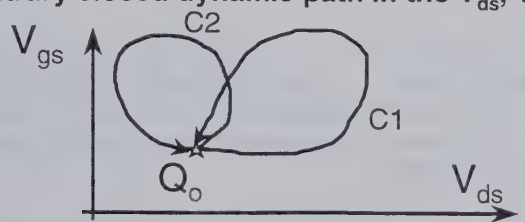

- The equations of Statz et al. [ED Feb. '87 p.160] represented an important step in improving the description of FET non-linear charge by introducing a semi-empirical formulation for the total Gate charge. This formulation is not conservative in terms of Q_{gs} and Q_{gd}. However, it may be argued on physical grounds that these charges are indeed not conserved in FET's under dynamic operation. The following example is quoted by Statz et al., based on a starting charge distribution corresponding to V_{S1} and V_{D1}:

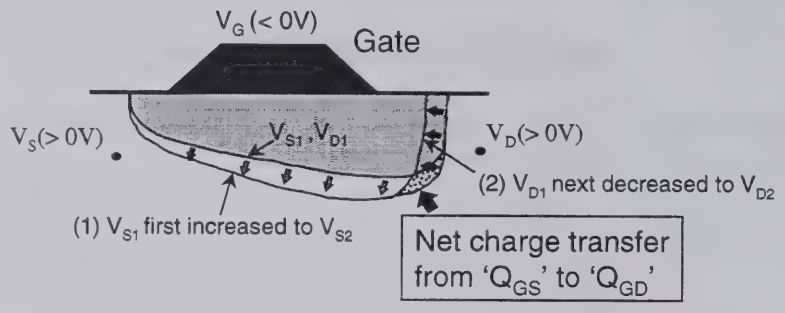

Simulator Issues for Charge Modelling

- Statz and similar equations create problems in the context of the conventional equivalent circuit topology when implemented in charge-based simulators (such as SPICE) as the lack of charge conservation causes spurious current components to be generated;
- This can be corrected by adding additional controlled current sources or 'transcapacitances' into the model. E.g. given a charge function $Q(V_1, V_2)$, we can write the full differential as:

$$dQ = C \cdot dV_1 + \tilde{C} \cdot dV_2 = \frac{\partial Q}{\partial V_1} \cdot dV_1 + \frac{\partial Q}{\partial V_2} \cdot dV_2$$

It is readily proven by vector algebra that 'conservation' or path-independence is assured if:

$$\frac{\partial C}{\partial V_2} = \frac{\partial \tilde{C}}{\partial V_1}$$

- Note that some simulation strategies (e.g. state-space solvers) can operate directly on the nonlinear capacitances C_{gs} and C_{gd}. Strictly speaking, these kinds of solution also cannot be conservative, because of the time-discretised nature of the numerical algorithm used, although with small time-steps and good algorithms, spurious effects of this kind can be kept to a minimum.

Dispersion in Drain Current

- The conventional approach to FET nonlinear modelling regards charge as quasistatic but has to contend with the well-known discrepancy between dynamic and static drain current characteristics (even at constant temperature);
- These 'dispersion' phenomena are thought to orginate from channel/ interface traps and surface charge, and are characterised by rather low-frequency relaxation times (1kHz - 1MHz). They are process-dependent and often more severe for MESFET's than for HEMT's;
- The effect is that primarily drain-source conductance is affected, by being increased significantly, but so also is transconductance, by being reduced;
- Pulsed DC measurements are a valuable tool for exposing this behaviour as described in a number of recent papers. However, it can be difficult experimentally to separate thermal and 'dispersion' phenomena;

Dispersion Correction Strategies

- A first-order dispersion correction is possible by adding an RC branch in parallel across the (quasi-static) drain current;
- To correct for g_m and g_{ds} over a wide bias range, a second nonlinear generator may be added used as shown;
- Even better adjustment is possible by also adding an extra nonlinear conductance g_x;
- The determination of C_x and its bias-dependence is facilitated by pulsed DC measurements.

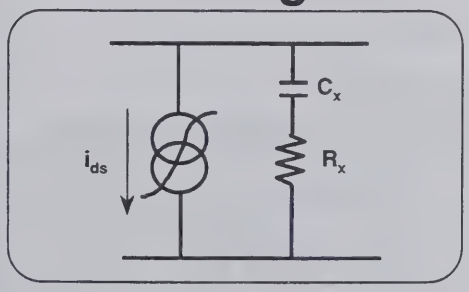

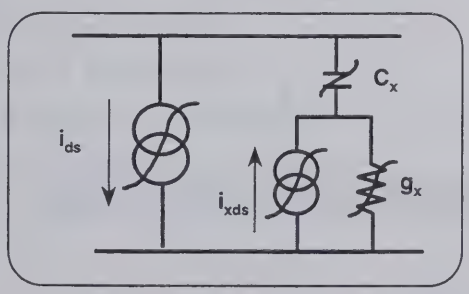

Thermal Issues in Device Modelling

- pulsed, multi-bias DC/S-parameter measurements are sometimes made, since results are then expected to be more appropriate to the temperature at the given Q-point
- in reality, bias point (and temperature) change with increasing RF power levels, and also as circuit conditions change
- full electro-thermal non-linear simulation is needed properly to account for all the interactions involved

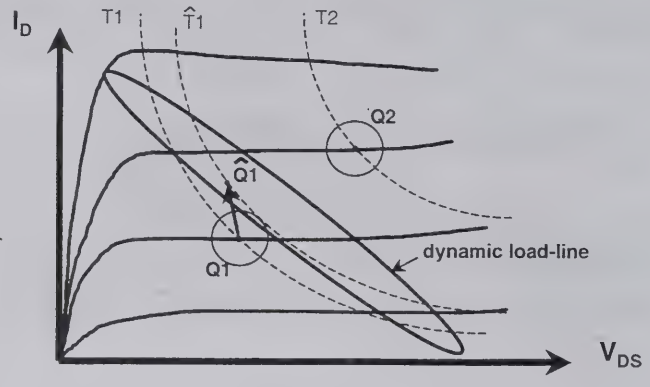

COBRA Model

COMET - FET Model Extractor

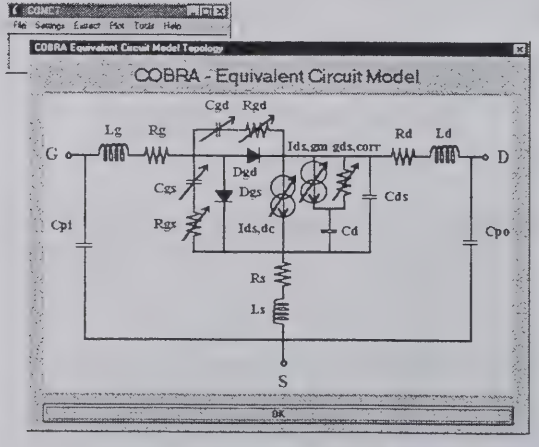

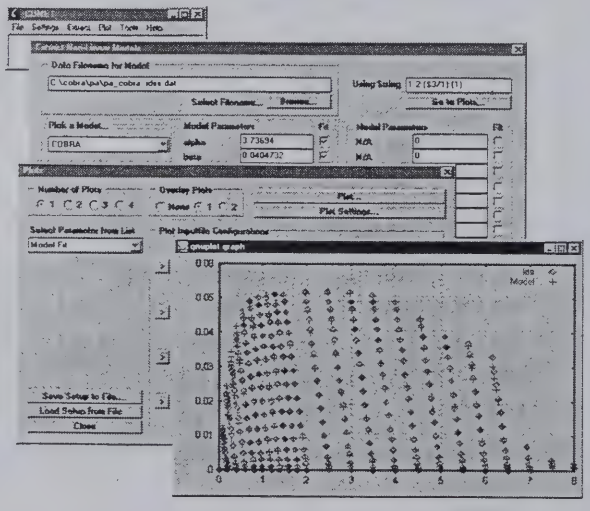

Single-tone large-signal test results (9 GHz) for a 0.2x(6x50)μm PHEMT, using the *COBRA* model scaled from 0.2x(4x30)μm (*Vpo* = -1.0V).

	Vgs	Vds
a)	-0.9V,	+0.6V;
b)	-0.9V,	+6.0V;
c)	-0.6V,	+3.0V;
d)	0.0V,	+0.6V.

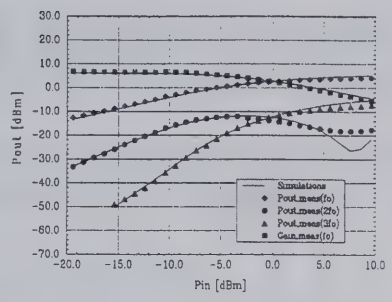

a)

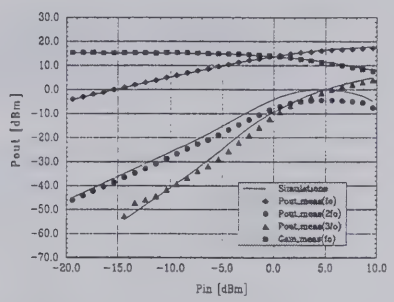

b)

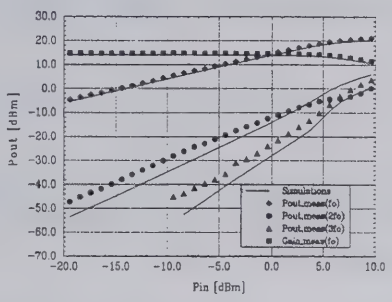

c)

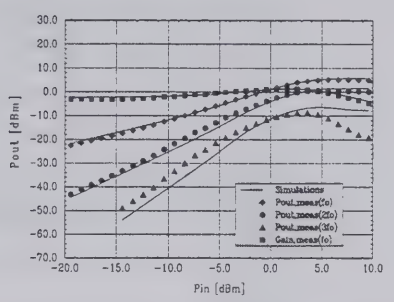

d)

Modelling of HBT Devices

- The HBT is a relatively complex device, for which there is now considerable demand for effective CAD-oriented modelling support;
- GaAs-based HBT's have been under development for a longer time and have illustrated some of the difficulties in adapting standard BJT models for linear or nonlinear modelling;
- SiGe HBT's show significant differences: the thermal issue is important but perhaps not so critical, however base push-out (the Kirk Effect) is considerably more important;
- Users require compact, robust model implementations in commercial simulation environments, backed up by clear parameter extraction procedures. There is still much work to be done to meet these needs.

Problems Applying the Gummel-Poon Model to III-V Based HBT's

- Many devices do not exhibit any useful 'constant current gain' region, yet the existence of such a region is a fundamental principle of the GP model;
- In the high-current region of the Gummel Plot, the measured curves tend to deviate from linearity, but for a fixed V_{BE} these deviations are generally *unequal* for the HBT, rather than ~equal as predicted by GP;
- For HBT's, the deviation from linearity for I_C may be larger than that of I_B or the other way round;
- Temperature must be solved for explicitly rather than being assigned in advance. 'Gain collapse' due to thermal instability can occur in even in non-power processes.

AlGaAs/GaAs HBT Characteristics

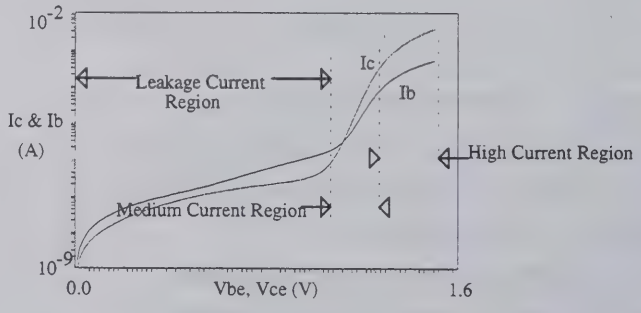

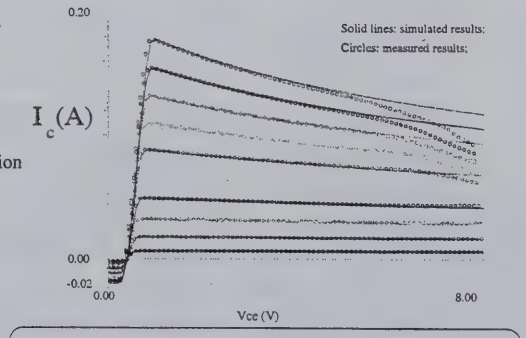

Transistor Nonidealities in Static GP Model

Non-Ideal Effect (Forward)	SPICE G-P	III-V-based HBT	SiGe-based HBT
B/E Recombination	Yes	Yes	Yes
Leakage	No	Yes	Yes
Base-Width Modulation (Early Voltage)	Yes	No	No
High-Level Injection (Webster Effect)	Yes	No	No
Base Push-Out (Kirk Effect)	Yes	(No)	YES
Local Thermal Effects	No	YES	(No)

Gain Advantage SiGe vs. BJT

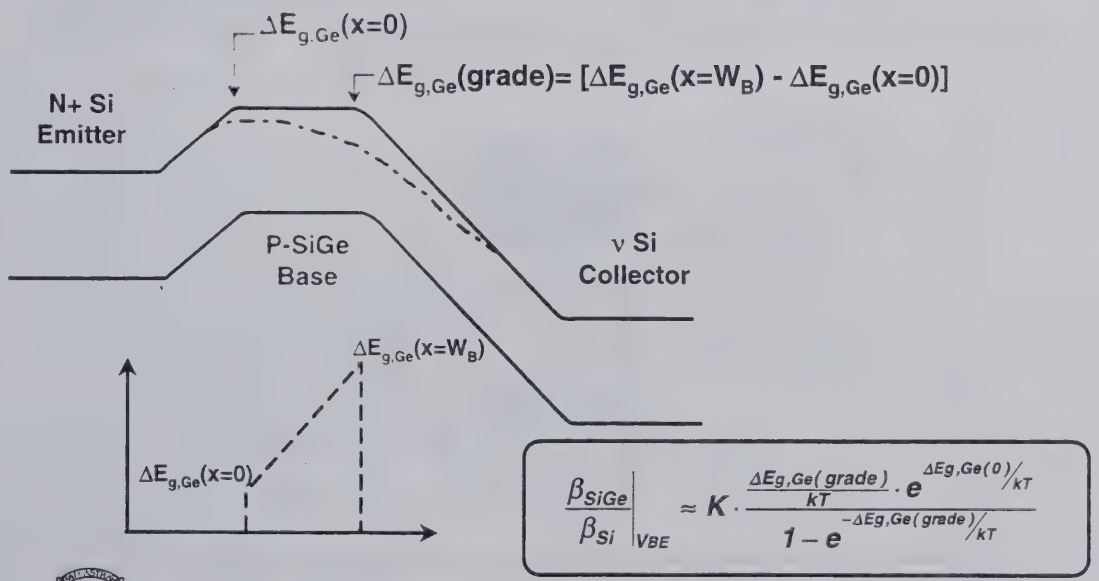

$$\left.\frac{\beta_{SiGe}}{\beta_{Si}}\right|_{VBE} \approx K \cdot \frac{\frac{\Delta Eg,Ge(grade)}{kT} \cdot e^{\Delta Eg,Ge(0)/kT}}{1 - e^{-\Delta Eg,Ge(grade)/kT}}$$

Kirk Effect (Base Push-Out)

- When a bipolar is operated such that high-level injection effects occur in the collector, minority carriers are injected into the collector region adjacent to the base, widening the electrical width of the base and leading to a degradation in current gain and high frequency performance;
- This effect is equivalent to 'quasi-saturation' where the internal base-collector metallurgical junction becomes forward biased while the external base collector-terminals are reverse biased;

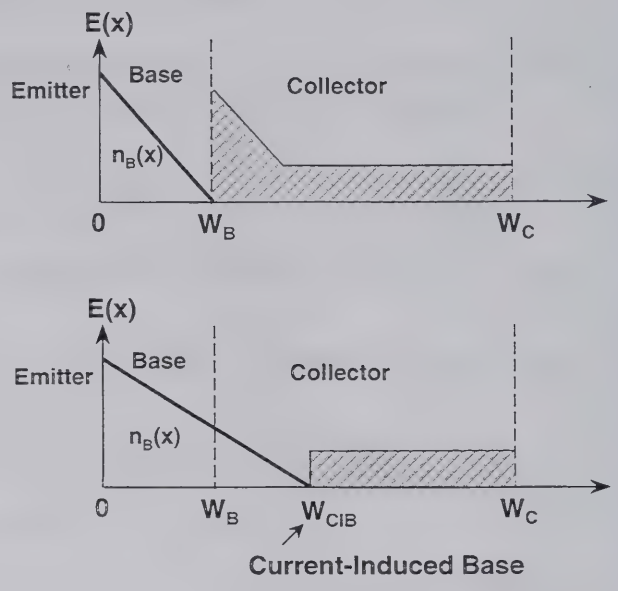

Basis of MMIC Sensitivity Analysis and Yield Forecasting in EDGE

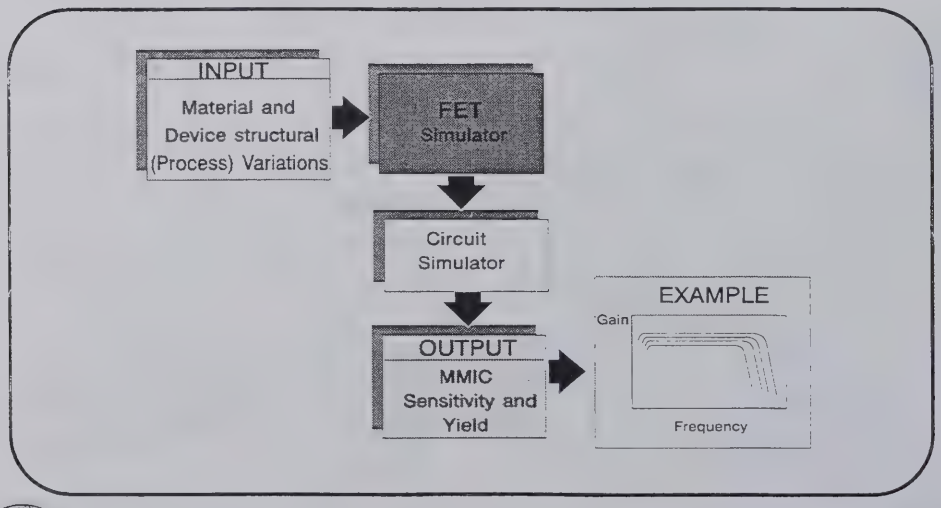

Test of Yield Forecasting Software In EDGE

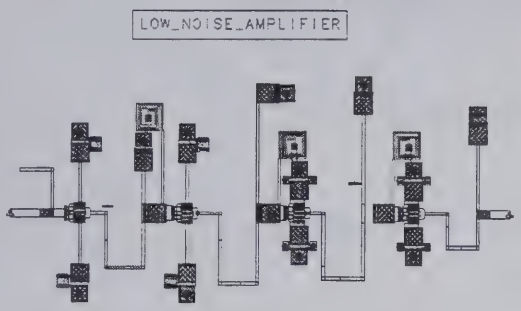

Dassault Electronique Test MMIC

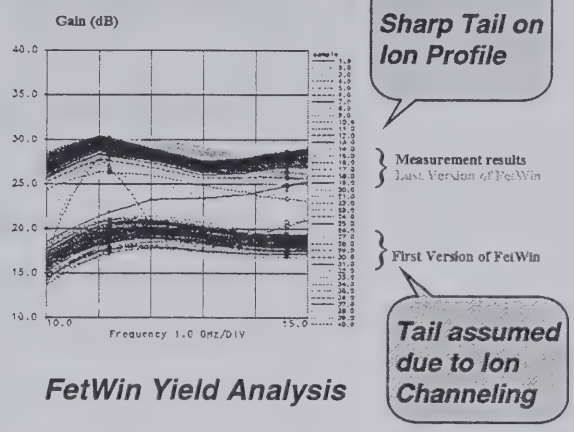

FetWin Yield Analysis

Comparison between Physics-Based Yield Predictor (FetWin) and measurements of 100 samples: histogram of S21 (dB) at 10 GHz.

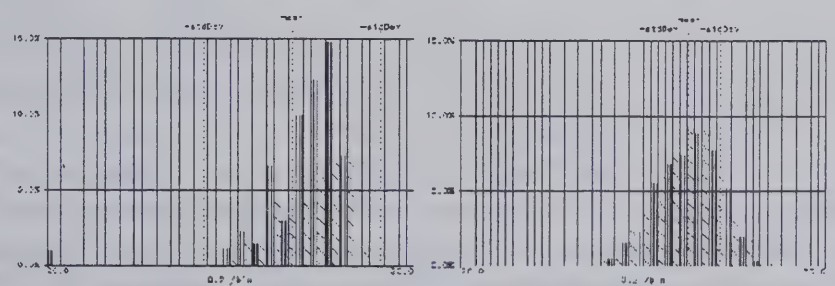

Measurements *Simulation*

- **Simulation Techniques**
  - ✶ Time-Domain Methods;
  - ✶ Volterra Series;
  - ✶ Harmonic Balance Techniques;
  - ✶ Circuit Envelope;
  - ✶ Convolution Methods;
  - ✶ Behavioural Models

Non-Linear High-Frequency Simulation

- The central problem is that the *linear* parts of the system are best described in the *frequency-domain* (S-parameters...) whereas the *non-linear* parts tend to produce integro-differential equations in the *time-domain*. The numerical challenge is to find methods which optimally handle both domains;
- The many formats adopted for digital wireless communications present particular challenges in calculating efficiency, very low distortion levels, 'adjacent channel interference', etc. mainly because of the spectral resolution and range required (e.g. ~ 50Hz resolution up to many harmonics of 2GHz, perhaps with multiple simultaneous tones)

TIME-DOMAIN & REAL FREQUENCY-DOMAIN RELATIONSHIPS .

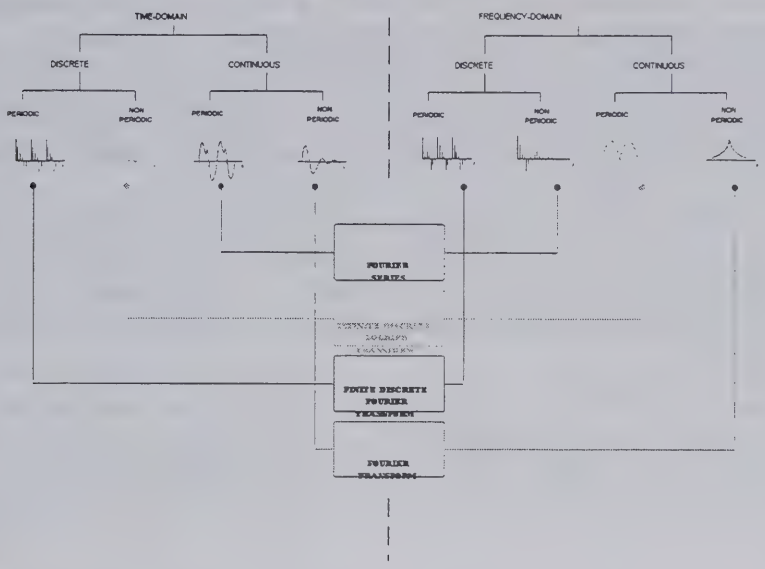

Time-Domain Methods (SPICE-type)

Circuit is described using a nodal-numbering scheme, and a wide range of ideal linear and non-linear elements are possible, including ideal transmission lines;

DC solution involves formulation of circuit equations using Modified Nodal Analysis as a non-linear algebraic system which is solved iteratively (LU decomposition, pivoting and sparse matrix techniques). Non-linear resistive elements are transformed to a linearised (source/resistance) "companion" form at each iteration.

For transient analysis, the solution interval in the time domain [0,T] is divided up into distinct time-steps, t_k, t_{k+1}... The Sparse Tableau differential equation formulation for the vector x of solution variables, is:

$$F(\dot{x}, x, t) = 0, \quad x(0) = x_o$$

the dimension of the vector is (2.b+n), where b= number of branches, n= number of nodes;

- This system is solved numerically using a single-step implicit scheme (e.g. trapezoidal), starting from the DC solution. This implicit formulation effectively reduces the non-linear dynamic circuit functions (including charge and flux) to equivalent non-linear resistances. Thus transient analysis becomes a sequence of non-linear algebraic solutions, or, in effect, repeated DC solutions;
- Problems with "stiff" systems (widely-varying time constants) make it desirable to incorporate some form of adaptive time-step control, based on meeting a local truncation error tolerance. Unfortunately, the stability properties of the algorithm become very difficult to predict in this situation;
- If a steady-state solution is of interest, the solution must be run until the initial transient period has died away, and then Fourier Analysis may be performed over a cycle via the FFT to compute harmonic levels.

Advantages of Time-Domain

- Solution starts from DC and follows a physically-consistent trajectory in phase-space. If parametric effects, spurious oscillations, or even chaos are possible they can appear in the solution;
- Very general excitations in the time-domain are possible;
- Solution is usually quite accurate and the numerical procedures show high level of robustness;

Disadvantages of Time-Domain

- Method can be very inefficient if only a steady-state answer is of interest, and a long transient must be solved. Variations such as the "shooting" method may help, but they are complex and not widely available;
- The adaptive time-stepping severely compromises the 'noise-floor' of the FFT - important in sensitive calculations of distortion products;
- Description of realistic, arbitrary distributed external circuit microwave environments is not possible.

Harmonic Balance

Introduction

- This method is based on the assumption that the (forced) non-linear system has a unique periodic solution, and that both the nature of the excitation, and the degree of non-linearity, are such that a relatively small number of harmonics (K) can describe all waveforms completely;
- In practical application of HB, an iteration takes place in which a trial solution vector (with each element described by a truncated Fourier Series), is passed on the one hand through the linear external network in the frequency domain, and on the other hand through a non-linear sub-system described in the time-domain. The objective of the iteration is to adjust the unknown coefficients in order to "balance" all harmonic components, so that the final representation is consistent in each domain;
- If a good initial guess is available, very rapid determination of the steady-state solution is possible. The method is is offered within all commercial software environments, and is very widely used in non-linear CAD.

Basic Method of Harmonic Balance:

- Let $P(T_o)$ be the set of bounded periodic waveforms in T_o. Let $u \varepsilon P(T_o)$ be a stimulus waveform in a DE of the form (f continuous and real):

$$f(x, \dot{x}, u) = 0$$

- Assume that the solution x exists, is real and $x \varepsilon P(T_o)$. Then:

$$x(t) = \sum_{k=-\infty}^{+\infty} X(k) \cdot e^{jk\omega_0 t}, \quad \text{and} \quad u(t) = \sum_{k=-\infty}^{+\infty} U(k) \cdot e^{jk\omega_0 t} \quad \text{where} \quad \omega_0 = \frac{2\pi}{T_o}$$

- Substitute the assumed solution and its derivatives into f, which must now also be $\varepsilon P(T_o)$. It can therefore be written as a Fourier Series:

$$f\left(x(t), \dot{x}(t), u(t)\right) = \sum_{k=-\infty}^{+\infty} F(X, U, k) \cdot e^{jk\omega_0 t}$$

where:

$$X = \left[\cdots, X(-1), X(0), X(1), \cdots\right]^T$$

$$U = \left[\cdots, U(-1), U(0), U(1), \cdots\right]^T$$

- Solve the following system of non-linear algebraic equations for X:

$$\boxed{F(X, U, k) = 0 \quad \forall\, k \varepsilon Z}$$

Formulating the Harmonic Balance Equation

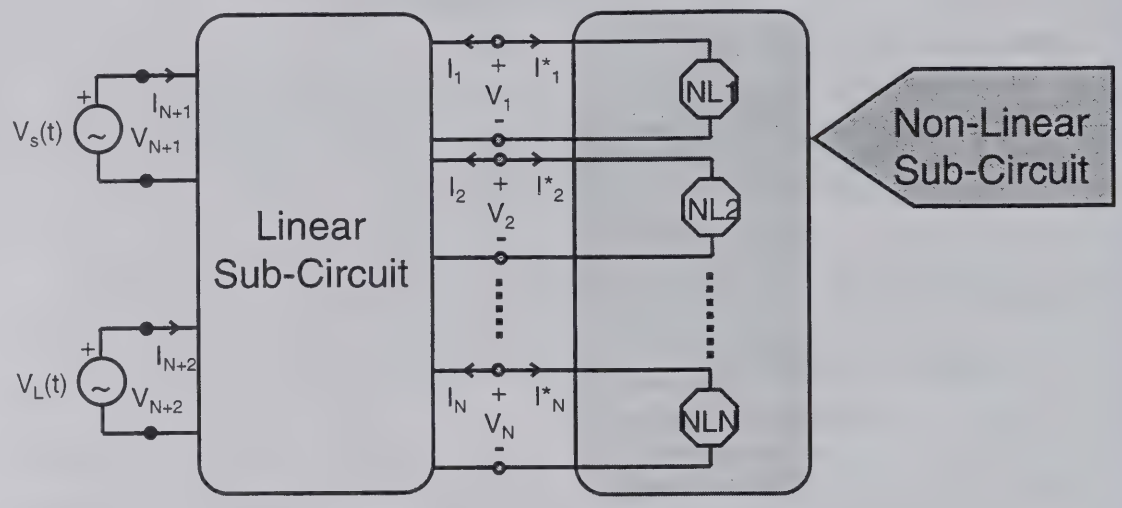

Let Y be the linear circuit admittance matrix, I_s be a vector of Norton excitations, and $Q(V)$ and $I_G(V)$ represent non-linearities, then we require a solution for V = vector of (unknown) voltages at Ports 1 -- N:

$$E(V) = I_s + Y_{NxN}.V + j\Omega.Q(V) + I_G(V) = 0$$

Solving the Harmonic Balance Equation

A great deal of research effort has been directed towards finding efficient, reliable methods for solution of the HB Equation. Possible methods include optimisation, splitting, reflection... A conventional technique with good convergence properties from a close initial guess, is that of Newton or quasi-Newton:

$$V^{(k+1)} = V^{(k)} - \alpha_k \cdot \left[J\left(V^{(k)}\right)\right]^{-1} \cdot E\left(V^{(k)}\right)$$

α_k is a scalar relaxation parameter ε [0, 1], and $J(\,)$ is the Jacobian of E with respect to V. However. with several ports and numerous harmonics, the matrices involved can become extremely large. Note, also, that high accuracy in computing the Jacobian is very desirable (analytical formulations are preferable, wherever possible);

Krylov Techniques

- Up to recently, HB methods struggled with the numerical complexity required to solve large circuits with many tones as required by digital wireless applications;
- An important recent advance has been the application of special methods for solving very large, relatively sparse, asymmetric equations of the form $A.x = b$. In particular, methods have been proposed based on generating a basis for the so-called Krylov sub-space, spanned by b, $A.b$, $A^2.b$, --- $A^{(k-1)}.b$. One example is the Generalised Minimal Residual Method (*GMRES* - see below);
- These methods have been recently introduced into commercial simulators (*ADS* - HP-EEsof; *Serenade 7.5* - Ansoft). There are reports of successful analysis of circuits with 1000's of tones and over 100 active devices, each described by a full non-linear equivalent circuit model.

Generalised Minimal Residual Method (GMRES)

- Start with an initial iterate x_o, using a *Preconditioning Matrix H* which is an approximation to A^{-1}: $x_o = H.b$. The residual error is then $[b - A.x_o]$.
- It can be shown that successive iterates can then be constructed using H, so that after k iterations, the solution estimate is:

$$x_k = x_o + H \cdot \left[r_o + (I - AH) \cdot r_o + \cdots + (I - AH)^{(k-1)} \cdot r_o \right]$$

with residual: $r_m = (I - AH)^k \cdot r_o$

- In GMRES, coefficients α_o, α_1, $\alpha_{(k-1)}$ are added as follows which are adjusted to minimise the Euclidean norm of r_m :

$$x_k = x_o + H \cdot \left[\alpha_o \cdot r_o + \alpha_1 \cdot (I - AH) \cdot r_o + \cdots + \alpha_{(k-1)} \cdot (I - AH)^{(k-1)} \cdot r_o \right]$$

- To achieve this, QR decomposition can be used to construct an upper Hessenberg matrix of size $(k+1) \times k$. Using $k \sim 10$, means the problem is of manageable proportions and easy to solve.

Sources of Error in Harmonic Balance

(1) Using Insufficient Harmonics. *It can be difficult to decide* a priori *what is an approriate number for K. Using too many harmonics is inefficient. Engineering judgement, or even approximate analytical solutions can give guidance and also provide good solution-vector starting estimates*;

(2) Aliasing Errors in the FFT. *The FFT is an exact method for computing Fourier Series, but only for band-limited signal spectra and subject to the Nyquist condition. Practical non-linearities do not preserve band-limiting, and then the FFT causes neglected high-frequency components to appear as error components on calculated (especially high-valued) harmonics. This problem can be reduced by retaining sufficient harmonics and* over-sampling *in the time-domain to preserve accuracy in calculated levels;*

(3) Iteration Closing Error: *This arises from the non-exact, numerical solution of the HB equation.*

Advanced Harmonic Balance

- A number of generalisations of Harmonic Balance have been developed in recent years, which allow the method to be used in a wide range of applications, e.g. mixers and oscillators. Another important case is multi-tone excitation of amplifiers, where several strong tones are applied simultaneously, at perhaps incommensurate frequencies;
- Where the frequencies are commensurate, the most straightforward approach is to use a fundamental period sufficiently long to produce periodicity. Very long-record FFT's may be required however;
- If the frequencies are incommensurate, it is generally still possible to find a time period over which the waveform is approximately periodic. A number of "almost-periodic" transform (APT) techniques have been developed for this case. For example, representing the voltage by:

$$v(t) = \sum_{k=0}^{K-1} \left[V_{ak} \cdot Cos(\omega_k t) + V_{bk} \cdot Sin(\omega_k t) \right]$$

and by (carefully!) choosing sufficient irregularly-spaced time samples, the RHS coefficients may be determined.

Frequency-Domain Nonlinear Analysis Methods / Spectral Balance

- Many of the problems with HB (especially in the multi-frequency case) are related to the FFT operation linking time- and frequency-domains. However, the FFT may be eliminated entirely by treating both linear and nonlinear parts of the system in the frequency domain
- This is achieved by expressing signal variables at the interface by pre-defined truncated summations of complex phasors, and expressing the non-linear relationships between these in functional form;
- Various forms of functional relationship have been described, including Generalised Power Series (Steer), Chebyshev expansions (Narhi), rational functions (Limiti)... ;
- Practical application requires careful 'bookkeeping' to keep track of frequency components. The most complex operations are the nonlinear ones of multiplication/division (convolution/de-convolution);

Advantages of Harmonic Balance

- Complex linear circuit environments may be easily and efficiently included in analysis;
- Periodic solution can be obtained without needing a (perhaps) very-long transient period to elapse;
- Solution can be very fast if non-linearity is moderate and/or a good initial guess is available. Recent improvements to the algorithm incorporating Krylov-subspace techniques have greatly extended the scale and complexity of problems which can be successfully tackled;

Disadvantages of Harmonic Balance

- Prior assumption of unique periodic solution may not always be justified;
- In spite of great advances in numerical implementation, convergence failure (or extremely slow convergence) is still not uncommon at very large drive levels;
- The method does not work well where the response of interest is not essentially steady-state but is instead a true transient.

Circuit Envelope Techniques

- Several research groups have sought to combine the best features of Hamonic Balance and Time-Domain within a single simulator technology.
- The Circuit Envelope simulator promoted by HP-EEsof, may be viewed as an extension to Harmonic Balance. Now each of the Fourier Series coefficients is considered as a complex-valued function of time which can represent an arbitrary modulating spectrum around each tone:

$$u(t) = \sum_{k=-K}^{+K} U_k(t) \cdot e^{jk\omega_0 t}$$

- A time-domain solution is performed consisting of a sequence of HB solutions at each time-step. However, the most critical point is that the transient analysis time-step is determined by the modulation waveform, not by the high-frequency tone(s). Some modifications to standard HB are then required. For example, a linear capacitor now returns a k^{th} harmonic current component given by:

$$I_k = jk\omega_o C \cdot U_k(t) \quad + \frac{d(C \cdot U_k(t))}{dt}$$

transient envelope component

Diagrammatic Representation of Circuit Envelope

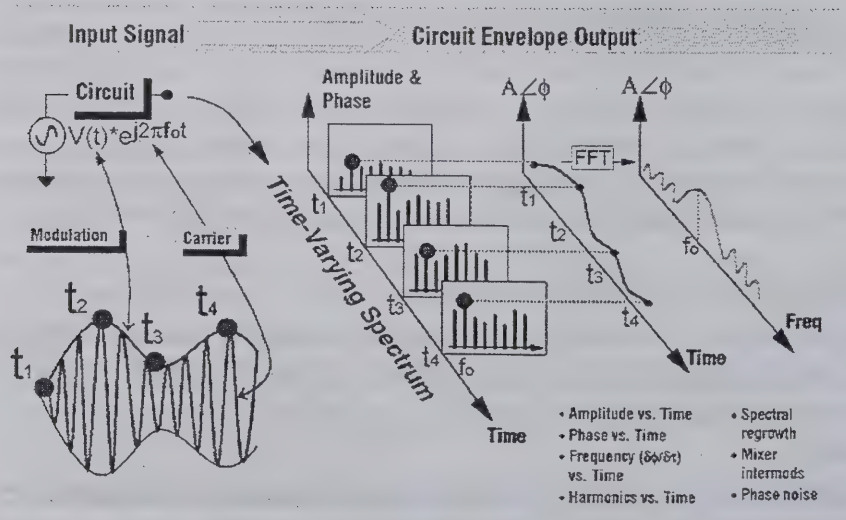

Discrete Convolution Analysis

In principle, convolution methods provide an attractive approach to incorporate arbitrary frequency domain blocks within a time-domain transient simulation. In practice, considerable care is needed in numerical implementations to achieve causality, stability and accuracy;

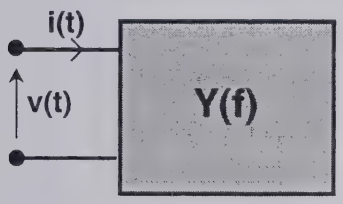

Linear 1-Port

Frequency-Domain:

$$I(f) = Y(f) \cdot V(f)$$

Time-Domain:

$$i(t) = \int_{-\infty}^{t} h_y(t-\tau) \cdot v(\tau) \cdot d\tau$$

where: $h_y(t) = \int_{-\infty}^{+\infty} Y(f) \cdot e^{j2\pi ft} \cdot df$

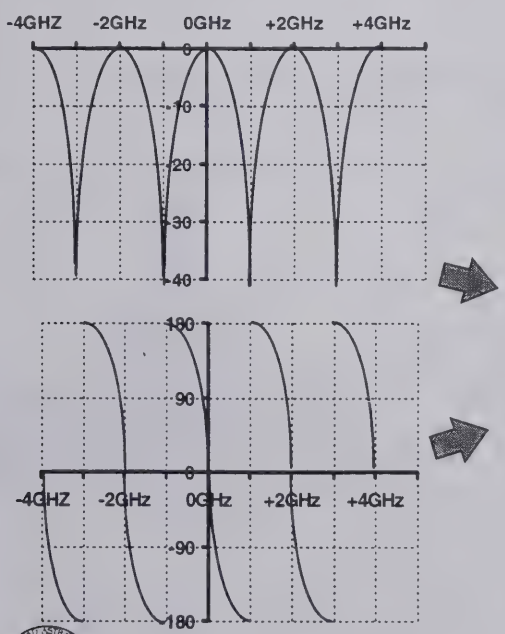

Periodic System Function in Frequency-Domain has Exact Discrete Impulse Response Equivalence

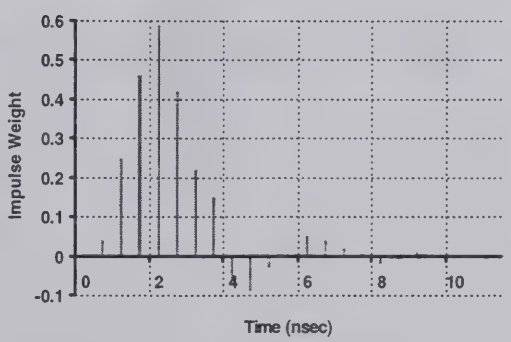

Two-Tone Intermodulation Test, PHEMT Amplifier
f_1= 10GHz Δf=2.5MHz (Convolution Analysis)

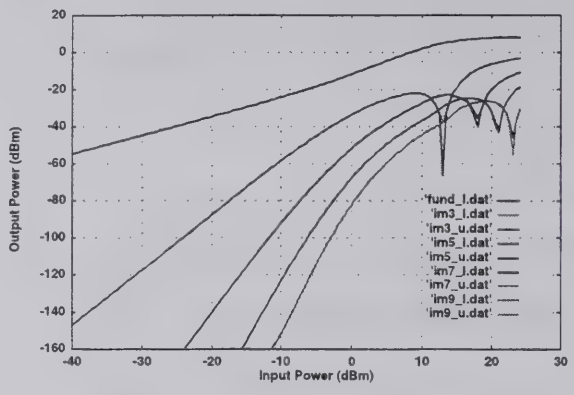

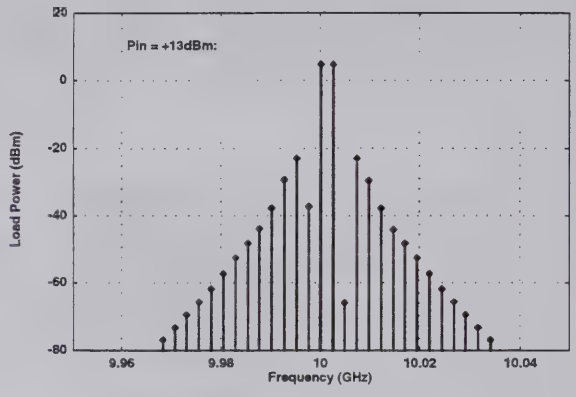

Test with 8 Tones [f_1= 10GHz, Δf=2.5MHz]

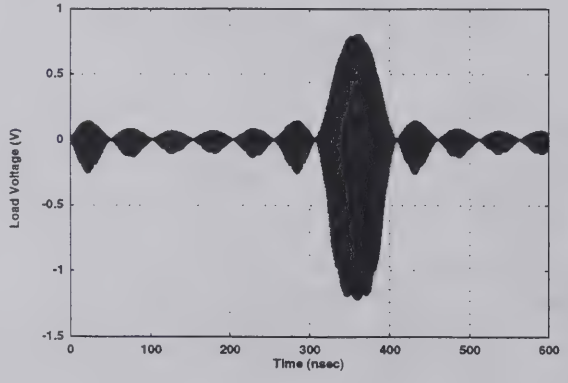

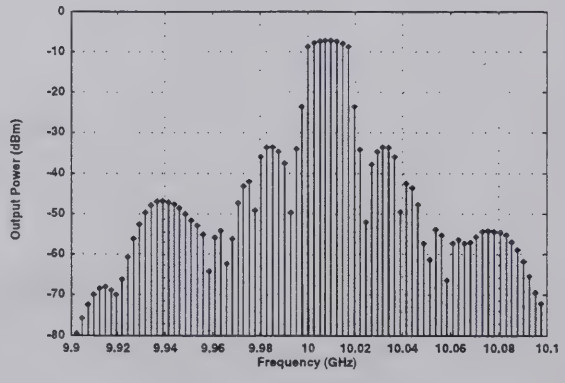

Conclusions

- Modern high-frequency CAD provides a powerful set of tools which can provide key strategic advantages in meeting new design challenges;
- The down-side is that the range and sophistication of these tools is now placing considerable demands on the user;
- Nonlinear active device modelling remains a critical concern. Coping with emerging new technologies and process variations within existing technologies compound the modelling problem;
- Significant progress has been made in recent years in meeting the simulation challenges posed by complex RF systems carrying digitally modulated signals.